Université de Montréal

Régulation et fonctions de la phosphatase PP2A-Twins pendant la mitose chez *Drosophila melanogaster*.

Par

Myreille Larouche

Département de Biochimie et médecine moléculaire, Institut de recherche en immunologie et en cancérologie (IRIC), Faculté de Médecine

Thèse présentée en vue de l'obtention du grade de Ph. D. en Biochimie et médecine moléculaire

Juin 2021

Université de Montréal

Département de Biochimie et médecine moléculaire, Institut de recherche en immunologie et en cancérologie (IRIC), Faculté de Médecine

Cette thèse intitulée

Régulation et fonctions de la phosphatase PP2A-Twins pendant la mitose chez *Drosophila melanogaster*.

Présentée par

Myreille Larouche

A été évaluée par un jury composé des personnes suivantes

Éric Lecuyer
Président-rapporteur

Vincent Archambault
Directeur de recherche

Sébastien Carréno
Membre du jury

Steve Jean
Examinateur externe

Résumé

L'entrée en mitose est initiée par le complexe cycline B – Cdk1. La phosphorylation de ses substrats déclenche des transformations incluant la condensation des chromosomes, le bris de l'enveloppe nucléaire et la formation d'un fuseau mitotique. Ces transformations permettent à la cellule de se diviser. La protéine phosphatase 2A (PP2A) en complexe avec sa sous-unité B55/Twins (Tws) reconnaît et déphosphoryle les substrats de cycline B – Cdk1. Pour éviter la déphosphorylation précoce des phosphoprotéines mitotiques, PP2A-B55/Tws est inhibée en entrée de mitose. Cette inhibition de la phosphatase est attribuable au module Greatwall (Gwl) – endosulfines. Activée en entrée de mitose, la kinase Gwl phosphoryle les endosulfines, qui inhibent alors de manière spécifique PP2A-B55/Tws. Gwl est exportée du noyau vers le cytoplasme en prophase, avant le bris de l'enveloppe nucléaire. Les mécanismes de régulation spatiotemporelle du module Gwl – endosulfines – PP2A-B55/Tws ne sont pas entièrement élucidés. De plus, les substrats ciblés par PP2A-B55/Tws en sortie mitose ne sont pas tous identifiés à ce jour.

Dans mon travail de thèse, j'ai trouvé que Tws peut transiter par le noyau via un signal de localisation nucléaire (NLS), mais que ses fonctions essentielles sont au cytoplasme. De plus, j'ai trouvé que l'unique endosulfine présente chez *Drosophila melanogaster*, Endos, a une localisation cytoplasmique. Cette localisation est requise pour qu'Endos soit efficacement phosphorylée par la forme active et cytoplasmique de Gwl. Endos phosphorylée lie ensuite PP2A-Tws pour l'inhiber. Empêcher la localisation cytoplasmique d'Endos avant le bris de l'enveloppe nucléaire entraîne des défauts mitotiques dépendants de l'activité de PP2A-Tws.

Les substrats mitotiques de PP2A-Tws ne sont pas tous connus. Par des cribles de phosphoprotéomique, j'ai identifié des substrats mitotiques potentiels de PP2A-Tws. L'un des candidats hyperphosphorylés suite à la déplétion de Tws, Otefin (Ote), est une protéine de l'enveloppe nucléaire. Les sites de phosphorylation d'Otefin identifiés dans

mes cribles sont adjacents à son domaine d'interaction avec BAF, une protéine liant l'ADN et certaines protéines de l'enveloppe nucléaire. L'introduction de mutations phosphomimétiques à ces sites abolit l'association d'Otefin avec BAF, en plus de retarder le recrutement d'Otefin à l'enveloppe nucléaire en sortie de mitose. Par ailleurs, l'association Otefin – BAF dépend de l'activité de PP2A-Tws. Enfin, la perte d'Otefin dans l'embryon syncytial de mouche affecte le développement.

En somme, mes travaux ont permis d'approfondir notre compréhension mécanistique de la régulation spatiotemporelle du module Gwl – endosulfines – PP2A et d'identifier de nouveaux substrats potentiels de PP2A-Tws.

Mots-clés : Mitose, Greatwall, endosulfines, PP2A, phosphatases, phosphoprotéomique, Otefin.

Abstract

Mitosis is triggered by the cyclin B – Cdk1 complex that phosphorylates multiple substrates to promote transformations such as chromosome condensation, nuclear envelope breakdown and mitotic spindle formation. These transformations are required for cell division. The protein phosphatase 2A (PP2A) in complex with its B55/Twins (Tws) subunit dephosphorylates cyclin B – Cdk1 substrates. To prevent premature dephosphorylation of the mitotic phosphoproteins, PP2A-B55/Tws is inhibited upon mitotic entry. The Greatwall (Gwl) – endosulfines pathway is responsible for PP2A-B55/Tws inhibition. Activated upon mitotic entry, the Gwl kinase phosphorylates small proteins called endosulfines to turn them into specific inhibitors of PP2A-B55/Tws. Gwl is exported from the nucleus to the cytoplasm before nuclear envelope breakdown. However, the mechanisms of spatiotemporal regulation of the Gwl – endosulfines – PP2A module are not entirely elucidated. Moreover, the identity of the proteins targeted by PP2A-Tws during mitotic exit is still unclear.

During my PhD training, I found that Tws can transit through the nucleus via a nuclear localization signal (NLS), but its essential functions are cytoplasmic. Moreover, the sole endosulfine present in *Drosophila melanogaster*, Endos, has a cytoplasmic localization. Such localization is required for efficient phosphorylation of Endos by active and cytoplasmic Gwl. Once phosphorylated, Endos binds PP2A-Tws to inhibit its activity. Preventing the cytoplasmic localization of Endos prior to nuclear envelope breakdown causes mitotic defects that are PP2A-Tws-dependent.

The mitotic substrates of PP2A-Tws are not all identified. By phosphoproteomic screening, I identified potential novel PP2A-Tws substrates. Among the hits that are hyperphosphorylated following Tws depletion, there is the nuclear envelope protein Otefin (Ote). The identified phosphosites on Otefin are adjacent to its domain of interaction with BAF, a protein binding DNA and nuclear envelope proteins. Introducing phosphomimetic mutations at these sites abolishes the Otefin – BAF association and delays Otefin recruitment at the reforming nuclear envelope during mitotic exit.

Moreover, the Otefin – BAF association is PP2A-Tws-dependent. Finally, loss of Otefin in the syncytial embryo of the fly impairs development.

Altogether, my results deepen our understanding of the spatiotemporal coordination of the Gwl – endosulfines – PP2A module and provide potential novel PP2A-Tws substrates.

Table des matières

Liste des tableaux

Liste des figures

Liste des sigles et abréviations

A

aa : Acide aminé
ADN : Acide désoxyribonucléique
ANOVA : Analysis of variance
AP : Affinity purification
APC/C : Anaphase-promoting complexe/cyclosome
ARN : Acide ribonucléique
Arpp19 : cAMP-regulated phosphoprotein 19
ATM : Ataxia telangiectasia mutated
ATR : Ataxia telangiectasia and Rad3-related
avgSPC : Average spectral counts

B-C

BAF : Barrier-to-autointegration factor
BPR : Bipartite polybasic region
CAK : CDK-activating kinase
CDK : Cyclin-dependent kinase
Cdk1 : Cyclin-dependent kinase 1
CDS : Coding sequence
Chk1 : Checkpoint 1
Chk2 : Checkpoint 2
CIP2A : Cancerous inhibitor of PP2A
CKI : CDK inhibitor
CPC : Chromosomal passenger complex

D-I

dsRNA : Double-stranded RNA
ENSA : α-endosulfine
ER : Endoplasmic reticulum
Fcp1 : Factor 2F-associating C-terminal domain phosphatase 1
FISH : Fluorescent *in situ* hybridization
GO : Gene ontology
GSK3 : Glycogen synthase kinase 3
Gwl : Greatwall
H2A : Histone 2A
HEAT : huntingtin, elongation factor, A subunit, target of rapamycin
IF : Immunofluorescence
Igo : Initiation of G0
IP : Immunoprecipitation

K-M

KASH : Klarsicht, ANC-1, Syne homology
kDa : kilodalton
KLC : Kinesin light chain
LC : Liquid chromatography
LEM : LAP2-emerin-MAN1
LEM-D : LEM domain
LINC : Linker of the nucleoskeleton and cytoskeleton
LMB : Leptomycin B
MASTL : Microtubule-associated serine/threonine kinase-like
MCC : Mitotic checkpoint complex
Mps1 : Monopolar spindle kinase 1
MS : Mass spectrometry
Mts : Microtubule star

N-O

NA : Numerical aperture
NE : Nuclear envelope
NEB : Nuclear envelope breakdown
Nek : NIMA-related kinase
NES : Nuclear export signal
NER : Nuclear envelope reformation
NHK-1 : Nucleosomal histone kinase 1
NIMA : Never in mitosis A
NLS : Nuclear localization signal
NPC : Nuclear pore complex
NSP : Nucleolar stress response pathway
Nup : Nucleoporin
OA : Okadaic acid
Ote : Otefin

P-R

PB : Polar body
PDB : Protein data bank
PKA : Protein kinase A
Plk1 : Polo-like kinase 1
PPP : Phosphoprotein phosphatase
PP1 : Protein phosphatase 1
PP2A : Protein phosphatase 2A
PRC1 : Protein regulator of cytokinesis 1
Rb : Retinoblastoma
RNAi : RNA interference

ROI : Region of interest

S

SAC : Spindle-assembly checkpoint
Scant : Scott of the Antarctic
SCF : Skp, cullin, F-box
SD : Standard deviation
SDC : Sodium deoxycholate
SEM : Standard error of the mean
SILAC : Stable isotope labeling by amino acids in cell culture
SLIM : Short linear-interaction motif
SP : SAINT score
SUN : Sad1 and UNC-84

T-Z

TM : Transmembrane
Tws : Twins
UAS : Upstream activating sequence
Ubi : Ubiquitin
UTR : Untranslated region
VRK1 : Vaccinia-related kinase 1
WB : Western blot
WT : Wildtype
YA : Young arrest

« Omnis cellula e cellula. »

- *Rudolf Virchow*

« Rien ne sert de courir, l'autobus est déjà passé. »

- *Charles Patenaude*

Remerciements

Le parcours de doctorant est à la fois incroyablement solitaire et profondément collaboratif. Ainsi, malgré le défi individuel qu'il représente, je ne me suis jamais sentie autant entourée que pendant mon doctorat. On oublie souvent que la science est immensément humaine. Merci à tous ceux qui m'ont soutenue au fil de cette aventure, mes mots auront certainement du mal à traduire la reconnaissance que j'éprouve à votre endroit.

J'aimerais commencer par remercier **Vincent**, sans qui rien de tout cela n'aurait eu lieu. Merci de m'avoir donné ma première chance comme stagiaire à l'été 2013, même si je ne connaissais absolument rien à l'époque. J'ai beaucoup appris sous ta supervision, à plusieurs niveaux. J'aimerais souligner les multiples opportunités que tu m'as données de « me faire les dents », que ce soit en termes d'écriture, de congrès ou même d'enseignement. Je retiendrai certainement la valeur du dur labeur et l'importance de se tenir debout pour ses idées. Merci d'avoir généreusement partagé ton expérience (et tes blagues épicées) à de nombreuses reprises, je ne pense pas que tous les directeurs de thèse le font aussi ouvertement. Et finalement, je n'oublierai jamais l'importance de la symbiose intellectuelle!

Quelques mots pour remercier les membres de mon comité de thèse, qui m'ont suivie pendant plusieurs années : merci à mon président, **Jim** Omichinski, et également à **Lea** Harrington. Merci à tous les deux pour votre franchise et votre apport constructif; bien que stressants en amont, je suis ressortie ragaillardie de mes comités. Je garderai un très bon souvenir de ces rencontres.

J'ai eu la chance de côtoyer plusieurs scientifiques plus expérimentés que moi depuis mon arrivée à l'IRIC comme stagiaire. Certains sont devenus d'excellents amis; tous ont plus que généreusement partagé leurs connaissances avec moi à un moment ou un autre. Un grand merci à **Peng**, mon tout premier superviseur. En congé paternité ou en rédaction, tu avais toujours du temps pour m'apprendre les techniques de base et répondre à mes questions ☺ Je me rappellerai toujours de ton enthousiasme légendaire et de ton énergie à revendre, une vraie machine!

Mon bref passage au sein du labo Labbé aura été riche en apprentissages. J'aimerais remercier **Jean-Claude** de m'avoir acceptée dans son équipe et initiée à *C. elegans*. Merci également pour les questions et discussions toujours constructives que nous avons eues par la suite. Un merci très spécial à **Abby**, qui me supervisait dans le labo Labbé. Génétique, microscopie, quantifications – j'ai tellement appris en peu de temps à tes côtés! Merci d'avoir partagé ton expérience scientifique et personnelle avec la jeune mêlée que j'étais.

Un gros merci à ma famille scientifique : David, Karine et Damien ☺ Qu'on en a vécu des choses ensemble! **David**, je suis passée de laveuse de carreaux à co-auteure – une pas pire progression non? ;) Maître incontesté des WB, DJ à ses heures, communicateur hors pair; merci d'avoir pris le temps de m'enseigner une tonne de choses. Ce que l'on conçoit bien s'énonce clairement, et les mots pour le dire viennent aisément!! Je n'oublierai jamais l'ADN des mammouths non plus..! Merci énormément pour tout, je suis très fière d'avoir publié à tes côtés. On a réussi! **Karine**, la personne la plus gentille et patiente que je connaisse. Tu es le secret le mieux gardé de l'UdeM je pense! Comme tu as dû être découragée souvent par mes gaffes au labo… Grâce à toi j'ai appris à être (plus) rigoureuse et disciplinée, à noter les détails importants, et à mener des enquêtes efficaces pour les clonages louches. Merci pour ton écoute et ta grande humanité. **Damien**, tu rivalises avec Karine pour la patience. Je ne compte plus les heures que tu as passées à m'expliquer (et me ré-expliquer..!) les dessous de la génétique et de la microscopie. Tes enseignements m'ont permis de devenir une drosophiliste potable, même si je ne cuisine pas couramment la polenta! Je me souviendrai toujours de notre voyage à Roscoff, et des exercices de respiration que tu m'as fait faire avant ma présentation :P Merci pour toutes les discussions, et pour ton support indéfectible quand la vie se complique! MERCI à tous les trois pour l'amitié et la solidarité dans les moments difficiles. Un petit McFlury bientôt? ;)

J'en profite pour remercier Maxime et Guillaume, collègues du passé qui ont égayé la vie au labo. Merci à **Jingjing** pour les quelques mois que nous avons passés ensemble. Ta bonne humeur est contagieuse, je te souhaite beaucoup de succès pour les années à venir. Moltes graciès à **Laia**, ma cyster! Les escargots, le drama, les

sacres, les mille stories IG; la vie au labo était certainement plus intéressante quand The Destroyer était aux alentours ;) Vive la tancat!

Les amis hors du labo ont aussi été essentiels ces dernières années à l'IRIC. Merci aux membres de **l'école intergalactique d'été 2014**, c'est en votre compagnie que j'ai embarqué dans les études graduées et que j'y ai pris goût. Merci aux **Tobbleroners**, aux **GBMs** et aux différentes **gangs de l'asso** qui se sont ajoutés par la suite. 5 à 7 infinis, défis sportifs, soirées Randolph, partys d'Halloween, partys de Noël, 2Ps, Canada Day, canot-camping des moustiques, chalets d'hiver, raclettes et tartiflettes à profusion, pique-niques en folie - les aventures à vos côtés ont pimenté toutes ces années! Merci pour les bouffées d'air frais, à l'IRIC ou en dehors. Mentions spéciales à **Vi**, **Alex**, **Marine**, **Chacha** et **Shasha**! Et merci aux **coureurs du zigzag** pour les sorties endorphines, été comme hiver ☺

Je tiens à remercier les personnes qui sont du côté obscur, souvent oublié, de l'IRIC. Merci à **Pascale** et **Julie** des affaires académiques, pour votre support et votre porte toujours ouverte. Merci **Lyndou**, pour ta présence rassurante au quotidien. Combien de fois je suis venue te voir pour du réconfort! Un IMMENSE merci à la dream team des comm! **Noé** la joggeuse, **Léa** et ses scoops, Sandy, Hélène, Lynn – vous avez toutes été importantes à votre façon. Merci **Cris** pour la complicité et les rires. Merci **Cathou** pour l'écoute et les conseils. Pour la confiance surtout. Sans vous, DLC n'aurait jamais vu le jour. J'ai appris tellement de nouveaux concepts et d'expressions savoureuses à vos côtés, vous êtes le gravy de mon doctorat! Merci spécial à **Zviane**, que je n'aurais jamais espéré rencontrer et qui a illustré mes travaux de doc (Annexe 2)!

Aux copains du quotidien, je vous remercie infiniment de m'avoir permis de garder un équilibre mental à peu près (!) sain. **Audelar Laram** et **Kev**, les biochimistes de la première heure qui savent, merci d'y avoir cru pour moi par moments. **Fatéma** – longue vie à nos séances de ventilation extrême. On va réussir à prendre notre bière un jour! **Lolito**, les Indes nous attendent – matante ça vaaaa! Merci **Bambi** (et la famille dysfonctionnelle des Hurricanes!) pour les marches et le support et la team tomate! Merci au **moussaillon Newtown** pour le surf et les vagues en pleine face, vive la MM..! Merci **Jackouille** pour les bons moments, avec ou sans chialage, souvent avec du bon manger ☺ Quarante-quinze mercis à **Dave** et ses biceps, je ne peux pas lister toutes les

aventures ici mais je les résumerai à : rond-point. Un merci très spécial à **Marjo** et **Kéké** (les Kevjo!) de m'avoir adoptée comme 3rd wheel officielle pour les soupers à 100$, les vacances sur la route et toutes les autres aventures. Pilou pilou! Merci à mon **Toto** pour l'ensemble de l'œuvre, depuis cette fameuse conversation en salle de culture (à quand un film?!) jusqu'à notre incorporation (!!). Vive nos synapses communes, tes clés hélicoptères, tes rires fous, nos petites angoisses de bébés et nos projets infinis!

Je suis infiniment reconnaissante à ma garde rapprochée, celle que je peux appeler en renfort à toute heure, dans n'importe quel état, quand je perds pied. Merci à **Amandine** (la ptite) de me prendre comme je suis et de me partager ta force de caractère. Merci **Clau** pour ce lien solide, loyal et vrai qui résiste aux années sans jamais s'amenuiser. Merci à **Cél**, qui reste proche malgré la distance, pour les lumières, le philosophage du dimanche et les folies multiples. Merci **Eugene**, de cette première napkin de schémas de croisements à tes poèmes quotidiens; merci pour la sollicitude, les enseignements, les discussions, les initiatives citoyennes, la culture avec un grand C. Merci à **Élizabi** pour la décennie de complicité +++, les gestions de crises, la présence indéfectible dans toutes les situations. Merci de prendre mon bord, et de me brasser au besoin. À toutes, merci d'être là. Merci de calmer mes (nombreuses) angoisses. Vous êtes ma forteresse.

Enfin, quelques mots pour les familles Noël et Larouche, pour qui je reste la même peu importe l'issue des manips. Merci **Charlot** pour la joie que tu apportes déjà à mon quotidien. Merci à ma **grand-maman Nicole**, véritable star parmi mes amis, pour le modèle de détermination et d'authenticité que tu es. Merci **les parents** pour le support, les encouragements, la fierté, la curiosité… et les lifts quand il faut trier des mouches le 31 décembre! Merci d'avoir embarqué sans jamais douter dans cette aventure bien loin de la comptabilité. Et merci À **JD**, Jid, Jdouille : le meilleur frère et le meilleur coloc. À bien des égards j'ai l'impression que c'est moi qui suis tes traces. Merci d'endurer mes délires quotidiens! Ça change tout de savoir sa famille à ses côtés pour les moments heureux comme pour ceux plus difficiles.

Chapitre 1

1. Introduction

1.1 Le cycle cellulaire eucaryote

La cellule constitue l'unité structurelle de base des organismes vivants. Les organismes multicellulaires se développent à partir d'une unique cellule fertilisée, le zygote. De nombreuses rondes de divisions cellulaires permettent à cette cellule initiale de se multiplier et de générer différents types cellulaires composant un organisme complet. Le corps humain adulte étant composé d'environ $3,7 \times 10^{13}$ cellules, on estime à environ 10^{16} le nombre de divisions cellulaires se déroulant pendant la vie humaine (Bianconi et al., 2013; Rangarajan and Weinberg, 2003). En plus d'être nécessaires au développement, les divisions cellulaires permettent de remplacer les cellules qui meurent de façon naturelle ou qui sont endommagées, lors de blessures par exemple. Les cellules cyclent ainsi entre les différentes phases de ce qui constitue le cycle cellulaire. Cette série d'étapes, qui se succèdent dans un ordre précis, mènent à la division d'une cellule dite mère en deux cellules-filles génétiquement identiques. Le cycle cellulaire eucaryote comporte deux phases principales. L'interphase permet aux cellules de croître et de dupliquer leur génome. La phase M permet quant à elle la division égale du matériel génétique dupliqué entre les deux cellules-filles naissantes.

1.1.1 L'interphase

L'interphase constitue généralement la phase la plus longue du cycle cellulaire. C'est une phase préparatoire qui permet à la cellule de croître en taille et de dupliquer son contenu, notamment son génome. L'interphase peut être subdivisée en phase S (synthèse), pendant laquelle il y a réplication de l'ADN, et en phases de croissance G (*gap phases*) (Baserga, 1965). Comme tous les cycles cellulaires ne sont pas équivalents, l'enchaînement des phases peut varier chez certaines espèces et/ou types cellulaires (Morgan, 2007). Par exemple, les phases de croissance sont absentes dans l'embryon précoce de *Drosophila melanogaster*, ce qui résulte en une succession rapide de phases S et M. Ainsi, le cycle cellulaire est adapté en fonction des besoins d'un type

cellulaire donné. Toutefois, la plupart des cellules se divisent selon un cycle cellulaire «
classique », pour lequel se succèdent, en ordre, les phases G1, S, et G2 pendant
l'interphase (Norbury and Nurse, 1992).

Dans le cycle cellulaire classique, la phase de croissance G1 prend place entre
les phases M et S (Figure 1.1). La croissance cellulaire correspond à l'augmentation de
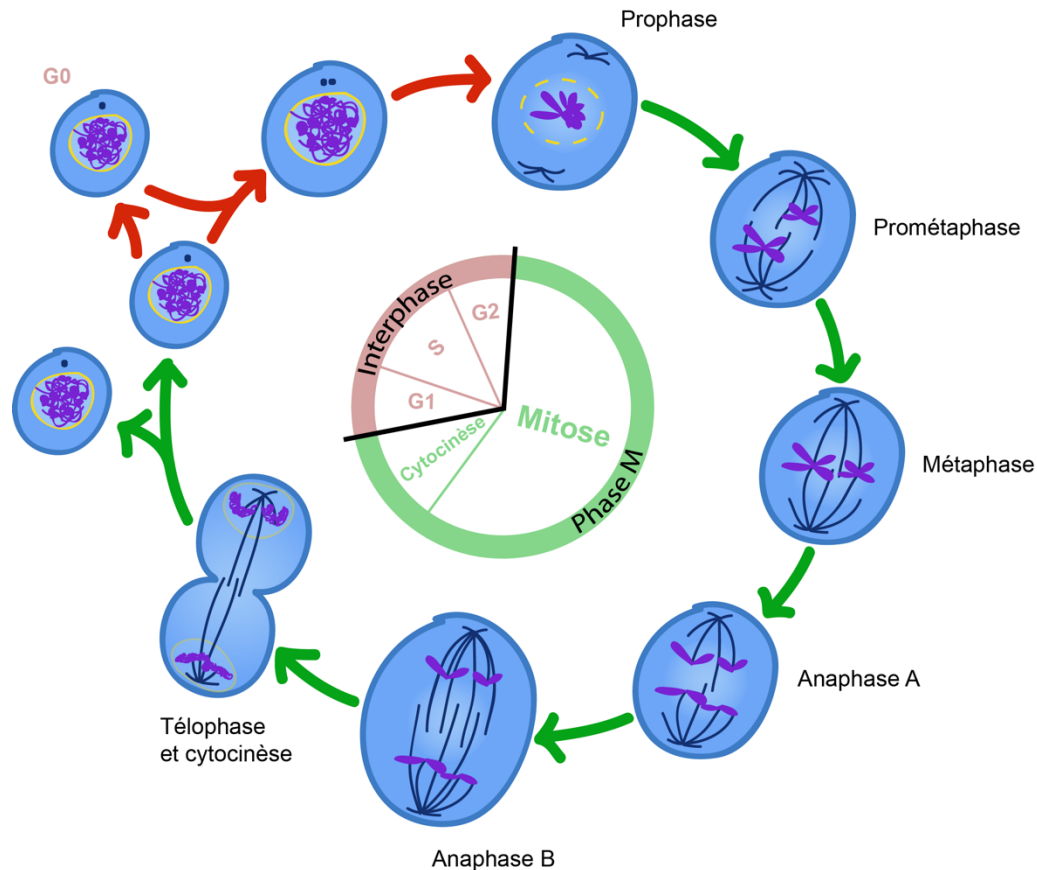
Figure 1.1. Les phases du cycle cellulaire eucaryote classique.

Les deux principales phases du cycle cellulaire sont l'interphase et la phase M (schéma
non représentatif de leur durée; l'interphase est en général plus longue que la phase M).
Dans un cycle classique, l'interphase est constituée des phases G1, S et G2. Les cellules
en G1 peuvent entrer en quiescence (G0). La phase M est constituée de la mitose
(prophase, prométaphase, métaphase, anaphase et télophase) et de la cytocinèse (pour
les divisions résultant en la partition physique des cellules filles).

la taille et de la masse de la cellule, et non du nombre de cellules (Malumbres and Barbacid, 2001). Elle s'accompagne d'une augmentation de la synthèse protéique (Campbell et al., 2020; Marguerat et al., 2012). Cette croissance cellulaire permet de générer des cellules-filles qui sont de taille similaire à la cellule-mère (Wilson, 1925). La cellule en G1 intègre des informations externes, comme la disponibilité des nutriments ou des signaux mitogènes, pour décider de poursuivre sa progression vers la phase S ou de s'arrêter dans un état de quiescence réversible (phase G0) (Fantes and Nurse, 1977; Fantes, 1977; Johnston et al., 1977). La présence de facteurs de croissance est requise jusqu'à ce que la cellule atteigne le point de restriction (R) en fin de G1, moment à partir duquel elle s'engage de façon irréversible à entrer en phase S (Blagosklonny and Pardee, 2002; Pardee, 1974).

L'événement principal caractérisant la phase S est la duplication fidèle et complète du génome de la cellule (Baserga, 1965; Howard and Pelc, 1953). La réplication correcte de l'ADN est cruciale au maintien de l'intégrité génomique de la cellule. Il est notamment important que le génome ne soit répliqué qu'une seule fois, pour éviter des problèmes comme la polyploïdie (Archambault et al., 2005; Green and Li, 2005; Melixetian et al., 2004; Zhu et al., 2004). Pour ce faire, la synthèse de l'ADN est initiée à des endroits précis, les origines de réplication, qui ne peuvent être activées qu'une seule fois par cycle cellulaire (Bell and Dutta, 2002; DePamphilis, 2016). Le nombre élevé d'origines de réplication combiné à la vélocité de la machinerie de réplication permet de répliquer l'entièreté du génome en quelques heures (environ 8 heures pour les cellules mammifères) (Alexiades and Cepko, 1996; DePamphilis, 2016; Masai et al., 2010; Morgan, 2007). Les brins d'ADN nouvellement synthétisés demeurent associés sous forme de chromatides; chaque chromosome dupliqué correspond donc à une paire de chromatides sœurs. Bien que la réplication de l'ADN soit l'événement principal de la phase S, elle s'accompagne de la synthèse de nombreuses protéines, notamment des protéines qui structurent la chromatine, comme les histones (Morgan, 2007). Les centrosomes, composés d'une paire de centrioles et agissant comme centres d'organisation des microtubules, sont également dupliqués pendant la phase S (Cavalier-Smith, 1974; Dippell, 1968; Kuriyama and Borisy, 1983;

Robbins et al., 1968). Chaque centriole-père se duplique dès le début de la phase S pour former un centriole-fils dans un angle orthogonal (Rattner and Phillips, 1973; Robbins et al., 1968; Vorobjev and Chentsov Yu, 1982).

La phase de croissance G2 s'insère entre les phases S et M (Norbury and Nurse, 1992). C'est en G2 que la cellule complète sa préparation pour la phase M. Elle y poursuit la synthèse protéique requise pour sa division (Burke and Church, 1991). Les centrioles-fils terminent leur élongation et les centrosomes complètent leur maturation (Casenghi et al., 2003; Palazzo et al., 2000; Rattner and Phillips, 1973; Robbins et al., 1968; Vorobjev and Chentsov Yu, 1982). En fin de G2, les centrosomes matures commencent à se séparer, ce qui leur permettra de former un fuseau mitotique bipolaire (Bahe et al., 2005; Mayor et al., 2000). D'autres organelles, comme l'appareil de Golgi et les mitochondries, se préparent également à la division cellulaire (Colanzi et al., 2007; Hidalgo Carcedo et al., 2004; Imoto et al., 2011; Mishra and Chan, 2014). Enfin, la cellule intègre les derniers signaux lui dictant sa progression en phase M, ou son arrêt en G2.

1.1.2 La phase M

La deuxième phase principale du cycle cellulaire est la phase M. Généralement plus courte que l'interphase, elle est toutefois beaucoup plus spectaculaire. C'est pendant la phase M que la mitose (division nucléaire) et la cytocinèse (partition du cytoplasme) ont lieu. Ces étapes visent à séparer également le génome dupliqué de la cellule-mère entre deux cellules-filles. Comme la longueur totale de l'ADN génomique dépasse largement le diamètre de la cellule, la mitose et la cytocinèse nécessitent d'importantes modifications structurelles du noyau et du cytosquelette (McIntosh, 2016).

1.1.2.1 La mitose

C'est en 1882 que le terme *mitosen* (du grec *mitos*, « filament ») est utilisé pour la première fois par Walther Flemming (Flemming, 1882; Paweletz, 2001). Avec Anton Schneider, il fut l'un des premiers à décrire précisément les modifications nucléaires se succédant pendant la division cellulaire (Flemming, 1882; Schneider, 1873). Ses travaux

ont fortement contribué à la conception actuelle de la mitose, qui est généralement sous-divisée en cinq phases chez les cellules eucaryotes : prophase, prométaphase, métaphase, anaphase et télophase (Figure 1.1).

La prophase débute avec la compaction des chromosomes dupliqués en courtes unités denses et distinguables. Les chromatides sœurs condensées demeurent connectées au niveau de leur centromère. La transcription et la synthèse protéique sont toutes deux fortement ralenties lorsque la cellule entre en prophase (Martinez-Balbas et al., 1995; McIntosh, 2016; Prescott and Bender, 1962; Sivan et al., 2007; Taylor, 1960). Les microtubules interphasiques se désassemblent, les centrosomes migrent vers les pôles de la cellule et forment des asters de microtubules mitotiques (Karsenti and Vernos, 2001; Maller, 1986; Vandre et al., 1986). L'appareil de Golgi se désassemble et le réticulum endoplasmique se repositionne vers la périphérie de la cellule (West et al., 2011). Enfin, dans les mitoses « ouvertes » des eucaryotes supérieurs, l'enveloppe nucléaire, barrière qui protège le génome des cellules, est désassemblée pour permettre aux microtubules du fuseau mitotique d'accéder aux chromosomes. Plusieurs mécanismes contribuent au bris de l'enveloppe nucléaire et seront présentés dans la section 1.4.4.5.2. Le bris de l'enveloppe nucléaire est l'événement qui marque la fin de la prophase des mitoses ouvertes. Chez les levures, la mitose est dite « fermée » puisque l'enveloppe nucléaire demeure intacte (Cavalier-Smith, 2010; Patterson, 1999; Zhang and Oliferenko, 2013). Pour ségréger les chromosomes dans ce type de mitose, des organelles nommées corps polaires du fuseau, insérés dans la membrane nucléaire et fonctionnellement similaires aux centrosomes, initient la formation d'un fuseau bipolaire dans le noyau à partir de microtubules nucléaires (Ding et al., 1997). D'autres organismes, tels *Caenorhabditis elegans* et *Drosophila melanogaster*, peuvent présenter des mitoses « semi-fermées » pour lesquelles le bris de l'enveloppe nucléaire est partiel (De Souza and Osmani, 2007).

En prométaphase, les extrémités « plus » des microtubules s'allongent à partir des asters pour former le fuseau mitotique. Les microtubules mitotiques sont dynamiques : leur extrémité plus se polymérise et se dépolymérise rapidement, leur permettant de capturer les chromosomes condensés via un complexe protéique lié au

centromère, le kinétochore (Belmont et al., 1990; Kirschner and Mitchison, 1986; Magidson et al., 2015; Saxton et al., 1984). Les chromosomes attachés migrent vers le centre du fuseau, la plaque équatoriale; un processus nommé congression des chromosomes (Miyazaki and Orr-Weaver, 1994). Progressivement, chaque chromatide sœur est ainsi capturée par les microtubules. La métaphase correspond au court moment où toutes les chromatides sœurs sont attachées aux microtubules et alignées à la plaque métaphasique.

Dès que tous les kinétochores sont attachés et sous tension, les chromosomes s'alignent à l'équateur de la cellule et l'anaphase s'enclenche. La cohésion centromérique entre les chromatides sœurs est éliminée, ce qui permet la ségrégation d'une copie de chaque chromosome vers chaque pôle du fuseau mitotique (Uhlmann, 2001). Deux types de mouvements s'enchaînent pendant l'anaphase. D'abord, pendant l'anaphase A, la distance entre les chromosomes et leur pôle respectif est réduite par le raccourcissement des microtubules, à la fois aux kinétochores et aux pôles (Maddox et al., 2000; Mitchison et al., 1986). Des moteurs protéiques présents aux kinétochores contribuent également à ségréger les chromosomes vers les pôles pendant l'anaphase A (Sharp et al., 2000; Tanaka et al., 2007; Yang et al., 1997). L'anaphase B consiste ensuite en l'élongation du fuseau central, composé de microtubules interpolaires non liés à des kinétochores (Maddox et al., 2000; McIntosh et al., 1979). En parallèle, les microtubules des asters contribuent à rapprocher les centrosomes de la membrane plasmique (Aist et al., 1991; Civelekoglu-Scholey and Scholey, 2007; Fink et al., 2006). Ces actions concertées ont pour effet d'allonger la cellule, ce qui sépare davantage les pôles et, conséquemment, les chromosomes.

En télophase, les masses de chromosomes rejoignent les pôles. Les chromosomes commencent à se décondenser et les protéines de l'enveloppe nucléaire sont progressivement recrutées à la chromatine pour reformer des noyaux dans les cellules-filles. La reformation de l'enveloppe nucléaire sera abordée à la section 1.4.4.5.2 et dans le Chapitre 3.

1.1.2.2 La cytocinèse

La cytocinèse est l'étape finale de la division cellulaire qui permet de partitionner le cytoplasme des cellules-filles (Rieder and Khodjakov, 2003). Elle doit être précisément coordonnée spatiotemporellement avec la ségrégation des chromosomes afin que chaque cellule-fille reçoive une copie complète du génome. Tout comme la mitose, la cytocinèse est donc un enchaînement d'étapes bien définies et hautement régulées.

Pendant l'anaphase, les microtubules antiparallèles du fuseau central permettent de positionner le futur plan de clivage (Bement et al., 2005; Mishima et al., 2002; Wheatley and Wang, 1996). Avec leurs protéines associées, ils orchestrent la formation de l'anneau contractile, composé notamment d'actine et de myosine II, au cortex cellulaire (Bement et al., 2006; Piekny et al., 2005). La contraction de l'anneau d'actomyosine compacte graduellement le fuseau central, ce qui le remodèle en un pont intercellulaire transitoire au milieu duquel se trouve une structure sphérique portant le nom de corps central (Mullins and Biesele, 1977). La cytocinèse se termine avec l'abcission cellulaire, possible par la scission des membranes et la relâche du corps central, générant deux cellules-filles physiquement séparées (Byers and Abramson, 1968; Caballe and Martin-Serrano, 2011; Guizetti and Gerlich, 2012).

Lors du développement de certains tissus, la cytocinèse est incomplète et les cellules-filles demeurent connectées une fois la mitose complétée pour former un syncytium (Burgos and Fawcett, 1955; Fawcett, 1961; Robinson and Cooley, 1996; Robinson and Cooley, 1997). C'est notamment le cas dans la lignée germinale des métazoaires (Burgos and Fawcett, 1955; Fawcett, 1961; Haglund et al., 2010; Hime et al., 1996; Pepling et al., 1999; Robinson and Cooley, 1996; Robinson and Cooley, 1997). Dans ces cellules, le pont intercellulaire est stabilisé, permettant l'échange de macromolécules et même d'organelles entre les cellules-filles (Robinson and Cooley, 1996; Zani and Edelman, 2010). Par ailleurs, la cytocinèse peut être absente à certains stades développementaux, dans l'embryon syncyctial de *Drosophila melanogaster* par exemple (Rabinowitz, 1941).

1.2 La régulation du cycle cellulaire

La progression du cycle cellulaire se fait selon un enchaînement précis des différentes phases présentées ci-haut. Plusieurs mécanismes de contrôle sont en place pour veiller à ce que chaque étape soit dûment complétée avant que ne s'entame la prochaine. Les principales actrices moléculaires régulant les transitions entre les phases du cycle cellulaire sont les cyclines et les kinases dépendantes des cyclines (CDKs, pour *cyclin-dependent kinases*), elles-mêmes précisément contrôlées. La cellule compte également sur divers points de contrôle, qui agissent comme mécanismes de surveillance dictant la poursuite ou l'arrêt du cycle cellulaire.

1.2.1 Les kinases dépendantes des cyclines (CDKs)

Les années 1980 ont été le théâtre de grandes avancées dans la compréhension de la régulation du cycle cellulaire. Les gènes *cdc2* et *CDC28* ont d'abord été identifiés comme étant essentiels pour la progression du cycle cellulaire chez *Schizosaccharomyces pombe* et *Saccharomyces cerevisiae* (Hartwell et al., 1974; Nurse et al., 1976). Ils correspondent tous deux à *Cdk1* chez l'humain, gène qui code pour la kinase dépendante des cyclines 1 (Cdk1) (Draetta et al., 1987; Lee and Nurse, 1987). Peu après, des protéines successivement synthétisées puis dégradées au fil du cycle cellulaire furent identifiées dans des embryons d'oursins de mer : les cyclines (Evans et al., 1983). Ce sont des expériences chez *Xenopus laevis* qui permirent ensuite de montrer que Cdk1 fonctionnait en complexe avec ces cyclines (Lohka et al., 1988). De fait, les CDKs constituent les sous-unités catalytiques d'une grande famille de complexes cycline – CDK.

Les CDKs sont des kinases qui ciblent les sérines et les thréonines (Hindley and Phear, 1984; Lorincz and Reed, 1984; Reed et al., 1985; Simanis and Nurse, 1986). Leur site consensus optimal (ou fort) est **S/T**-P-x-K/R, mais elles peuvent également reconnaître le motif minimal **S/T**-P (Endicott et al., 1999; Songyang et al., 1994). Le nombre de CDKs augmente avec l'évolution : de six chez la levure, leur nombre passe à vingt chez l'humain (Cao et al., 2014). Constituées de 250 à 1500 acides aminés, les

CDKs possèdent toutes les deux lobes typiques des kinases (Malumbres, 2014). Comme chez la levure, Cdk1 est la seule CDK qui est essentielle au cycle cellulaire mammifère (Santamaria et al., 2007). Contrairement à ceux des cyclines, les niveaux des CDKs sont stables tout au long du cycle cellulaire (Morgan, 1995). D'autres mécanismes sont donc requis pour la régulation temporelle de leur activité.

1.2.2 Mécanismes de régulation de l'activité des CDKs

1.2.2.1 Association aux cyclines

Les CDKs doivent s'associer aux cyclines, qui agissent comme sous-unités activatrices, pour fonctionner (Draetta and Beach, 1988; Solomon et al., 1990). L'expression périodique des cyclines permet ainsi d'activer séquentiellement leurs CDKs associées (Figure 1.2).
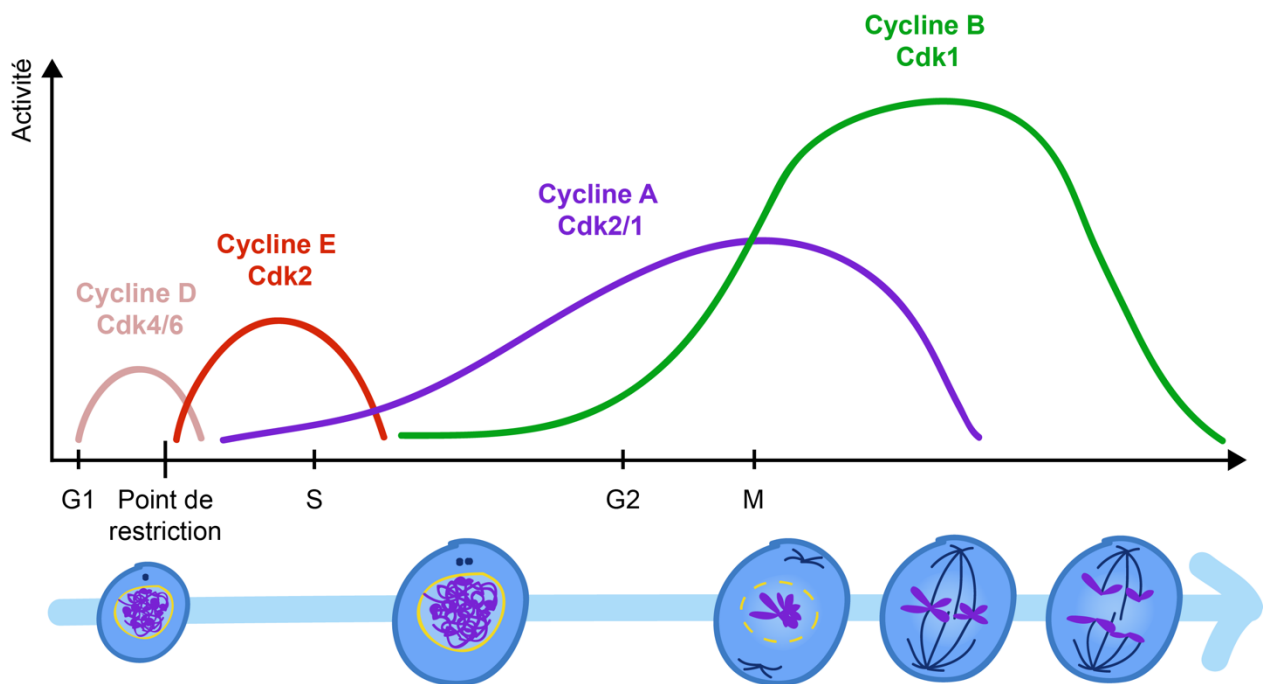
Figure 1.2. Les niveaux des cyclines oscillent pendant le cycle cellulaire.

Les cyclines sont exprimées séquentiellement et périodiquement pendant le cycle cellulaire. Les cyclines lient les CDKs pour les activer et leur donner leur spécificité de substrats. Les complexes cyclines – CDKs ainsi activés temporellement sont les principaux moteurs de la progression du cycle cellulaire. Inspiré de (Holder et al., 2019).

Les cyclines D sont les seules cyclines qui sont synthétisées en réponse à la stimulation par les facteurs de croissance (Assoian and Zhu, 1997). Elles s'associent avec Cdk2 et Cdk4 pour permettre l'entrée en G1 (Sherr, 1994). Leur activité mène entre autres à l'expression en G1 de la cycline E qui, en s'associant avec Cdk2, permet la transition de la G1 à la phase S (Ohtsubo et al., 1995). Le complexe cycline A – Cdk2 est par la suite requis pour la complétion de la phase S (Girard et al., 1991; Walker and Maller, 1991). En fin de G2, la cycline A en complexe avec Cdk1 initie l'entrée en mitose, transition qui est complétée par l'activité du complexe cycline B – Cdk1 (Arellano and Moreno, 1997; King et al., 1994). Enfin, en plus d'orchestrer l'activation temporelle des CDKs, les cyclines leur confèrent leur spécificité envers leurs substrats (Booher et al., 1989; Draetta et al., 1989; Minshull et al., 1990).

1.2.2.2   Inhibiteurs

À l'inverse des cyclines qui jouent un rôle activateur, d'autres protéines peuvent lier les CDKs pour inhiber leur activité : ce sont les inhibiteurs de CDKs (CKIs, pour *CDK inhibitors*). Les CKIs sont rassemblés en deux familles : les protéines INK4 et les protéines Cip/Kip (Sherr and Roberts, 1995). Les protéines INK4 lient directement Cdk4 et Cdk6, empêchant leur association avec les cyclines D (Carnero and Hannon, 1998). Les protéines Cip/Kip agissent quant à elles en liant les complexes cycline – CDK de la transition G1/S et de la phase S pour les inactiver (Harper et al., 1995; Lee et al., 1995; Polyak et al., 1994).

1.2.2.3   Phosphorylations activatrices et inhibitrices

En plus de leur association aux cyclines, les CDKs doivent être phosphorylées sur une thréonine située dans la boucle d'activation de leur domaine catalytique pour être complètement actives (Jeffrey et al., 1995). La liaison aux cyclines induit un changement de conformation qui expose le site de phosphorylation à la kinase activatrice des CDKs (CAK, pour *CDK-activating kinase*) (Jeffrey et al., 1995; Nigg, 1996).

Les CDKs impliquées dans le contrôle de la division cellulaire sont aussi inhibées par la phosphorylation d'une tyrosine conservée (Tyr15) (Gould and Nurse, 1989). Chez les eucaryotes multicellulaires, la phosphorylation d'un second site (Thr14) est également inhibitrice (Krek and Nigg, 1991; Norbury et al., 1991). Wee1 est la kinase majoritairement responsable de la phosphorylation de la Tyr15 (Gould and Nurse, 1989; McGowan and Russell, 1993; Russell and Nurse, 1987). Chez les vertébrés, la kinase Myt1 peut phosphoryler les deux sites (Mueller et al., 1995). Ce sont les phosphatases de la famille Cdc25 qui déphosphorylent les CDKs pour les activer (Gould and Nurse, 1989; Lew and Kornbluth, 1996; Strausfeld et al., 1991).

1.2.3 Protéolyse

Pour assurer la progression unidirectionnelle du cycle cellulaire, certaines protéines régulatrices sont dégradées par le complexe du protéasome 26S. Cette protéolyse cible notamment les cyclines, les protéines qui assurent la cohésion entre les chromatides sœurs (les cohésines), les CKIs et certaines kinases mitotiques (Glotzer et al., 1991; Lindon and Pines, 2004; Meghini et al., 2016; Uhlmann et al., 1999). Les ubiquitine ligases (ou ligases E3) dirigent la protéolyse des régulateurs du cycle cellulaire en catalysant leur attachement covalent à des unités d'ubiquitine activées (Hershko, 1983; Hershko and Ciechanover, 1998). Les protéines ainsi polyubiquitinées sont reconnues et dégradées par le protéasome. Les deux ubiquitine ligases impliquées dans la progression du cycle cellulaire sont le complexe Skp, cullin, F-box (SCF) et le complexe promoteur de l'anaphase, ou cyclosome (APC/C, pour *anaphase-promoting complex/cyclosome*) (Castro et al., 2005; Feldman et al., 1997; Nakayama and Nakayama, 2006).

Le complexe SCF est actif tout au long du cycle cellulaire et reconnaît ses substrats en fonction de leur état de phosphorylation, via des motifs nommés phosphodégrons (Castro et al., 2005; Nguyen and Busino, 2020). La spécificité du complexe SCF vient des différentes sous-unités F-box qui peuvent lui être associées (Bai et al., 1994; Bai et al., 1996). Celles-ci recrutent des substrats spécifiques, dont plusieurs sont phosphorylés par les CDKs, permettant d'induire la protéolyse à des

moments précis du cycle cellulaire (Ang and Wade Harper, 2005). Ces particularités font du complexe SCF un acteur clé de la progression du cycle cellulaire entre la fin de la phase G1 et l'initiation de la mitose (Castro et al., 2005). SCF est notamment responsable de la dégradation de la cycline E en phase S pour éviter la ré-réplication de l'ADN (Hwang and Clurman, 2005; Malumbres and Barbacid, 2005).

Contrairement au complexe SCF, l'APC/C n'est actif que pendant la sortie de mitose et la phase G1 (Hershko et al., 1994; Sudakin et al., 1995). L'activation de l'APC/C nécessite le recrutement de l'un de ses deux co-activateurs, Cdc20 ou Cdh1, eux-mêmes activés successivement par déphosphorylation (Figure 1.3) (Hilioti et al., 2001; Kramer et al., 2000; Labit et al., 2012; Sorensen et al., 2001; Visintin et al., 1998;
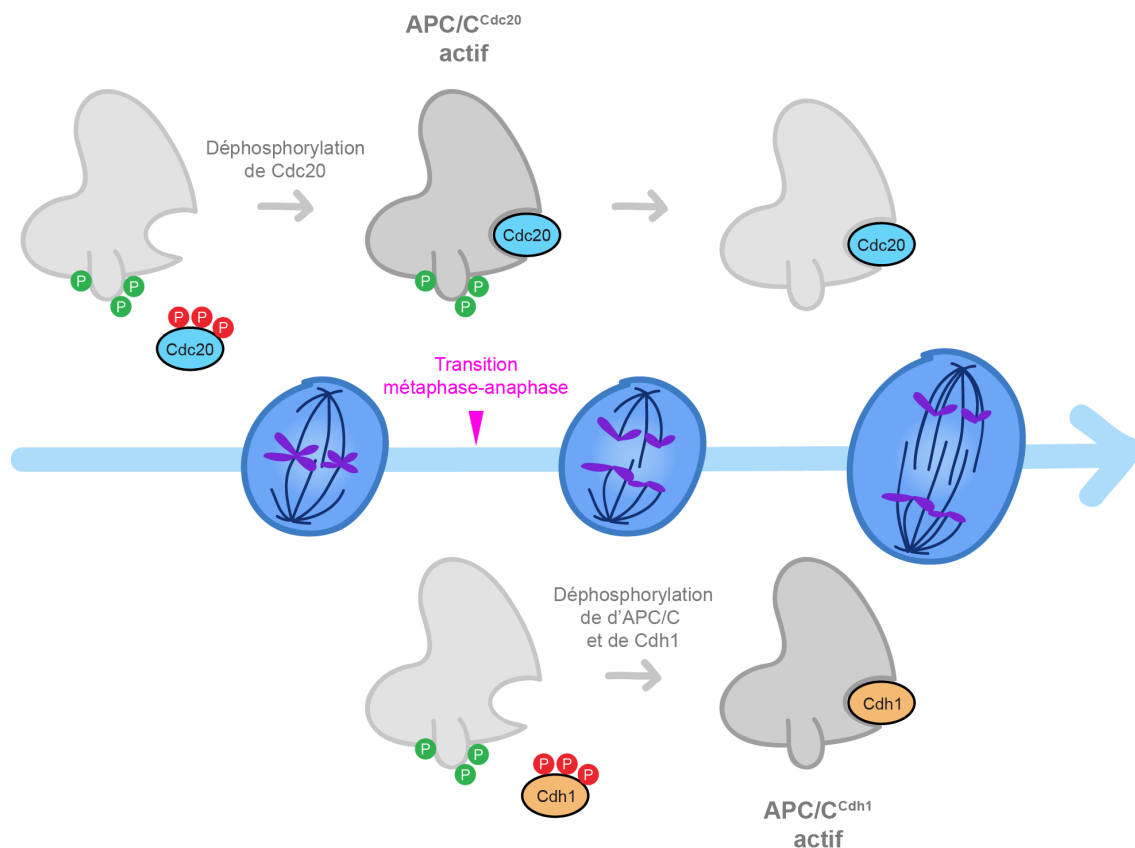
Figure 1.3. La phosphorégulation de l'APC/C^{Cdc20} et l'APC/C^{Cdh1} permet de les activer séquentiellement.

Le recrutement de Cdc20 nécessite la phosphorylation de l'APC/C. Cdc20 doit être déphosphorylé pour lier l'APC/C et initier l'anaphase. La déphosphorylation de l'APC/C inactive l'APC/C^{Cdc20}, mais n'empêche pas l'activation de l'APC/C^{Cdh1}, qui nécessite toutefois la déphosphorylation de Cdh1.

Visintin et al., 1997; Yudkovsky et al., 2000; Zachariae et al., 1998; Zachariae et al., 1996).

À l'inverse, la phosphorylation de l'APC/C par Cdk1 est requise pour son recrutement de Cdc20 (Fujimitsu et al., 2016; King et al., 1995; Kraft et al., 2003; Qiao et al., 2016; Sudakin et al., 1995; Zhang et al., 2016). Les détails de cette phosphorégulation seront abordés dans la section 1.4.4.4. Les déphosphorylations séquentielles de Cdc20 et Cdh1 font en sorte que l'APC/C^{Cdc20} est activé à la métaphase, alors que l'APC/C^{Cdh1} n'est activé qu'en fin de mitose (Hein et al., 2017; Yamano, 2019). Lorsqu'ils sont activés, Cdc20 et Cdh1 dirigent le recrutement de substrats spécifiques à l'APC/C via la reconnaissance de motifs de dégradation (Castro et al., 2002; Glotzer et al., 1991; Hilioti et al., 2001; Lorca et al., 1992; Pfleger and Kirschner, 2000). L'activité ainsi régulée de l'APC/C permet l'initiation de l'anaphase et la sortie de mitose (Castro et al., 2005).

1.2.4 Des points de contrôle à satisfaire pour continuer

L'expression « point de contrôle » (*checkpoint* en anglais) a été proposée en 1989 pour référer aux mécanismes de surveillance permettant d'assurer la succession ordonnée des événements du cycle cellulaire (Hartwell and Weinert, 1989). Certaines conditions doivent être réunies pour satisfaire les points contrôle, qui dictent à la machinerie cellulaire si la progression doit s'arrêter ou se poursuivre vers la phase suivante.

1.2.4.1   Le point de restriction

Le premier point de contrôle du cycle cellulaire, le point de restriction, se trouve en G1. Tel que mentionné précédemment, le point de restriction est un point de non-retour, au-delà duquel la cellule s'engage dans le cycle cellulaire. Ce contrôle assure que les conditions nutritives et de croissance requises soient réunies avant que la cellule n'entame sa division. La disponibilité de nutriments et l'intégration de signaux mitogènes induisent la synthèse des cyclines D (Assoian and Zhu, 1997; L'Allemain et al., 1997; Sherr, 1996). Celles-ci s'associent aux Cdk4/6 et initient la phosphorylation

des protéines de la famille du rétinoblastome (Rb) (Connell-Crowley et al., 1997; Kitagawa et al., 1996). Dans sa forme hypophosphorylée, Rb lie les facteurs de transcription E2F pour inhiber leur activité (Giacinti and Giordano, 2006). La phosphorylation de Rb par CycD – Cdk4/6 la dissocie partiellement de E2F, qui compte les cyclines E et A parmi ses cibles transcriptionnelles (Bartek et al., 1996; Duronio et al., 1996; Resnitzky and Reed, 1995; Sanchez and Dynlacht, 1996; Sherr, 1996). Une fois exprimée, la cycline E s'associe avec Cdk2 pour compléter la phosphorylation des protéines Rb, ce qui les inactive de façon irréversible. Le complexe CycA – Cdk2 contribue à l'inactivation complète de Rb (Morgan, 1997). Cet événement rend les cellules indépendantes des stimuli externes et leur permet de franchir le point de restriction (Malumbres and Barbacid, 2001).

1.2.4.2 Les points de contrôle des dommages à l'ADN

L'un des principaux défis du cycle cellulaire est le maintien de l'intégrité génomique. Des mécanismes de surveillance arrêtent ainsi le cycle cellulaire pour permettre à la cellule de réparer son ADN lorsqu'il est endommagé. Variant d'une phase à l'autre, les points de contrôle des dommages à l'ADN impliquent néanmoins tous la kinase mutée du syndrome d'ataxie télangiectasie (ATM, de *ataxia telangiectasia mutated*), qui est recrutée aux sites de cassures double-brin.

1.2.4.2.1 En G1

Lorsque des dommages à l'ADN surviennent en G1, ATM est recrutée au site de cassure, d'où elle phosphoryle la kinase Checkpoint 2 (Chk2) (Matsuoka et al., 1998). ATM et Chk2 stabilisent le facteur de transcription p53, ce qui résulte en l'expression de différentes cibles transcriptionnelles, incluant l'inhibiteur des CDKs p21 (Harper et al., 1993; Harper et al., 1995; Siliciano et al., 1997). p21, qui fait partie de la famille Cip/Kip des CKIs, lie ensuite les complexes CycD – Cdk4/6 pour les inhiber et arrêter la progression du cycle cellulaire, empêchant ainsi la réplication de l'ADN endommagé (Ko and Prives, 1996). Comme cette réponse transcriptionnelle est relativement lente, des voies complémentaires plus rapides permettent d'empêcher la transition vers la phase S. ATM peut effectivement directement induire la dégradation protéasome-dépendante

de la cycline D en la phosphorylant (Choo et al., 2009; Hitomi et al., 2008). De façon similaire, la phosphorylation de la phosphatase Cdc25A par Chk2 mène à sa destruction protéolytique (Mailand et al., 2000). Cela empêche la déphosphorylation activatrice de Cdk2 et bloque l'entrée en phase S.

1.2.4.2.2 En phase S

La réponse aux dommages à l'ADN diffère en phase S, puisqu'elle peut additionnellement être déclenchée par des bris simple-brin (Shaltiel et al., 2015). Ceux-ci activent la kinase du syndrome d'ataxie télangiectasie liée à Rad3 (ATR, de *ataxia telangiectasia and Rad3-related* (Zou and Elledge, 2003). L'activité d'ATR, tout comme celle de son effecteur la kinase Checkpoint 1 (Chk1), est dépendante de Cdk2, ce qui empêche son activation avant la phase S (Myers et al., 2007; Xu et al., 2012). En phase S, ATR contribue avec ATM à stabiliser p53 via Chk1 et Chk2, mais l'accumulation subséquente de p21 est empêchée pendant la réplication de l'ADN pour éviter la ré-réplication (Abbas et al., 2008; Kim et al., 2008). Le point de contrôle de la phase S dépend plutôt de l'activation de Wee1 (Chow et al., 2003; O'Connell et al., 1997; Watanabe et al., 1995). Une fois phosphorylée par Chk1 et Chk2, Wee1 cible Cdk2 pour l'inactiver (Chow et al., 2003; O'Connell et al., 1997; Watanabe et al., 1995). Chk1 et Chk2 ciblent également Cdc25A pour qu'elle soit dégradée, ce qui accentue l'inhibition de Cdk2 et ralentit la phase S (Beck et al., 2010; Hughes et al., 2013).

1.2.4.2.3 En G2

Le point de contrôle en G2 implique ATM, mais dépend essentiellement d'ATR pour maintenir un arrêt stable (Brown and Baltimore, 2003; Liu et al., 2000; Rainey et al., 2008; Shibata et al., 2010; Takai et al., 2000). Les kinases effectrices Chk1 et Chk2 ciblent Wee1 et Cdc25A, Cdc25B et Cdc25C pour empêcher l'activation de Cdk2 et Cdk1 (Shaltiel et al., 2015). Il en résulte un arrêt avant l'entré en mitose. La stabilisation de p53 par les voies ATM-Chk2 et ATR-Chk1 mène aussi à l'inhibition de Cdk2 en G2, puisque p21 n'y est plus dégradé (Bunz et al., 1998). Enfin, ATM et ATR peuvent induire l'activation de la kinase p38, qui inhibe Cdc25A et Cdc25B (Reinhardt et al., 2007).

1.2.4.2.4 En phase M

La réponse aux dommages à l'ADN est atténuée en mitose, principalement grâce aux activités de la Polo-like kinase 1 (Plk1), qui empêche l'activation de Chk1 et Chk2, et de Cdk1, qui bloque le recrutement d'effecteurs aux sites de cassures ainsi que les mécanismes de réparation de l'ADN (Mailand et al., 2006; Orthwein et al., 2014; Terasawa et al., 2014; van Vugt et al., 2010).

1.2.4.3   Le point de contrôle du fuseau

Le point de contrôle du fuseau (SAC, de *spindle-assembly checkpoint*) assure la ségrégation correcte des chromatides sœurs en empêchant l'anaphase tant que tous les kinétochores ne sont pas i) attachés aux microtubules et ii) sous tension (Musacchio and Salmon, 2007). La transition de la métaphase vers l'anaphase requiert l'activité de l'APC/C^{Cdc20}, qui cible deux principaux substrats, la cycline B et la sécurine, pour mener à leur dégradation par le protéasome 26S (Funabiki et al., 1996; King et al., 1995; Sudakin et al., 1995). La dégradation de la cycline B cause l'inactivation de Cdk1, ce qui favorise la sortie de mitose (Peters, 2006). La protéolyse de la sécurine permet quant à elle de lever l'inhibition de sa cible, la protéase séparase (Ciosk et al., 1998; Cohen-Fix et al., 1996; Funabiki et al., 1996; Uhlmann et al., 1999). Il en résulte le clivage par la séparase des cohésines centromériques qui lient les chromatides sœurs, ce qui permet la ségrégation des chromosomes vers les deux pôles (Ciosk et al., 1998; Cohen-Fix et al., 1996; Funabiki et al., 1996; Uhlmann et al., 1999).

L'effecteur du SAC est un complexe protéique qui inhibe l'activité de l'APC/C^{Cdc20} : le complexe MCC (pour *Mitotic Checkpoint Complex*) (Sudakin et al., 2001). Celui-ci est composé des protéines BubR1, Bub3, Mad2 et Cdc20 qui s'assemblent aux kinétochores non-attachés (Alfieri et al., 2016; Chao et al., 2012; Fang et al., 1998; Hardwick et al., 2000; Izawa and Pines, 2015; Sudakin et al., 2001). Le complexe MCC lie l'APC/C qui est déjà en complexe avec son co-activateur Cdc20 (Izawa and Pines, 2015; Primorac and Musacchio, 2013). Le MCC inhibe l'activité de l'APC/C^{Cdc20} en l'empêchant de reconnaître les motifs de dégradation des substrats, en changeant la conformation de son site catalytique et en bloquant la synthèse de chaînes

d'ubiquitine (Alfieri et al., 2016; Herzog et al., 2009; Yamaguchi et al., 2016). Les kinases Plk1 et Aurora B contribuent également au SAC en déstabilisant les microtubules incorrectement attachés aux kinétochores (Ahonen et al., 2005; Lampson et al., 2004; Pinsky et al., 2006; Salimian et al., 2011). Lorsque les kinétochores sont correctement attachés et sous tension, le MCC se désassemble et les phosphorylations inhibitrices sont contrées par des phosphatases des familles PP1 et PP2A (Emanuele et al., 2008; Foley et al., 2011; Posch et al., 2010; Suijkerbuijk et al., 2012). L'APC/C^{Cdc20} peut alors induire la dégradation de la cycline B et de la sécurine, permettant la ségrégation des chromosomes et la sortie de mitose.

1.3 Régulation de la mitose par phosphorylation réversible

Comme la transcription et la traduction sont réprimées lorsque les cellules entrent en phase M, ce sont principalement les modifications post-traductionnelles qui orchestrent la mitose (Prescott and Bender, 1962; Tanenbaum et al., 2015; Taylor, 1960). La phosphorylation joue notamment un rôle crucial : on rapporte plus de 32 000 événements de phosphorylation sur plus de 5000 protéines pendant la mitose (Olsen et al., 2010; Sharma et al., 2014). Pour compléter leur division, les cellules doivent se départir de ces phosphorylations. Tel qu'abordé précédemment, l'APC/C dirige la protéolyse de la cycline B et de la sécurine pour initier la sortie de mitose (Funabiki et al., 1996; King et al., 1995; Sudakin et al., 2001). L'inactivation de Cdk1 résultant de la dégradation de la cycline B empêche le renouvellement des événements de phosphorylations. Compte tenu de la très grande stabilité des phosphorylations, des mécanismes dynamiques comme la protéolyse et la déphosphorylation sont nécessaires pour les retirer (Lad et al., 2003). Outre la cycline B et la sécurine, il n'y a toutefois qu'une faible proportion des protéines qui sont dégradées en sortie de mitose (environ 2,5% chez l'humain, entre 10 et 20% chez la levure) (Kuilman et al., 2015; Min et al., 2014). C'est donc la déphosphorylation qui constitue le principal mécanisme permettant de renverser les événements de phosphorylation et de sortir de mitose (Holder et al., 2020). La déphosphorylation des substrats mitotiques doit se dérouler dans un ordre précis, et différent de celui de leur phosphorylation en entrée de mitose,

pour que les événements de la sortie de mitose aboutissent correctement à la formation de deux cellules-filles (Bouchoux and Uhlmann, 2011; Sullivan and Morgan, 2007). L'incapacité à respecter scrupuleusement cet enchaînement ordonné entraîne l'échec de la mitose (Burgess et al., 2010; McCloy et al., 2014).

1.3.1 Kinases mitotiques

Les complexes cycline A/B – Cdk1 provoquent les principaux événements associés à l'entrée en mitose en phosphorylant de nombreux substrats comme les condensines, les lamines nucléaires et des protéines liant les microtubules (Andersen, 1999; Kimura et al., 1998; Lowe et al., 1998; Nigg, 1995). Il en résulte notamment la condensation des chromosomes, le bris de l'enveloppe nucléaire et la formation du fuseau mitotique (Andersen, 1999; Kimura et al., 1998; Lowe et al., 1998; Nigg, 1995). Les complexes cycline – Cdk1 sont requis jusqu'à la métaphase; l'activation de l'APC/C, à laquelle contribue Cdk1, entraîne la dégradation des cyclines et l'inactivation de Cdk1 qui sont nécessaires à la sortie de mitose.

Malgré son rôle de premier plan, Cdk1 n'est pas la seule kinase nécessaire au bon déroulement de la mitose (Kettenbach et al., 2011). Deux autres kinases ciblant les sérines et les thréonines ont été initialement identifiées chez *Drosophila melanogaster* comme étant essentielles à la formation d'un fuseau mitotique bipolaire : les kinases Polo et Aurora (Glover et al., 1995; Llamazares et al., 1991; Sunkel and Glover, 1988). Elles sont toutes deux fortement conservées évolutivement, des levures aux mammifères (Brown et al., 2004; de Carcer et al., 2011). Leurs homologues forment les familles des kinases Aurora et Plks (*Polo-like kinases*) (Bischoff et al., 1998; Golsteyn et al., 1994; Holtrich et al., 1994; Sen et al., 1997). Enfin, une quatrième famille, celle des kinases Neks (pour *NIMA-related kinases*), est impliquée en mitose (O'Connell et al., 2003). « Never in mitosis A » (NIMA) a d'abord été identifié chez le champignon *Aspergillus nidulans* comme étant requise pour la transition G2/M (Osmani et al., 1991; Osmani et al., 1988).

Deux kinases similaires de la famille des Aurora, Aurora A et Aurora B, jouent des rôles importants en mitose chez les métazoaires (Nigg, 2001). Aurora A est

essentielle à la maturation et à la séparation des centrosomes, à la transition G2/M et à la formation d'un fuseau bipolaire (Barr and Gergely, 2007; Berdnik and Knoblich, 2002; Hannak et al., 2001; Lindqvist et al., 2009; Nigg, 2001; Palazzo et al., 2000). Aurora B fait partie du complexe passager des chromosomes (CPC, de *chromosomal passenger complex*). Elle est importante pour la cohésion des chromatides sœurs, l'attachement des microtubules aux kinétochores, la régulation du SAC et la cytocinèse (Carmena et al., 2012b; van der Horst and Lens, 2014). Par ailleurs, Aurora A et Aurora B agissent toutes deux comme activatrices de Plk1 (Carmena et al., 2012b; Joukov et al., 2014; Kachaner et al., 2014; Macurek et al., 2008; Seki et al., 2008; Shao et al., 2015).

Des cinq Plks présentes chez les mammifères, seule Plk1 est active en phase M. Elle contribue à la maturation des centrosomes, à l'activation de cycline B – Cdk1, à la formation d'un fuseau bipolaire, à la ségrégation des chromosomes et à la formation du sillon de clivage pendant la cytocinèse (Descombes and Nigg, 1998; Lane and Nigg, 1996; Ohkura et al., 1995; Roshak et al., 2000; Toyoshima-Morimoto et al., 2001).

Parmi les 13 Neks identifiées chez l'humain, Nek2 est l'homologue structurelle et fonctionnelle de NIMA (Schmit and Ahmad, 2007). Elle contribue à la séparation des centrosomes, à la stabilisation du fuseau mitotique et à la régulation du SAC (Faragher and Fry, 2003; Fry et al., 1998; Fu et al., 2007; Jeong et al., 2007; Lou et al., 2004; Sonn et al., 2009; Wei et al., 2011).

1.3.2 Phosphatases mitotiques

Il a longtemps été considéré que les substrats mitotiques étaient déphosphorylés suite à l'inactivation des kinases mitotiques, par des phosphatases constitutivement actives (Trinkle-Mulcahy and Lamond, 2006). Cela peut expliquer le faible intérêt accordé jusqu'à récemment à l'étude des phosphatases mitotiques. Or, la déphosphorylation des substrats mitotiques ne se produit pas nécessairement au moment de l'inactivation des kinases mitotiques (Sullivan and Morgan, 2007). Par ailleurs, l'activité des phosphatases mitotiques s'est avérée, tout comme celle des kinases, finement régulée (Mochida and Hunt, 2007; Skoufias et al., 2007). De fait, la déphosphorylation des substrats mitotiques nécessaire à la sortie de mitose est un

processus ordonné qui est orchestré par différentes phosphatases (Bouchoux and Uhlmann, 2011; Holder et al., 2020; Sullivan and Morgan, 2007). Parmi les principales phosphatases impliquées dans la sortie de mitose, deux sous-familles font partie de la grande famille des phosphoprotéines phosphatases (PPPs) : les protéines phosphatases 1 (PP1) et les protéines phosphatases 2A (PP2A), qui sont des complexes multimériques (Booher and Beach, 1989; Chen et al., 2007; Doonan and Morris, 1989; Mayer-Jaekel et al., 1993). À celles-ci s'ajoute la phosphatase Fcp1 (pour *Factor 2F-associating C-terminal domain phosphatase 1*), également requise pour la complétion de la mitose (Visconti et al., 2012). Les phosphatases PP1, PP2A et Fcp1 collaborent ensemble pour permettre la sortie de mitose. Ce relais entre les phosphatases sera abordé en section 1.4.4.2. En plus de cibler les substrats des kinases mitotiques, les phosphatases mitotiques participent à la régulation de l'activité de ces mêmes kinases. PP1, par exemple, déphosphoryle directement Plk1 et Aurora B dans leurs boucles d'activation pour réguler négativement leur activité (Macurek et al., 2008; Posch et al., 2010; Seki et al., 2008; Yamashiro et al., 2008). Chez la levure bourgeonnante, la phosphatase responsable de la sortie de mitose est Cdc14, mais cette fonction ne semble pas conservée chez les animaux (Berdougo et al., 2008; Mocciaro et al., 2010; Stegmeier and Amon, 2004).

L'action concertée des phosphatases mitotiques permet donc de renverser dans un ordre précis la phosphorylation des substrats mitotiques. Pour que la séquence d'événements se déroule correctement, une combinaison de mécanismes agissent comme « horloges » et comme « règles » moléculaires (Figure 1.4) (Vagnarelli, 2021).

Le modèle des horloges réfère à la régulation basée sur le temps : les caractéristiques biochimiques des substrats de même que la réactivation coordonnée de leur phosphatase contrôlent temporellement leur déphosphorylation. Le modèle des règles suggère plutôt que des senseurs locaux coordonnent la déphosphorylation des substrats en fonction de leur position dans la cellule. Il est proposé que les deux modèles ne fonctionnent pas de façon indépendante, mais qu'ils s'influencent mutuellement, permettant d'intégrer des signaux temporels et spatiaux (Vagnarelli, 2021).
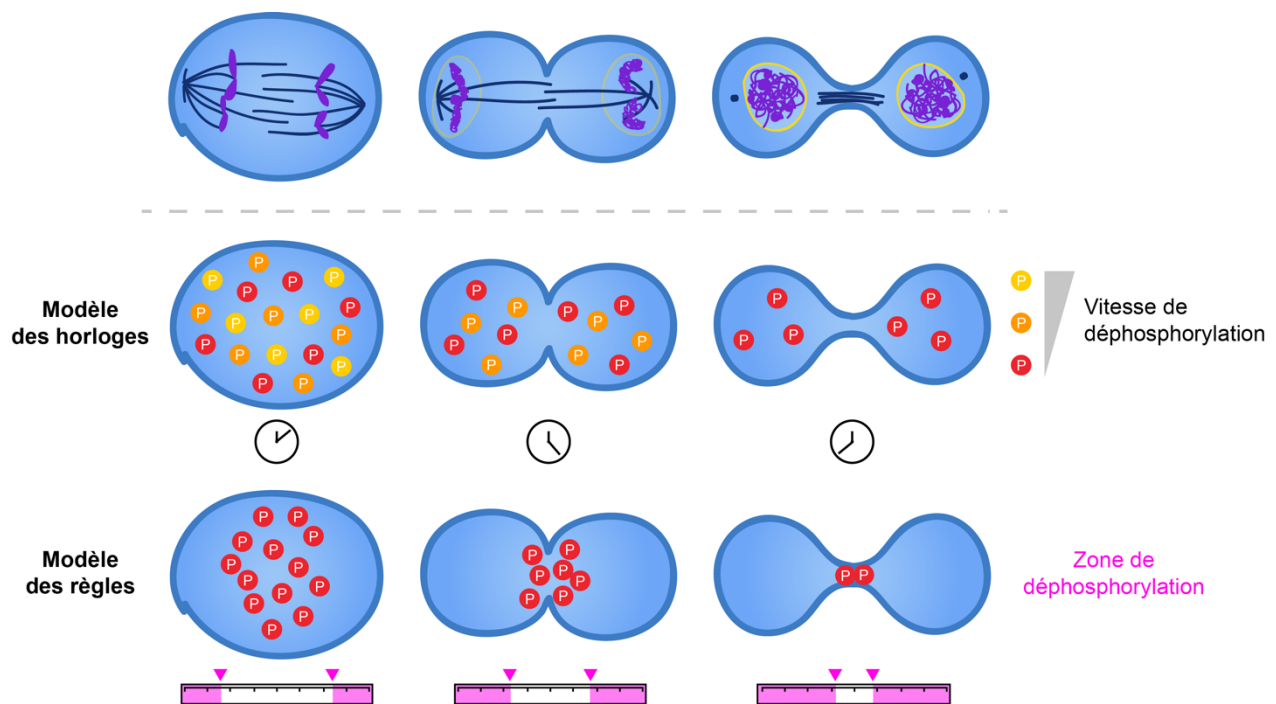
Figure 1.4. Modèles de régulation de la sortie de mitose par déphosphorylation.

Le modèle des horloges propose que la réactivation ordonnée des phosphatases et leur affinité pour leurs substrats coordonnent la sortie de mitose par des événements de déphosphorylation contrôlés temporellement. Le modèle des règles propose plutôt des événements de déphosphorylation contrôlés par la spatialité des activités enzymatiques et des substrats. Inspiré de (Vagnarelli, 2021).

1.3.3 Régulation spatiotemporelle des régulateurs mitotiques

La régulation de la mitose par phosphorylation est souvent décrite comme une vague de phosphorylation en entrée de mitose, concomitante avec l'activation des kinases et l'inactivation des phosphatases mitotiques, suivie d'une vague de déphosphorylation lorsque les activités enzymatiques sont inversées en sortie de mitose. La phosphorégulation de la mitose est toutefois plus complexe; elle nécessite la coordination dynamique d'activités kinases et phosphatases s'opposant dans le temps et l'espace cellulaires tout au long de la mitose. Différents mécanismes, comme la translocation d'un compartiment cellulaire à un autre ou le recrutement à des structures cellulaires spécifiques, permettent d'amplifier localement l'activité des kinases et phosphatases mitotiques ou, à l'inverse, de séquestrer leur activité pour protéger certains substrats.

À titre d'exemple, le complexe cycline B – Cdk1 est principalement cytoplasmique en interphase, mais il se relocalise au noyau lors de son activation en début de phase M (Gavet and Pines, 2010a; Gavet and Pines, 2010b; Pines and Hunter, 1991; Santos et al., 2012). Chez la drosophile, Polo passe elle aussi du cytoplasme au noyau en fin de G2 (Kachaner et al., 2017). Sa translocation nucléaire lui permet d'activer la phosphatase Cdc25, contribuant ainsi à l'activation de Cdk1 et à la transition G2/M (Kachaner et al., 2017). Polo/Plk1 est également recrutée aux centromères, aux centrosomes et au fuseau central pendant la mitose, de même qu'au corps central lors de la cytocinèse (Bruinsma et al., 2012; Carmena et al., 2012a; Glover, 2005; Kang et al., 2006; Moutinho-Santos et al., 1999). De façon similaire, l'association d'Aurora A avec différents co-facteurs dicte sa localisation aux centrosomes et aux microtubules du fuseau mitotique (Asteriti et al., 2015; Barr and Gergely, 2007; Carmena and Earnshaw, 2003). Aurora B, qui fait partie du complexe passager des chromosomes, passe quant à elle successivement des centromères, au fuseau central puis au cortex cellulaire (Carmena and Earnshaw, 2003; Schumacher et al., 1998). Tout comme Plk1, elle se localise au corps central pendant la cytocinèse (Carmena and Earnshaw, 2003; Schumacher et al., 1998).

Les phosphatases mitotiques sont elles aussi soumises à une régulation spatiale. De fait, PP1 et PP2A sont recrutés à différentes structures cellulaires par leurs sous-unités régulatrices associées. Une population de PP2A est ainsi enrichie aux kinétochores, alors qu'une autre se localise plutôt au fuseau mitotique (Espert et al., 2014; Torres et al., 2010). De même, PP1 peut être ciblée au cortex cellulaire, à la chromatine ou encore à l'enveloppe nucléaire (Fisher et al., 2014; Kunda et al., 2012; Steen et al., 2003). En somme, le recrutement des enzymes mitotiques dans des compartiments spécifiques ou à des structures particulières ajoute un niveau supplémentaire à la régulation de leurs activités pendant la mitose.

1.4 Le module Greatwall – endosulfines – PP2A

L'une des principales phosphatases ciblant les substrats phosphorylés de Cdk1 est PP2A en complexe avec sa sous-unité B55 (Ferrigno et al., 1993; Mayer-Jaekel et al., 1993; Mochida et al., 2009). Haute en interphase, son activité catalytique est inhibée en entrée de mitose (Mochida et al., 2009). La kinase Greatwall (Gwl), via ses cibles les endosulfines, est responsable de cette inhibition (Figure 1.5) (Castilho et al., 2009; Gharbi-Ayachi et al., 2010; Mochida et al., 2010; Rangone et al., 2011; Vigneron et al., 2009; Wang et al., 2011; Yu et al., 2004). L'action inhibitrice de Gwl est levée lorsque s'amorce la sortie de mitose, ce qui permet à PP2A-B55 de retrouver son activité et de contribuer à la déphosphorylation des substrats mitotiques de Cdk1. Les prochaines sections traiteront de façon détaillée des trois acteurs clés de l'axe Greatwall – endosulfines – PP2A.
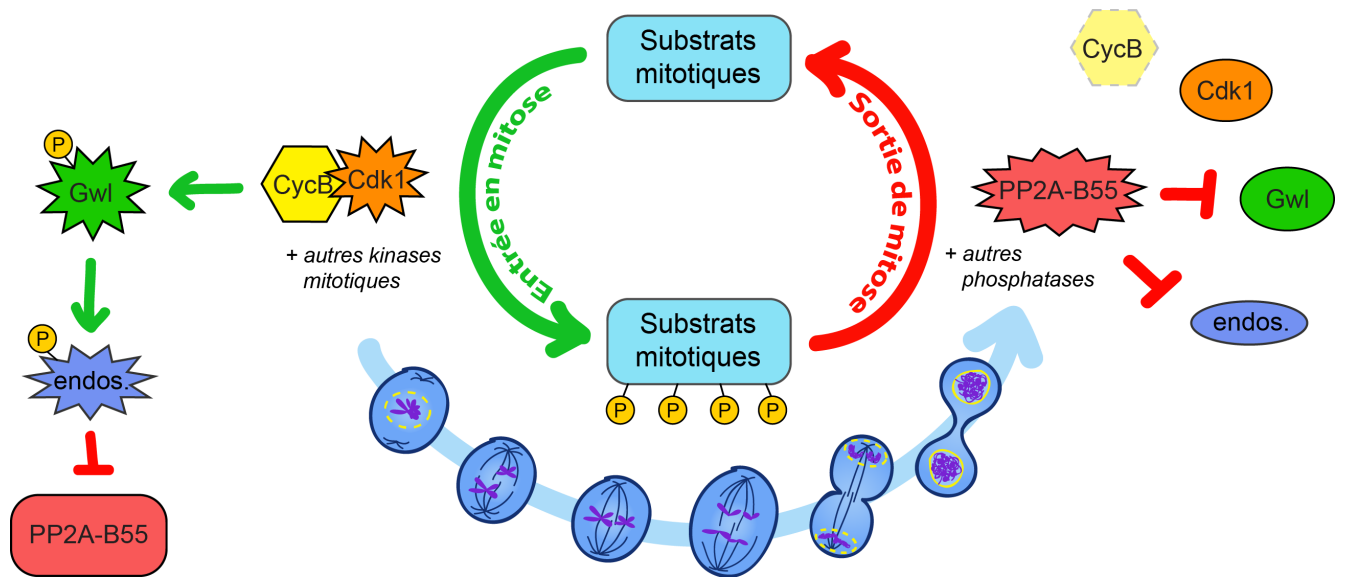
Figure 1.5. Le module Greatwall – endosulfines – PP2A pendant la mitose.

L'activité du complexe cycline B – Cdk1 et d'autres kinases mitotiques, déclenche les transformations cellulaires requises pour la progression mitotique. Les phosphatases mitotiques, dont PP2A-B55, cible les substrats mitotiques phosphorylés en sortie de mitose pour permettre aux cellules de compléter leur division. L'activation de la kinase Greatwall (Gwl), initiée par Cdk1, mène à la phosphorylation des endosulfines (endos.), qui peuvent alors lier et inhiber PP2A-B55. Cet événement est requis pour protéger l'état phosphorylé des substrats mitotiques. Suite à la dégradation de la cycline B par l'APC/C^{Cdc20}, Cdk1 est inhibée, Gwl et les endosulfines sont déphosphorylées et PP2A-B55 retrouve son activité. PP2A-B55 contribue elle-même à l'inactivation complète de Gwl et des endosulfines.

1.4.1 PP2A-B55 : une enzyme phosphatase trimérique requise pour la complétion de la mitose

1.4.1.1 Structure et formation du complexe PP2A

Les phosphatases PP2A sont des métalloenzymes ciblant les sérines et thréonines phosphorylées. Elles sont constituées d'un dimère central, composé d'une sous-unité structurale (A) et d'une sous-unité catalytique (C), auquel peut s'associer une sous-unité régulatrice (B) (Figure 1.6A). Il existe plusieurs isoformes des différentes sous-unités, encodées par des gènes distincts ou issues de l'épissage alternatif d'un même gène (Janssens and Goris, 2001). Cette diversité permet l'assemblage d'une

grande variété d'hétérotrimères différents; on estime à une centaine le nombre de combinaisons possibles chez certaines espèces (Nasa and Kettenbach, 2018).

A

Sous-unité
structurale (A)

Sous-unité
régulatrice (B55)

Sous-unité
catalytique (C)

B

Cavité de liaison
des substrats

C

Potentiel électrostatique
négatif

Potentiel électrostatique
positif
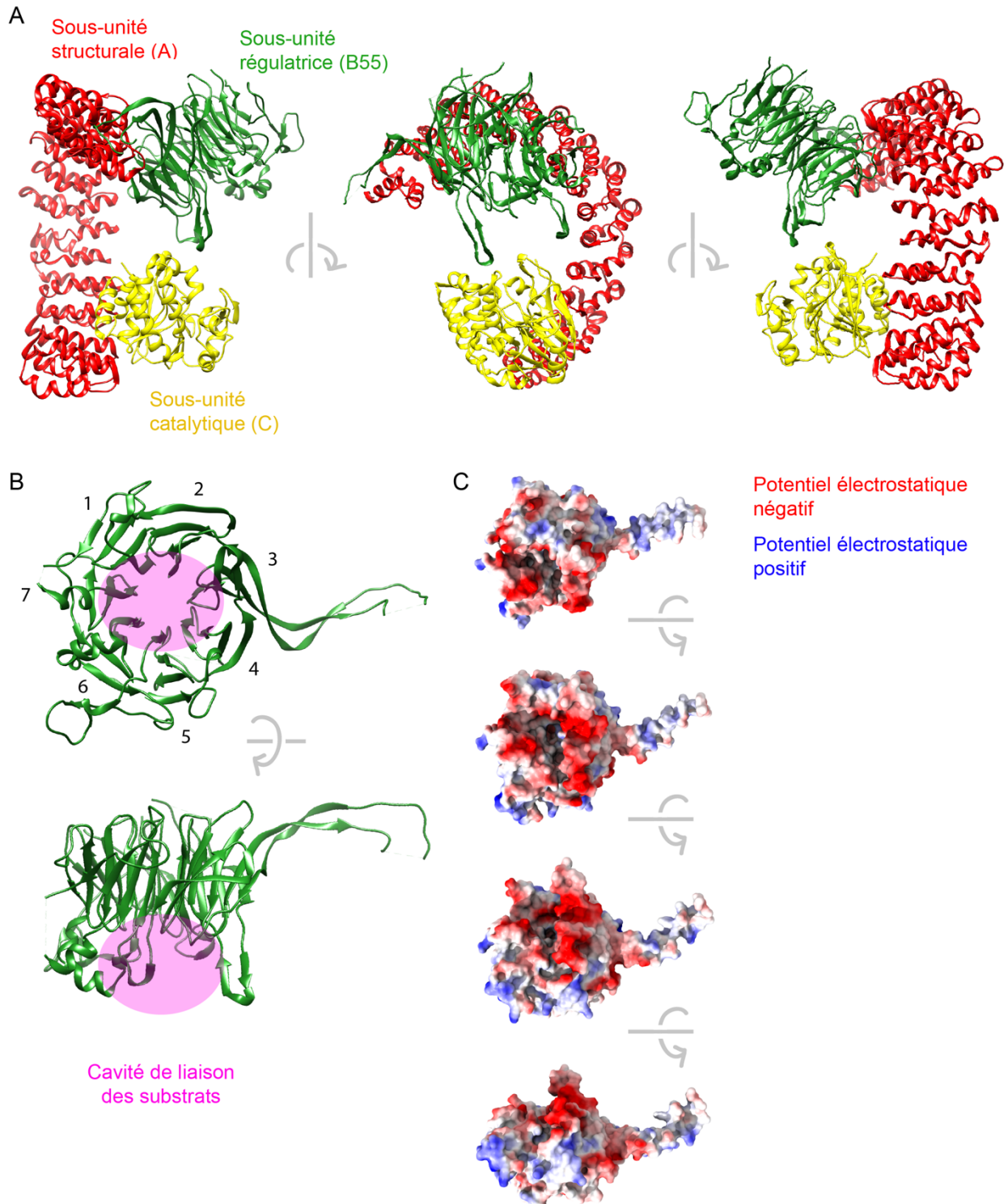
Figure 1.6. Structure du complexe PP2A-B55.

(A) PP2A-B55 est composée d'une sous-unité structurale A (en rouge) qui lie la sous-unité catalytique C (en jaune) et la sous-unité régulatrice B55 (en vert). Structure montrant PP2A-B55α en complexe avec la microcystine-LR (numéro d'accession Protein Data Bank : 3DW8) (Xu et al., 2008). (B) Structure en « β-propeller » à sept lames WD40 de la sous-unité B55. La cavité de liaison des substrats est indiquée en rose. (C) La cavité de liaison des substrats de la sous-unité B55 a une surface fortement acide. Les potentiels électrostatiques négatifs apparaissent en rouge; les positifs, en bleu. Rendu des structures effectué avec Chimera 1.11 (Pettersen et al., 2004) et ChimeraX (Pettersen et al., 2021) de l'University of California, San Francisco.

Chez les mammifères, on trouve deux isoformes différentes de la sous-unité catalytique (C), toutes deux exprimées de façon ubiquitaire (Arino et al., 1988; Green et al., 1987; Jones et al., 1993; Khew-Goodall et al., 1991; Stone et al., 1987). Bien que codée par deux gènes distincts, leur séquence primaire est néanmoins identique à 97% (Arino et al., 1988; Green et al., 1987; Jones et al., 1993; Khew-Goodall et al., 1991; Stone et al., 1987). La sous-unité catalytique de PP2A est effectivement l'une des enzymes les mieux conservées dans l'évolution, de la levure à l'humain (Arino et al., 1993; Cohen et al., 1990; Cormier et al., 1991; Kinoshita et al., 1990; MacKintosh et al., 1990; Orgad et al., 1990; Van Hoof et al., 1995). Malgré leur grande similarité, les deux isoformes de la sous-unité catalytique ne sont pas complètement redondantes (Gotz et al., 1998; Gu et al., 2012). La sous-unité catalytique adopte le repliement α/β qui est typique des phosphoprotéines phosphatases (PPPs) ciblant les sérines et les thréonines (Barford, 1996). Le site catalytique de la sous-unité C contient deux ions de manganèse qui sont cruciaux à la réaction de déphosphorylation des substrats (Barford et al., 1998).

La sous-unité structurale (A) se présente également en deux isoformes encodées par des gènes exprimés de façon ubiquitaire chez les mammifères (Hemmings et al., 1990). Les deux isoformes partagent 86% d'identité de séquence (Hemmings et al., 1990). La sous-unité structurale est composée de 15 motifs de 39 acides aminés répétés en tandem, nommés motifs HEAT (parce que présents chez les protéines huntingtin, elongation factor, sous-unité A de PP2A et target of rapamycin) (Hemmings et al., 1990; Walter et al., 1989). Chaque motif HEAT forme deux hélices-α.

Globalement, la sous-unité structurale a une architecture en forme de C (Groves et al., 1999).

Le génome humain contient 16 gènes codant des sous-unités régulatrices (B) de PP2A (Seshacharyulu et al., 2013). Celles-ci sont regroupées en quatre familles : B55 (PR55/B), B56 (PR61/B'), B72 (PR72/B'') et Striatin (PR93/B''') (Seshacharyulu et al., 2013). Contrairement aux sous-unités A et C, il n'y a pas de similarité de séquence entre les sous-unités B des différentes familles. Comme ce sont les sous-unités régulatrices qui déterminent la spécificité de PP2A, leur diversité permet de cibler une multitude de substrats (Agostinis et al., 1992; Agostinis et al., 1990; Agostinis et al., 1987; Imaoka et al., 1983; Mayer-Jaekel et al., 1994; Ogris et al., 1997). Les sous-unités B55 et B56 sont les plus impliquées en mitose; B56 est principalement importante jusqu'à la métaphase, alors que B55 joue des rôles de premier plan pour la sortie de mitose (Foley et al., 2011; Funabiki and Wynne, 2013).

La sous-unité B55 (dont le nom vient de sa masse de 55 kDa) est encodée par quatre gènes chez les mammifères, qui sont exprimés de façon spécifique dans certains tissus (Healy et al., 1991; Mayer et al., 1991; Strack et al., 1999; Strack et al., 1998; Zolnierowicz et al., 1994). B55α et B55δ sont exprimées de façon ubiquitaire, alors que l'expression de B55β et B55γ est restreinte aux cellules du cerveau (Healy et al., 1991; Mayer et al., 1991; Strack et al., 1999; Strack et al., 1998; Zolnierowicz et al., 1994). Les sous-unités B55 contiennent sept motifs WD40, une séquence de 40 acides aminés se terminant par un tryptophane et un acide aspartique (Neer et al., 1994; Xu et al., 2008). Chaque motif WD40 forme une « lame » de 4 feuillets-β antiparallèles, donnant une structure globale de « β-propeller » à sept lames aux sous-unités B55 (Figure 1.6B) (Wall et al., 1995; Xu et al., 2008). Les motifs WD40 permettent des interactions protéine-protéine (Neer et al., 1994). Deux boucles en épingle β et deux hélices-α s'ajoutent à cette structure centrale et contribuent à former la cavité de liaison des substrats (Xu et al., 2008). La surface de cette cavité est fortement acide (Figure 1.6C) (Xu et al., 2008).

Le complexe PP2A est minimalement composé d'un dimère des sous-unités structurale et catalytique, dimère auquel peut s'associer une sous-unité régulatrice (Cayla et al., 1990; Kremmer et al., 1997). La sous-unité catalytique interagit avec les motifs HEAT 11 à 15 de la sous-unité structurale pour former le dimère (Xing et al., 2006). Le tiers des complexes PP2A sont sous forme dimérique (Kremmer et al., 1997).

L'association des sous-unités régulatrices au dimère A/C est mutuellement exclusive et, de par la grande diversité de sous-unités B disponibles, donne aux complexes PP2A un grand nombre de spécificités de substrats (Mayer-Jaekel et al., 1994). Les sous-unités B55 lient le dimère A/C via les motifs HEAT 1 à 7 de la sous-unité structurale (Xu et al., 2008). Cette dernière sert donc d'échafaudage, orientant la cavité de liaison des substrats de B55 face au site catalytique de la sous-unité C (Xu et al., 2008).

L'association de B55 au dimère A/C est influencée par différentes modifications post-traductionnelles. La carboxyméthylation de la leucine 309 du motif TPDYFL de la sous-unité catalytique, motif conservé de la levure à l'humain, est requise pour le recrutement de B55 *in vivo* (Bryant et al., 1999; Evans and Hemmings, 2000; Gentry et al., 2005; Lee and Stock, 1993; Ogris et al., 1997; Tolstykh et al., 2000; Wei et al., 2001; Wu et al., 2000; Xie and Clarke, 1993; Xie and Clarke, 1994; Yu et al., 2001). La phosphorylation de la thréonine 304 et de la tyrosine 307 du motif a l'effet inverse, empêchant la liaison de B55 (Longin et al., 2007). Par ailleurs, un site de phosphorylation dépendant de Cdk1 a été identifié sur B55α; la phosphorylation de la sérine 167 de B55α empêche sa liaison au dimère A/C (Schmitz et al., 2010). La formation de complexes PP2A-B55 pourrait donc être régulée au cours du cycle cellulaire via différentes modifications post-traductionnelles.

1.4.1.2 L'implication de PP2A-B55 en mitose

Ce sont des expériences *in vitro* et dans des extraits de *Xenopus laevis* qui ont initialement permis d'attribuer l'activité phosphatase anti-Cdk1 à PP2A (Agostinis et al., 1992; Ferrigno et al., 1993). En parallèle, des expériences génétiques menées chez *Drosophila melanogaster* ont mis en lumière l'importance fonctionnelle de la sous-unité

B55/PR55 de PP2A (Gomes et al., 1993; Mayer-Jaekel et al., 1993; Uemura et al., 1993). Le nom de *twins* (*tws*) a été attribué au gène codant la sous-unité de 55 kDa de PP2A chez la drosophile puisque sa mutation cause la duplication symétrique d'une partie du disque imaginal de l'aile, structure à partir de laquelle l'aile est formée (Uemura et al., 1993). Des défauts de condensation et de ségrégation des chromosomes pendant l'anaphase ont également été observés dans les neuroblastes en division des larves mutantes (Gomes et al., 1993; Mayer-Jaekel et al., 1993). La mutation de *twins* est létale, stoppant le développement des mouches au stade de pupes (Gomes et al., 1993). Un an plus tard, toujours chez la mouche, il est montré que la mutation de *twins* diminue fortement l'activité phosphatase de PP2A envers des substrats de Cdk1; suggérant que les défauts mitotiques observés résultent de l'absence de déphosphorylation de substrats de Cdk1 par PP2A-Tws (Mayer-Jaekel et al., 1994). Enfin, différentes expériences biochimiques dans des extraits de xénope ont révélé que l'activité phosphatase anti-Cdk1 de PP2A-B55 est cyclique : haute en interphase et basse en phase M (Mochida and Hunt, 2007; Mochida et al., 2009). De plus, l'activité de PP2A-B55 est requise pour la sortie de mitose (Manchado et al., 2010; Mochida et al., 2009). Ces résultats suggèrent une régulation précise de l'activité de PP2A-B55 au cours du cycle cellulaire.

1.4.2 La kinase Greatwall

1.4.2.1 Identification

Différentes expériences génétiques menées chez *Drosophila melanogaster* ont permis d'identifier Greatwall comme étant une importante kinase mitotique. En 1996, un premier allèle mutant, *Scant*, a été identifié dans un crible pour identifier des gènes mitotiques (White-Cooper et al., 1996). *Scant*, pour <u>*Sc*</u>ott of the <u>*Ant*</u>arctic, est un allèle dominant gain-de-fonction qui tient son nom du phénotype ayant permis sa découverte : des fuseaux mitotiques dont l'un des centrosomes se détache du pôle dans l'embryon syncytial, causant des mitoses défectueuses puis la mort des embryons (White-Cooper et al., 1996). Quelques années plus tard, un allèle récessif ralentissant la transition G2/M et causant des défauts de condensation des chromosomes fut identifié (Yu et al.,

2004). Le nom *greatwall* (*gwl*) fut attribué au gène impliqué, puisqu'il semblait protéger la structure des chromosomes mitotiques (Yu et al., 2004). À la même époque, Greatwall était identifiée dans un crible pour identifier des kinases mitotiques dans des cellules en culture de drosophile (Bettencourt-Dias et al., 2004). Sa déplétion affecte la morphologie du fuseau mitotique ainsi que la congression et la ségrégation des chromosomes (Bettencourt-Dias et al., 2004). Ce n'est que quelques années plus tard que le lien entre *Scant* et *gwl* est établi : *Scant* est en fait un allèle de *gwl* qui introduit une mutation ponctuelle rendant Gwl constitutivement active (Archambault et al., 2007). Cette même étude a aussi mis en lumière les contributions méiotiques de Gwl par l'analyse d'un mutant perte de fonction spécifique à la lignée germinale femelle (Archambault et al., 2007). En absence de Gwl, les ovocytes présentent des chromatides anormalement séparées sur des fuseaux allongés en méiose I (Archambault et al., 2007). Enfin, le premier article publié par notre groupe de recherche a permis de montrer que Gwl s'oppose à PP2A-Tws en mitose et en méiose chez la drosophile (Wang et al., 2011).

D'importantes avancées ont été faites en parallèle par des expériences biochimiques dans des extraits de xénope. Il a d'abord été déterminé que Gwl est activée en phase M, probablement par Cdk1 (Yu et al., 2006). La perte de Gwl empêche l'entrée en phase M; un phénotype renversé par l'inhibition des phosphatases PP1 et PP2A, ce qui suggère que Gwl participe à la boucle d'activation de Cdk1 en contrant une phosphatase inhibitrice (Yu et al., 2006). La perte de Gwl provoque également la sortie de mitose en induisant la déphosphorylation des substrats mitotiques, et ce même en présence de Cdk1 actif (Vigneron et al., 2009). Cette déphosphorylation est dépendante de PP2A-B55 et cible les substrats de Cdk1 (Castilho et al., 2009; Vigneron et al., 2009). Ces expériences contribuèrent à identifier la double fonction de l'inhibition de PP2A-B55 par Gwl en mitose : favoriser l'activation de Cdk1 et empêcher la déphosphorylation des substrats mitotiques de Cdk1 (Goldberg, 2010). En absence de Gwl, l'incapacité à inhiber PP2A-B55 résulte en la déphosphorylation trop rapide des substrats de Cdk1 et à l'échec de la mitose (Alvarez-Fernandez et al., 2013; Burgess et al., 2010; Manchado et al., 2010; Voets and Wolthuis, 2010).

1.4.2.2 Régulation de l'activité kinase de Gwl

Gwl fait partie de la famille des kinases AGC (Yu et al., 2004). Elle se distingue des autres kinases de cette famille par la présence d'une longue région centrale non conservée qui sépare son domaine kinase en deux (Figure 1.7A) (Yu et al., 2004). Contrairement au domaine kinase, la séquence de la région centrale de Gwl est peu conservée entre les espèces et n'est pas essentielle à l'activité kinase de Gwl (Blake-Hodek et al., 2012; Vigneron et al., 2011). L'activité de Gwl est basse en interphase, elle augmente subitement en entrée de mitose et diminue lorsque s'enclenche la sortie de mitose (Hara et al., 2012; Yu et al., 2006). Cycline B – Cdk1 initie l'activation de Gwl en phosphorylant deux sites de la boucle T de son domaine kinase (Thr193 et Thr206 chez *Xenopus lavelis*, correspondant à Thr194 et Thr207 chez l'humain et à Ser220 et Thr227 chez *Drosophila melanogaster*) (Figure 1.7B) (Blake-Hodek et al., 2012). L'activation partielle de Gwl entraîne un changement conformationnel qui permet son auto-phosphorylation sur sa queue C-terminale (SerS883 chez *Xenopus laevis*, Ser875 chez l'humain et Ser840 chez *Drosophila melanogaster*) résultant en sa pleine activation (Blake-Hodek et al., 2012).

A
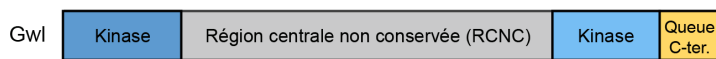
B
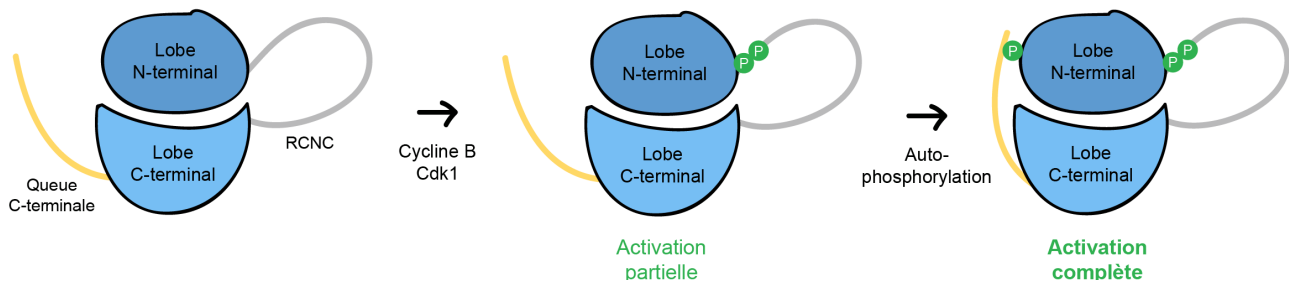
Figure 1.7. Structure et activation de la kinase Greatwall.

(A) La séquence de Greatwall (Gwl) est caractérisée par un domaine kinase scindé par une longue région centrale dont la séquence n'est pas bien conservée. (B) L'activation de Gwl se fait en deux étapes : cycline B – Cdk1 phosphoryle deux sites positionnés dans la boucle T de son domaine kinase (représentée en gris) pour initier un changement conformationnel qui permet à Gwl de s'auto-phosphoryler sur un site de sa queue C-terminale (représentée en jaune).

1.4.2.3 Régulation de la localisation de Gwl en entrée de mitose

En plus d'être régulée au niveau de son activité kinase, Gwl est également soumise à une régulation spatiotemporelle. La région centrale désordonnée de Gwl contient au moins un signal de localisation nucléaire (NLS, pour *Nuclear Localization Signal*) chez le xénope et les mammifères alors qu'elle en contient deux chez la drosophile (Alvarez-Fernandez et al., 2013; Wang et al., 2013; Yamamoto et al., 2014). D'un à trois signaux d'export nucléaire (NES, pour *Nuclear Export Signal*) sont également présents dans la région centrale de Gwl (Alvarez-Fernandez et al., 2013; Wang et al., 2016). La liaison des importines-α et β aux NLS de Gwl l'envoie au noyau en interphase (Yamamoto et al., 2014; Yu et al., 2004). Cycline B – Cdk1 s'accumule au noyau en s'activant, ce qui lui permet d'y phosphoryler Gwl. En plus d'initier son activation, cycline B – Cdk1 promeut l'export nucléaire de Gwl en phosphorylant des sites adjacents à son NLS (Wang et al., 2016). Chez la drosophile, des sites additionnels sont ciblés par Polo (Wang et al., 2013). L'inactivation des NLSs cause la translocation de Gwl du noyau vers le cytoplasme en prophase, avant le bris de l'enveloppe nucléaire (Alvarez-Fernandez et al., 2013; Wang et al., 2013; Yamamoto et al., 2014). L'export nucléaire de Gwl est médié par l'exportine-1 (CRM1) chez la drosophile et chez l'humain, et par les importines chez le xénope (Alvarez-Fernandez et al., 2013; Wang et al., 2016; Yamamoto et al., 2014). Perturber l'export nucléaire de Gwl en prophase entraîne des défauts mitotiques semblables à ceux observés suite à la perte de Gwl (Alvarez-Fernandez et al., 2013; Wang et al., 2013). Il est suggéré que l'export de Gwl permet l'inhibition de PP2A-B55 au cytoplasme avant le bris de l'enveloppe nucléaire, ce qui protégerait l'état phosphorylé des substrats mitotiques nucléaires lors du bris de l'enveloppe nucléaire (Alvarez-Fernandez et al., 2013; Wang et al., 2013; Wang et al., 2016). Or, les mécanismes moléculaires nécessitant la relocalisation de Gwl du noyau vers le cytoplasme en prophase n'ont pas été formellement investigués. Le projet présenté au Chapitre 2 est né de cette question et porte sur la régulation spatiotemporelle du module Gwl – endosulfines – PP2A. La régulation de Gwl en sortie de mitose sera quant à elle abordée en section 1.4.4.2.

1.4.3 Endosulfines

1.4.3.1 Identification

Comme il n'y a pas de site de phosphorylation de Gwl sur PP2A-B55, l'hypothèse d'une troisième protéine agissant comme intermédiaire entre les deux a été proposée (Mochida et al., 2010). Deux cribles menés parallèlement dans des extraits de *Xenopus laevis* validèrent cette hypothèse par l'identification des deux substrats de Gwl : α-endosulfine (ENSA) et la phosphoprotéine 19 régulée par cAMP (Arpp19) (Gharbi-Ayachi et al., 2010; Mochida et al., 2010). ENSA et Arpp19 font partie de la famille des endosulfines. Il n'y a qu'une endosulfine chez la mouche : Endos. *endos* est un gène essentiel au développement de la mouche (Von Stetina et al., 2008). Des mutations hypomorphes permettent le développement somatique, mais entraînent des défauts de bris de l'enveloppe nucléaire et de formation du fuseau méiotique dans la majorité des œufs, rendant les femelles stériles (Von Stetina et al., 2008). Dans les rares cas où la méiose femelle est complétée chez ces mutants, des défauts de fuseau apparaissent pendant les divisions mitotiques de l'embryon syncytial (Von Stetina et al., 2008). La déplétion d'Endos en cellules de mouche entraîne les mêmes défauts mitotiques que la perte de Gwl, soit des problèmes de congression des chromosomes sur des fuseaux allongés ainsi qu'une anaphase retardée (Goshima et al., 2007; Rangone et al., 2011). La double déplétion de Gwl et d'Endos n'aggrave pas les défauts, suggérant que les deux protéines fonctionnent dans la même voie (Rangone et al., 2011). Enfin, la perte d'Endos peut être compensée par la suppression des sous-unités A (structurale), C (catalytique) et B55, mais pas des autres sous-unités régulatrices, de PP2A (Kim et al., 2012; Rangone et al., 2011). Ces résultats suggèrent qu'Endos a une fonction opposée à celle de PP2A-B55 chez la mouche également.

Bien que pouvant être phosphorylées par Cdk1 et PKA (protéine kinase A) *in vitro*, c'est la phosphorylation par Gwl sur la sérine du motif conservé FD**S**GDY de la région centrale des endosulfines (Ser67 pour ENSA, Ser62 pour Arpp19, Ser68 pour Endos) qui mène à l'inhibition de PP2A-B55 (Gharbi-Ayachi et al., 2010; Mochida et al., 2010; Rangone et al., 2011). Les endosulfines phosphorylées par Gwl interagissent

physiquement avec PP2A-B55 pour l'inhiber spécifiquement (Gharbi-Ayachi et al., 2010; Mochida et al., 2010). L'interaction de la région centrale contenant la sérine phosphorylée implique les sous-unités catalytique et B55 de PP2A, mais pas sa sous-unité structurale; suggérant un positionnement dans la cavité de liaison des substrats de PP2A-B55, près de son site catalytique (Mochida, 2014). La phosphorylation des endosulfines par Cdk1 augmente faiblement leur inhibition de PP2A-B55 *in vitro*, mais l'importance fonctionnelle de cette phosphorylation reste à déterminer (Mochida, 2014). La phosphorylation par PKA est quant à elle importante pour la fonction méiotique d'Arpp19 et sera abordée en section 1.4.6.1.

1.4.3.2 Les endosulfines sont les substrats privilégiés de PP2A-B55

Une étude par le groupe de Mike Goldberg a permis de mieux comprendre le mécanisme d'inhibition spécifique de PP2A-B55 par les endosulfines (Williams et al., 2014). Les travaux du groupe ont notamment montré que les endosulfines phosphorylées par Gwl sont à la fois des inhibiteurs et des substrats de PP2A-B55 (Williams et al., 2014). De fait, c'est PP2A-B55 qui est la phosphatase responsable de la déphosphorylation des endosulfines pendant la sortie de mitose (Williams et al., 2014).

Les paramètres cinétiques de cette déphosphorylation diffèrent grandement de ceux d'autres substrats phosphorylés par Cdk1 (Williams et al., 2014). La réaction de déphosphorylation des endosulfines (constante catalytique, $k_{cat} \sim$ 0,02-0,06 sec^{-1}) est beaucoup plus lente que celles des autres substrats de Cdk1 testés ($k_{cat} \sim$ 20-25 sec^{-1}) (Williams et al., 2014). De plus, l'affinité de PP2A-B55 pour les endosulfines phosphorylées par Gwl ($K_m \sim$ 1 nM) est nettement plus forte que celle des autres substrats phosphorylés par Cdk1 testés ($K_m \sim$ 90 µM) (Williams et al., 2014). Ces caractéristiques particulières sont à l'origine du nom d'inhibition par « compétition déloyale » donné au modèle proposé : pendant la phase M, la forte liaison et la lente déphosphorylation des endosulfines font en sorte qu'elles monopolisent le site catalytique de PP2A-B55, empêchant la phosphatase de cibler d'autres substrats mitotiques moins « privilégiés » (Williams et al., 2014). Comme les endosulfines sont en excès par rapport à PP2A-B55 dans la cellule (ratio 5 :1), le modèle d'inhibition par

compétition déloyale est très plausible pour expliquer l'inactivation rapide et quasi complète de PP2A-B55 en entrée de mitose (Cundell et al., 2013; Williams et al., 2014).

1.4.3.3   Les endosulfines possèdent tous les atouts pour battre la compétition

Même dans leur état non phosphorylé par Gwl, les endosulfines ont un potentiel intrinsèque d'inhibition de PP2A-B55 (IC$_{50}$ ~ 500 nM - 2 µM) (Mochida, 2014; Williams et al., 2014). Une combinaison de caractéristiques préférentielles expliquent le net avantage qu'ont les endosulfines pour lier le site actif de PP2A-B55.

La cavité de liaison des substrats de B55 contient plusieurs résidus d'acides aminés aux chaînes latérales acides (Xu et al., 2008). Cela favorise la liaison de substrats possédant des motifs basiques de part et d'autre de leur site de phosphorylation pour former un motif polybasique bipartite (BPR, pour *bipartite polybasic region*) (Cundell et al., 2016). Par ailleurs, des analyses biochimiques ont depuis un moment établi la préférence inhérente des complexes PP2A envers les thréonines phosphorylées par rapport aux sérines phosphorylées (Deana et al., 1982; Deana and Pinna, 1988). Des analyses protéomiques plus récentes ont permis de confirmer que cette préférence était également valide pour PP2A en complexe avec B55 (Cundell et al., 2016; Hein et al., 2017). Il est proposé que la structure légèrement plus grosse et hydrophobique des phosphothréonines augmenterait leur affinité pour le site actif de PP2A-B55 par rapport aux phosphosérines (Egloff et al., 1995; Mant et al., 2009; Rogers et al., 2016b). PP2A-B55 arrive tout de même à déphosphoryler les sérines lorsqu'elles sont adjacentes à des résidus d'acides aminés aromatiques et acides, qui contribuent à l'interaction des substrats avec le site catalytique de PP2A (Cundell et al., 2016; Xu et al., 2008). La présence d'une proline en position +1 du site
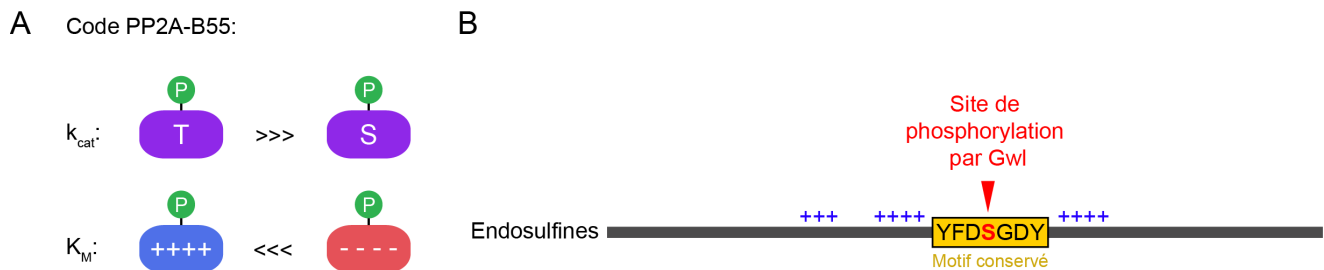
Figure 1.8. Les endosulfines sont les substrats privilégiés de PP2A-B55.

(A) PP2A-B55 catalyse plus rapidement la déphosphorylation des phosphothréonines que celle des phosphosérines, et a une plus forte affinité pour les motifs basiques. Inspiré (Holder et al., 2019). (B) Le site de phosphorylation par Gwl est une sérine située dans un motif fortement conservé entre les endosulfines et entouré d'un nombre saturant de résidus d'acides aminés basiques qui forment un motif polybasique bipartite (BPR).

de phosphorylation favorise aussi la déphosphorylation par PP2A-B55 (Kruse et al., 2020). Il est suggéré que la proline en +1, en nuisant à la formation de structures secondaires, rend la région du site de phosphorylation plus flexible et donc plus accessible pour le site actif (Rogers et al., 2016b; Theillet et al., 2014). Les motifs basiques, la nature du site de phosphorylation ainsi que les résidus d'acides aminés qui lui sont adjacents encodent donc la reconnaissance et la vitesse de déphosphorylation des substrats de PP2A-B55 (Figure 1.8A).

Le site de phosphorylation par Gwl est situé dans une région hautement basique des endosulfines (Figure 1.8B) (Cundell et al., 2016). De fait, le site de phosphorylation est entouré d'un nombre saturant de résidus d'acides aminés basiques formant un BPR (Cundell et al., 2016). Qui plus est, le site phosphorylé est une sérine faisant partie du motif conservé YFDSGDY des endosulfines, qui contient des résidus d'acides aminés aromatiques et acides. Le motif ne contient pas de proline en +1, mais cela pourrait être compensé par le fait que les endosulfines sont de petites protéines (112 à 174 acides aminés, selon les espèces) désordonnées. Enfin, le site phosphorylé par Gwl est une sérine, ce qui explique sa lente déphosphorylation (Cundell et al., 2016; Williams et al., 2014). Les endosulfines possèdent donc tous les atouts pour lier fortement PP2A-B55 tout en étant lentement déphosphorylées, leur permettant d'éclipser les autres substrats dans la compétition pour lier le site actif.

1.4.4 Réactivation de PP2A-B55 et sortie de mitose

Tel qu'abordé précédemment, la sortie de mitose est plus complexe que le renversement biochimique de l'activité kinase de Cdk1, qui résulterait simplement en

l'inversion des événements de l'entré de mitose et un retour en G2. Les cellules poursuivent plutôt leur progression en mitose pour compléter leur division. Deux mécanismes régulés imposent une direction à la sortie de mitose : la protéolyse et la déphosphorylation.

1.4.4.1 La sortie de mitose : une alternance de protéolyse et de déphosphorylation

Lorsque le point de contrôle du fuseau est satisfait, la dégradation de la cycline B par APC/C^{Cdc20} est l'élément clé qui déclenche l'anaphase. La protéolyse de la cycline B entraîne l'inactivation de Cdk1. Ainsi, la baisse progressive des niveaux de cycline B provoque la réactivation ordonnée des phosphatases mitotiques (Bouchoux and Uhlmann, 2011; Holder et al., 2020). Celles-ci coordonnent ensuite la déphosphorylation de centaines de substrats pendant l'anaphase. Une fois Cdk1 inactivée, les événements de déphosphorylation permettant la sortie de mitose sont indépendants de l'activité de l'APC/C (Holder et al., 2020). La déphosphorylation ordonnée des substrats mitotiques constitue donc le mécanisme principal de sortie de mitose (Holder et al., 2020). La protéolyse médiée par l'APC/C a majoritairement lieu en aval de l'anaphase, suite à l'activation par déphosphorylation de l'APC/C^{Cdh1} (Holder et al., 2020). Celui-ci collabore avec l'APC/C^{Cdc20} en fin de mitose pour, entre autres, induire la dégradation des kinases Plk1 et Aurora et permettre le retour en G1 (Floyd et al., 2008). La protéolyse est donc requise pour initier et terminer la sortie de mitose; alors que la déphosphorylation ordonnée en est le principal moteur.

1.4.4.2 Les phosphatases se relaient pour orchestrer la sortie de mitose

Tout comme celle de PP2A-B55, l'activité de PP1 est réduite en entrée de mitose pour favoriser l'augmentation globale de la phosphorylation et l'état mitotique de la cellule. Cette inhibition est en partie causée par la phosphorylation inhibitrice de PP1 par cycline B – Cdk1 (Dohadwala et al., 1994; Kwon et al., 1997). À cela s'ajoute la liaison de protéines inhibitrices qui sont phosphorylées en mitose (Ceulemans and Bollen, 2004; Leach et al., 2003; Wu et al., 2009). Comme PP1 s'auto-déphosphoryle, l'inactivation de cycline B – Cdk1 à la transition métaphase-anaphase lui permet d'initier

rapidement sa propre réactivation (Figure 1.9) (Wu et al., 2009). PP1 actif initie l'inactivation de Gwl en ciblant son site d'auto-phosphorylation (Heim et al., 2015; Ma et al., 2016; Ren et al., 2017; Rogers et al., 2016a). La phosphatase Fcp1, qui ne fait pas partie des PPPs, serait aussi impliquée dans la désactivation de Gwl (Della Monica et al., 2015; Hegarat et al., 2014). Son mécanisme d'action n'est toutefois pas clairement élucidé.

L'inactivation partielle de Gwl suspend la phosphorylation soutenue des endosulfines; celles déphosphorylées par PP2A-B55 ne sont donc plus remplacées (Williams et al., 2014). Comme l'excès stochiométrique des endosulfines n'est que d'environ cinq fois, PP2A-B55 peut assez rapidement toutes les déphosphoryler (Williams et al., 2014).
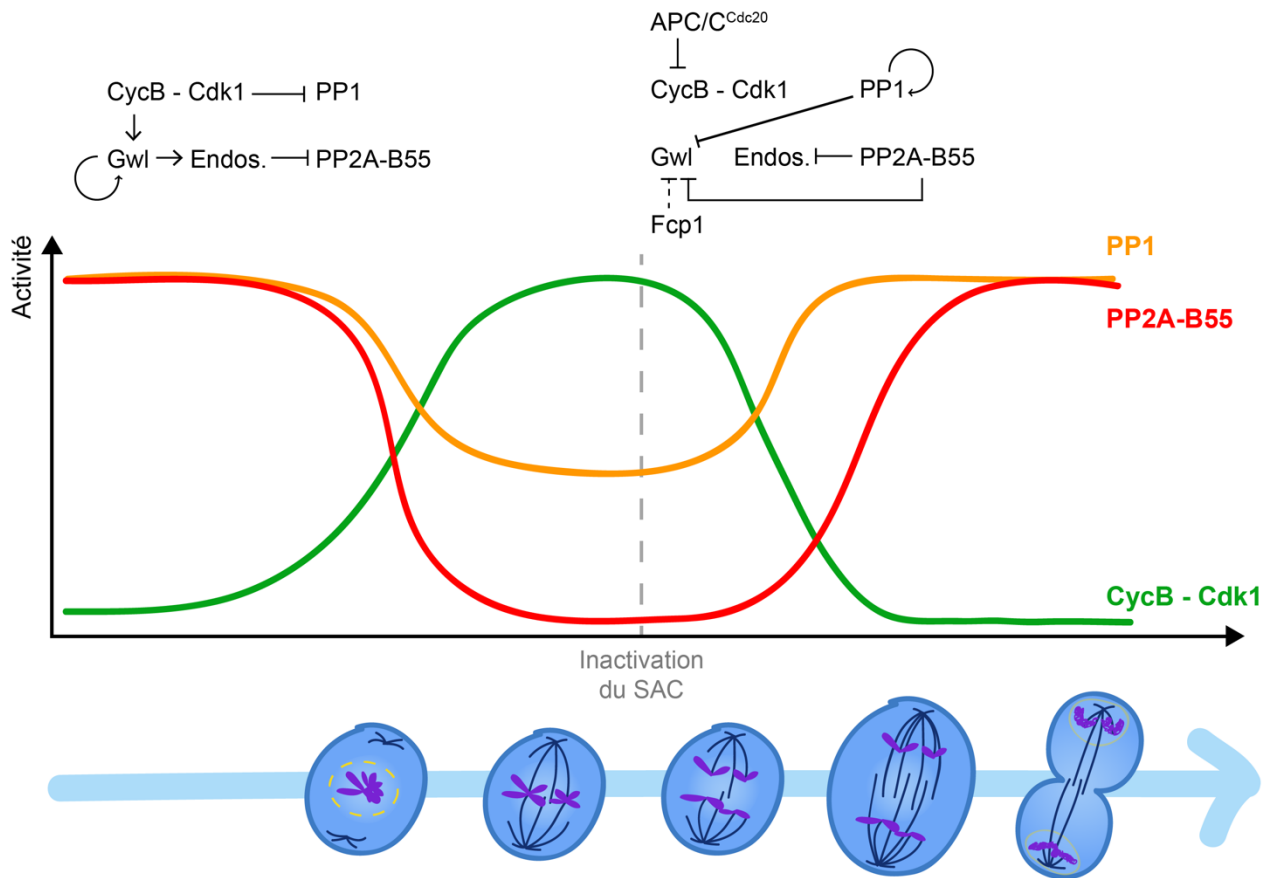
Figure 1.9. La sortie de mitose nécessite les réactivations coordonnées de PP1 et PP2A-B55.

Les niveaux d'activation de cycline B – Cdk1 (CycB – Cdk1, en vert), PP1 (en orangé) et PP2A-B55 (en rouge) sont représentés en fonction de la progression mitotique. En entrée de mitose, l'activité de cycline B – Cdk1 provoque l'inhibition des phosphatases PP1 et PP2A-B55. Suite à l'inactivation du SAC, la cycline B est dégradée par l'APC/C^{Cdc20} et Cdk1 est inactivée. L'inhibition de PP1 est levée, ce qui lui permet de s'auto-déphosphoryler pour s'activer. Elle initie ensuite l'inhibition de Greatwall (Gwl). La phosphatase Fcp1 participerait aussi à la réactivation partielle de Gwl par un mécanisme incompris pour l'instant. Partiellement inactivée, Gwl ne peut soutenir aussi efficacement la phosphorylation des endosulfines, ce qui permet à PP2A-B55 de les déphosphoryler. PP2A-B55 complète ensuite l'inactivation de Gwl et cible ses autres substrats.

Une fois libérée des endosulfines, PP2A-B55 complète l'inactivation de Gwl en ciblant ses sites d'activation phosphorylés par Cdk1, ce qui lui permet de redevenir pleinement active envers ses autres substrats (Rogers et al., 2016a). La déphosphorylation de Gwl par PP2A-B55 promeut aussi son retour au noyau en télophase (Wang et al., 2016). Chez la levure, PP1 lierait directement PP2A-B55 pour initier sa réactivation (Grallert et al., 2015). Une fois réactivées, PP1 et PP2A catalysent la transition de la phase M vers l'interphase en déphosphorylant leurs substrats de façon ordonnée.

1.4.4.3   L'ordre de déphosphorylation est encodé par les substrats

La succession d'événements menant à la sortie de mitose se déroule dans un ordre précis, qui nécessite la coordination des activités phosphatases. Une fois réactivées, les phosphatases ne déphosphorylent pas leurs substrats de façon aléatoire; elles les font plutôt selon un programme établi. On retrouve ainsi des substrats rapides, des substrats intermédiaires et des substrats tardifs (Figure 1.10) (Bouchoux and Uhlmann, 2011; Kuilman et al., 2015; McCloy et al., 2015). Cette hiérarchie de substrats fait en sorte que les protéines impliquées dans l'inactivation du SAC, l'élongation du fuseau et la ségrégation des chromosomes sont déphosphorylées en premier; tandis que celles impliquées dans la décondensation des chromosomes, la reformation de l'enveloppe nucléaire et la cytocinèse sont déphosphorylées plus tardivement (Bouchoux and Uhlmann, 2011; Kuilman et al., 2015; McCloy et al., 2015). Tel que présenté en section 1.4.3.3, les caractéristiques intrinsèques des substrats impactent la cinétique de leur déphosphorylation. Les préférences observées pour PP2A-B55 sont partagées par PP1 et partiellement par Cdc14 chez la levure, et s'appliquent donc globalement aux événements de déphosphorylation de la sortie de mitose (Holder et al., 2020; McCloy et al., 2015; Touati et al., 2018).

Deux principales caractéristiques déterminent les préférences des phosphatases : leur affinité pour le substrat et l'efficacité catalytique de déphosphorylation (Bouchoux and Uhlmann, 2011). Ces caractéristiques discriminent les substrats entre eux, établissant l'ordre de leur déphosphorylation (Bouchoux and

Uhlmann, 2011). Tout comme pour PP2A-B55, les phosphatases mitotiques ont globalement une plus grande affinité pour les substrats basiques (Cundell et al., 2016; Holder et al., 2020; Touati et al., 2018).
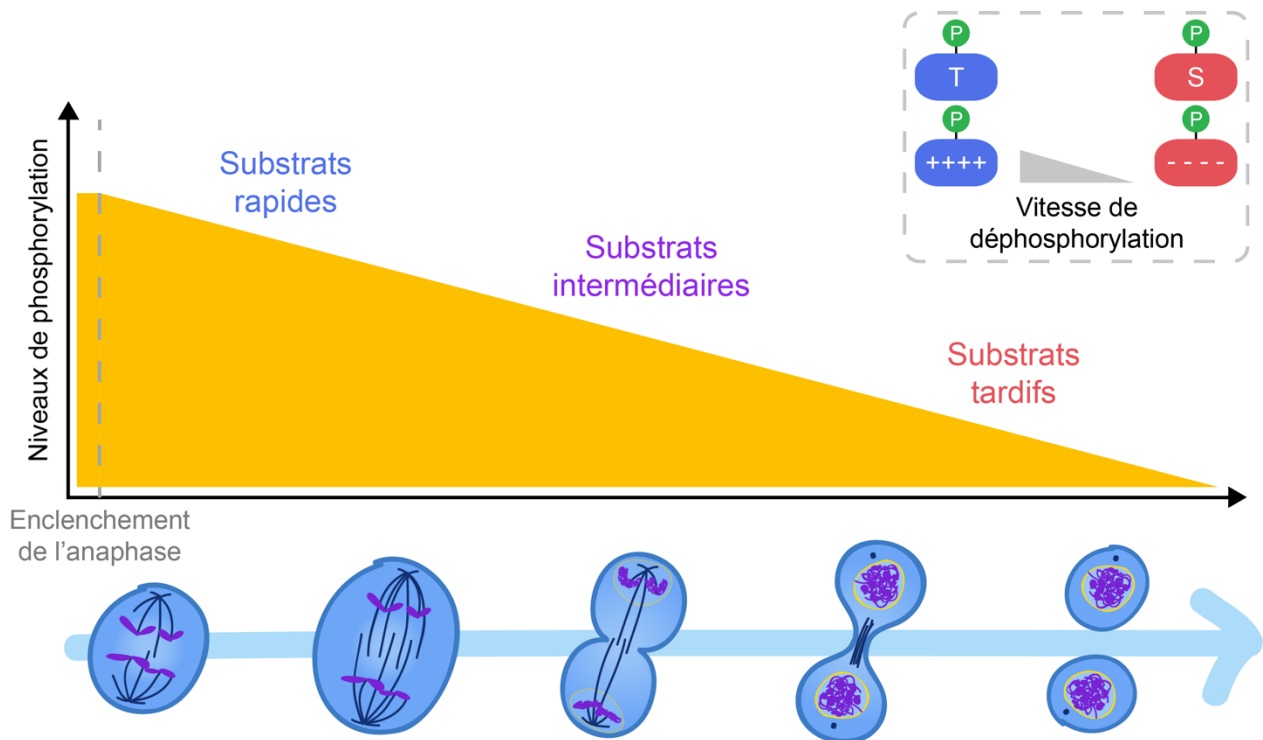
Figure 1.10. La déphosphorylation ordonnée des substrats pendant la sortie de mitose.

Les substrats des phosphatases sont ciblés selon un programme établi encodé par leurs caractéristiques. Les phosphothréonines situées dans des régions basiques sont généralement déphosphorylées plus rapidement; on les retrouve sur des protéines impliquées dans les premiers événements de la sortie de mitose (substrats rapides). À l'opposé, les substrats qui sont déphosphorylés en dernier sont moins basiques et contiennent généralement des phosphosérines. Ces substrats tardifs sont impliqués dans les étapes finales de la division, comme la cytocinèse.

Ainsi, les substrats les plus basiques, notamment ceux impliqués dans la régulation du fuseau mitotique, sont ceux qui sont déphosphorylés le plus tôt (Cundell et al., 2016; Holder et al., 2020; Touati et al., 2018). Les protéines déphosphorylées plus lentement sont moins basiques et incluent des protéines comme les nucléoporines (Cundell et al., 2016). Ces différences d'affinités assurent la progression correcte de la

sortie de mitose, par exemple que la reformation de l'enveloppe nucléaire se déroule en aval de la ségrégation des chromosomes. L'efficacité catalytique est quant à elle influencée par la nature du site de phosphorylation et des acides aminés qui lui sont adjacents (Hein et al., 2017; Holder et al., 2020; McCloy et al., 2015). Les phosphothréonines sont globalement déphosphorylées plus rapidement que les phosphosérines en sortie de mitose (Cundell et al., 2016; Deana et al., 1982; Deana and Pinna, 1988; Donella-Deana et al., 1991; Godfrey et al., 2017; Hein et al., 2017; Holder et al., 2020; Malik et al., 2009; McCloy et al., 2015). Ainsi, il y a un enrichissement de phosphothréonines chez les protéines impliquées dans les premiers événements de la sortie de mitose (Hein et al., 2017; Holder et al., 2020; McCloy et al., 2015). Les protéines requises pour les événements tardifs sont plutôt phosphorylées sur des sérines (Hein et al., 2017; Holder et al., 2020; McCloy et al., 2015). Chez la levure bourgeonnante, la situation est inversée puisque Cdc14 cible préférentiellement les phosphosérines (Kuilman et al., 2015).

À ces mécanismes qui dictent la temporalité (modèle des horloges) de la déphosphorylation, s'ajoutent les mécanismes régulant sa spatialité (modèle des règles) (de Castro et al., 2018). Ceux-ci impliquent un gradient d'activité d'Aurora B au fuseau mitotique pour contrebalancer les activités phosphatases (Afonso et al., 2014; Fuller et al., 2008; Neurohr et al., 2011). Le ratio des activités kinase/phosphatase est ainsi élevé dans la zone médiane du fuseau, et diminue graduellement jusqu'à être inversé aux pôles (Afonso et al., 2014; Fuller et al., 2008; Neurohr et al., 2011). Ce mécanisme « mesure » la position des chromosomes par rapport à l'axe de division et empêche leur décondensation et la reformation de l'enveloppe nucléaire tant que la ségrégation n'est pas suffisamment avancée (Afonso et al., 2014; Fuller et al., 2008; Neurohr et al., 2011).

Malgré des préférences communes au niveau catalytique, les phosphatases ont tout de même leur spécificité; elles ne ciblent pas toutes les mêmes substrats. PP1 et les sous-unités régulatrices de PP2A reconnaissent des motifs d'interactions courts et linéaires (SLIMs, pour *short linear-interaction motifs*) (Choy et al., 2014; Egloff et al., 1997; Hendrickx et al., 2009; Hertz et al., 2016; Kumar et al., 2016; Terrak et al., 2004). La phosphorylation de ces motifs peut bloquer (dans le cas de PP1) ou à l'inverse

favoriser (pour PP2A-B56 par exemple) leur interaction avec la phosphatase qui les reconnaît (Hertz et al., 2016; Liu et al., 2010; Qian et al., 2015). La phosphorégulation des SLIMs contribue ainsi à réguler temporellement et spatialement les interactions des phosphatases. Enfin, les protéines interagissant avec PP1 peuvent présenter une combinaison de SLIMs, ce qui module leur affinité d'interaction (Choy et al., 2014; Qian et al., 2015).

1.4.4.4 Quelques substrats mitotiques connus de PP2A-B55

Malgré les avancées récentes sur les mécanismes de reconnaissance des substrats par les phosphatases, l'identité de la majorité des substrats de PP2A-B55 demeure inconnue à ce jour. L'un des premiers substrats mitotiques de PP2A-B55 à avoir été identifié est GM130, une protéine ciblée par Cdk1 qui contribue à la structure de l'appareil de Golgi et aux transferts entre le réticulum endoplasmique et l'appareil de Golgi (Lowe et al., 2000).

Un autre substrat spécifique de PP2A-B55 est la protéine régulatrice de la cytocinèse 1 (PRC1) (Cundell et al., 2013). PRC1 est recrutée au fuseau central en sortie de mitose, où elle est requise pour l'élongation du fuseau en anaphase et pour la cytocinèse (Li et al., 2018; Walczak and Shaw, 2010). Sa déphosphorylation par PP2A-B55 renverse une phosphorylation inhibitrice placée par Cdk1 en entrée de mitose et permet son recrutement au fuseau central (Cundell et al., 2013; Jiang et al., 1998; Mollinari et al., 2002; Zhu and Jiang, 2005; Zhu et al., 2006).

La déphosphorylation de la kinase du SAC Mps1 (pour *monopolar spindle kinase 1*) est également dépendante de PP2A-B55 (Diril et al., 2016). La phosphorylation de Mps1 est requise pour le recrutement de certains effecteurs du SAC aux kinétochores; sa déphosphorylation par PP2A-B55 promeut donc la transition métaphase-anaphase (Diril et al., 2016).

Il a été montré *in vitro* que PP2A-B55 pouvait retirer les phosphorylations activatrices sur APC1, une sous-unité de l'APC/C, ainsi que les phosphorylations inhibitrices des co-activateurs Cdc20 et Cdh1 (Hein et al., 2017; Labit et al., 2012;

Mochida et al., 2009; Yudkovsky et al., 2000). Les sites de phosphorylation activateurs d'APC1 sont des sérines; les sites inhibiteurs de Cdc20 sont des thréonines, alors que ceux de Cdh1 sont des sérines (Hein et al., 2017). Compte tenu de la préférence de PP2A-B55 pour les phosphothréonines, PP2A-B55 permet l'activation séquentielle de l'APC/C^{Cdc20} puis de l'APC/C^{Cdh1} (Hein et al., 2017). De fait, un délai est observé entre la déphosphorylation de Cdc20 et celle d'APC1, ce qui procure une fenêtre d'activité à l'APC/C^{Cdc20} (Hein et al., 2017). L'APC/C^{Cdh1} ne nécessite pas la phosphorylation d'APC1 pour être actif; ainsi lorsque PP2A-B55 déphosphoryle les sérines d'APC1 et de Cdh1, l'APC/C^{Cdc20} est inactivée alors que l'APC/C^{Cdh1} est activée (Hein et al., 2017).

Malgré tout, les substrats mitotiques confirmés de PP2A-B55 demeurent peu nombreux. C'est avec l'objectif d'identifier de nouveaux substrats de PP2A-B55 que le projet présenté au Chapitre 3 a été initié.

1.4.4.5 L'implication de PP2A-B55 pour la reformation de l'enveloppe nucléaire

1.4.4.5.1 Organisation de l'enveloppe nucléaire

L'une des transformations importantes se produisant pendant la sortie de mitose est la reformation de l'enveloppe nucléaire. Chez les cellules eucaryotes, l'enveloppe nucléaire permet de compartimenter le noyau. Elle est composée de deux bicouches lipidiques spécialisées : la membrane nucléaire externe et la membrane nucléaire interne (Figure 1.11) (Agrawal and Lele, 2019). Les membranes externes et internes sont biochimiquement distinctes. La membrane nucléaire externe est le prolongement du réticulum endoplasmique; la membrane nucléaire interne a quant à elle une composition protéique qui lui est propre (Boni et al., 2015; Ungricht et al., 2015).
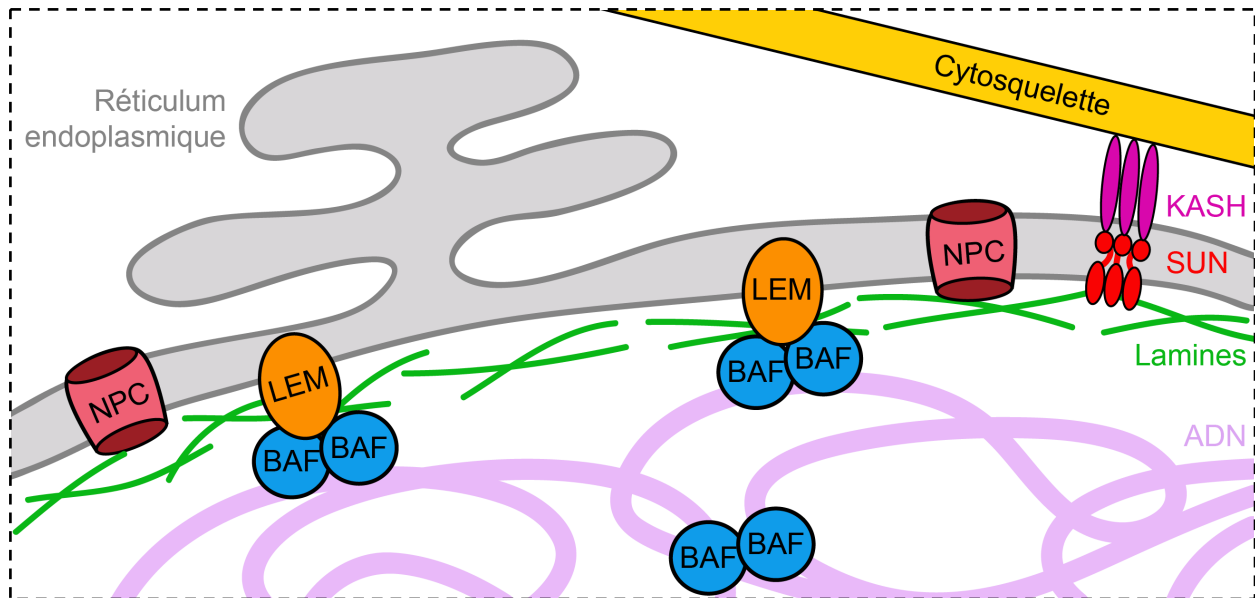
Figure 1.11. La structure de l'enveloppe nucléaire.

L'enveloppe nucléaire est constituée de deux bicouches lipidiques : les membranes nucléaires interne et externe (représentées en gris). La membrane nucléaire externe est le prolongement du réticulum endoplasmique et fusionne avec la membrane nucléaire interne au niveau des pores nucléaires. Ceux-ci sont occupés par les complexes des pores nucléaires (NPCs) qui dirigent le transport nucléocytoplasmique. Plusieurs protéines associées à la membrane nucléaire interne forment un réseau structurant et permettent la communication entre le noyau et le reste de la cellule. Parmi celles-ci se trouvent les lamines nucléaires, les protéines LEM et les protéines SUN. Les lamines et les protéines LEM interagissent entre elles et avec des protéines qui lient la chromatine (représentée en mauve pâle), telle BAF, servant à la fois de support mécanique et de lien entre la chromatine et l'enveloppe nucléaire. Les protéines SUN s'associent avec les protéines KASH pour former les complexes LINC et lier le nucléosquelette au cytosquelette.

Les deux membranes nucléaires fusionnent à de multiples endroits pour former des pores (Knockenhauer and Schwartz, 2016). Les pores nucléaires ne sont pas de simples trous; ils sont occupés par des complexes protéiques, les complexes des pores nucléaires (NPCs, pour *nuclear pore complexes*), qui agissent comme canaux de transport entre le nucléoplasme et le cytoplasme (Knockenhauer and Schwartz, 2016). Les NPCs sont formés de protéines nommées nucléoporines (Nups) (Alber et al., 2007; Kramer et al., 2008). Ils permettent la diffusion passive des petites macromolécules et régulent le passage de celles de plus de 40-60 kDa (Christie et al., 2016; Keminer and

Peters, 1999; Knockenhauer and Schwartz, 2016; Mohr et al., 2009; Paine and Feldherr, 1972; Paine et al., 1975; Ribbeck and Gorlich, 2001).

Un second mécanisme de communication entre le noyau et le cytoplasme implique les « complexes liant le nucléosquelette et le cytosquelette », ou complexes LINCs (pour *linker of the nucleoskeleton and cytoskeleton*) (Aureille et al., 2017; Chang et al., 2015; Maniotis et al., 1997; Schwager et al., 2019). Ces complexes sont formés des protéines à domaine KASH (pour *Klarsicht, ANC-1, Syne homology*), qui traversent la membrane nucléaire externe, et des protéines à domaine SUN (pour *Sad1 and UNC-84*), qui sont ancrées dans la membrane nucléaire interne (Malone et al., 1999; Sosa et al., 2013; Starr and Han, 2002). Les protéines KASH et les protéines SUN lient respectivement le cytosquelette et la lamine nucléaire; leur interaction dans l'espace périnucléaire permet donc de connecter la chromatine au microenvironnement cellulaire (Kim et al., 2015).

La lamina nucléaire est un réseau de filaments intermédiaires, les lamines de type A et B, qui interagissent avec les protéines de la membrane nucléaire interne et des protéines liant la chromatine (Gerace and Huber, 2012; Guttinger et al., 2009; Osmanagic-Myers et al., 2015; Schirmer and Gerace, 2005). La lamina nucléaire procure donc un support mécanique à l'enveloppe nucléaire et contribue à l'organisation de l'hétérochromatine (Boni et al., 2015; Osmanagic-Myers et al., 2015; Ungricht et al., 2015).

Parmi les protéines ancrées dans la membrane nucléaire interne, se trouvent les protéines de la famille LEM (pour LAP2-emerin-MAN1, les trois protéines LEM initialement identifiées). Ces protéines partagent un domaine LEM d'environ 40 acides aminés qui adopte un repliement globulaire, principalement composé de deux hélices-α stabilisées par des interactions électrostatiques intramoléculaires (Figure 1.12A) (Laguri et al., 2001; Lin et al., 2000; Wolff et al., 2001). Les protéines LEM possèdent aussi des régions intrinsèquement désordonnées qui sont modifiées au niveau post-traductionnel, entre autres par phosphorylation, au cours du cycle cellulaire (Ellis et al., 1998; Hirano et al., 2009; Yip et al., 2012). Les protéines LEM interagissent avec les lamines et

d'autres protéines de la membrane nucléaire interne, contribuant à l'architecture nucléaire et à l'organisation de la chromatine (Haque et al., 2010; Patel et al., 2014; Shin et al., 2013).

Le domaine LEM interagit directement avec les homodimères de BAF (pour *barrier-to-autointegration factor*), une petite protéine qui lie l'ADN (Figure 1.12B) (Cai et al., 2001; Cai et al., 2007; Cai et al., 1998; Lee et al., 2001; Mansharamani and Wilson, 2005; Shumaker et al., 2001). Comme chaque monomère de BAF lie l'ADN, sa dimérisation contribue à la compaction de l'ADN (Cai et al., 1998). Leurs sites de liaison à l'ADN et aux domaines LEM étant distincts, les dimères de BAF peuvent interagir simultanément avec la chromatine et les protéines LEM (Cai et al., 2007). BAF permet donc de faire le pont entre la chromatine et l'enveloppe nucléaire, tout en agissant comme régulateur épigénétique par son rôle dans la formation de l'hétérochromatine (Asencio et al., 2012; Margalit et al., 2005; Montes de Oca et al., 2011).
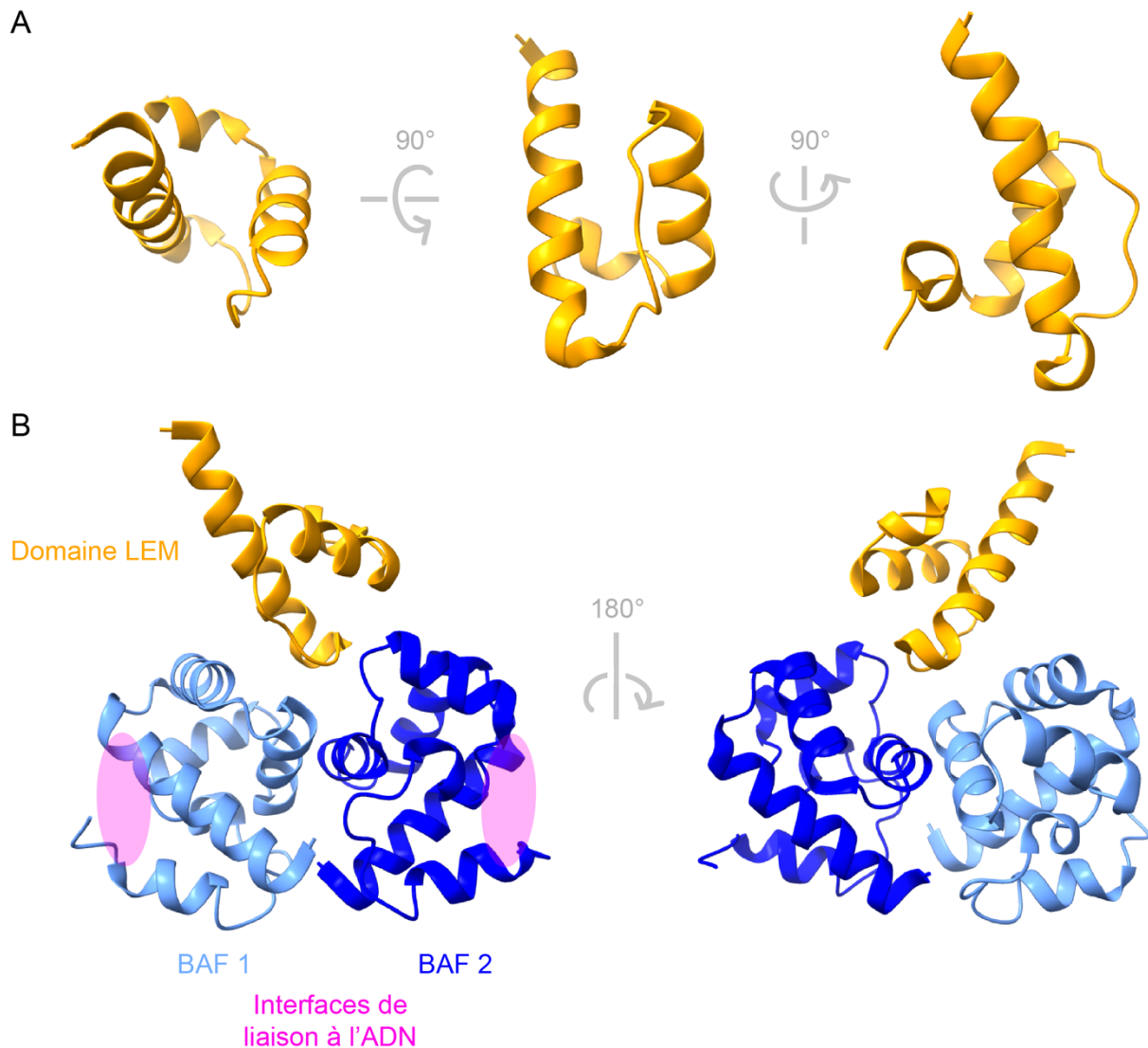
Figure 1.12 Le domaine LEM interagit avec BAF dimérique.

(A) Domaine LEM partagé par les protéines LEM. Il adopte un repliement globulaire formé de deux hélices-α (numéro d'accession Protein Data Bank : 2ODC) (Cai et al., 2007). (B) Le domaine LEM interagit avec les deux monomères de BAF (représentés en bleu) (numéro d'accession Protein Data Bank : 2ODG) (Cai et al., 2007). Les interfaces de liaison à l'ADN (indiquées en rose) étant distinctes, les dimères de BAF peuvent à la fois lier la chromatine et les protéines LEM; ce qui permet de faire le pont entre la chromatine et l'enveloppe nucléaire. Rendu des structures effectué avec ChimeraX (Pettersen et al., 2021) de l'University of California, San Francisco.

1.4.4.5.2 La régulation de l'enveloppe nucléaire au cours de la division cellulaire requiert PP2A-B55

Tel que mentionné plus tôt, l'enveloppe nucléaire est totalement ou partiellement désassemblée lors des mitoses ouvertes et semi-ouvertes. Le bris de l'enveloppe nucléaire est un processus qui se déroule de façon ordonnée, au cours duquel se succèdent le désassemblage des NPCs, la dépolymérisation de la lamina nucléaire et la rétraction des membranes nucléaires vers le réticulum endoplasmique (Alvarez-Fernandez and Malumbres, 2014). Ces événements sont initiés par l'activité de cycline B – Cdk1, qui phosphoryle plusieurs composantes de l'enveloppe nucléaire pour désengager la chromatine et perturber les interactions protéine-protéine maintenant la structure de l'enveloppe nucléaire (Figure 1.13) (Heald and McKeon, 1990; Peter et al., 1990; Tseng and Chen, 2011).
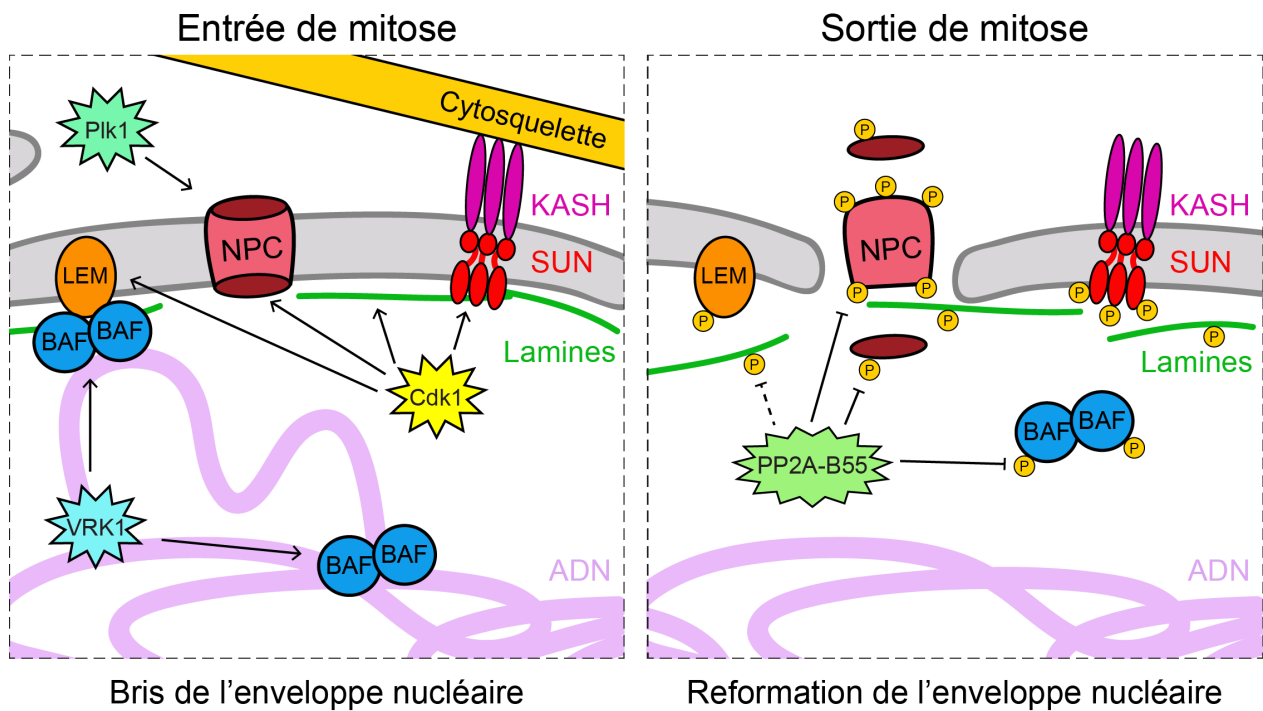
Figure 1.13. L'enveloppe nucléaire est régulée par phosphorylation pendant le cycle cellulaire.

Les activités kinase combinées de cycline B – Cdk1, Plk1 et VRK1/NHK-1 causent le désassemblage des NPCs, la dispersion de la lamina nucléaire et la dissociation de nombreuses interactions entre protéines de l'enveloppe nucléaires. Ces événements

provoquent le bris de l'enveloppe nucléaire. En sortie de mitose, PP2A-B55 est impliquée dans la déphosphorylation de BAF et de certaines nucléoporines, et est requise pour le recrutement de la lamine B. Ces événements promeuvent la reformation de l'enveloppe nucléaire.

La phosphorylation des nucléoporines, à laquelle participe aussi Plk1, cause le désassemblage rapide des NPCs (de Castro et al., 2018; Favreau et al., 1996; Glavy et al., 2007; Guttinger et al., 2009; Heald and McKeon, 1990; Laurell et al., 2011; Linder et al., 2017; Martino et al., 2017). La phosphorylation des lamines disperse la lamina nucléaire (Goss et al., 1994; Heald and McKeon, 1990; Mall et al., 2012; Peter et al., 1990; Torvaldson et al., 2015). De même, la phosphorylation de certaines protéines de la membrane nucléaire interne, comme les protéines SUN ou LAP2, les dissocie de la lamina nucléaire (Heald and McKeon, 1990; Patel et al., 2014; Peter et al., 1990; Tseng and Chen, 2011). De façon similaire, la phosphorylation de BAF par la kinase VRK1/NHK-1 (pour *vaccinia-related kinase 1*, ou *nucleosomal histone kinase 1* chez la drosophile) perturbe ses interactions avec la chromatine et les protéines LEM, contribuant au bris de l'enveloppe nucléaire (Gorjanacz et al., 2007; Margalit et al., 2007; Nichols et al., 2006).

En sortie de mitose, il faut reformer une enveloppe nucléaire autour des noyaux des deux cellules-filles naissantes. Un événement clé de ce processus est le recrutement de BAF aux chromosomes en télophase (Samwer et al., 2017). En recouvrant la surface des chromosomes ségrégés, les dimères de BAF les rassemblent en une seule masse d'ADN, menant à la formation d'un seul noyau par cellule-fille (Samwer et al., 2017). Suite à cette première étape, les NPCs sont réassemblés, les protéines de l'enveloppe nucléaire interne sont recrutées et les membranes nucléaires sont reformées à partir du réticulum endoplasmique (Gorjanacz et al., 2007; Haraguchi et al., 2001; Margalit et al., 2005).

PP2A-B55 joue différents rôles dans la reformation de l'enveloppe nucléaire. De fait, en son absence, la reformation de l'enveloppe nucléaire est retardée dans les cellules humaines et de drosophile (Mehsen et al., 2018; Schmitz et al., 2010). PP2A-B55 induit la déphosphorylation de BAF pour permettre son recrutement à la chromatine

et son interaction subséquente avec ses partenaires protéiques de l'enveloppe nucléaire (Asencio et al., 2012; Mehsen et al., 2018). De plus, des résultats en cellules humaines ont démontré le rôle de PP2A-B55 dans la déphosphorylation et le recrutement à la chromatine des nucléoporines Nup153 et Nup107 (Cundell et al., 2016). Chez la mouche, les recrutements de Nup107 et de la Lamine B aux noyaux naissants suite à la mitose dépendent aussi de PP2A-B55 (Mehsen et al., 2018).

1.4.5 Conservation du module

Bien que fortement conservé de la levure à l'humain, le module Gwl – endosulfines – PP2A présente une certaine plasticité entre les espèces (Tableau 1.1).

Tableau 1.1 Conservation du module Gwl – endosulfines – PP2A.
Les protéines homologues du module sont indiquées pour différents organismes.

Fonction	*S. pombe*	*S. cerevisiae*	*C. elegans*	*D. melanogaster*	*X. laevis*	*H. sapiens*
Kinase(s)	Ppk18 Cek1	Rim15	-	Greatwall	Greatwall	MASTL
Endosulfine(s)	Igo1/Mug134	Igo1 Igo2	ENSA	Endos	ENSA Arpp19	ENSA Arpp19
Phosphatase	PP2A-Pab1	PP2A-Cdc55	PP2A-SUR-6	PP2A-Tws	PP2A-B55	PP2A-B55

L'importance fonctionnelle du module pour l'entrée en mitose est généralement conservée, mais Gwl n'est pas essentielle dans tous les organismes. De fait, il n'y a pas d'orthologue de Gwl chez *Caenorhabditis elegans* et l'endosulfine ensa-1 n'y est pas essentielle (Kim et al., 2012). Comme les niveaux de PP2A-B55 sont faibles dans cet organisme, la présence d'un mécanisme d'inhibition robuste de son activité n'est potentiellement pas requise pour la progression en mitose (Kim et al., 2012). Contrairement à Gwl, les endosulfines sont présentes dans toutes les espèces, de la levure à l'humain (Kim et al., 2012). Elles semblent issues d'un gène eucaryote ancestral ayant subi des duplications et des délétions, expliquant le nombre variable d'homologues entre les espèces (Hached et al., 2019; Labandera et al., 2015). De fait, *Caenorhabditis elegans* et *Drosophila melanogaster* n'ont qu'une endosulfine, alors que

les levures et les mammifères en ont deux (Hached et al., 2019). Des études récentes suggèrent des rôles spécifiques et distincts pour les deux paralogues mammifères des endosulfines. Il a effectivement été montré qu'Arpp19 est essentielle pour le développement embryonnaire par son rôle en mitose, contrairement à ENSA qui est plutôt requise pour la réplication de l'ADN pendant la phase S (Charrasse et al., 2017; Hached et al., 2019). PP2A-B55 et un homologue de Gwl (IRE) sont également présents chez les plantes (Lillo et al., 2014; Mochida, 2014; Yu et al., 2004). De plus, trois protéines homologues aux endosulfines ont été identifiées chez *Arabidopsis thaliana*, mais leurs rôles précis restent à caractériser (Labandera et al., 2015).

Chez les organismes multicellulaires, Gwl et les endosulfines inhibent la phosphatase PP2A-B55, agissant comme un interrupteur moléculaire qui promeut l'entrée en mitose et en méiose (Gharbi-Ayachi et al., 2010; Mochida et al., 2009; Mochida et al., 2010; Von Stetina et al., 2008). Chez *Saccharomyces cerevisiae*, le module contribue à l'entrée en mitose d'une façon légèrement différente à celle des autres organismes. De fait, Rim15 (Gwl) phosphoryle les endosulfines Igo1 et Igo2 (pour *Initiation of G0* 1 et 2) pour induire l'activation et l'export nucléaire de la phosphatase PP2A-Cdc55, l'homologue de PP2A-B55 (Juanes et al., 2013). Comme le rôle de PP2A-Cdc55 chez la levure est de promouvoir plutôt que d'inhiber l'activation de Cdk1, Rim15 et Igo1/2 y favorisent néanmoins l'entrée en mitose (Harvey et al., 2011; Lin and Arndt, 1995; Minshull et al., 1996; Pal et al., 2008; Yang et al., 2000).

Par ailleurs, on retrouve un module similaire au module Gwl – endosulfines – PP2A dans le système nerveux. MAST3, une kinase de la même famille que Gwl/MASTL, y est spécifiquement exprimée dans les cellules du striatum (Garland et al., 2008). Arpp16 est un variant d'épissage d'Arpp19, plus court de 16 acides aminés et exclusivement exprimé dans le cerveau, particulièrement dans le striatum (Brene et al., 1994; Dulubova et al., 2001; Girault et al., 1990; Horiuchi et al., 1990). Il est suggéré qu'Arpp16 phosphorylé par MAST3 agit comme inhibiteur constitutif de PP2A dans les neurones du striatum (Andrade et al., 2017). La voie est donc conservée entre les espèces dans un contexte mitotique, mais semble également avoir évolué dans différents systèmes pour accomplir des rôles diversifiés.

1.4.5.1 *Drosophila melanogaster* pour étudier le module Gwl – endosulfines – PP2A.

Drosophila melanogaster est un puissant organisme pour l'étude du cycle cellulaire. Son génome compact a été complètement séquencé, et 60% de ses gènes sont conservés chez l'humain (Adams et al., 2000; Celniker and Rubin, 2003). Les principaux régulateurs du cycle cellulaire font partie des gènes conservés. Par ailleurs, 75% des gènes humains causant des pathologies sont conservés chez *Drosophila melanogaster* (Reiter and Bier, 2002).

La drosophile constitue un bon modèle expérimental par la facilité de sa maintenance et la multitude d'outils qu'elle offre. Le cycle de vie de la drosophile est d'environ 10 jours à 25°C, ce qui permet d'obtenir plusieurs générations rapidement, et comporte quatre principaux stades développementaux distincts : embryonnaire, larvaire, pupal et adulte. Après la fertilisation, treize cycles de divisions nucléaires s'enchaînent de façon rapide (environ 10 minutes par cycle) et synchronisée dans l'embryon syncytial, ce qui en fait un système intéressant pour étudier la machinerie mitotique.

La drosophile est particulièrement utile pour les expériences génétiques puisqu'elle est facile à manipuler génétiquement. Il est possible de l'utiliser pour explorer différentes questions à propos des rôles développementaux et fonctionnels de gènes d'intérêt donnés. Elle peut aussi être utilisée inversement pour identifier les gènes impliqués dans une processus donné. De nombreuses ressources sont accessibles aux drosophilistes, notamment des lignées transgéniques et mutantes. Par ailleurs, il est relativement facile de générer des mouches transgéniques pour exprimer différentes versions d'un gène d'intérêt, ou même le silencer, de façon spécifique à un tissu. De plus, différentes lignées de cellules en culture sont disponibles. Les lignées cellulaires les plus couramment utilisées (Schneider 2, S2R+ et Kc) sont toutes dérivées d'embryons (Echalier and Ohanessian, 1969; Schneider, 1972; Yanagawa et al., 1998). Permettant des approches génétiques, biochimiques, protéomiques et microscopiques, l'utilisation de la drosophile et des nombreux outils développés par les drosophilistes facilite l'étude de processus biologiques variés et conservés.

Le génome simplifié de la drosophile en fait un organisme intéressant pour l'étude du module Gwl – endosulfines – PP2A. *Drosophila melanogaster* ne compte effectivement qu'une endosulfine, Endos. De plus, il y a moins de redondance dans les gènes encodant les sous-unités de PP2A. Contrairement aux mammifères, il n'y a qu'un seul gène pour les sous-unités catalytique (*microtubule star*) et structurale (*PP2A-29B*). De la même façon, il n'y a que cinq gènes encodant des sous-unités régulatrices : *twins* (famille B/B55), *widerborst* (famille B'/B56 type 1), *well rounded* (famille B'/B56 type 2), *CG4733* (famille B''/PR72) et *connector of kinase to AP-1* (B''/Striatin) (Hannus et al., 2002; Mayer-Jaekel et al., 1992; Ribeiro et al., 2010; Snaith et al., 1996; Uemura et al., 1993; Viquez et al., 2006). Ainsi, un maximum de cinq hétérotrimères différents de PP2A peuvent être formés chez la drosophile, ce qui facilite grandement leur caractérisation.

1.4.6 Fonctions non mitotiques de Gwl et des endosulfines

La principale fonction associée à Gwl est sa promotion de la phase M via la voie endosulfines – PP2A-B55. Des fonctions non mitotiques sont toutefois associées au module. Certaines de ces fonctions impliquent les endosulfines; d'autres semblent impliquer des voies différentes qui restent à caractériser. De fait, malgré les efforts faits en ce sens, aucun autre substrat de Gwl n'a été identifié à ce jour.

1.4.6.1 Les fonctions méiotiques

La réduction des dosages de *gwl* et d'*endos* rend les drosophiles femelles stériles, soulignant leur importance pour la méiose femelle (Archambault et al., 2007; Von Stetina et al., 2008). Les drosophiles hypomorphes pour *gwl* produisent des ovocytes qui échouent à maintenir la métaphase I et ont des défauts de cohésion des chromatides sœurs (Archambault et al., 2007). Un des allèles ayant permis d'identifier les contributions méiotiques de *gwl* est *gwl^{Sr18}*. Ce mutant empêche l'épissage de la plus longue des deux isoformes de Gwl (Archambault et al., 2007). Or, l'isoforme longue est la seule qui est exprimée dans la lignée germinale femelle (Archambault et al., 2007). Les cellules somatiques produisent quant à elles les deux formes, qui y sont redondantes fonctionnellement (Archambault et al., 2007). L'allèle *gwl^{Sr18}* affecte donc

spécifiquement la lignée germinale femelle, qui dépend de l'isoforme longue, sans impacter la mitose dans les autres tissus (Archambault et al., 2007). Les mutants *endos* présentent aussi des défauts en méiose : le bris de l'enveloppe nucléaire est retardé dans les ovocytes mutants et ceux-ci échouent à progresser en métaphase I (Von Stetina et al., 2008). Les mouches mutantes pour *endos* sont stériles, puisque leurs ovocytes ne se développent pas (Drummond-Barbosa and Spradling, 2004; Von Stetina et al., 2008). La promotion de la maturation méiotique par Endos est dépendante de sa phosphorylation par Gwl (Kim et al., 2012).

Ces fonctions méiotiques sont conservées. La perte de Gwl cause des défauts dans les ovocytes de souris, de porc et d'étoile de mer, sans toutefois bloquer la méiose I (Adhikari et al., 2014; Li et al., 2013; Okumura et al., 2014). Par ailleurs, les ovocytes de souris déplétés pour ENSA sont bloqués en prophase I (Matthews and Evans, 2014). Gwl semble donc requise pour la progression en méiose II, alors que le rôle des endosulfines semble plutôt être en méiose I. Comme chez la drosophile, la phosphorylation d'Arpp19 par Gwl promeut la maturation méiotique chez le xénope (Dupre et al., 2013). La phosphorylation additionnelle par PKA maintient l'arrêt en prophase I chez cet amphibien (Dupre et al., 2014). À l'inverse, chez la mouche, la phosphorylation d'Endos par PKA n'est pas requise en méiose (Kim et al., 2012).

1.4.6.2 L'arrêt du cycle en cas de carence nutritive

Chez les levures à fission et bourgeonnante, Gwl est activée par le manque de nutriments (Chica et al., 2016; Moreno-Torres et al., 2015; Wanke et al., 2005). La phosphorylation subséquente des endosulfines permet d'enclencher le programme de quiescence des cellules (Bontron et al., 2013; Talarek et al., 2010). Un rôle similaire n'a pas été rapporté pour l'instant chez les animaux.

1.4.6.3 La protection de l'intégrité génomique

Greatwall porte bien son nom de protectrice des chromosomes à plusieurs égards. D'abord, son inhibition de PP2A-B55 est requise pour la reprise du cycle cellulaire après un arrêt induit par la réponse au dommage à l'ADN (Peng et al., 2010;

Wong et al., 2016). De façon similaire, Gwl est nécessaire pour récupérer de l'arrêt en G2 induit par l'irradiation aux rayons ultraviolets de cellules de mélanome humain (Pavey et al., 2020). Fait intéressant, chez la drosophile, PP2A-B55 est impliquée dans la réponse aux dommages à l'ADN induite par ATM (Merigliano et al., 2017).

Par ailleurs, chez l'humain, l'endosulfine ENSA stabilise la protéine Treslin, requise pour l'activation des origines de réplication en phase S, en empêchant sa déphosphorylation par PP2A-B55 (Charrasse et al., 2017). En absence d'ENSA, et dans une moindre mesure en absence de Gwl, les niveaux de Treslin diminuent et la phase S est allongée (Charrasse et al., 2017).

1.4.7 Le module Gwl – endosulfines – PP2A-B55 et les cancers

Les défauts de cycle cellulaire sont répandus dans les cancers. Les cellules tumorales accumulent des mutations qui mènent à une prolifération altérée, à de l'instabilité génomique et/ou à de l'instabilité chromosomique (Manchado et al., 2012). Perturber la voie Gwl – endosulfines – PP2A-B55 cause des défauts de ségrégation des chromosomes et de cytocinèse, défauts qui peuvent mener à de l'instabilité chromosomique (Alvarez-Fernandez et al., 2013; Burgess et al., 2010; Cundell et al., 2013; Diril et al., 2016).

Les complexes PP2A sont globalement perçus comme des suppresseurs de tumeur puisque leur inhibition chimique avec de l'acide okadaïque génère des tumeurs chez la souris (Fujiki and Suganuma, 1993). PP2A-B55 a également été rapporté comme suppresseur de tumeurs par différentes études. Empêcher l'association de B55 au dimère A/C de PP2A en la séquestrant avec des particules virales promeut la transformation cellulaire (Dilworth, 2002; Skoczylas et al., 2004). De plus, des délétions et mutations inactivant B55 ont été identifiées dans des tumeurs du sein, de la prostate et de l'ovaire, de même que dans la leucémie primaire du plasma et la leucémie myéloïde aiguë (Cheng et al., 2011; Curtis et al., 2012; Kamada et al., 2012; Mosca et al., 2013; Shouse et al., 2016). Par ailleurs, les niveaux d'expression de B55 sont diminués dans plusieurs cancers, notamment ceux du poumon, de la thyroïde, de la prostate et la leucémie myéloïde aiguë (Bluemn et al., 2013; Kalev et al., 2012; Ruvolo

et al., 2011). B55 agirait comme suppresseur de tumeur par sa régulation négative de la kinase AKT, qui elle promeut la survie des cellules cancéreuses (Ruvolo, 2016; Ruvolo et al., 2011). PP2A-B55 pourrait toutefois également avoir un rôle oncogénique dans certains contextes; cela a notamment été rapporté dans le cancer du pancréas (Bajpai et al., 2004; Hein et al., 2016; Ory et al., 2003).

Par sa fonction inhibitrice de PP2A-B55, Gwl agit plutôt comme un oncogène. Son expression est augmentée dans de nombreux cancers, incluant des cancers colorectaux, gastriques, du sein, du foie et du cerveau (Alvarez-Fernandez et al., 2018; Cao et al., 2019; Dahlhaus et al., 2016; Rogers et al., 2018; Sun et al., 2017; Tian et al., 2017; Uppada et al., 2018; Vera et al., 2015; Zhuge et al., 2017). Les niveaux élevés de Gwl dans ces cancers corrèlent avec une augmentation de la prolifération, de la migration et de l'invasion cellulaires (Rogers et al., 2018; Uppada et al., 2018; Vera et al., 2015; Wang et al., 2014a). Il est suggéré que le rôle oncogénique de Gwl serait via la régulation de la kinase GSK3 (pour *Glycogen Synthase Kinase 3*), mais il n'est pas clair pour l'instant si c'est par son activation ou son inhibition (Uppada et al., 2018; Vera et al., 2015). Malgré cette incertitude, les niveaux élevés de Gwl corrèlent avec l'activation d'AKT et de la voie anti-apoptotique impliquant la β-Caténine et c-Myc (Uppada et al., 2018; Vera et al., 2015). Par ailleurs, l'inactivation soutenue de PP2A-B55 causée par la surexpression de Gwl entraînerait des défauts mitotiques résultant en instabilité chromosomique (Rogers et al., 2018). Les mécanismes causant la surexpression de Gwl ne sont pas élucidés à ce jour. De plus, les taux de mutations de Gwl dans les cancers sont bas, et les conséquences fonctionnelles de ces mutations sont incomprises (Marzec and Burgess, 2018).

Chez les endosulfines, une surexpression associée à la tumorigenèse a été rapportée pour Arpp19 dans des cancers du sein, du larynx, du foie, de l'estomac, de l'utérus de même que dans la leucémie myéloïde aiguë (Gong et al., 2018; Lu et al., 2015; Ma et al., 2020; Makela et al., 2019; Song et al., 2014; Xie et al., 2020). La surexpression d'Arpp19 dans ces cancers est causée par la diminution des niveaux de microARNs la ciblant (Gong et al., 2018; Lu et al., 2015; Ma et al., 2020; Makela et al., 2019; Song et al., 2014; Xie et al., 2020). Contrairement à Arpp19, la surexpression

d'ENSA ne semble pas avoir d'effet oncogénique (Vera et al., 2015). Cela pourrait s'expliquer par les rôles différents que semblent jouer Arpp19 et ENSA dans la cellule.

L'étude de la voie Gwl – endosulfines – PP2A dans des conditions physiologiques et pathologiques demeure donc importante pour en décortiquer les mécanismes d'actions et développer les outils thérapeutiques permettant de la corriger au besoin.

1.4.8 Objectif général

L'objectif général de ma thèse visait à caractériser en termes mécanistiques la régulation et les fonctions de la phosphatase PP2A-Tws pendant la mitose chez *Drosophila melanogaster*.

1.4.9 Objectifs spécifiques

Objectif 1 : Élucider comment le module Gwl – Endos – PP2A-Tws fonctionne au niveau spatio-temporel, notamment comprendre la nécessité de l'export nucléaire de Gwl en prophase (Chapitre 2).

Objectif 2 : Identifier les substrats mitotiques spécifiques de PP2A-Tws (Chapitre 3).

Chapitre 2

2. Article 1 – Spatiotemporal coordination of Greatwall-Endos-PP2A promotes mitotic progression.

Myreille Larouche[1,2,*], David Kachaner[1,2,*], Peng Wang[1,2], Karine Normandin[1], Damien Garrido[1,2], Changfu Yao[3], Maxime Cormier[1], Kristen M. Johansen[3], Jørgen Johansen[3], Vincent Archambault[1,2,#]

[1] Institut de recherche en immunologie et en cancérologie, Université de Montréal, Montréal, Québec, Canada

[2] Département de Biochimie et médecine moléculaire, Université de Montréal, Montréal, Québec, Canada

[3] Roy J. Carver Department of Biochemistry, Biophysics, and Molecular Biology, Iowa State University, Ames, Iowa, United States of America.

*Contributed equally.

#Corresponding author: vincent.archambault.1@umontreal.ca

2.1 Contexte

De précédents travaux effectués chez la drosophile et dans les cellules mammifères ont montré que Gwl doit se relocaliser au cytoplasme avant le bris de l'enveloppe nucléaire pour remplir correctement ses fonctions (Alvarez-Fernandez et al., 2013; Wang et al., 2013). En théorie, la cible de Gwl, Endos, est assez petite pour pourvoir diffuser librement entre le noyau et le cytoplasme. L'objectif du présent chapitre était de déterminer comment la relocalisation de Gwl sert sa fonction en mitose.

2.2 Contributions des auteurs

Myreille Larouche a conceptualisé, conçu et réalisé les expériences (Figure 2.1B-D, Figure 2.2, Figure 2.3B-F, Figure 2.4A-B, Figure 2.5A-B, D, Figure 2.7A, Figure 2.8, Figure 2.9, Figure S2.1A-B, D-E, Figure S2.2, Figure S2.3C-D, Figure S2.4B-E, Figure S2.5C-F), analysé les données, préparé les figures pour le manuscrit, écrit le manuscrit.

David Kachaner a conceptualisé, conçu et réalisé les expériences (Figure 2.3A, Figure 2.4A-B, Figure 2.5, Figure 2.6, Figure S2.3A-B, Figure S2.4F, Figure S2.5A-B).

Peng Wang a conceptualisé, conçu et réalisé les expériences de la Figure 2.1A.

Karine Normandin a participé aux expériences présentées à la Figure 2.3B-F et a réalisé les expériences dans les cellules humaines et préparé la Figure 2.4C-D.

Damien Garrido a analysé et préparé les images pour la Figure 2.5.

Changfu Yao a conçu et réalisé les expériences d'injection dans l'embryon présentées à la Figure 2.5C.

Maxime Cormier a généré des réactifs et réalisé des expériences préliminaires pour la Figure 2.3 et la Figure S2.3A-B.

Kristen M. Johansen a supervisé le travail réalisé pour la Figure 2.5C.

Jørgen Johansen a supervisé le travail réalisé pour la Figure 2.5C.

Vincent Archambault a conceptualisé, conçu et réalisé les expériences (Figure 2.2, Figure S2.1C-D, Figure S2.4A-B), analysé les données, préparé les figures pour le manuscrit, écrit le manuscrit.

2.3 Abstract

Mitotic entry involves inhibition of Protein Phosphatase 2A bound to its B55/Tws regulatory subunit (PP2A-B55/Tws), which dephosphorylates substrates of mitotic kinases. This inhibition is induced when Greatwall phosphorylates Endos, turning it into an inhibitor of PP2A-Tws. How this mechanism operates spatiotemporally in the cell is incompletely understood. We previously reported that the nuclear export of Greatwall in prophase promotes mitotic progression. Here we examine the importance of the localized activities of PP2A-Tws and Endos for mitotic regulation. We find that Tws shuttles through the nucleus via a conserved Nuclear Localization Signal (NLS), but expression of Tws in the cytoplasm and not in the nucleus rescues the development of *tws* mutants. Moreover, we show that Endos must be in the cytoplasm before nuclear envelope breakdown (NEB) to be efficiently phosphorylated by Greatwall, and to bind and inhibit PP2A-Tws. Disrupting the cytoplasmic function of Endos before NEB results in subsequent mitotic defects. Evidence suggests that this spatiotemporal regulation is conserved in humans.

2.4 Introduction

Reversible phosphorylation plays a major role in the regulation of the cell division cycle. In this process, hundreds of proteins are sequentially phosphorylated and dephosphorylated by an evolutionarily conserved network of kinases and phosphatases. Cyclin-dependent kinase 1 (Cdk1) is a key initiator of mitosis, triggering chromosome condensation, nuclear envelope breakdown (NEB) and spindle formation (Lindqvist et al., 2009; Morgan, 2007). Mostly cytoplasmic in interphase, Cyclin B-Cdk1 is concentrated in the nucleus as it becomes active before NEB (Gavet and Pines, 2010a; Gavet and Pines, 2010b; Pines and Hunter, 1991). Other mitotic kinases, including those of the Polo and Aurora families, are also required for mitotic entry and progression (Archambault and Glover, 2009; Carmena et al., 2012b). Changes in localization are extensively and variously used by these kinases to help them reach their substrates during mitosis (Archambault and Glover, 2009; Carmena et al., 2009; Pintard and

Archambault, 2018).

To allow cells to complete mitosis and re-enter interphase, many mitotic substrates must be dephosphorylated. Several phosphatases contribute to this transition (mitotic exit), including Protein Phosphatases 1 and 2A (PP1 and PP2A) (Holder et al., 2019; Moura and Conde, 2019). PP2A generally functions as a heterotrimeric enzyme comprising a catalytic subunit (C), a scaffold subunit (A) and a regulatory subunit. The latter can be of several types (B, B', B'', B''') that differ in their structures and subcellular localizations, conferring substrate specificity to PP2A (Lambrecht et al., 2013). In animal cells, PP2A in complex with its B-type/B55 regulatory subunits (Tws in *Drosophila*) promotes mitotic exit as it dephosphorylates substrates of Cdk1 and other mitotic kinases (Castilho et al., 2009; Cundell et al., 2016; Mayer-Jaekel et al., 1994; Mochida et al., 2009; Schmitz et al., 2010).

Inhibition of PP2A-B55 is required during mitotic entry to promote the phosphorylated state of mitotic kinase substrates (Mochida et al., 2009). The Greatwall kinase (Gwl; Mastl in humans) antagonizes PP2A-B55 (Castilho et al., 2009; Vigneron et al., 2009; Wang et al., 2011; Yu et al., 2004). Gwl targets Endosulfines (ENSA and Arpp19 in *Xenopus* and humans, Endos in *Drosophila*) to turn them into potent and selective inhibitors of PP2A-B55 (Gharbi-Ayachi et al., 2010; Mochida et al., 2010; Rangone et al., 2011). Gwl activation requires its CDK-dependent phosphorylation in the activation loop and its autophosphorylation in the C-terminal tail (Blake-Hodek et al., 2012; Yu et al., 2006). Activated Gwl phosphorylates a conserved site corresponding to Ser68 of *Drosophila* Endos. Once phosphorylated by Gwl, Endosulfines become substrates of PP2A-B55 with very high affinity but very slow dephosphorylation kinetics, effectively acting as competitive inhibitors of PP2A-B55 (Mochida, 2014; Williams et al., 2014). At the onset of mitotic exit, the Anaphase-Promoting Complex / Cyclosome (APC/C) triggers the degradation of Cyclin B, resulting in Cdk1 inactivation, which in turn facilitates PP1-dependent inactivation of Gwl (Heim et al., 2015; Ma et al., 2016). Because most PP2A-B55 substrates have a much lower affinity to PP2A-B55 than Endosulfines, their dephosphorylation is inhibited as long as Gwl is active (Williams et

96

al., 2014). This mechanism helps in the ordering of events of mitotic exit (Cundell et al., 2013).

The Gwl-Endos-PP2A module is strongly conserved, regulating mitosis in fungi, insects and vertebrates (Garcia-Blanco et al., 2019). In frog and starfish oocytes, Gwl is required for M-phase entry and maintenance (Hara et al., 2012; Lorca et al., 2010; Yu et al., 2006). In HeLa cells, complete depletion of Mastl can also result in a G2 arrest, but cells partially depleted of Mastl enter a defective mitosis (Burgess et al., 2010; Voets and Wolthuis, 2010). In *Drosophila* cells and mouse embryonic fibroblasts, the loss of Gwl or Endosulfine function does not prevent mitotic entry, but leads to mitotic defects where chromosomes become partially decondensed and scattered along aberrant mitotic spindles (Alvarez-Fernandez et al., 2013; Rangone et al., 2011; Voets and Wolthuis, 2010; Yu et al., 2004). *gwl* and *endos* are essential for viability in *Drosophila*, and hypomorphic mutants are defective in female meiosis (Archambault et al., 2007; Von Stetina et al., 2008).

Like the other major mitotic kinases, Gwl relies on spatial regulation for its function (Alvarez-Fernandez and Malumbres, 2014; Wang et al., 2014b). In *Drosophila*, Gwl is strongly concentrated in the nucleus in interphase (Yu et al., 2004). Nuclear import of Gwl is mediated by two Nuclear Localization Signals (NLSs) within a central region that interrupts the kinase domain (Wang et al., 2013). In prophase, Gwl suddenly relocalizes to the cytoplasm until it is excluded from the nucleus before NEB. This relocalization requires Gwl kinase activity, phosphorylation of Gwl near its NLSs, and Crm1-dependent export of Gwl (Wang et al., 2013; Wang et al., 2016). This spatial regulation of Gwl is generally conserved in vertebrates (Alvarez-Fernandez et al., 2013; Yamamoto et al., 2014). In both *Drosophila* and mammalian cells, preventing Gwl nuclear localization in interphase or its cytoplasmic localization in prophase disrupts its function, resulting in mitotic defects and collapse (Alvarez-Fernandez et al., 2013; Wang et al., 2013). Disrupting the nuclear localization of Gwl in *Xenopus* eggs prevents mitotic entry in extracts from these eggs (Yamamoto et al., 2014).

Because Gwl activation requires its phosphorylation at CDK sites, and because active Cyclin B-Cdk1 is imported into the nucleus at the G2/M transition, the nuclear

localization of Gwl likely helps its activation (Alvarez-Fernandez et al., 2013; Wang et al., 2013). However, it is unclear why Gwl needs to relocalize to the cytoplasm. We hypothesized that the phosphorylation by Gwl of Endosulfines to induce their binding and inhibition of PP2A-B55 before NEB is an obligatory cytoplasmic event. However, little is known about Endosulfines' localization dynamics and the functional importance of their localization. Moreover, while B55 regulatory subunits of PP2A appear mostly cytoplasmic in interphase in humans and *Drosophila*, the functional requirements and regulation of their localization are poorly understood (Alvarez-Fernandez et al., 2013; Mayer-Jaekel et al., 1994; Santos et al., 2012).

Here, we show that in *Drosophila,* Endos and PP2A-Tws must be in the cytoplasm to play their essential roles in mitotic regulation. We show that active Gwl must access the cytoplasm to phosphorylate Endos and induce its inhibitory interaction with PP2A-Tws. Failures in this process lead to mitotic defects. Our findings provide a mechanistic understanding of the essential spatiotemporal regulation of the Gwl-Endosulfine-PP2A module.

2.5 Results

2.5.1 PP2A-Tws functions primarily in the cytoplasm.

To begin investigating the spatiotemporal dynamics of the Gwl-Endos-PP2A module, we examined the localization of Tws. We found that Tws-GFP is more concentrated in the cytoplasm than in the nucleus in D-Mel (d.mel-2) cells in culture (Figure 2.1Aa). This is consistent with immunofluorescence results for Tws in embryos and with the localization of B55α and B55δ in human cells (Alvarez-Fernandez et al., 2013; Mayer-Jaekel et al., 1994; Santos et al., 2012). Because we detected some Tws-GFP in the nucleus, we tested if it shuttles between the cytoplasm and the nucleus. We treated cells with Leptomycin B (LMB), an inhibitor of Crm1-dependent nuclear export. As a result, Tws-GFP accumulates in the nucleus (Figure 2.1Ab). This accumulation is also observed for Tws-Flag (Figure S2.1A). We used live imaging to visualize the localization shift of Tws-GFP. Within 180 minutes after LMB addition, the

nuclear/cytoplasmic ratio of Tws-GFP intensity increases almost 10-fold (Figure 2.1B-C). Therefore, Tws-GFP can transit through the nucleus. We searched for a Nuclear Localization Signal (NLS) in Tws, and found a candidate motif that is conserved in human B55α (and B55δ), where it is part of a loop oriented outwards in the crystal structure (Figure 2.1D). Mutation of this motif abolishes the nuclear retention of Tws-GFP upon treatment of cells with LMB (Figure 2.1Ac-d, B and C). We conclude that Tws-GFP undergoes nucleocytoplasmic shuttling.
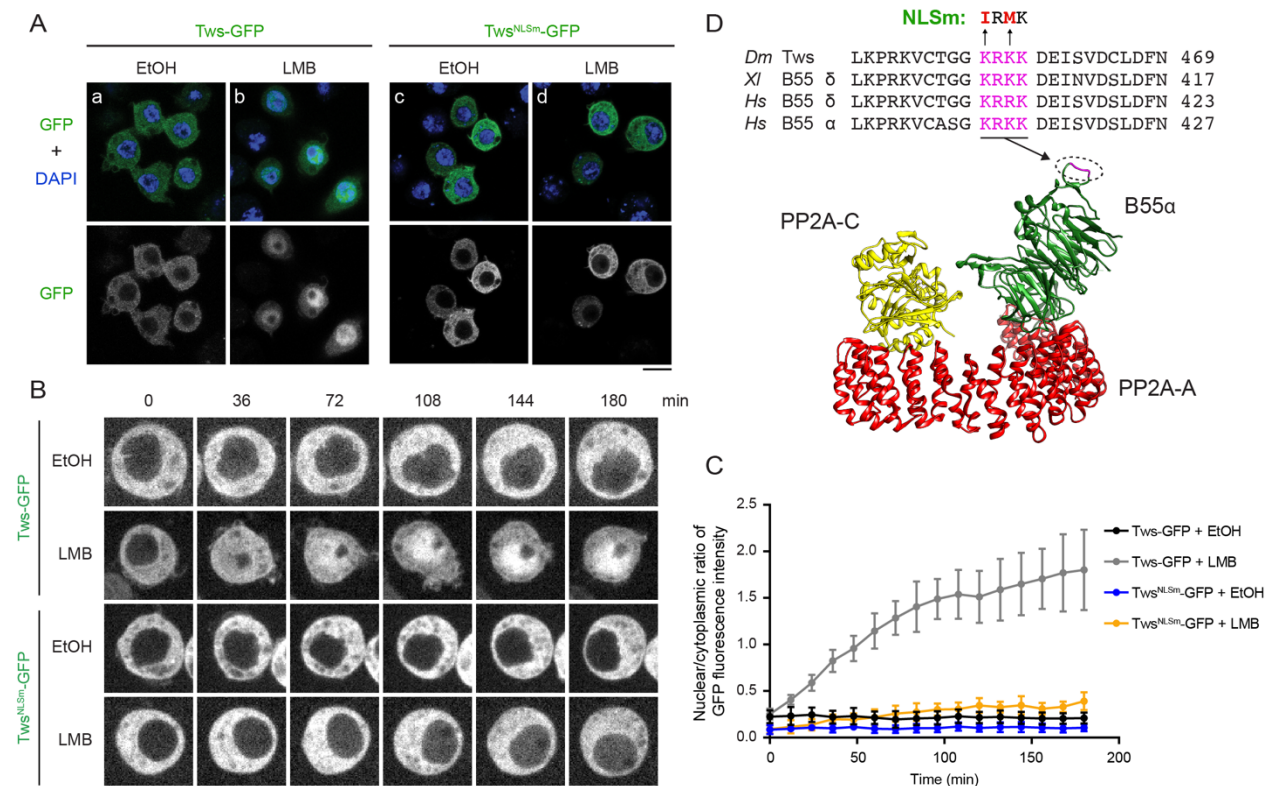
Figure 2.1. Tws is primarily cytoplasmic but shuttles through the nucleus.

(A) D-Mel cells expressing Tws-GFP or Tws^{NLSm}-GFP (NLS mutant: K455I, K457M) were treated with 50 nM Leptomycin B (LMB; b-d) or 0,1% ethanol (EtOH, mock control, a-c) for 2 hours before fixation and DNA staining with DAPI. Scale bar: 10 μm. (B) Cells expressing Tws-GFP or Tws^{NLSm}-GFP were treated with LMB or EtOH and imaged. Scale bar: 5 μm. (C) The nuclear/cytoplasmic ratio of GFP fluorescence intensity from movies in B was quantified through time (10 cells for each condition, mean ± SD). (D) Tws contains a NLS that is conserved in vertebrate B55 orthologs. Top: sequence alignment showing the NLS in magenta. *Dm*: *Drosophila melanogaster*; *Xl*: *Xenopus laevis*; *Hs*: *Homo sapiens*. Mutations introduced to inactivate the NLS in Tws are shown in red. Bottom: location of the identified NLS in the structure of the human PP2A-B55α complex bound to microcystin-LR (PDB 3DW8)(Xu et al., 2008).

To test the genetic requirements of Tws localization *in vivo*, we generated flies allowing for inducible expression of various GFP-fused forms of Tws with altered localizations using the Gal4-UAS system (Figure 2.2A). In addition to Tws-GFP and Tws^{NLSm}-GFP, we generated a form of Tws-GFP fused to 2 repeats of the NLS from the SV40 virus (NLS^{SV40}-Tws-GFP) to force its localization into the nucleus. As a control, we created an analogous variant where amino-acid substitutions were introduced to inactivate the NLS (NLSm^{SV40}-Tws-GFP). To assess the differences in localization of Tws variants, we expressed them ubiquitously using the *Ubiquitin-Gal4* (*Ubi-Gal4*) driver, which allows moderate overexpression relative to endogenous Tws (Figure S2.1B).
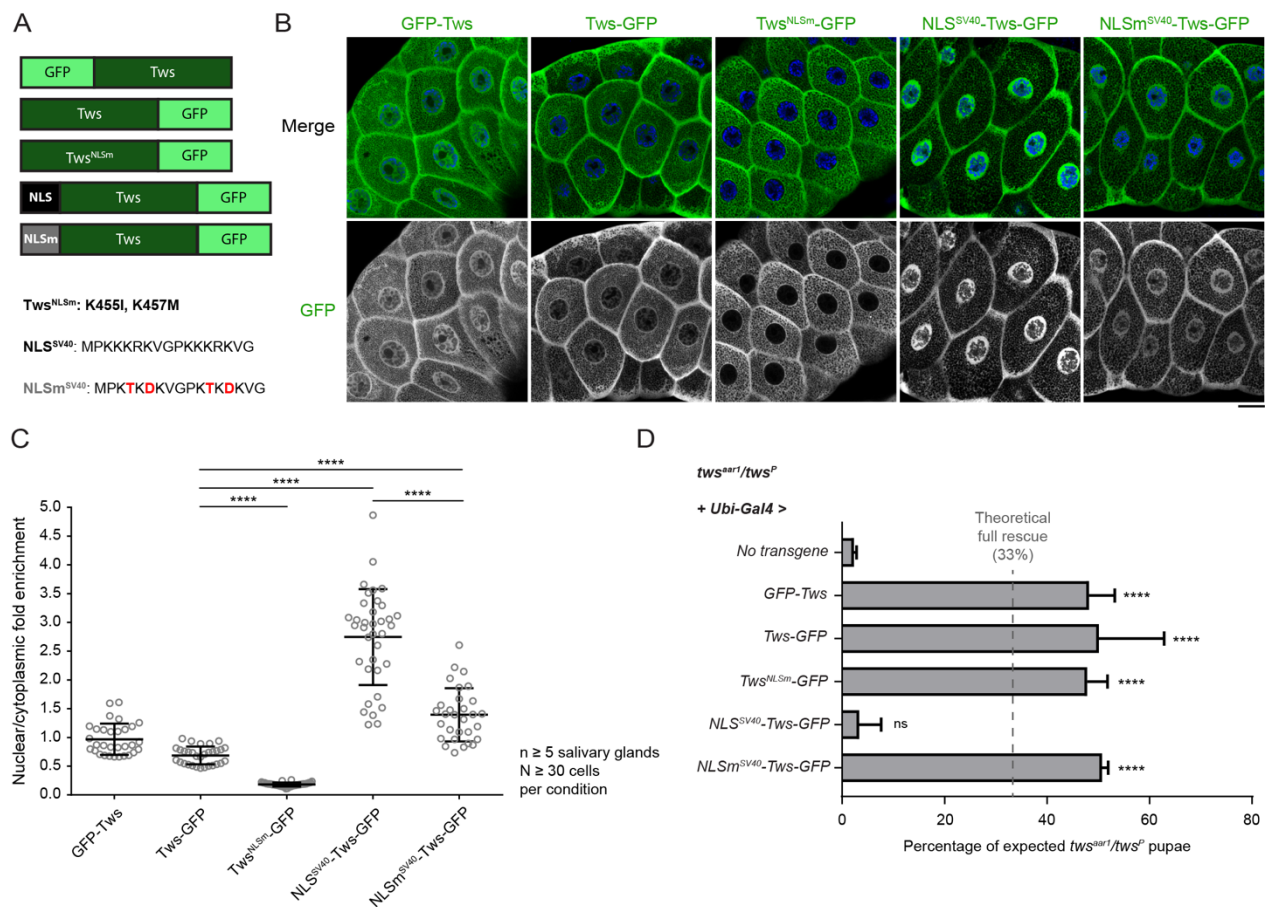
Figure 2.2 Tws function is required in the cytoplasm.

(A) Tws-GFP variants constructed for transgenic expression. Tws-GFP was fused to two copies of the SV40 virus NLS (NLS^{SV40}) or to a mutated form (NLSm^{SV40}, substitutions in red). (B) The localization of Tws variants fused to GFP was visualized in 3rd instar larval tissues. Salivary glands cells are shown (see also brain cells in Fig S2.1). Transgenes were under the *UASp* promoter and expression was driven by *Ubi-Gal4*. Merge images show GFP (green) and DNA stained with Hoescht 33342 (blue). Scale bar: 20 μm. C. The nuclear/cytoplasmic ratio of GFP intensity was quantified (mean ± SD). D. Genetic rescue of *tws^{aar1}/tws^P* mutant flies by the expression of the indicated Tws variants. Values shown correspond to percentages of eclosed *tws^{aar1}/tws^P* pupae (*Tb$^+$*) relative to the expected number of *tws^{aar1}/tws^P* pupae calculated from the total number of eclosed pupae. See Materials & Methods for details. Values are averages of 3 independent experiments in which between 110 and 1252 eclosed pupae were scored for each cross. Error bars: SD. **** *p* ≤ 0.0001. ns: non-significant.

None of the constructions are toxic in this context as animals develop into healthy adults. In addition, all GFP-fused Tws variants are capable of assembling into trimeric complexes with PP2A-29B and Mts (Figure S2.1C). In all tissues examined, Tws-GFP is concentrated in the cytoplasm. Differences in localization between the Tws-GFP variants are most obvious in the large endoreplicating cells of the larval salivary glands (Figure 2.2B-C). We found that while a minor fraction of Tws-GFP is nuclear, Tws^{NLSm}-GFP is completely restricted to the cytoplasm. Conversely, NLS^{SV40}-Tws-GFP is enriched in the nucleus, as expected. Mutation of the NLS^{SV40} abrogates this nuclear enrichment. Similar localization patterns are observed in proliferating cells of the larval brain (Figure S2.1D). GFP-Tws (N-terminal tag) generally localizes largely to the cytoplasm although its nuclear and cytoplasmic levels are similar in salivary glands. In addition, all variants localize to the cell cortex in this tissue (Figure 2.2B).

We then tested the ability of these Tws variants to rescue the development of *tws* mutant flies. We expressed the Tws variants in developing animals transheterozygous for the *tws^{aar1}* and *tws^P* strongly hypomorpic alleles (Gomes et al., 1993; Uemura et al., 1993). These animals die mostly in late pupal development, with rare eclosing adults (Mayer-Jaekel et al., 1994). We found that ubiquitous expression of either GFP-Tws or Tws-GFP using the *Ubi-Gal4* driver efficiently rescues development until adulthood (Figure 2.2D), indicating that both fusion proteins are functional (although rescued flies

tend to die in the food quickly after eclosion). A full rescue is also obtained with the expression of Tws^{NLSm}-GFP, which restricts Tws activity to the cytoplasm. This result indicates that Tws activity in the nucleus is not required, and that Tws activity in the cytoplasm is sufficient for *Drosophila* development to adulthood. Moreover, expression of NLS^{SV40}-Tws-GFP does not rescue *tws^{aar1}/tws^P* animals, while expression of the NLSm^{SV40}-Tws-GFP control does rescue them (Figure 2.2D). The failure of NLS^{SV40}-Tws-GFP to rescue may be partly due to its reduced incorporation into PP2A trimers (Figure S2.1C). Nevertheless, this result is consistent with the full rescue obtained with Tws^{NLSm}-GFP from which we conclude that PP2A-Tws function is required in the cytoplasm but not in the nucleus during development.

2.5.2 Endos binding and inhibition of PP2A-Tws is mainly controlled by its Gwl phosphorylation site.

Before exploring Endos spatiotemporal dynamics, we wished to determine more precisely the structural requirements for Endos to bind and inhibit PP2A-Tws in *Drosophila*. Several lines of evidence indicate that the inhibition of PP2A-B55 enzymes by Endosulfines is strongly enhanced by the phosphorylation by Gwl at a serine residue within a conserved motif (Ser68 in Endos; Figure S2.2) (Gharbi-Ayachi et al., 2010; Mochida, 2014; Mochida et al., 2010; Rangone et al., 2011; Williams et al., 2014). However, unphosphorylated ENSA from *Xenopus* was shown to partially inhibit PP2A-B55δ, and unphosphorylated Endos from *Drosophila* has been shown to interact with Tws *in vitro* (Kim et al., 2012; Mochida, 2014). Thus, we examined the relative contributions of the Ser68 phosphorylation site in Endos versus its phosphorylation-independent interaction with Tws to the inhibition of PP2A-Tws. As expected, co-immunoprecipitations revealed that a phosphomimetic mutation of Endos at its Gwl site (Endos^{S68D}-Flag) enhances its ability to interact with GFP-Tws (Figure 2.3A). Using a GST pulldown assay, we also verified that the S68D mutation in Endos enhances its ability to interact with Tws-Flag (Figure 2.3B). Nevertheless, Endos^{WT} and Endos^{S68A} also interact specifically with Tws in both assays, indicating that unphosphorylated

102

Endos is also capable of a weak interaction (Figure 2.3A-C). These observations are consistent with previous results where GST-Endos was used to pulldown *in vitro* translated Tws (Kim et al., 2012).
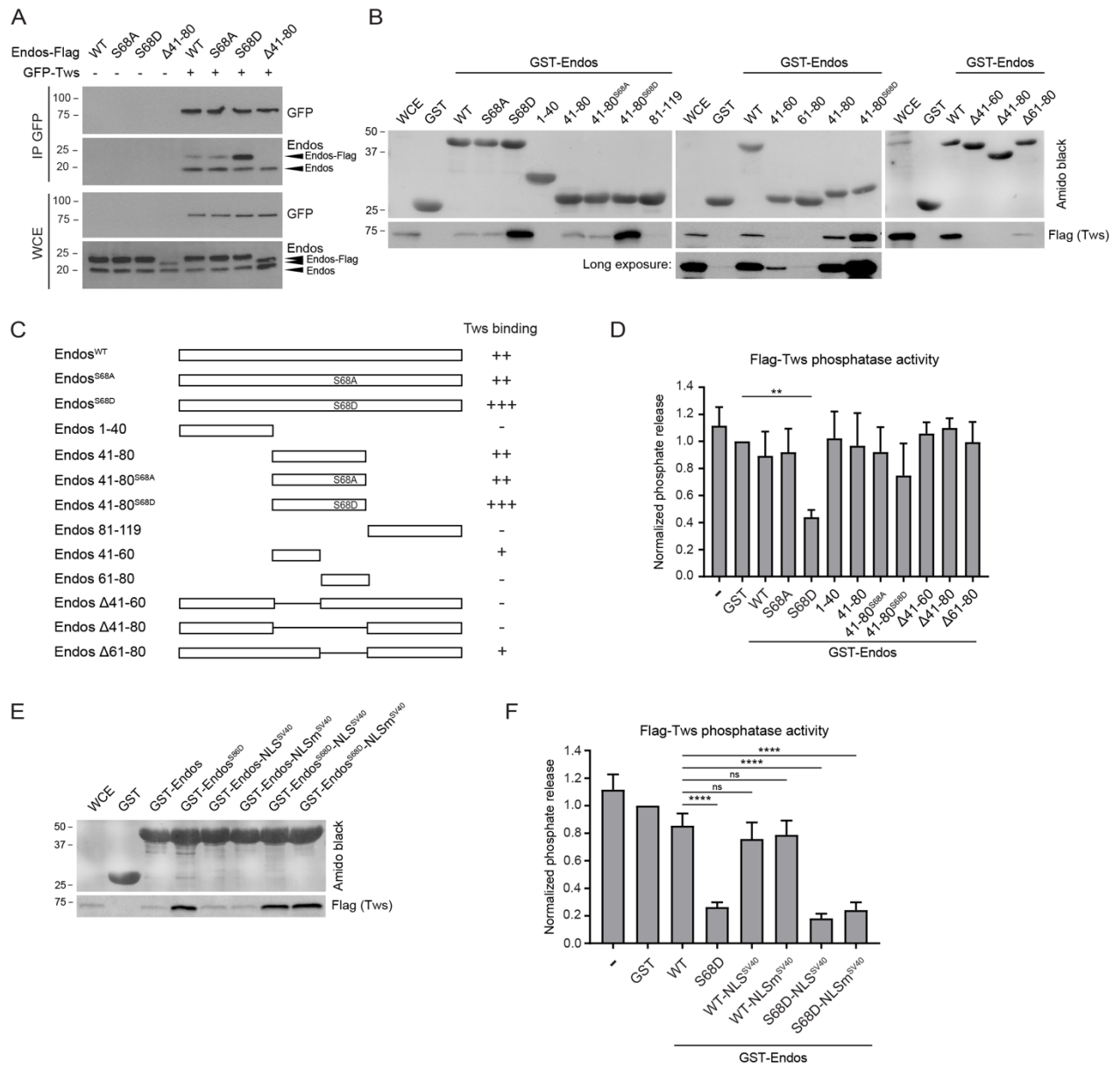
Figure 2.3. Endos binding and inhibition of PP2A-Tws depends mainly on its Gwl phosphorylation site.

(A) D-Mel cells transfected with the indicated proteins were submitted to GFP-Tws immunoprecipitation and products were analyzed by Western blots for GFP and Endos. WCE: whole cell extract. (B) The indicated variants of GST-Endos (or GST alone) were tested for their ability to pulldown Tws-Flag from a cell extract (detected with anti-Flag). (C) Summary of Endos variants tested in panels A and B for their interaction with Tws. (D) The ability of the indicated GST-Endos variants to inhibit PP2A-Tws phosphatase activity towards a phosphopeptide was quantified. ** p = 0.0022. (E-F) C-terminal fusion of the SV40 NLS to Endos does not prevent its ability to bind Tws (E - GST pulldown as in B) or to inhibit PP2A-Tws (F - phosphatase assay as in D). **** p ≤ 0.0001. ns: non-significant. Bars: mean ± SD, n = 3.

To search for the region of Endos responsible for its Ser68-independent association with Tws, we tested truncations of Endos, starting with N-terminal (aa 1-40), central (aa 41-80) and C-terminal (aa 81-119) fragments (Figure 2.3C and S2.2). Of these, only the central fragment of Endos can interact with Tws, similarly to full-length Endos (Figure 2.3B). As expected, the S68D mutation within the central fragment enhances its binding to Tws, while the S68A mutation has no effect. Consistent with these results, deletion of the central region of Endos (Δ41-80) eliminates its interaction with Tws (Figure 2.3A-C). Interestingly, deletion of residues 41-60 also eliminates the interaction, but deletion of residues 61-80 still allows the interaction with Tws (Figure 2.3B-C). Moreover, residues 41-60 of Endos are sufficient for an interaction with Tws, although this binding is weaker compared to the whole central region or full-length Endos. These results indicate that Endos is capable of a weak interaction with Tws even without the Gwl phosphorylation site at Ser68 or residues immediately adjacent to it. Although deletion of residues 61-80 removes the Gwl phosphorylation motif in Endos, it leaves several residues conserved in Endos orthologs, including positively charged residues shown to promote the dephosphoylation of human ENSA by PP2A-B55 (Figure S2.2) (Cundell et al., 2016).

We then tested the ability of the various forms of Endos to inhibit PP2A-Tws phosphatase activity. Flag-Tws was expressed in D-Mel cells, purified and used to measure phosphatase activity *in vitro.* Purified GST-Endos variants were added to the reactions to assess their ability to inhibit PP2A-Tws activity. We found that the S68D

form of Endos markedly inhibits the phosphatase activity, while other forms have little or no effect (Figure 2.3D). While the unphosphorylated central region of *Xenopus* ENSA was found to be capable of PP2A-B55 inhibition *in vitro* (Mochida, 2014), we did not detect a significant inhibition by the unphosphorylated central region of *Drosophila* Endos in our assay. These results suggest that the ability of Endos to bind and inhibit PP2A-Tws is mainly controlled by the Gwl phosphorylation site, and that the phosphorylation-independent interaction between Endos and Tws does not inhibit PP2A-Tws.

Because targeting Tws-GFP to the nucleus by N-Terminal fusion to the NLS^{SV40} reduces its ability to assemble into PP2A trimers in embryos (Figure S2.1C), we wondered if NLS^{SV40} fusion causes a gross misfolding or steric hindrance effect on PP2A-Tws. We used our GST pulldown and phosphatase assay to test it. We found that fusion of the NLS^{SV40} to Tws preserves the catalytic activity of PP2A-Tws and its ability to bind and be inhibited by Endos, indicating that the complex is biochemically functional (Figure S2.1E-F).

2.5.3 Endos is a predominantly cytoplasmic protein.

It was hypothesized that the export of Gwl is required for its phosphorylation of Endos in the cytoplasm, leading to PP2A-Tws inhibition in the cytoplasm before NEB, thereby preventing mitotic collapse after NEB (Alvarez-Fernandez et al., 2013; Wang et al., 2013). To begin testing this hypothesis, we wished to determine the subcellular localization of Endos. We first examined Endos in fusion with various fluorescent or epitope tags in D-Mel cells in culture. While Endos-Flag and Endos-PrA are enriched in the cytoplasm, Endos-Myc, Endos-GFP and Endos-RFP are more evenly distributed between the cytoplasm and the nucleus (Figure S2.3A). These distributions are confirmed by subcellular fractionation (Figure S2.3B). Thus, fusion of a tag on Endos (a small protein of 119 aa residues) can affect its nucleo-cytoplasmic distribution in interphase. To determine the localization of endogenous Endos, we raised polyclonal antibodies against Endos. The purified antibodies recognize a band near the expected

molecular mass of 13 kDa, and this band is not detected upon Endos RNAi (Figure 2.4A). In immunofluorescence, anti-Endos antibodies reveal a cytoplasmic staining with little or no signal in the nucleus in interphase (Figure 2.4B). This cytoplasmic signal is strongly decreased following Endos RNAi, indicating that the signal is specific to Endos. In addition, subcellular fractionation shows that endogenous Endos is strongly enriched in the cytoplasmic fraction (Figure S2.3B). Treating cells with LMB causes an only minor increase in nuclear Endos staining, suggesting that Endos does not actively shuttle through the nuclear pores (Figure S2.3C). In mitotic cells, our antibodies do not reveal Endos staining to particular structures (Figure S2.3D).
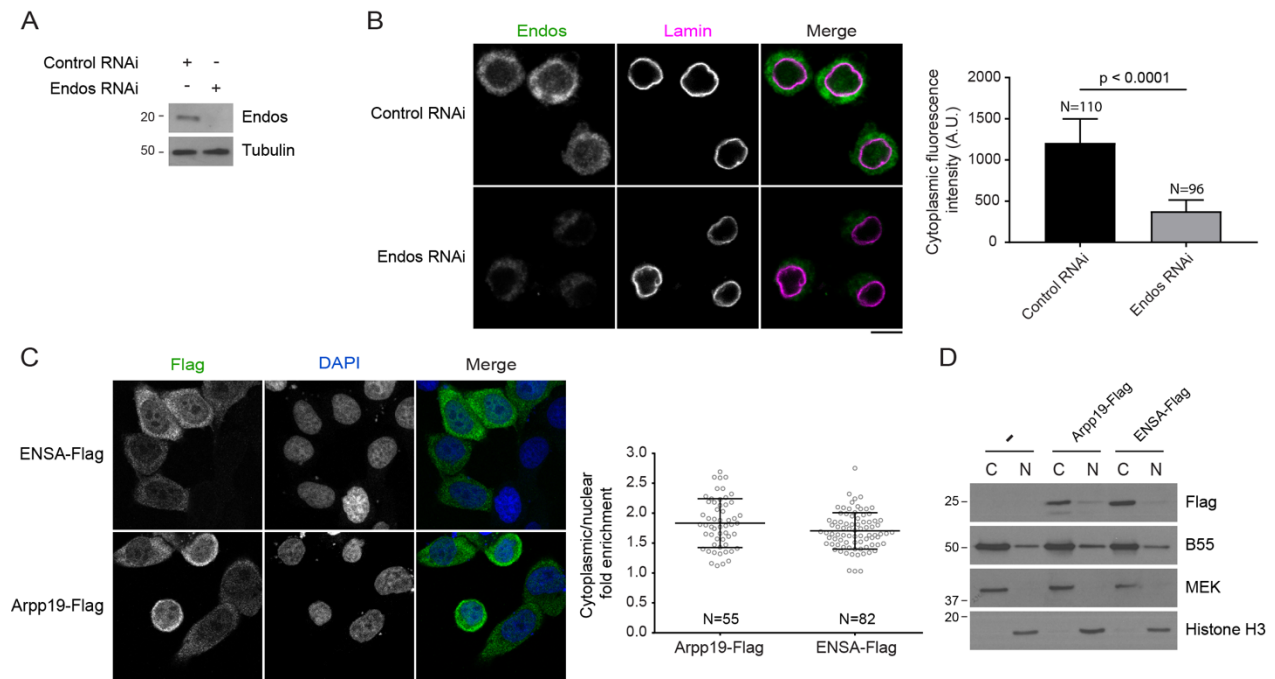
Figure 2.4. Endos and its human orthologs are enriched in the cytoplasm.

(A) The specificity of antibodies against Endos is verified by RNAi and Western blot. (B) Immunofluorescence reveals that Endos is mainly cytoplasmic. Left: representative images. Scale bar: 5 μm. Right: quantifications of the cytoplasmic signal. (C) Immunofluorescence reveals that Endos-Flag and Arpp19-Flag are mainly cytoplasmic. Left: representative images. Scale bar: 20 μm. Right: quantifications of the cytoplasmic/nuclear ratio of signal intensities. (D) Subcellular fractionation and Western blots show the relative amounts of cytoplasmic, C, and nuclear, N, proteins. MEK and Histone H3 are controls as cytoplasmic and nuclear proteins, respectively. Bars: mean ± SD. N = number of cells quantified.

The subcellular localizations of human ENSA and Arpp19, the two human orthologs of Endos, have not been firmly established and staining patterns reported with commercially available antibodies diverge. We generated ENSA-Flag and Arpp19-Flag fusions and examined their localization in HeLa cells by immunofluorescence. Both ENSA-Flag and Arpp19-Flag are enriched in the cytoplasm (Figure 2.4C). This is also confirmed by subcellular fractionation (Figure 2.4D). These results suggest that like *Drosophila* Endos, human ENSA and Arpp19 are predominantly cytoplasmic proteins.

2.5.4 Endos-RFP and GFP-Tws show dynamic localizations in syncytial embryos.

The only previous attempt to determine the localization of Endos examined Endos fused to GFP (Rangone et al., 2011). In syncytial embryos, Endos-EGFP concentrates in the nuclear/spindle areas as nuclei enter mitosis, before dispersing back in the cytoplasm after anaphase (Rangone et al., 2011). The significance of this localization dynamics remained unknown. We observed a very similar localization pattern with embryos expressing Endos-RFP (Figure 2.5A), indicating that it is not specific to the EGFP tag.
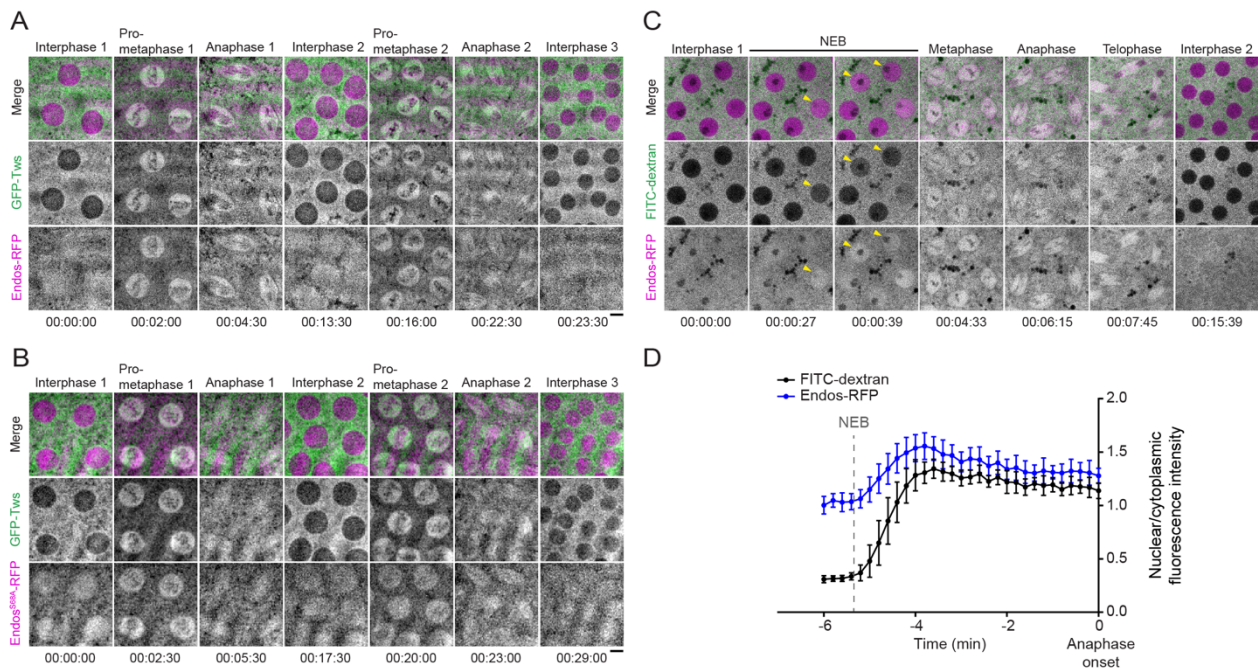
Figure 2.5. Dynamic localization of Endos-RFP and GFP-Tws in syncytial embryos.

(A) Time-lapse imaging reveals that GFP-Tws is enriched in the cytoplasm in interphase and becomes enriched in the nuclear/spindle area simultaneously with Endos-RFP in prometaphase until anaphase. (B) The S68A mutation does not alter the localization dynamics of Endos-RFP. For A-B, images from multiple z-steps were combined in an average intensity projection. (C) Time-lapse imaging of an embryo expressing Endos-RFP and injected with 70 kDa FITC-dextran to mark the time of NEB. Endos-RFP is homogenously dispersed throughout the syncytial embryo in interphase until NEB, when it becomes enriched in the nuclear/spindle area. Images shown are for a single focal plane. (D) The nuclear/cytoplasmic ratios of FITC-dextran and Endos-RFP fluorescence intensities from movie in C were quantified through time relative to anaphase onset. Values are averages of 14 nuclei. Error bars: SD. Scale bars: 5 μm.

Morever, immunofluorescence against endogenous Endos in embryos similarly reveals an enrichment of Endos in the nuclear areas in prometaphase, along with a cytoplasmic pool (Figure S2.4A). We also verified that ubiquitous expression of Endos-RFP completely rescues the development of $endos^1/Df$ flies, indicating that Endos-RFP is fully functional (Figure S2.4B). As expected, expression of Endos^{S68A}-RFP or Endos$^{\Delta 41-80}$-RFP does not rescue the mutant. To examine how the localization of Endos-RFP relates to the localization of its target Tws in embryos, we generated transgenic flies co-expressing Endos-RFP and GFP-Tws. Interestingly, GFP-Tws shows similar dynamics to Endos-RFP, as both proteins become concentrated in the nuclear/spindle areas when nuclei enter mitosis (Figure 2.5A). However, unlike Endos-RFP, GFP-Tws is strongly concentrated in the cytoplasm in interphase, appearing largely excluded from nuclei in interphase. We hypothesized that Endos-RFP is recruited to the nuclear/spindle areas by its interaction with Tws. However, we found that the S68A mutation in Endos-RFP does not abolish its concentration to nuclear/spindle areas, nor does the S68D mutation affect it in an obvious manner (Figure 2.5B, S2.4C). Moreover, deletion of Endos residues 41-60 or 41-80 which are required for its interaction with Tws, does not abrogate Endos-RFP enrichment to the spindle areas (Figure S2.4D-E). Therefore, the localization of Endos-RFP to the nuclear/spindle areas in mitosis is not mediated by its interaction with Tws.

To test if Endos-RFP is actively imported into the nucleus before NEB in syncytial embryos, we injected FITC-coupled 70 kDa dextran in interphase. This FITC-dextran is

too large to diffuse through the nuclear pores and can only enter the nuclear area after NEB. We found that Endos-RFP becomes enriched in the nuclear areas simultaneously with FITC-dextran, after NEB (Figure 2.5C-D). Thus, the localization dynamics of Endos-RFP does not reflect an active nuclear import through nuclear pores before NEB. Rather, the mitotic localization of Endos-RFP and GFP-Tws resembles the spindle matrix, a gel-like structure derived from an array of nuclear proteins that appears particularly clearly in *Drosophila* syncytial embryos (discussed below) (Johansen and Johansen, 2009; Johansen et al., 2011; Woodruff, 2018). Other cell cycle regulators are known to be enriched or excluded from the spindle matrix, but the functional significance of these localizations is still unclear (Huang et al., 2018; Lince-Faria et al., 2009; Schweizer et al., 2014; Yao et al., 2018).

2.5.5 Gwl phosphorylates Endos in the cytoplasm to promote its interaction with Tws.

Our results have established that Endos is a predominantly cytoplasmic protein in interphase, and we previously showed that Gwl is exported from the nucleus to the cytoplasm in prophase (Wang et al., 2013; Wang et al., 2016). Thus, we next sought to test if the phosphorylation of Endos by Gwl is an obligatory cytoplasmic event. To this end, we overexpressed in D-Mel cells various forms of Gwl-Myc with different localizations and kinase activity levels (Figure 2.6A). We monitored Endos phosphorylation levels using a phosphospecific antibody against pS68-Endos (Figure S2.4F). Overexpression of Gwl^{WT}-Myc has at most a marginal effect on pS68-Endos levels (Figure 2.6B). This was expected because Gwl is thought to become fully active only when cells enter mitosis (Castro and Lorca, 2018). Expression of the kinase-dead Gwl^{K87R}-Myc has no effect (Figure 2.6B). To make a constitutively active form of Gwl, we introduced the K97M (Scant) mutation (Archambault et al., 2007). Again, no increase in pS68-Endos levels is observed, consistent with the fact that Gwl^{K97M}-Myc is restricted to the nucleus in interphase (Figure 2.6A), while Endos is in the cytoplasm. To force the localization of Gwl to the cytoplasm, we mutated the two previously reported NLS motifs

(Wang et al., 2013). Cytoplasmic retention of Gwl^{NLSm}-Myc in interphase is not sufficient to induce an increase in pS68-Endos, again consistent with the idea that Gwl becomes fully active only as cells enter mitosis. Strikingly, when mutations making Gwl constitutively active and cytoplasmic are combined (Gwl$^{K97M,\ NLSm}$-Myc), pS68-Endos levels are clearly increased (Figure 2.6B). Mutation of the NES in Gwl has no effect. To test if the levels of pS68-Endos obtained with the expression of the various forms of Gwl correlate with the ability of Endos to interact with PP2A-Tws, we probed the interaction by co-immunoprecipitation between the endogenous proteins. As expected, the interaction between Endos and Tws is increased only with active Gwl in the cytoplasm (Gwl$^{K97M,\ NLSm}$-Myc, Figure 2.6C). We conclude that the presence of active Gwl in the cytoplasm is necessary and sufficient for the phosphorylation of Endos at Ser68 and for its interaction with PP2A-Tws.
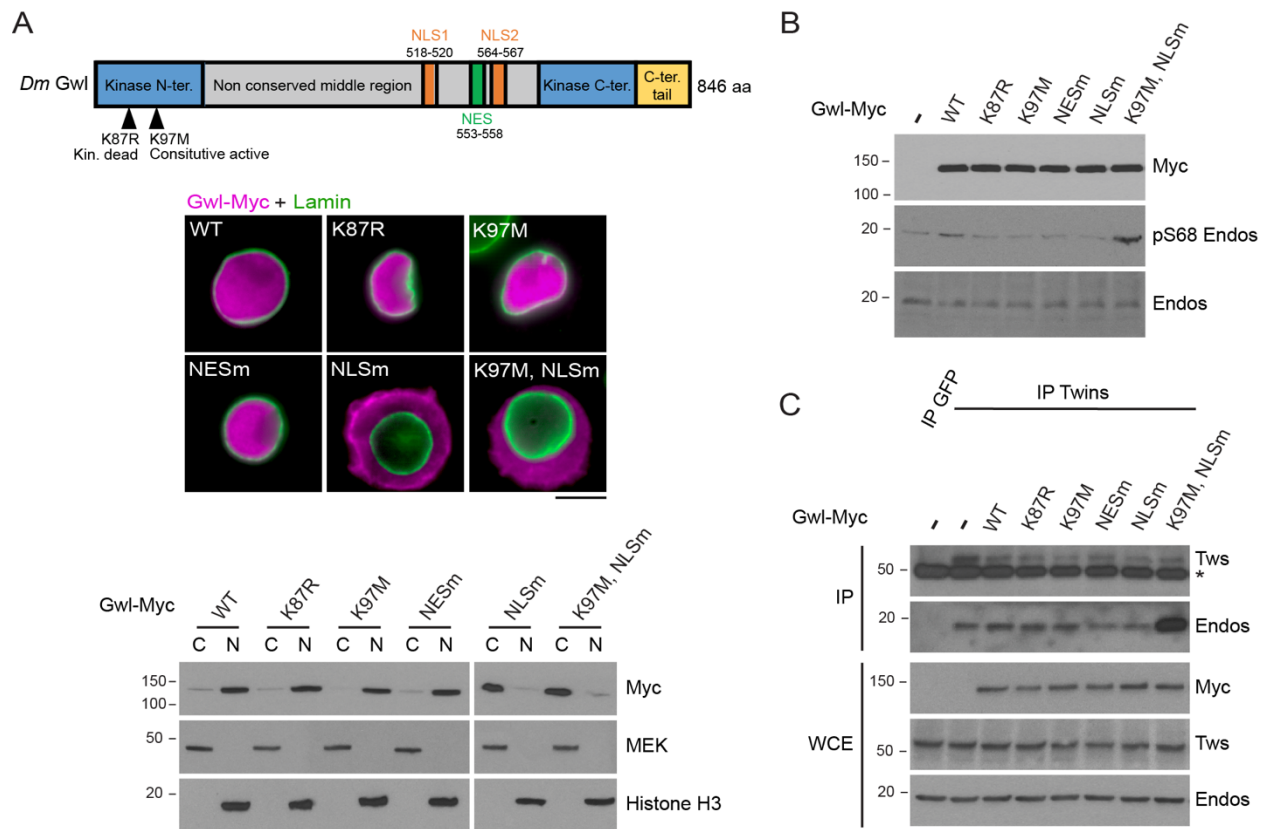
Figure 2.6. Active Gwl in the cytoplasm is necessary and sufficient for the induction of Endos phosphorylation and interaction with PP2A-Tws.

(A) Mutations in Gwl used to alter its kinase activity and localization. Top: location of the mutations in the primary structure. Middle: Immunofluorescence showing the localization of the Gwl-Myc variants. Bottom: subcellular fractionation and Western blots showing the relative amounts of cytoplasmic, C, and nuclear, N, proteins. MEK and Histone H3 are controls as cytoplasmic and nuclear proteins, respectively. (B) Expression of the constitutively active and cytoplasmic Gwl^{K97M,NLSm}-Myc increases levels of pS68-Endos. Cells were transfected with the indicated constructs, treated with 100 nM okadaic acid for 1 h and analyzed by Western blots. (C) Expression of the constitutively active cytoplasmic Gwl^{K97M,NLSm}-Myc enhances the interaction between Endos and Tws. Cells were transfected with the indicated constructs and submitted to Tws immunoprecipitations. Products were analyzed by Western blots. *IgG. WCE: whole cell extract.

To test if the cytoplasmic localization of Endos is required for its phosphorylation by Gwl and its interaction with PP2A-Tws, we disrupted the localization of Endos-Flag. We fused Endos to the SV40 NLS. The resulting Endos-NLS^{SV40}-Flag is strongly enriched in the nucleus, unlike Endos-Flag, which is mainly cytoplasmic (Figure 2.7A). As a control, we generated a variant with the SV40 NLS inactivated by mutations. The resulting Endos-NLSm^{SV40}-Flag localizes to the cytoplasm, like Endos-Flag. Subcellular fractionation confirms these results (Figure 2.7B).
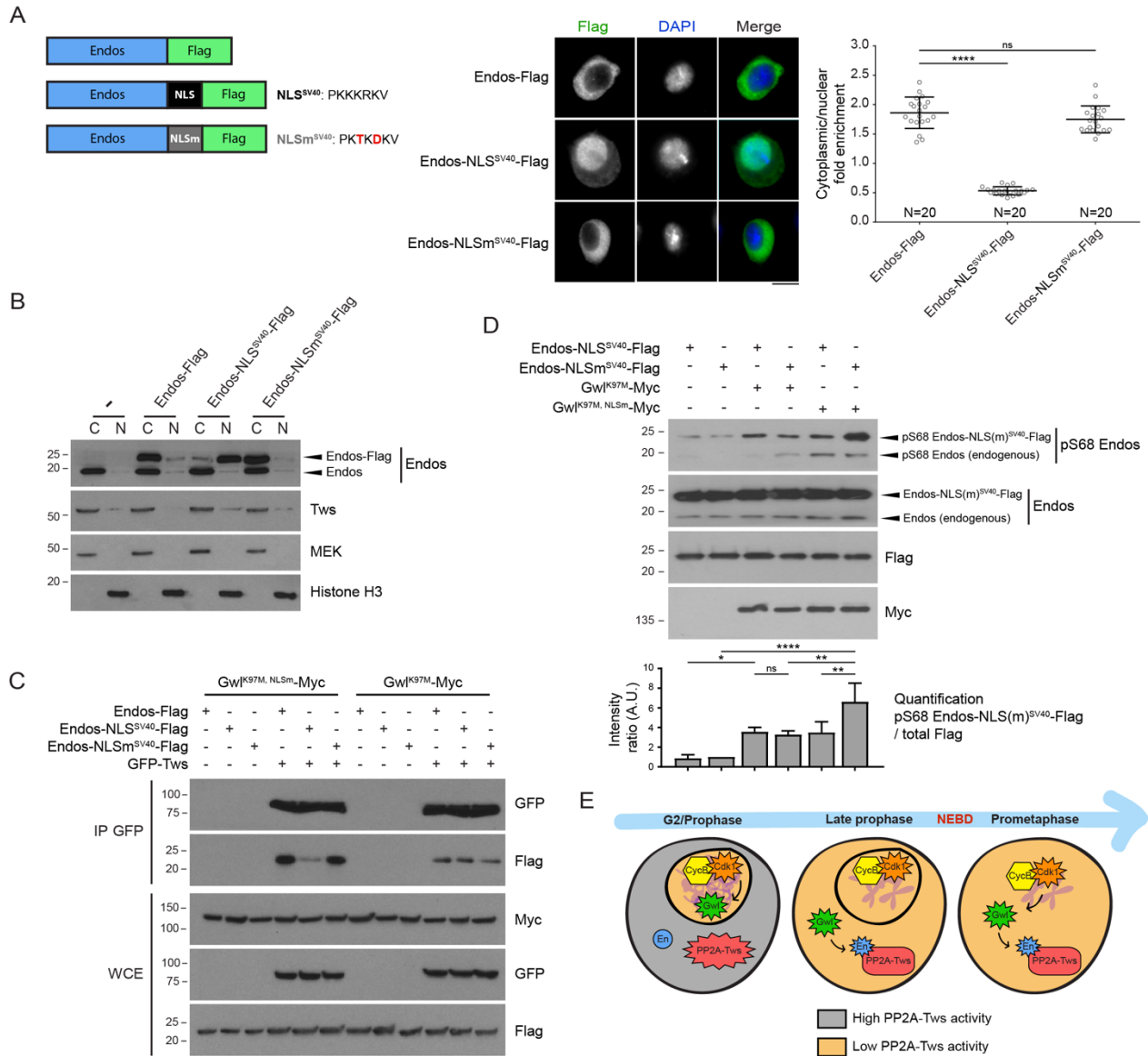
Figure 2.7. Endos must be in the cytoplasm to be phosphorylated by Gwl.

(A) Fusion of the SV40 NLS to Endos-Flag targets it to the nucleus. Left: Endos-Flag variants analyzed. Center: representative immunofluorescence images. Scale bar: 5 μm. Right: quantifications of the cytoplasmic/nuclear ratio of signal intensities (bars: mean ± SD). N = number of cells quantified. Error bars: SD. **** p = 0.0001, ns: non-significant. (B) Subcellular fractionation and Western blots show the relative amounts of cytoplasmic, C, and nuclear, N, proteins. MEK and Histone H3 are controls as cytoplasmic and nuclear proteins, respectively. (C) Active and cytoplasmic Gwl (K97M, NLSm) enhances Endos interaction with Tws if Endos is in the cytoplasm but not in the nucleus. Cells were transfected with the indicated constructs and submitted to GFP-Tws immunoprecipitations. Products were analyzed by Western blots. WCE: whole cell extract. (D) Gwl phosphorylates Endos more efficiently in the cytoplasm than in the nucleus. Cells were transfected with the indicated constructs and analyzed by Western

112

blots. Quantifications of the pS68 Endos-NLS(m)^{SV40}-Flag / total Flag band intensities are shown (mean ± SD, n = 3). **** $p < 0.0001$, ** $0.001 < p < 0.01$, * $p < 0.05$, ns: non-significant. (E) Model for the spatiotemporal dynamics of the Gwl-Endos-PP2A-Tws module. In prophase, Cyclin B-Cdk1 activates Gwl and promotes its export to the cytoplasm where Gwl phosphorylates Endos to induce its binding and inhibition of PP2A-Tws before NEB. After NEB, Cyclin B-Cdk1 keeps Gwl active and Gwl keeps Endos phosphorylated and PP2A-Tws inhibited during prometaphase. Spiky shapes: activated proteins.

We verified that fusion of Endos to NLS^{SV40} or NLSm^{SV40} does not interfere with its ability to bind and inhibit PP2A-Tws *in vitro*, ruling out any potential direct disruption of the functionality of Endos (Figure 2.3E-F). We tested the ability of the 3 variants of Endos-Flag to interact with GFP-Tws in a co-precipitation assay, where Gwl^{K97M,NLSm}-Myc was also expressed to enhance Endos phosphorylation and interaction with PP2A-Tws in interphase. We found that forcing Endos to the nucleus strongly abrogates its interaction with GFP-Tws (Figure 2.7C). Moreover, expression of nuclear and active Gwl^{K97M}-Myc does not cause nuclear Endos-NLS^{SV40}-Flag to bind PP2A-Tws more strongly than Endos-Flag, consistent with the idea that most PP2A-Tws is cytoplasmic and thus inaccessible to nuclear Endos. In addition, we found that the phosphorylation of nuclear Endos by nuclear active Gwl is less efficient than the phosphorylation of cytoplasmic Endos by cytoplasmic active Gwl (Figure 2.7D). Altogether, these results reinforce the idea that Endos must be phosphorylated by Gwl in the cytoplasm, so that Endos can bind and inhibit PP2A-Tws in the cytoplasm prior to NEB as cells enter mitosis (Figure 2.7E).

2.5.6 The cytoplasmic localization of Endos is required for its function.

We then tested the importance of this spatiotemporal regulation of the Gwl-Endos-PP2A module for mitotic progression. To examine the consequences of a loss of Endos function in mitosis, we conducted time-lapse imaging of D-Mel cells expressing Histone 2A (H2A)-RFP and Lamin-GFP. We found that depletion of Endos causes widespread mitotic collapse with abnormally condensed chromosomes scattered on mitotic spindles, as previously reported (Figure S2.5A-B) (Rangone et al., 2011). To test

the importance of the cytoplasmic localization of Endos for mitotic progression, we took advantage of our variants of Endos with altered localizations. We generated stable cell lines allowing their copper-inducible expression using the pMT promoter. Endogenous Endos was simultaneously silenced using RNAi targeting its 3' untranslated region (3'UTR) (Figure S2.5C). We then examined the mitotic phenotypes by immunofluorescence (Figure 2.8A-C). Cells expressing Endos-Flag, Endos-NLS^{SV40}-Flag or Endos-NLSm^{SV40}-Flag display normal chromosome alignment when endogenous Endos is not depleted (Control RNAi). This suggests that a gain of Endos function in the cytoplasm or in the nucleus is not detrimental. When endogenous Endos is depleted, cytoplasmic Endos-Flag and Endos-NLSm^{SV40}-Flag largely rescue chromosomal alignment defects, indicating that the fusion proteins are functional. By contrast, Endos-NLS^{SV40}-Flag (nuclear in interphase) fails to rescue chromosomal alignment defects. Similar results were obtained with cells expressing the Endos-Flag variants from the constitutive pAC5 promoter (Figure S2.5D-E).
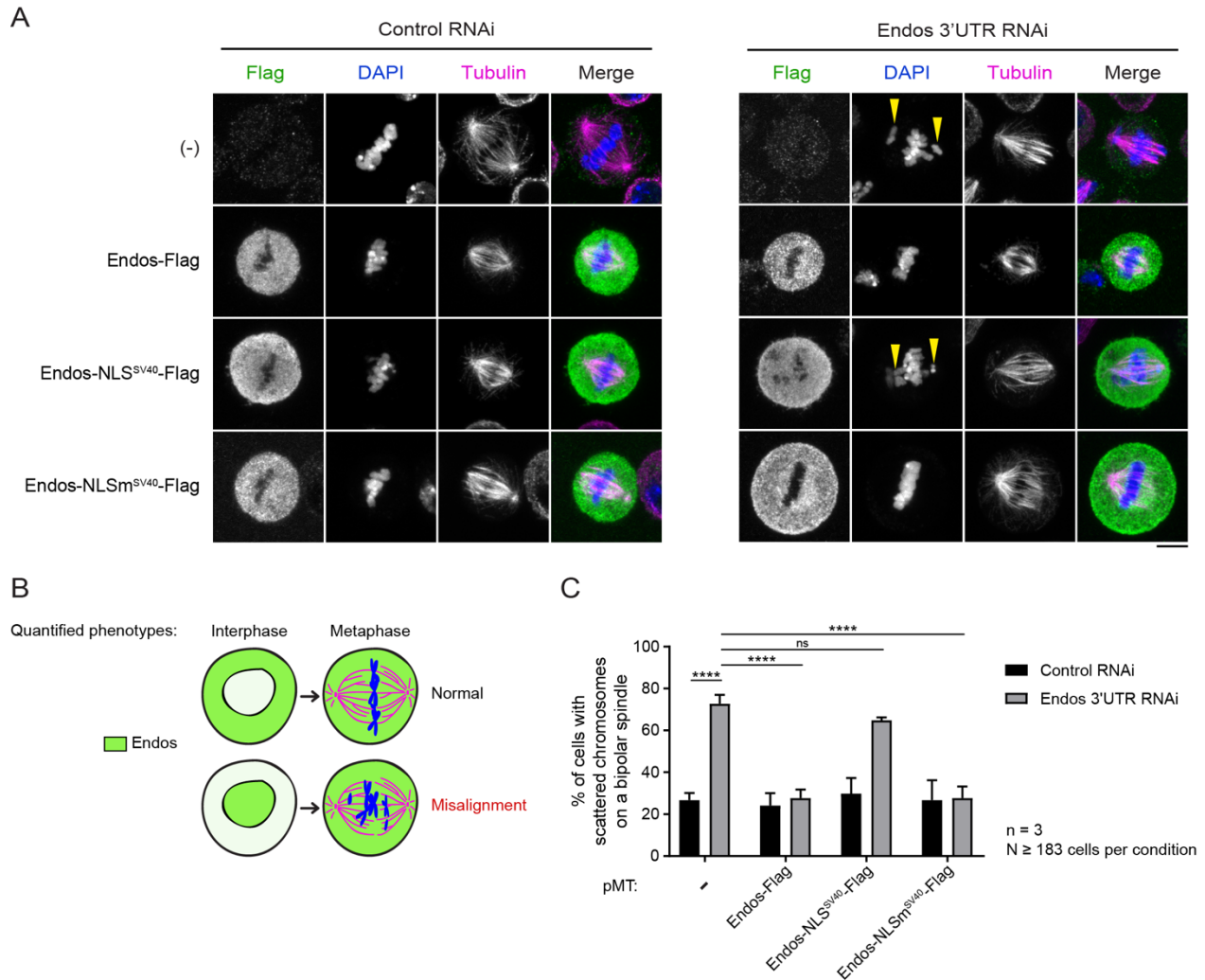
Figure 2.8. Endos must be in the cytoplasm before NEB to promote correct mitotic entry.

(A) Expression of the indicated proteins was induced and cells were transfected with dsRNA targeting endogenous Endos (3'UTR) or non-target control dsRNA. Representative immunofluorescence images are shown. Arrowheads indicate scattered chromosomes on a bipolar spindle (as illustrated in B). Scale bar: 5 μm. (C) Quantification of the percentages of mitotic cells with scattered chromosomes on a bipolar spindle (mean ± SD, $n = 3$). **** $p \leq 0.0001$. ns: non-significant.

To assess if the defects observed upon the loss of function of Endos in the cytoplasm are caused by a gain of function of PP2A-Tws, we additionally depleted Tws by RNAi (Figure S2.5F). Strikingly, we found that knockdown of Tws suppresses the chromosomal alignment defects observed when Endos-NLS^{SV40}-Flag is expressed in the

115

absence of endogenous Endos (Figure 2.9A-B). We conclude that Endos is required in the cytoplasm before NEB to inhibit PP2A-Tws and for correct chromosome alignment subsequently in mitosis.
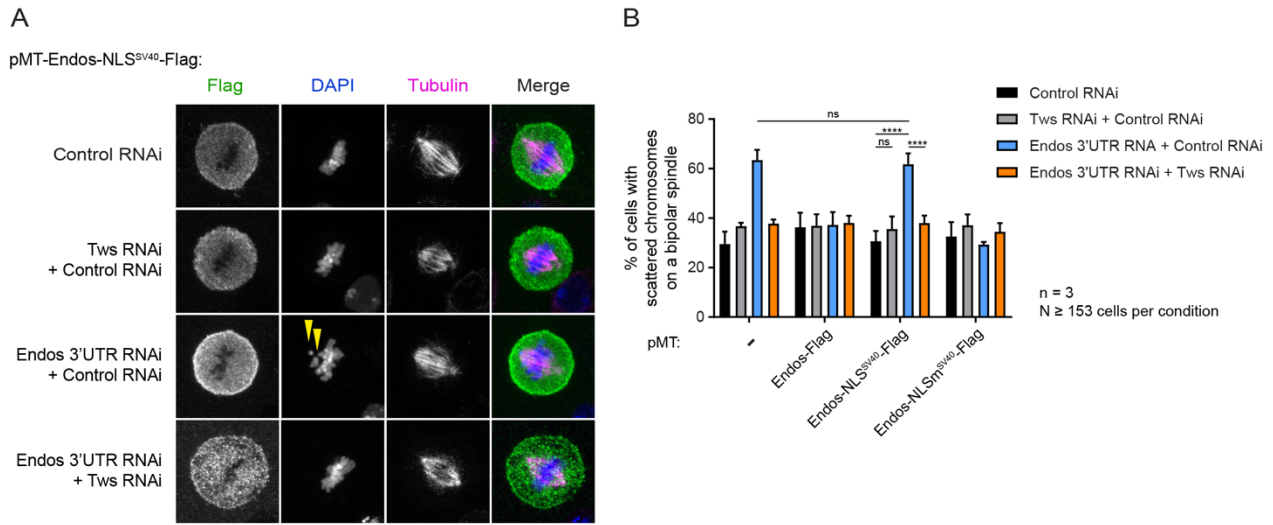
Figure 2.9. Depletion of Tws rescues mitotic defects resulting from the loss of Endos function in the cytoplasm.

(A) Expression of the indicated proteins was induced and cells were transfected with dsRNA targeting endogenous Endos (3'UTR), Tws and/or non-target control dsRNA. Representative immunofluorescence images are shown. Arrowheads indicate scattered chromosomes on a bipolar spindle. Scale bar: 5 μm. (B) Quantification of the percentages of mitotic cells with scattered chromosomes on a bipolar spindle (mean ± SD, n = 3). **** p ≤ 0.0001. ns: non-significant.

2.6 Discussion

Our results provide a more complete understanding of the spatiotemporal coordination of mitotic entry through the molecular Gwl-Endos-PP2A module that is likely conserved in vertebrates (Figure 2.7E). The nuclear localization of Gwl probably helps its activation by Cyclin B-Cdk1 (Alvarez-Fernandez et al., 2013; Wang et al., 2013). In the nucleus, Gwl may also be protected from PP2A-Tws/B55, which is mainly cytoplasmic and capable of dephosphorylating Gwl (Alvarez-Fernandez et al., 2013; Heim et al., 2015; Ma et al., 2016; Santos et al., 2012; Wang et al., 2016). Gwl suddenly translocates to the cytoplasm in prophase (Alvarez-Fernandez et al., 2013; Wang et al.,

2013). This rapid change in localization may be facilitated by the fact that Gwl is constantly shuttling between the nucleus and the cytoplasm even in interphase (Wang et al., 2016). The relocalization of Gwl to the cytoplasm in prophase was shown to promote Gwl function in both *Drosophila* and mammalian cells but the underlying reason was unclear (Alvarez-Fernandez et al., 2013; Wang et al., 2013). The present paper indicates that Endos is mostly cytoplasmic and must be cytoplasmic to bind and inhibit PP2A-Tws before NEB as cells enter mitosis. This requirement logically imposes the need for activated Gwl to translocate from the nucleus to the cytoplasm to phosphorylate Endos, as we have shown. The specific timing and localization of these events ensures that PP2A-Tws activity is inhibited in the cytoplasm just before NEB occurs. By this mechanism, phosphorylated substrates of mitotic kinases in the nucleus are presumably protected from premature dephosphorylation by PP2A-Tws between NEB and mitotic exit. The identity of these substrates is still unclear, but they likely include the Spindle Assembly Checkpoint kinase Mps1 and factors of the DNA damage repair machinery (Bisteau et al., 2020; Diril et al., 2016). Moreover, it would be interesting to explore if the spatiotemporal mechanism described here is essential for the ability of Gwl and Endosulfines to promote the G2/M transition in various systems (see introduction).

We found that Tws shuttles between the nucleus and the cytoplasm, but is concentrated in the cytoplasm at steady state. The nuclear import of Tws occurs via a novel NLS that is conserved in vertebrate B55 orthologs. Inactivation of this NLS does not prevent essential functions of Tws during *Drosophila* development. In the cytoplasm, PP2A-Tws likely contributes to stabilize interphase and ensure robust switch-like mitotic entry and exit by promoting the dephosphorylation of multiple substrates (Santos et al., 2012). Potential functions of Tws in the nucleus remain unknown and could be specific to particular contexts including certain cell types or stresses. Mutations in *tws* were shown to disrupt the G2/M DNA damage checkpoint and lead to frequent chromosomal aberrations in larval brain cells (Merigliano et al., 2017). The same study also showed that Tws becomes enriched in the nucleus and on γH2Av foci upon irradiation. By mutation of the NLS that we identified, the nuclear function of PP2A-Tws in the DNA damage response could be tested. Our results suggest that the assembly of PP2A-

Tws/B55 holoenzymes, which requires several enzymatic steps (Goguet-Rubio et al., 2020), takes place preferentially in the cytoplasm. It will be interesting to determine whether the whole PP2A-Tws holoenzyme can be translocated across nuclear pores or if Tws is transported alone via its NLS.

Our results in cultured cells established that Endos must be cytoplasmic to be efficiently phosphorylated by Gwl, and consequently bind and inhibit PP2A-Tws. When Endos is restricted to the nucleus, it cannot fulfill its mitotic function, resulting in mitotic collapse. We attempted experiments to test the ability of the Endos-Flag variants (WT, fused to NLS^{SV40} or to NLSm^{SV40}) to rescue *endos* mutant flies (Annexe 1). However, all Endos-Flag variants could rescue the viability of the *endos^1/Df(3L)ED4536* null mutant when their expression was driven by the strong driver *Ubi-Gal4*. On the other hand, none of the Endos-Flag variants could rescue the fertility of the sterile *endos^1/endos^{EY01105}* hypomorphic mutant when driven by the female germline driver *nanos-Gal4*; however, in this case, the transgenic expression was very weak. Thus, potential effects of changing Endos localization on its function may be detectable only within a restricted window of expression levels *in vivo*.

The mere fact that Endos is enriched in the cytoplasm relative to the nucleus in *Drosophila* cells is intriguing. With its mass of 13 kDa, Endos is in principle small enough to freely cross the nuclear pores which have an exclusion limit of approximately 40 kDa for passive diffusion (Wente and Rout, 2010). We considered the idea that the constitutive pSer68-independent interaction between Endos and PP2A-Tws may maintain Endos in the cytoplasm. However, depleting Tws did not markedly alter the nucleocytoplasmic ratio of Endos (our unpublished observations). Endomembranes are another possible anchor of Endos in the cytoplasmic compartment as ENSA engages in interactions with membranes (Boettcher et al., 2008). Alternatively, Endos dynamics may be restricted if it undergoes multimerization or liquid-liquid phase separation. The fact that Endos-NLS^{SV40}-Flag (17 kDa) is retained in the nucleus suggests that Endos does not need a cytoplasmic anchor to be prevented from diffusion through nuclear pores. The predicted intrinsically disordered nature of Endos coupled with the alternation of positively and negatively charged stretches of amino acid residues are features often

118

found in various proteins that phase-separate (Bergeron-Sandoval et al., 2016). Moreover, our results suggest that during embryonic mitoses, Endos becomes enriched in the nuclear/spindle matrix, a structure organized by liquid-liquid phase separation (Huang et al., 2018; Johansen et al., 2011; Woodruff, 2018). It would be interesting to investigate if Endos and its orthologs engage in such higher structures and how this may contribute to Endos function.

We found that, like *Drosophila* Endos, human ENSA and Arpp19 (Flag tagged) are more concentrated in the cytoplasm than in the nucleus. Human Mastl/Gwl also needs to be exported from the nucleus to the cytoplasm in prophase and B55α and B55δ, the main B-type regulatory subunits of PP2A, are mostly cytoplasmic in interphase (Alvarez-Fernandez et al., 2013; Santos et al., 2012). Previous results suggested that ENSA and Arpp19 are concentrated in the nucleus of HeLa cells, but the specificity of the antibodies used in immunofluorescence remained unclear (Charrasse et al., 2017; Hached et al., 2019). Nevertheless, the same studies provide convincing evidence that while human Arpp19 regulates mitosis, human ENSA is required for normal initiation of DNA replication (Charrasse et al., 2017; Hached et al., 2019). In this context, a transient nuclear localization of B55 via the NLS we identified could contribute to the correct regulation of the DNA replication cycle. It would be interesting to investigate if Mastl, perhaps activated by Cyclin A-Cdk2, phosphorylates a nuclear pool of ENSA to inhibit specifically a nuclear pool of PP2A-B55 that could otherwise interfere with the DNA replication initiation machinery.

Intriguingly, while PP2A-Tws/B55 localizes mainly to the cytoplasm and promotes interphase in flies and vertebrates, the budding yeast ortholog PP2A-Cdc55 localizes mainly to the nucleus, and its nuclear export, which depends on the Endos orthologs Igo1 and Igo2, promotes mitosis (Juanes et al., 2013). Spatiotemporal regulation is a fundamental but still incompletely understood dimension of cell cycle controls. It plays a major part in the proper function of the main mitotic regulators including several kinases and phosphatases. Plasticity at this level may allow cell type-specific changes during development and adaptations during evolution.

2.7 Materials and methods

2.7.1 Plasmids and mutagenesis

Drosophila cells expression vectors were generated by Gateway recombination (Invitrogen). Coding sequences were first cloned into the pDONR221 entry vector and then recombined into the relevant destination vectors for expression from copper-inducible (pMT) or constitutive (pAC5) promoters. The following expression vectors were generated: pAc5-Endos-Flag, pAc5-Endos-NLS^{SV40}-Flag, pAc5-Endos-NLSm^{SV40}-Flag, pAc5-Endos-Myc, pAc5-Endos-GFP, pAc5-Endos-RFP, pAc5-Endos-PrA, pAc5-Endos^{S68A}-Flag, pAc5-Endos^{S68D}-Flag, pAc5-Endos$^{\Delta41-80}$-Flag, pMT-Endos-RFP, pMT-Endos^{S68A}-RFP, pMT-Endos^{S68D}-RFP, pMT-Endos$^{\Delta41-60}$-RFP, pMT-Endos$^{\Delta41-80}$-RFP, pAc5-Gwl-Myc, pAc5-Gwl^{K87R}-Myc, pAc5-Gwl^{NLSm}-Myc, pAc5-Gwl^{NESm}-Myc, pAc5-Gwl^{K97M}-Myc, pAc5-Gwl^{K97M,NLSm}-Myc, pAc5-Flag-Tws, pAc5-Tws-Flag, pAc5-NLS^{SV40}-Tws-Flag, pMT-Tws-GFP, pMT-Tws^{NLSm}-GFP, pMT-H2A-RFP, pAc5-Lamin-GFP, pMT-Endos-Flag, pMT-Endos-NLS^{SV40}-Flag, pMT-Endos-NLSm^{SV40}-Flag. The coding sequences of the longest isoforms annotated in Flybase were used to clone Gwl and Tws. pCMV-Arpp19-Flag and pCMV-ENSA-Flag were constructed from a pCMV-dMoeTA-PC-TEV-Flag3x plasmid (gift from S. Carréno, Université de Montréal, Montréal, Canada). GST-Endos (WT, S68A, S68D, 1-40, 41-80, 41-80^{S68A}, 41-80^{S68D}, 41-60, 61-80, 81-119, Δ41-60, Δ41-80, Δ61-80, WT-NLS^{SV40}, WT-NLS^{SV40m}, S68D-NLS^{SV40}, S68D-NLS^{SV40m}) plasmids were constructed into the pGEX4T vector. pUASp-Endos-RFP (WT, S68A, S68D, Δ41-60, Δ41-80), pUASp-GFP-Tws and pUASp-Tws-GFP (WT, Tws^{NLSm}, NLS^{SV40}-Tws, NLS^{SV40m}-Tws) were constructed in the pUAS-K10attB vector. Amino-acid substitution mutants were generated using QuikChange Lightning Site-Directed Mutagenesis Kit (Agilent) following the manufacturer's protocol. For SV40 NLS and NLSm fusions to Endos, the following sequences were inserted: MPKKKRKV and MPK**TKD**KV, respectively (Kalderon et al., 1984; Makkerh et al., 1996). For fusions to Tws, 2 copies of SV40 NLS and NLSm were introduced: MPKKKRKVGPKKKRKVG and MPK**TKD**KVGPK**TKD**KVG. Their cDNAs were introduced in the PCR cloning primers. All sequences of oligonucleotides used for the generation of plasmids used in this study are provided in Tableau S2.1.

2.7.2 Cell culture, transfections and cell lines

Except for Figure 2.4C-D, all cells were in the D-Mel (d.mel-2) background and were cultured in Express Five medium (Invitrogen) supplemented with glutamine, penicillin and streptomycin (Wisent). Transfections were performed using X-tremeGENE HP DNA Transfection Reagent (Roche) following the manufacturer's instructions. All stable cell lines were selected in medium containing 20 µg/ml blasticidin. While inducible pMT-based vectors contain the blasticidin resistance gene, pAc5-based vectors were co-transfected with pCoBlast to confer blasticidin resistance to the cells. Expression of the copper-inducible transgenes was induced with $CuSO_4$ (300 µM or 500 µM) for at least 8 h. For phospho-Endos detection by WB, cells were treated with Okadaic Acid (100 nM) for 1 hour to inhibit PP2A. For Leptomycin B (LMB) treatment, cells were incubated in media containing 50 nM of LMB for 2 hours (Figure 2.1A) or 4 hours (Figures S2.1 and Figure S2.3) before fixation.

For RNA interference, dsRNAs were generated from PCR amplicons using a Ribomax kit (Promega). All sequences of oligonucleotides used in the PCRs are provided in Tableau S2.1. Cells were transfected in six-well plates with 20 µg of Endos double-stranded RNA (dsRNA), 40 µg of Endos 3′ UTR dsRNA or 40 µg of Tws dsRNA using Transfast reagent (Promega). The control dsRNA was generated against the sequence of the bacterial kanamycin resistance gene. Cells were analyzed 24 h or 48 h later by immunoblotting, immunofluoressence or live-cell imaging.

HeLa cells were cultured in DMEM medium supplemented with 10% fetal bovine serum (FBS) and with penicillin/streptomycin (Wisent). For IF and subcellular fractionation experiments (Figure 2.4), 400 000 HeLa cells/ml were seeded and transfected using Lipofectamine 2000 (Invitrogen) following the manufacturer's protocol.

2.7.3 Western blotting and immunofluorescence

Primary antibodies used in western blotting and immonufluorescence (IF) were anti-Flag M2 from mouse (#F1804, Sigma, at 1:2000 dilution for WB in D-Mel cells, at

1:5000 dilution for WB in HeLa cells, at 1:200 dilution for IF in D-Mel cells, 1:300 dilution for IF in HeLa cells), anti-GFP from rabbit (#A6455, Invitrogen, at 1:5000 dilution for WB), anti-GFP from mouse (#1218, Abcam, at 1:5000 dilution for WB), peroxidase-conjugated ChromPure rabbit IgG for PrA detection (#011-030-003, Jackson Immuno Research, at 1:3000 dilution for WB), anti-α-tubulin DM1A from mouse (#T6199, Sigma, at 1:10,000 dilution for WB), anti-Myc 9E10 from mouse (#sc-40, Santa Cruz Biotechnology, Inc., at 1:2000 dilution for WB, at 1:500 dilution for IF), anti-Lamin Dm0 (DSHB Hybridoma Product ADL84.12, ADL84.12 was deposited to the DSHB by Fisher, P. A., at 1:100 dilution for IF), anti-α-tubulin YL1/2 from rat (#MCA77G, Bio-Rad, at 1:100 dilution for IF in D-Mel cells, at 1:50 dilution in HeLa cells), anti-MEK from rabbit (#9122, NEB, at 1:2000 dilution for WB), anti-Histone H3 from rabbit (#9717, NEB, at 1:1000 dilution for WB), anti-Endos from rabbit (custom-made by Thermo Fisher Scientific, dilution 1:500 for WB, dilution 1:500 for IF), anti-phospho-Endos from rabbit (a gift from M. Goldberg, Cornell University, Ithaca, USA, 1:1000 dilution for WB), anti-Tws from rabbit (custom-made by Thermo Fisher Scientific, dilution 1:1000 for WB), anti-PP2A B subunit from rabbit (#2290P, NEB, at 1:1000 dilution for WB) and anti-PP2A A subunit from rabbit (#2039. Cell Signaling, at 1:1000 for WB). Secondary antibodies were coupled to Alexa-488 (Jackson, at 1:300 dilution in D-Mel cells, at 1:200 dilution in HeLa cells), Alexa-555 (Invitrogen, at 1:300 dilution), Texas red (Invitrogen, at 1:300 dilution) or Peroxidase (Jackson, at 1:5000 dilution). DNA was marked with DAPI.

For Western blot quantification, the intensity of the pS68 Endos-NLS(m)^{SV40}-Flag and total Flag bands were quantified using ImageJ software. Backgrounds were subtracted. Ratios were normalized to the Endos-NLSm^{SV40}-Flag/No Gwl condition.

For IF in D-Mel2 cells, cells were fixed in PBS containing 4% formaldehyde during 20 min. Cells were permeabilized and blocked in PBS containing 0.2% Triton X-100 and 1% bovine serum albumine (BSA) (PBSTB). Cells were incubated with primary antibodies diluted in PBSTB for 2 h at RT, washed three times in PBS and incubated with secondary antibodies and DAPI diluted in PBSTB for 1 h at RT. Cells were washed three times in PBS before being mounted in Vectashield medium (Vector Laboratories).

For IF in HeLa cells, cells were plated on poly-L-lysine coated round coverslips in

a 24-well plate. 48 h later, cells were washed with PHEM buffer (60 mM Pipes, 25 mM HEPES, 10 mM EGTA, 4 mM $MgSO_4$, pH 6.9) at 37 °C before fixation in PHEM buffer containing 4% formaldehyde for 20 min at 37 °C. Cells were then washed four times with TBS-tween 0.1% and a 1-h block with PHEM buffer containing 2% BSA and 0.1% Triton X-100 was done before addition of the primary antibody diluted in PHEM buffer containing 2% BSA for 2 h at RT. Coverslips were then washed three times with TBS-Tween 0.1%, before addition of the secondary antibody diluted at 1:200 in PHEM buffer containing 2% BSA. Cells were incubated for 90 min at RT and washed again three times before being mounted on slide using Vectashield medium containing DAPI (Vector Laboratories).

For IF in embryos, flies were allowed to lay eggs on grape-juice containing agar in a cage. Embryos were collected every 2 h and dechorionated in 50% bleach. There were then fixed with a 1:1 mixture of Bouin's fluid (0.66% picric acid, 9.5% formalin, and 4.7% acetic acid) and heptane with vigorous shaking at room temperature. The vitelline membrane was removed with agitation in methanol. Embryos were re-hydrated with a 1:1 mixture of methanol and PBS, and then washed in PBT (PBS + 0,1% Triton X). A 1 h block was done with PBT + 5% Bovine Serum Albumin (BSA) at room temperature. Embryos were then incubated overnight at 4°C with anti-Endos (1:500) and anti-α-tubulin DM1A (1:250) in PBT + 5% BSA. After 3 washes of 20 min in PBT, embryos were incubated for 2 h at room temperature with anti-Rabbit-Alexa 488 (1:200) and anti-Mouse-Cy3 (#115-185-166, Jackson, 1:200) in PBT + 5% BSA. They were washed 3 times with PBT and once with PBS. DNA was stained by incubation with DAPI in PBS for 10 min. Embryos were mounted in Mowiol on microscopic slides.

2.7.4 Production of GST-fusion proteins

Overnight cultures of BL21 *Escherichia coli* transformed with pGEX-Endos (WT or mutants), were used to inoculate 110 ml of LB medium. At an OD_{600} between 0.4 and 0.6, expression was induced with 1 mM IPTG for 3 h at 37°C. Cells were pelleted at 3000 *g* for 10 min at 4°C and resuspended in 5 ml of PBS, 0.4% Sarcosyl and

supplemented with 1 mM phenylmethylsulfonyl fluoride (PMSF), 10 µg/ml aprotinin and 10 µg/ml leupeptin. Bacterial cell suspensions were lysed by sonication and Triton X-100 was added (1% final). Extracts were incubated on wheel for 20 min at 4°C and centrifugated at 23,500xg for 20 min. For preparation of beads, 10 ml of clarified extract were incubated with 300 µl of washed Glutathion Sepharose 4B beads (GE Healthcare) for 1 h at 4°C. Beads were washed four times with PBS, 1 mM PMSF, 10 µg/ml aprotinin, 10 µg/ml leupeptin, 1% Triton X-100. Beads were flash freezed and stored in 90-µl aliquots at -80°C until use. For beads prepared for phosphatase assays, PBS was replaced in all buffers by Tris-HCl pH 7.5 20 mM, NaCl 150 mM.

2.7.5 GST-pulldown assay

Pelleted D-Mel cells expressing Tws-Flag from confluent 75-cm^2 flasks were lysed in 75 mM K-HEPES pH 7.5, 150 mM KCl, 2 mM EGTA, 2 mM MgCl$_2$, 5% glycerol, 0.2% Triton X-100, 1 mM PMSF, 10 µg/ml aprotinin and 10 µg/ml leupeptin, and lysates were centrifuged at 4900xg during 15 min at 4 °C. Clarified lysates were incubated with sepharose beads bound to purified GST–Endos (WT or mutants) or GST during 90 min at 4 °C. Beads were washed five times with lysis buffer before SDS–PAGE and immunoblotting.

2.7.6 Immunoprecipitation

For immunoprecipitation of GFP-Tws or endogenous Tws, pelleted cells from confluent 25-cm^2 flasks were lysed in 50 mM Tris-HCl pH 7.5, 150 mM NaCl, 1mM EDTA, 10% glycerol, 0.2% Triton X-100, 1 mM PMSF, 10 µg/ml aprotinin and 10 µg/ml leupeptin, and lysates were centrifuged at 19 000xg during 10 min at 4 °C. Lysates were incubated with anti-GFP (#A6455, Invitrogen) or anti-Tws (Thermo Fisher Scientific) antibodies for 1 h at 4 °C and then incubated with 20 µl of Protein A-conjugated Dynabeads (Invitrogen) for 45 min at 4 °C, before being washed in lysis buffer as above.

2.7.7 Affinity purifications from embryos

Embryos expressing GFP-fused variants of Tws were collected every 2 hours. GFP affinity purifications were done with GFP-Trap agarose (Chromotek) essentially as described (Lipinszki et al., 2014). Embryos aged 0-3 h old were dechorionated with 50% bleach and rinsed in water. For each genotype, 50 mg embryos were crushed in 100 µl of lysis buffer (50 mM Tris pH 7.5, 150 mM NaCl, 0.5 mM EGTA, 2 mM MgCl2, 1 mM DTT, 5% glycérol, 0.5% Triton X-100, PMSF, pepstatin, aprotinin). Another 400 µl of lysis buffer was then added. Samples were incubated with agitation at 4°C for 15 min, and then centrifugated at 14 000 rpm for 5 min at 4°C. The supernatants were collected into new tubes, avoiding the top fat layer. To each sample, 25 µl of pre-equilibrated GFP-Trap Agarose (Chromotek) was added. Samples were incubated with agitation at 4°C for 1 h. The resin was washed 4 times 5 min with 1 ml of wash buffer (50 mM Tris pH 7.5, 150 mM NaCl, 0.5 mM EGTA, 2 mM MgCl2, 1 mM DTT, 5% glycérol, 0.1% Triton X-100, PMSF, pepstatin, aprotinin). For the last wash, samples were transferred to new tubes. In each sample, 25 µl of 2X SDS-PAGE sample buffer was added before heating for electrophoresis and Western blot analysis.

2.7.8 Phosphatase assay

Phosphatase assays using malachite green were conducted essentially as described (Mehsen et al., 2018). Pelleted cells stably expressing Flag-Tws, Tws-Flag or NLS[SV40]-Tws-Flag were suspended in Tris buffer saline containing protease inhibitors: 1 mM PMSF, 10 µg/ml aprotinin and 10 µg/ml leupeptin. Cells were lysed in buffer containing 20 mM Tris-HCl pH 7.5, 150 mM NaCl, 2 mM EGTA, 0.5% NP-40, 1 mM DTT, and the protease inhibitors as above and incubated on a wheel for 15 min at 4°C, before being centrifugated at 4900x*g* rpm for 15 min at 4°C. Supernatants were incubated with anti-Flag antibody for 75 min on a wheel at 4°C and with Protein G-conjugated Dynabeads (Invitrogen) for an additional 45 min. Beads were washed 4 X 5 min with lysis buffer before being used as sources of enzyme for the phosphatase assay. Purified enzymes were pre-incubated with 20 µM of eluted GST-Endos (WT or

mutants, eluted in a buffer containing 50 mM Tris pH 8, 100 mM NaCl, 10 mM reduced gluthation, and 1 mM DTT) for 10 min at RT. In Figure 2.3D, a peptide corresponding to human PRC1 phosphorylated at site a PP2A-B55 site (pT481) was used as substrate: SKRRGLAPNpTPGKARKLNTTT (synthesized by Biobasic). In Figure 2.3F and Figure S2.1F, a peptide corresponding to human Knl1 phosphorylated at pT875 was used as a PP2A-Tws substrate: SEDDKNDMDIpTKSYTIEINHR (synthesized by Biobasic). The 2X reaction solutions contained 400 µM of peptides, 20 mM Tris pH 7.5, 5 mM $MgCl_2$, 1 mM EGTA, 20 mM β-mercaptoethanol, and 1.45 mg/ml of BSA. For the phosphatase reactions, equal volumes of 2X reaction solution and washed bead suspensions were combined and incubated at room temperature in 96-well plates. Reactions were stopped by the addition of 90 mM $HClO_4$. Phosphate release was revealed by the addition of one volume of 1 M malachite green solution. The absorbance was then measured at a wavelength of 620 nm using a plate reader (Tecan Infinite 200 PRO). Values for T_0 were subtracted from series. All values were normalized to the GST control.

2.7.9 Subcellular fractionations

Cytoplasmic and nuclear extracts were obtained using the NE-PER Nuclear and Cytoplasmic Extraction Reagents Kit (#78833) according to the manufacturer's instructions (Thermo Fisher Scientific).

2.7.10 Microscopy

Fixed D-Mel cells shown in Figure 2.1A were transiently transfected with pMT-Tws-GFP and pMT-Tws^{NLSm}-GFP and imaged using a LSM700 laser scanning confocal microscope (Zeiss) with a 63X oil objective (NA 1.4) and Zen software. Images of fixed D-Mel cells shown in Figure 2.5, Figure 2.6 and Figure S2.2 were acquired on an AxioImager microscope (Carl Zeiss) with a 100X oil objective (NA 1.4) and an AxioCam HRm camera (Carl Zeiss), using AxioVision software (Carl Zeiss). All other images of fixed D-Mel cells were acquired on a TCS SP8 DLS laser scanning microscope (Leica)

with a 63X oil objective (NA 1.4) using LAS X software. Fixed HeLa cells were imaged using a LSM880 laser scanning confocal microscope (Zeiss) with a 40X oil objective (NA 1.3) using Zen software.

Larval tissues were dissected in Express Five medium, stained with Hoechst 33342 10 μg/ml in medium for 5 to 30 min, and washed for 5 min in medium. They were then mounted in Express Five medium between the coverslip and a gas-permeable membrane before imaging with a TCS SP8 DLS laser scanning microscope (Leica) using 40X (NA 1.3) or 63X (NA 1.4) oil objectives for salivary glands and neuroblasts, respectively. Fixed embryos were imaged on the same microscope with the 63X oil objective (NA 1.4).

Live imaging was performed using a Spinning-Disk confocal system (Yokogawa CSU-X1 5000) mounted on a fluorescence microscope (Zeiss Axio Observer.Z1) using an Axiocam 506 mono camera (Zeiss), 63X oil objective (NA 1.4), and Zen software. For time-lapse microscopy of D-Mel cells, cells in culture were plated in a Lab-Tek II chambered coverglass (#155409, Thermo Fisher Scientific). For cell treatments with Leptomycin B (LMB), the cell medium in the chamber on the microscope stage was replaced with medium containing 50 nM LMB immediately before imaging. In the experiment shown in Figure 2.1B, cells used were stably transfected with pMT-Tws-GFP and pMT-Tws^{NLSm}-GFP. For live analysis of *Drosophila* syncytial embryos, 0-2 h-old embryos were first dechorionated in 50% bleach, aligned on a coverslip (#P35G-1.5-14-C, MatTek) and covered with halocarbon oil. Between 15 and 23 confocal sections of 1 μm were collected per time point for each embryo.

Time-lapse imaging of live syncytial embryos injected with FITC-labeled 70 kDa molecular mass dextrans were performed using a Leica TCS SP5 tandem scanning microscope as previously described (Yao et al., 2012; Yao et al., 2018). In short, 0-1.5 h embryos were collected from apple juice plates, and aged 1 h. The embryos were manually dechorinated, transferred onto a cover slip coated with a thin layer of heptane glue, and covered with a drop of Halocarbon oil 700. Time-lapse image sequences of a single z-plane or of z-stacks covering the depth of the mitotic apparatus were obtained using a Plan-apochromat 63X oil objective (NA 1.4). Injections of approximately 100-200

pl of FITC-labeled 70 kDa molecular mass dextrans (Invitrogen) into syncytial embryos were done with a Narishige Programmable Microinjector IM 300 system. Live imaging experiments were all conducted at room temperature.

Fluorescence quantifications and images treatment were performed using Zen software (Zeiss) and Fiji software (National Institutes of Health). Figure 2.1, Figure 2.3, Figure 2.6, Figure 2.7 and Figure S2.3A present images of single z-planes containing the nuclei. For images in Figure 2.2, Figure 2.8, Figure 2.9, Figure S2.1, Figure S2.3C-D, Figure S2.4 and Figure S2.5, a final projection was made on the z-planes containing the the nuclei and/or the condensed chromosomes. For embryo images in Figure 2.5A-B and Figure S2.5C-E, deconvolution was carried out using the Fiji software using "Diffraction PSF 3D" and "Iterative Deconvolution 3D" plugins. The number of iterations for deconvolution was set to 3. A final projection was made on the z-planes containing the nucleus. Fluorescence intensity ratios were calculated at a single z-plane (containing the nucleus) with the Zen or Fiji software, by dividing the mean fluorescence intensity of a nuclear region of interest (ROI) by the mean fluorescence intensity of a cytoplasmic ROI of the same size. The opposite ratio (cytoplasmic/nuclear) was calculated for Figure 2.4C and Figure 2.7A.

2.7.11 Fly genetics

Fly husbandry was conducted according to standard procedures. All crosses were performed at 25 °C. The WT strain used was Oregon R. Transgenic lines for expression of *UASp-GFP-Tws* and *UASp-Tws-GFP* (WT and mutants) were generated by site-directed insertions of our pUAS-K10attB-based vectors on the second chromosome in the attP40 strain (BestGene Inc, Chino Hills, CA, USA). Lines for expression of *UASp-Endos-RFP* (WT or mutants) were generated by site-directed insertions of our pUAS-K10attB-based vectors on the third chromosome in the attP154 strain, except for the *UASp-Endos-RFP* transgene used in Figure 2.3A, D, which was generated by random *P*-element mediated insertion (BestGene Inc, Chino Hills, CA, USA). Expression of transgenes in the early embryo was driven by *mat-α-tub-GAL4*

(#7062, Bloomington *Drosophila* Stock Center). For viability tests, flies were crossed and the number of observed hatching pupae relative to their expected number in the progeny was expressed as a percentage. Expression of Tws transgenes was driven by *Ubi-Gal4* (#32551, Bloomington *Drosophila* Stock Center). The tws^P and tws^{aar1} alleles were obtained from David Glover.

For the genetic rescue experiment shown in Figure 2.2D, males of the *UASp-Tws transgene/CyO; tws^{aar1}/TM6B Tb Hu* genotype were crossed with females of the *Ubi-Gal4/CyO; tws^P /TM6B Tb Hu* genotype. As a control, tws^{aar1}/*TM6B Tb Hu* males (no transgene) were crossed to *Ubi-Gal4/CyO; tws^P /TM6B Tb Hu* females. *Tb* is a dominant marker on the *TM6B* balancer chromosome III that makes pupae shorter. *CyO* is a balancer chromosome II. Both balancer chromosomes are homozygous embryonic lethal. All eclosing pupae in the progeny were scored for their *Tb* or Tb^+ (WT) phenotype. The mendelian ratio of expected Tb^+ (tws^{aar1}/tws^P) flies was 1/3. However, they could not be counted reliably as they often die in the food without becoming visible on the tube wall. Instead, we calculated the number of expected Tb^+ pupae (theoretically 1/3 of the progeny) by dividing the number of eclosing *Tb* pupae (theoretically 2/3 of total) by 2. The number of hatching Tb^+ pupae in the progeny was expressed as a percentage of the number of expected Tb^+ pupae for all crosses. Pupae of the tws^{aar1}/tws^P genotype also expressing the transgene are expected to represent 1/3 of the tws^{aar1}/tws^P pupae (theoretical full rescue, dotted line in Figure 2.2D); however observed values exceed this fraction because of higher stochastic mortality of the other genotypes caused by balancer chromosomes, and because a small fraction of escaper tws^{aar1}/tws^P pupae eclosed even without transgene expression.

For the genetic rescue experiment shown in Figure S2.4B, males of the *$endos^1$ UASp-Endos-RFP transgene/TM6C Tb Sb* genotype were crossed with females of the *Ubi-Gal4; Df(3L)ED4536/SM5-TM6B* genotype. The number of hatching Tb^+ pupae in the progeny was expressed as a percentage of the number of expected Tb^+ pupae.

2.7.12 Structure rendering

Structure rendering was done using University of California, San Francisco Chimera 1.11. The structure of human PP2A in complex with B55α bound to microcystin-LR (Protein Data Bank accession no. 3dw8 (Xu et al., 2008)) was used to generate Figure 2.1D.

2.7.13 Statistical Analysis

GraphPad software was used for graphing and statistical analyses. All results are expressed as mean ± SD unless otherwise indicated. Sample size (n) is given in each figure legend. One-way analysis of variance (ANOVA) followed by a pots hoc Dunnett's multiple comparisons was used in Figure 2.2C, Figure 2.2D, Figure 2.3D, Figure 2.3E, Figure 2.7A, Figure 2.7D and Figure S2.4B. Two-way ANOVA followed by Dunnetts's and Sidak's multiple comparisons was used in Figure 2.8C, Figure S2.1F and Figure S2.5F. Two-way ANOVA followed by Dunnetts's multiple comparisons was used in Figure 2.9B. Two-tailed Welch's t-test was used in Figure 2.4B, Figure S2.1A, Figure S2.3C and Figure S2.5B. In all figures, p values are represented as follows: *$p < 0.05$, **$p < 0.01$, ***$p < 0.001$, ****$p \leq 0.0001$, and n.s. (not significant) is $p > 0.05$. Data distribution was assumed to be normal, but this was not formally tested.

2.8 Supplemental material

2.8.1 Supplementary figures

Figure S2.1. Spatiotemporal regulation of Tws localization (complements to Figure 1 and 2).

(A) Left: D-Mel cells expressing Tws-Flag were treated with 50 nM Leptomycin B (LMB; b-d) or 0,1% ethanol (EtOH, mock control, a-c) for 4 hours before fixation, immunostaining and DNA staining with DAPI. Scale bar: 5 µm. Right: quantifications of the nuclear/cytoplasmic ratio of signal intensities (mean ± SD). (B) Western blot from 3rd instar larvae in which expression of the indicated Tws variants was driven by Ubi-Gal4. (C) All GFP-fused Tws variants can associate with Mts and PP2A-29B. 0-2 h old embryos expressing the indicated proteins were submitted to GFP-affinity purifications. Purification products were analyzed by Western blots. (D) Images of larval brains (ventral nerve cord) from 3rd instar larvae expressing Tws variants. DNA was stained with Hoescht 33342. Note the higher nuclear/cytoplasmic ratio of NLSm^{SV40}-Tws-GFP (arrows) compared with the other variants. Scale bar: 10 µm. (E) Fusion of NLS^{SV40} to Tws does not prevent its ability to bind Endos. A GST pulldown was done as in Figure 2.3B. (F) Fusion of NLS^{SV40} to Tws does not prevent its ability to be inhibited by Endos^{S68D}. A phosphatase assay was done as in Figure 2.3D. Top: quantification of the phosphatase activity (mean ± SD, n = 3). Bottom: visualization of the immunoprecipitated PP2A complexes used in the reactions. Error bar: SD. **** $p \leq 0.0001$.

Figure S2.2. Sequence alignment of *Drosophila* Endos with vertebrate orthologs.

The central region is the most conserved. It contains the Gwl phosphorylation site Ser68, which is the main determinant for Endos interaction with PP2A-Tws. Endos also engages in a phosphorylation-independent interaction with PP2A-Tws that requires a region upstream of the Gwl phosphorylation site. Residues in blue are positively charged and reported to promote ENSA dephosphorylation by PP2A-B55 (Cundell et al., 2016). *perfectly conserved residues. Based on an alignment obtained using Align from Uniprot.

Figure S2.3. Endos is a cytoplasmic protein and tags can perturb its nucleo-cytoplasmic distribution.

(A) Fluorescence images of fixed D-Mel cells expressing the indicated tagged forms of Endos. Note that GFP, RFP and Myc (6 copies), which are larger tags, make Endos more nuclear than cytoplasmic. Conversely, Flag (3 copies) and the Protein A IgG-binding domain (PrA), which are smaller tags, keep Endos in the cytoplasm. *(B)* Subcellular fractionation and Western blots show the relative amounts of cytoplasmic and nuclear proteins. MEK and Histone H3 are controls as cytoplasmic and nuclear proteins, respectively. *(C)* Inhibition of Crm1-dependent nuclear export does not cause a strong nuclear accumulatin of Endos. Left: D-Mel cells were treated with 50 nM LMB or 0,1% ethanol (Control) for 4 hours before fixation, immunostaining and DNA staining with DAPI. Scale bar: 5 µm. Right: quantifications of the nuclear/cytoplasmic ratio of signal intensities (mean ± SD). *(D)* Endos is mainly cytoplasmic throughout the cell cycle. Immunofluorescence showing the localization of endogenous Endos in the different phases of the mitotic cell cycle. Scale bar: 5 µm.

A

| Merge | Anti-Rabbit-488 | DAPI | α-Tubulin |

Anti-Endos

No Primary Ab

B

endos¹/Df(3L)ED4536

+ Ubi-Gal4 >

No transgene

Endos-RFP

Endos^{S68A}-RFP

Endos$^{Δ41-80}$-RFP

Theoretical full rescue

****

Percentage of expected *endos¹/Df(3L)ED4536* pupae

C

| | Interphase 1 | Pro-metaphase 1 | Anaphase 1 | Interphase 2 | Pro-metaphase 2 | Anaphase 2 | Interphase 3 |

Merge

GFP-Tws

Endos^{S68D}-RFP

00:00:00   00:02:00   00:04:30   00:12:30   00:15:00   00:18:30   00:24:00

D

| | Interphase 1 | Pro-metaphase 1 | Anaphase 1 | Interphase 2 | Pro-metaphase 2 | Anaphase 2 | Interphase 3 |

Merge

GFP-Tws

Endos$^{Δ41-80}$-RFP

00:00:00   00:02:00   00:04:30   00:12:00   00:14:00   00:16:30   00:21:30

E

| | Interphase 1 | Pro-metaphase 1 | Anaphase 1 | Interphase 2 | Pro-metaphase 2 | Anaphase 2 | Interphase 3 |

Merge

GFP-Tws

Endos$^{Δ41-80}$-RFP

00:00:00   00:02:00   00:05:30   00:18:30   00:21:00   00:24:30   00:31:30

F

Endos-Myc   Endos S68A-Myc

Okadaic acid
(100 nM, 1h)   −   +   −   +   −   +

37 −
25 −
20 −

pS68 Endos-Myc
pS68 Endos (endogenous)

pS68 Endos

37 −
25 −
20 −

Endos-Myc
Endos (endogenous)

Endos

135

Figure S2.4. Endos-RFP localization to the nuclear/spindle area is independent from interaction with PP2A-Tws.

(A) Immunofluorescence against endogenous Endos reveals specific staining in the nuclear area in prometaphase. Scale bar: 20 μm. B. Endos-RFP but not Endos^{S68A}-RFP or Endos$^{\Delta 41-80}$-RFP rescues the development of endos mutant flies. Transgenes were under the UASp promoter and driven ubiquitously by Ubi-Gal4. Values shown correspond to percentages of eclosed endos^{1}/Df pupae (Tb^{+}) relative to the expected number of endos^{1}/Df pupae calculated from the total number of eclosed pupae. The observed rescue exceeds the expected rescue because of higher stochastic mortality of the other genotypes caused by balancer chromosomes. Values are averages of 3 independent experiments in which between 193 and 325 eclosed pupae were scored for each cross. Error bars: SD. **** $p < 0.0001$. (C-E) Time-lapse imaging of embryos expressing GFP-Tws and variants of Endos-RFP. Scale bars: 5 µm. (C) Endos^{S68D}-RFP (gain of interaction with PP2A-Tws). (D) Endos$^{\Delta 41-60}$-RFP (loss of pS68-independent interaction with PP2A-Tws). (E) Endos$^{\Delta 41-80}$-RFP (complete loss of interaction with PP2A-Tws). Images from multiple z-steps were combined in an average intensity projection. (F) Validation of the phosphospecific antibody against pS68-Endos. Cells were transfected and treated as indicated and analyzed by Western blots.
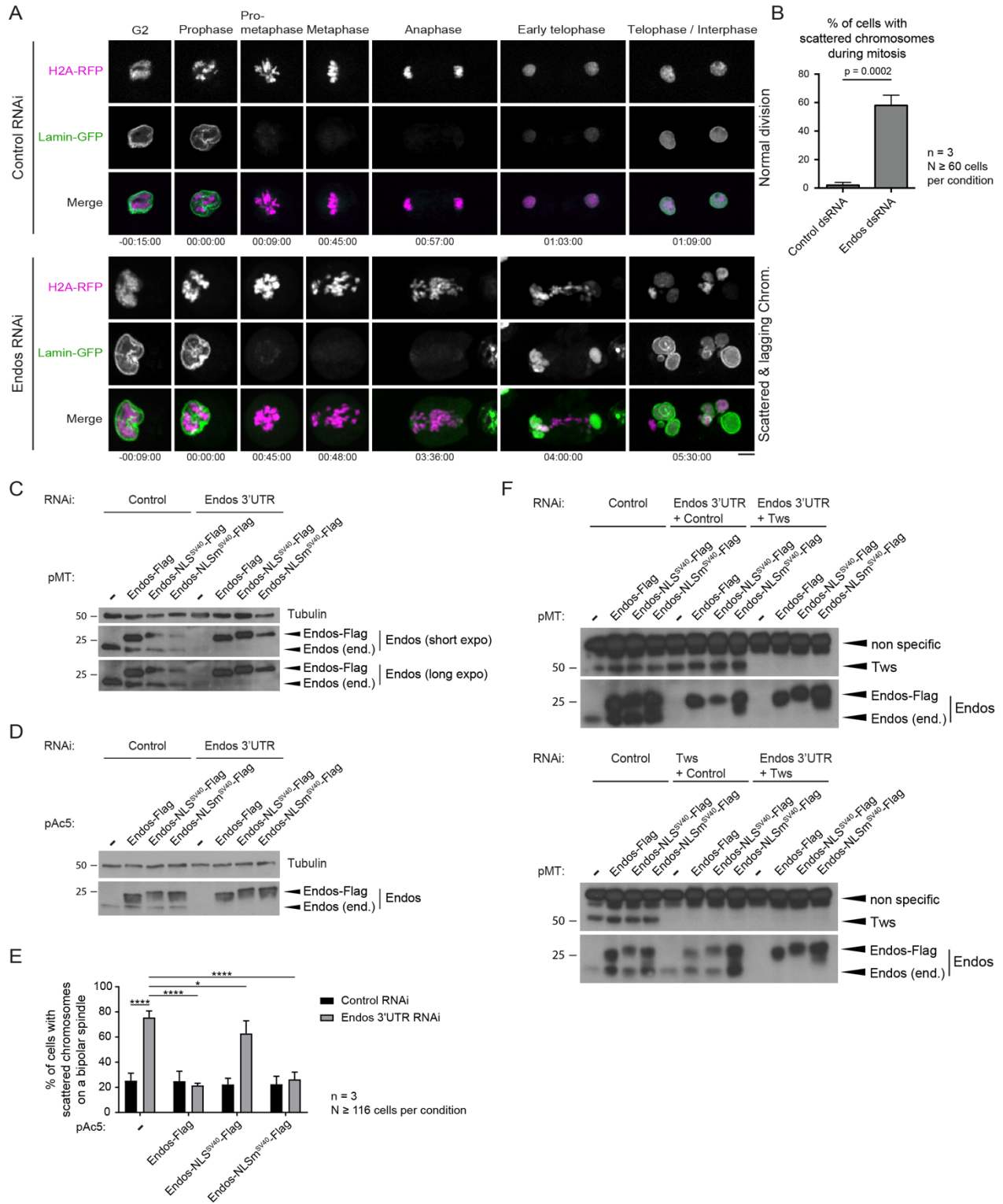
Figure S2.5. RNAi depletion of Endos or its targeting to the nucleus results in Tws-dependent mitotic defects (complements to Figures 2.8 and 2.9).

(A) Cells stably expressing H2A-RFP and Lamin-GFP were transfected with dsRNA against Endos or the bacterial KAN gene (non-target control). Cell divisions were then filmed on a Spinning-Disk microscope. Upon depletion of Endos, mitosis is delayed and chromosomes become scattered and/or lagging. Lamin-GFP is ultimately recruited aberrantly on dispersed chromatin masses. Scale bar: 5 µm. (B) Quantification of the percentages of mitotic cells displaying scattered chromosomes (mean ± SD). (C) Western blot validation of protein expression and RNAi depletion for experiment in Figure 2.8A. (D-E) Independent validation with cells constitutively expressing Endos-Flag variants under the pAC5 promoter. (D) Western blots. (E) Quantification of phenotypes (mean ± SD, n = 3).**** $p < 0.0001$, * $p < 0.05$. (F) Western blot validation of protein expression and RNAi depletion for experiments in Figure 2.9.

2.8.2 Supplementary tables

Tableau S2.1. Oligonucleotides used in this study.

Name	Sequence
Gateway cloning	
attB1-Tws-F	5'-GGGGACAAGTTTGTACAAAAAAGCAGGCTTAATGGGTCGCTGGGGACG-3'
attB2-Tws-R	5'-GGGGACCACTTTGTACAAGAAAGCTGGGTACTAAAATTTATCCTGAAA TATGAAGAGG-3'
attB2-TwsNoStop-R	5'-GGGGACCACTTTGTACAAGAAAGCTGGGTAAAATTTATCCTGAAATATGAAGAGG-3'
attB1-Gwl-F	5'-GGGGACAAGTTTGTACAAAAAAGCAGGCTTAATGGAAAACGCCGATGC
attB2-GwlNoStop-R	5'-GGGGACCACTTTGTACAAGAAAGCTGGGTATTCTTCTAGGGCAAAATTGG-3'
attB1-Endos-F	5'-GGGGACAAGTTTGTACAAAAAAGCAGGCTTAATGAGCTCCGCGGAAG-3'
attB2-EndosNoStop-R	5'-GGGGACCACTTTGTACAAGAAAGCTGGGTAGCTCGTCGCCGGGAAC-3'
attB2-<u>SV40NLS</u>-EndosNoStop-R	5'-GGGGACCACTTTGTACAAGAAAGCTGGGTA<u>AACCTTCCTCTTCTTCTTAGG</u>GCTCGTCGCCGGGAACTT-3'
attB2-<u>SV40NLS**mut**</u>-EndosNoStop-R	5'-GGGGACCACTTTGTACAAGAAAGCTGGGTA<u>AACCTT**ATC**CTTC**G**TCTTAGG</u>GCTCGTCGCCGGGAACTT-3'
attB2-Stop-3xFlag-R	5'-GGGGACCACTTTGTACAAGAAAGCTGGGTACTAGCTTACGTCACGTGGACCG-3'
*attB*1-2x<u>SV40NLS</u>-Tws-F	5'-GGGGACAAGTTTGTACAAAAAAGCAGGCTTAATG<u>CCTAAGAAGAAGAGGAAGG</u>-3'
*attB*1-2x<u>SV40NLS**mut**</u>-Tws-F	5'-GGGGACAAGTTTGTACAAAAAAGCAGGCTTAATG<u>CCTAAG**ACG**AAG**GAT**AAGG</u>-3'
pUAS-K10 cloning	
*Kpn*I-Endos-F	5'-GGGG<u>GGTACC</u>ATGAGCTCCGCGGAAGAAAACAG-3'
*Bam*HI-RFP-R	5'-GGGG<u>GGATCC</u>TTAGGCGCCGGTGGAGTG-3'
*Kpn*I-**2xSV40NLS**-Tws-F	5'-GGGG<u>GGTACC</u>ATG**CCTAAGAAGAAGAGGAAGGTTGGTCCCAAGAAGAAAAGAA AGGTC**GGTATGGGTCGCTGGGGACG-3'
*Kpn*I-**2xSV40NLSmut**-Tws-F	5'-GGGG<u>GGTACC</u>ATG**CCTAAGACGAAGGATAAGGTTGGTCCCAAGACGAAAGATAA GGTC**GGTATGGGTCGCTGGGGACG-3'
*Not*I-GFP-R	GGGG<u>GCGGCCGC</u>TTACTTGTACAGCTCGTCCATGCCG
*Kpn*I-GFP-F	GGGG<u>GGTACC</u>ATGGTGAGCAAGGGCGAGGAGC
*Kpn*I-Tws-F	5'-GGGG<u>GGTACC</u>ATGGGTCGCTGGGGACG-3'
*Not*I-Tws-R	GGGG<u>GCGGCCGC</u>TAAAATTTATCCTGAAATATGAAGAGGTTATTGG
pGEX-4T cloning	
*Nco*I-Endos-M1-F	5'-GGG<u>CCATGGG</u>GAAGCTCCGCGGAAGAAAACAGC-3'
*Nco*I-Endos-Y41-F	5'-GGGG<u>CCATGGG</u>ATATCCCAGCGGAATGC-3'
*Nco*I-Endos-K61-F	5'-GGGG<u>CCATGGG</u>AAAGGGGCAAAAGTTCTTCGACTCG-3'
*Nco*I-Endos-V81-F	5'-GGGG<u>CCATGGG</u>AGTCAAGCAGGTCTTTGCCAACAAG-3'
*Sma*I-Endos-K40-R	5'-GGGG<u>CCCGGGT</u>CACTTGGACTTGAGTTTCTCCTCCTCGATC-3'
*Sma*I-Endos-Q60-R	5'-GGGG<u>CCCGGGT</u>CACTGCAGCCTTTTCTGGAGGAAGG-3'
*Sma*I-Endos-G80-R	5'-GGGG<u>CCCGGGT</u>CAGCCGCCACC-3'
*Sma*I-Endos-S119-R	5'-GGG<u>CCCGGG</u>TTAGCTCGTCGCCGGGAA-3'
*Sma*I-Stop-**SV40NLS**-EndosNoStop-R	5'-GGGG<u>CCCGGG</u>TCA**AACCTTCCTCTTCTTCTTAGG**GCTCGTCGCCGGGAACTT-3'
*Sma*I-Stop-**SV40NLSmut**-EndosNoStop-R	5'-GGGG<u>CCCGGG</u>TCA**AACCTTATCCTTCGTCTTAGG**GCTCGTCGCCGGGAACTT-3'
pCMV cloning	
*Eco*RI-ARPP19-F	5'-GGGGAATTCATGTCTGCGGAAGTCCCCG-3'
*Bam*HI-ARPP19-NOStop-R	5'-GGGGGATCCACGCCAGCCAGCTTGCTAGC-3'
*Eco*RI-ENSA-F	5'-GGGGAATTCATGTCCCAGAAACAAGAAGAAGAGAACCC-3'
*Bam*HI-ENSA-NOStop-R	5'-GGGGGATCCACTTCAACTTGGCCACCCGC-3'
Mutagenesis	
Tws**NLSm(K455I, K457M)**-F	5'-GCACTGGCGGC**ATA**CGA**ATG**AAGGATGAGATCAGCGTGG-3'
Tws**NLSm(K455I, K457M)**-R	5'-CCACGCTGATCTCATCCTT**CAT**TCG**TAT**GCCGCCAGTGC-3'
Gwl-Scant-**K97M**-F	5'-GTCAGAGATGATCAAC**ATG**AACATGGTGTCCCAGG-3'
Gwl-Scant-**K97M**-R	5'-CCTGGGACACCATGTT**CAT**GTTGATCATCTCTGAC-3'
Gwl**K87R**-F	5'-CGCCATC**AGG**GTGATGCGC-3'
Gwl**K87R**-R	5'-GCGCATCAC**CCT**GATGGCG-3'
Gwl**NESm(L556A,I558A)**-F	5'-CACAGGAAATTGAAATC**GCT**AAT**GCT**GGCAGCACGCCCAAG-3'

Gwl**NESm(L556A,I558A)**-R	5'-CTTGGGCGTGCTGCTGCC**AGC**ATT**AGC**GATTTCAATTTCCTGTG-3'
Gwl**NLS1m(K518M,K520M)**-F	5'-CTTCCTGCGCGGCATG**ATG**CGA**ATG**ATCAATTTGGTCAATCG-3'
Gwl**NLS1m(K518M,K520M)**-R	5'-CGATTGACCAAATTGAT**CAT**TCG**CAT**CATGCCGCGCAGGAAG-3'
Gwl**NLS2m(K564M,R566L)**-F	5'-CAGCAGCACGCCC**ATG**AAG**CTC**AAGGCCCGTTCC-3'
Gwl**NLS2m(K564M,R566L)**-R	5'-GGAACGGGCCTTG**A**GCTT**C**A**TGGGCGTGCTGCTG-3'
Endos**S68A**-F	5'-CAAAAGTTCTTCGAC**GCG**GGCGATTACCAG-3'
Endos**S68A**-R	5'-CTGGTAATCGCC**CGC**GTCGAAGAACTTTTG-3'
Endos**S68D**-F	5'-GGGCAAAAGTTCTTCGAC**GAC**GGCGATTACCAGATGGC-3'
Endos**S68D**-R	5'-GCCATCTGGTAATCGCC**GTC**GTCGAAGAACTTTTGCCC-3'
Endos-del41-60-F	5'-GGAGAAACTCAAGTCCAAGAAGGGGCAAAAGTTCTTCG-3'
Endos-del41-60-R	5'-CGAAGAACTTTTGCCCCTTCTTGGACTTGAGTTTCTCC-3'
Endos-del41-80-F	5'-GAGAAACTCAAGTCCAAGGTCAAGCAGGTCTTTGCC-3'
Endos-del41-80-R	5'-GGCAAAGACCTGCTTGACCTTGGACTTGAGTTTCTC-3'
Endos-del61-80-F	5'-CCAGAAAAGGCTGCAGGTCAAGCAGGTCTTTG-3'
Endos-del61-80-R	5'-CAAAGACCTGCTTGACCTGCAGCCTTTTCTGG-3'
dsRNA	
T7-Endos-3'UTR-F	5'-<u>TAATACGACTCACTATAGGG</u>GAGACACCACTCAACACTCACCTC-3'
T7-Endos-3'UTR-R	5'-<u>TAATACGACTCACTATAGGG</u>GAGACCAGTAATGTACGAGAACGTG-3'
T7-Endos-F	5'-<u>TAATACGACTCACTATAGGG</u>GAGAGCAGCACACAATGAGCTC-3'
T7-Endos-R	5'-<u>TAATACGACTCACTATAGGG</u>GAGAGTCGCCGGGAACTTGT-3'
T7-Tws-F	5'-<u>TAATACGACTCACTATAGGG</u>GAGATCCTGCCTCAAAAGCC-3'
T7-Tws-R	5'-<u>TAATACGACTCACTATAGGG</u>GAGAGAAGGTCTCCTGATCCGA-3'
T7-Kan-F	5'-<u>TAATACGACTCACTATAGGG</u>GAGACGACAATCTATCGCTTGTATGG-3'
T7-Kan-R	5'-<u>TAATACGACTCACTATAGGG</u>GAGACCGTCAGCCAGTTTAGTCTG-3'

2.9 Acknowledgements

Chapitre 3

3. Article 2 - Phosphoproteome profiling uncovers Otefin as a PP2A-Tws target for nuclear envelope reformation after mitosis.

Myreille Larouche[1,2], Peter Kubiniok[1,3], Laia Jordana[1,2], Laura Frizzi[1], Mohammed Bourouh[1], Jingjing Li[1,2], Jean-David Larouche[1,4], Pierre Thibault[1,3], Vincent Archambault[1,2,*]

[1] Institute for Research in Immunology and Cancer, Université de Montréal, Montréal, Québec, Canada

[2] Department of Biochemistry and Molecular Medicine, Université de Montréal, Montréal, Québec, Canada

[3] Department of Chemistry, Université de Montréal, Montréal, Québec, Canada.

[4] Department of Molecular Biology, Université de Montréal, Montréal, Québec, Canada

[*]Corresponding author: vincent.archambault.1@umontreal.ca

3.1 Contexte

PP2A-Tws joue des rôles clés pour la sortie de mitose. Toutefois, peu de ses substrats directs ont été identifiés à ce jour. Nous avons adopté des approches de phosphoprotéomique pour identifier des sites de phosphorylation dépendants de l'activité de PP2A-Tws. Les sites plus phosphorylés en l'absence de PP2A-Tws représentent de potentiels substrats directs de la phosphatase.

3.2 Contributions des auteurs

Myreille Larouche a conceptualisé, conçu et réalisé les expériences, analysé les données, préparé les figures pour le manuscrit, écrit le manuscrit.

Peter Kubiniok a conceptualisé, conçu et co-réalisé les expériences de phosphoprotéomique, puis acquis et analysé les données brutes de spectrométrie de masse (Figures 3.1-3.4, Figure S3.1).

Laia Jordana a co-réalisé les expériences de la Figure 3.8A-B.

Laura Frizzi a généré des réactifs et participé aux expériences des Figures 3.5 et 3.7.

Mohammed Bourouh a co-réalisé les expériences de la Figure 3.5B-C.

Jingjing Li a généré des réactifs et participé aux expériences de la Figure 3.6E.

Jean-David Larouche a réalisé les analyses bioinformatiques pour générer les graphiques et diagrammes des Figures 3.2-3.4, S3.1D.

Pierre Thibault a conceptualisé, conçu et supervisé les expériences de phosphoprotéomique.

Vincent Archambault a conceptualisé, conçu et supervisé les expériences, révisé le manuscrit.

3.3 Abstract

Mitotic exit requires massive protein dephosphorylation events. PP2A in complex with its B55 regulatory subunit (called Tws in *Drosophila*) is crucial for this process, but many of its specific mitotic substrates are yet to be identified. We conducted SILAC-based and label-free quantitative phosphoproteomics screens in *Drosophila* cells to identify PP2A-Tws-dependent phosphosites. The intersection of the datasets revealed new potential PP2A-Tws substrates, among which the nuclear envelope protein Otefin.

We found that mutation of phosphosites identified near the LEM domain of Otefin impacts its association with BAF and delays its recruitment at reassembling nuclei during mitosis. Our results suggests that PP2A-Tws-dependent regulation of the Otefin – BAF interaction contributes to nuclear envelope reformation. This work uncovered potential novel PP2A-Tws substrates and deepens our understanding of the LEM-D/BAF complexes regulation in mitosis

3.4 Introduction

Mitotic progression requires a series of precisely ordered cellular events that lead to correct partitioning of the genetic material (Morgan, 2007). Transformations such as chromosome condensation, nuclear envelope breakdown (NEB) and microtubule spindle organization take place in a stepwise manner (Lindqvist et al., 2009; Morgan, 2007). The cyclin dependent kinase 1 (Cdk1) is considered the master regulator of mitosis as it triggers many cellular transformations through protein phosphorylation (Lindqvist et al., 2009; Morgan, 2007; Nigg, 2001; Nurse, 1990; Sharma et al., 2014). Kinases of the Polo and Aurora families are also required to promote mitotic entry and progression (Archambault et al., 2015; Carmena et al., 2009). Once the spindle assembly checkpoint is satisfied, APC/C-driven degradation of mitotic cyclins initiates mitotic exit (Wolf et al., 2007; Wolf et al., 2006). While some proteolysis does occur, dephosphorylation of the mitotic substrates by protein phosphatases is the major mechanism allowing proper mitotic exit (McCloy et al., 2015; Min et al., 2014; Olsen et al., 2010; Sharma et al., 2014; Wurzenberger and Gerlich, 2011).

Protein phosphatases 1 (PP1) and 2A (PP2A) as well as Fcp1 account for most of the phosphatase activity counteracting mitotic phosphorylation during mitotic exit (Booher and Beach, 1989; Chen et al., 2007; Doonan and Morris, 1989; Mayer-Jaekel et al., 1993; Visconti et al., 2012). PP2A is the major phosphoserine and phosphothreonine targeting phosphatase in eukaryotic cells (Nilsson, 2019; Virshup and Shenolikar, 2009). It is a heterotrimeric complex composed of a catalytic (C) subunit, a scaffold (A) subunit and a regulatory (B) subunit (Wlodarchak and Xing, 2016). There is wide range of B-

145

type subunits belonging to four families, B (B55), B' (B56), B'' (PR72) and B'''(PR93), each one conferring distinct substrate specificity to PP2A trimers (Lambrecht et al., 2013; Virshup and Shenolikar, 2009). PP2A in complex with B55 plays important roles for cell cycle progression as it opposes Cdk1 and other mitotic kinases (Castilho et al., 2009; Cundell et al., 2016; Mayer-Jaekel et al., 1994; Mochida et al., 2009; Schmitz et al., 2010).

PP2A-B55 must be inhibited at mitotic onset through the Greatwall-Endosulfine module to allow high levels of Cdk1-dependent phosphorylation of mitotic substrates (Castilho et al., 2009; Mochida et al., 2009; Vigneron et al., 2009). Greatwall (Gwl) is a nuclear kinase that, once fully activated by Cdk1 and autophosphorylation, relocalizes to the cytoplasm before NEB to phosphorylate Endosulfine proteins (ENSA and Arpp19 in vertebrates, Endos in *Drosophila*) (Gharbi-Ayachi et al., 2010; Mochida et al., 2010; Rangone et al., 2011; Wang et al., 2013). Gwl-phosphorylated Endosulfines then become potent and specific inhibitors of PP2A-B55 (Gharbi-Ayachi et al., 2010; Mochida et al., 2010; Rangone et al., 2011). They bind PP2A-B55 with very high affinity while being dephosphorylated with very slow kinetics, thereby outcompeting other substrates for binding PP2A-B55 catalytic site (Cundell et al., 2016; Mochida, 2014; Williams et al., 2014). Following cyclin B degradation by the APC/C, Cdk1 activity drops and PP1 initiates Gwl inactivation (Heim et al., 2015; Ma et al., 2016). Reduced Gwl activity decreases Endosulfines phosphorylation rate, allowing PP2A-B55 to gradually dephosphorylates them (Cundell et al., 2013; Williams et al., 2014). Once released from Endosulfines, PP2A-B55 can target its other substrates to promote mitotic exit (Williams et al., 2014). PP2A-B55 inactivation by the Gwl-Endosulfine molecular switch is strongly conserved from yeast to humans (Garcia-Blanco et al., 2019).

Work from many teams shed light on PP2A-B55's contributions for mitotic exit across species. In *Xenopus* egg extracts, loss of B55 accelerates mitotic entry (Mochida et al., 2009). Silencing the *Drosophila* ortholog of B55, encoded by *twins* (*tws*), causes pupal lethality, with larval neuroblasts displaying high chromosomal condensation and anaphase figures (Gomes et al., 1993; Mayer-Jaekel et al., 1993). Similar anaphase bridges and lagging chromosomes were observed upon Tws knockdown in *Drosophila*

146

cells in culture (Chen et al., 2007). In human and fly cells, loss of B55/Tws delays nuclear envelope reformation (NER) (Schmitz et al., 2010). Finally, B55 controls the mitotic spindle during mitotic exit (Cundell et al., 2013; Schmitz et al., 2010). PP2A-B55 is therefore required for proper mitotic completion in various systems. However, until recently, the specific PP2A-B55 substrates during mitotic exit were not identified. Knockdown of the Gwl homologue (Mastl) in HeLa cells allowed the identification of the spindle assembly checkpoint (SAC) kinase Mps1, the central spindle component PRC1 and the nucleoporin NUP153 as direct targets of PP2A-B55 (Cundell et al., 2013; Cundell et al., 2016; Diril et al., 2016).

In parallel to the current work, other groups performed phosphoproteomics studies to identify global phosphoproteome changes during mitosis and PP2A-B55-dependent phosphosites. Work in budding yeast and human cells revealed that the dephosphorylation events required for mitotic exit have to follow a precise temporal order (Bouchoux and Uhlmann, 2011; Kuilman et al., 2015; Malik et al., 2009; McCloy et al., 2015). Dephosphorylation kinetics have been shown to depend on the identity of both the phosphorylated residue and the amino acids surrounding it (Cundell et al., 2016; Hein et al., 2017; McCloy et al., 2015). PP2A-B55 dephosphorylates preferentially phosphothreonines over phosphoserines in human cells (Cundell et al., 2016; Hein et al., 2017). Moreover, PP2A-B55 has a preference for proline-directed phosphosites (Kruse et al., 2020). Finally, it was shown that PP2A-B55 substrates are recognized through a bipartite polybasic motif surrounding the phosphorylation site (Cundell et al., 2016). These physico-chemical characteristics explain why Endosulfines, which are phosphorylated on a serine surrounded by basic amino acids, strongly bind PP2A-B55 while being slowly dephosphorylated (Williams et al., 2014).

Increasing evidence points out to PP2A-B55 involvement in NER. Reforming a nuclear envelope around decondensing chromosomes is a stepwise process (de Castro et al., 2016; LaJoie and Ullman, 2017; Schellhaus et al., 2016). One of the primary events is recruitment of barrier-to-autointegration factor (BAF) homodimers at the anaphase chromosomes to shape a single nucleus (Samwer et al., 2017). Nuclear pore complexes (NPCs) also assemble early at the reforming nuclei in a coordinated manner

(Clever et al., 2012). These priming events are followed by the recruitment of other nuclear envelope proteins, such as lamins and proteins of the LEM-domain (LEM-D) family (Gorjanacz et al., 2007; Haraguchi et al., 2001; Margalit et al., 2005). These interactions allow recruitment of ER-derived membranes to the decondensing chromosomes during mitotic exit (Gorjanacz et al., 2007; Haraguchi et al., 2001; Margalit et al., 2005). In *C. elegans*, BAF reassociation with chromatin during mitotic exit depends on PP2A activity (Asencio et al., 2012). In HeLa cells, PP2A-B55 dephosphorylates NUP153 to promote its enrichment to chromatin and NPC reformation at the end of mitosis (Cundell et al., 2016). More recently, work in *Drosophila* revealed PP2A-Tws-dependent dephosphorylation of BAF to promote its recruitment to chromosomes in telophase and subsequent NER (Mehsen et al., 2018).

The LEM-D proteins include LAP2, emerin and MAN1, and directly bind BAF homodimers through their LEM domain (Cai et al., 2007; Lin et al., 2000). Phosphorylation of human BAF by VRK1/NHK-1 negatively impacts its interaction with LEM domains (Nichols et al., 2006). In *Xenopus laevis*, phosphorylation of LEM-domain proteins also reduces their ability to interact with BAF (Hirano et al., 2009; Hirano et al., 2005). The precise molecular mechanisms of such phosphoregulation as well as their biological importance are yet to be characterized.

Here we used *Drosophila* to identify novel PP2A-Tws substrates. We conducted phosphoproteomic screens, using both SILAC and label-free approaches, to uncover PP2A-Tws-dependent phosphosites. Our work unveiled interesting potential mitotic targets of PP2A-Tws, among which we found the *Drosophila* ortholog of the LEM-D protein emerin, Otefin. We identified two serine residues in Otefin, Ser50 and Ser54, as being hyperphosphorylated following PP2A-Tws inhibition. Moreover, we found that phosphoregulation of these two sites regulates Otefin's association with BAF and with other proteins. Our results uncover novel potential substrates of PP2A-Tws and provide new insights about the phosphoregulation of the LEM-D protein Otefin during mitosis.

3.5 Results

3.5.1 SILAC labeling of *Drosophila* cells for quantitative phosphoproteomics

To identify novel PP2A-Tws substrates, we conducted a quantitative phosphoproteomic screen. We hypothesized that PP2A-Tws-dependent phosphorylation sites would become hyperphosphorylated upon depletion or inhibition of PP2A-Tws in *Drosophila* cells in culture. We used stable isotopic labeling by amino acids in cell culture (SILAC) to accurately quantify phosphoproteome changes. The mass shift introduced by the use of isotopes allows the distinction of peptides coming from cells grown in "light" medium from the ones coming from cells grown in "heavy" medium. *Drosophila* S2 cells were grown in serum-free synthetic media containing light ($[^{12}C_6$, $^{14}N_4]$-L-Arg and $[^{12}C_6$, $^{14}N_2]$-L-Lys) or heavy ($[^{13}C_6$, $^{15}N_4]$-L-Arg and $[^{13}C_6$, $^{15}N_2]$-L-Lys) isotopes of lysine and arginine. We tested the incorporation of the metabolically labeled amino acids using two concentrations of supplemented isotopic amino acids: a low one (Arg 380 µM, Lys 640 µM), based on concentrations used with mice cells; and a high one (Arg 2 mM, Lys 20 mM), based on a previous study using SILAC in *Drosophila* cells (Sap et al., 2015) (Figure 3.1A). After an adaptation phase, during which cells grow in the SILAC media to incorporate labeled amino acids, labeling efficiency was measured by mass spectrometry (MS). Complete incorporation would be reached when the signal intensities from light and heavy peptides are in a 1:1 ratio (Figure 3.1B). After six cell doublings, only 65% of incorporation was reached when using the low concentration of amino acids (Figure 3.1C). This percentage increased to 80% with the highly concentrated medium. Nonetheless, incorporation was incomplete. We therefore extended the adaptation phase and tested cells after nine doublings. Incorporation was still incomplete (78%) for cells grown in the low-concentrated medium but reached a satisfying 93% for cells grown with high isotopes concentrations. Thus, further experiments were performed with cells grown in high concentration SILAC media for at least nine doublings. Of note, we observed that cells grown in serum-free synthetic

SILAC media had a longer doubling time (about 1.5-2-fold increase) and a high mortality rate.
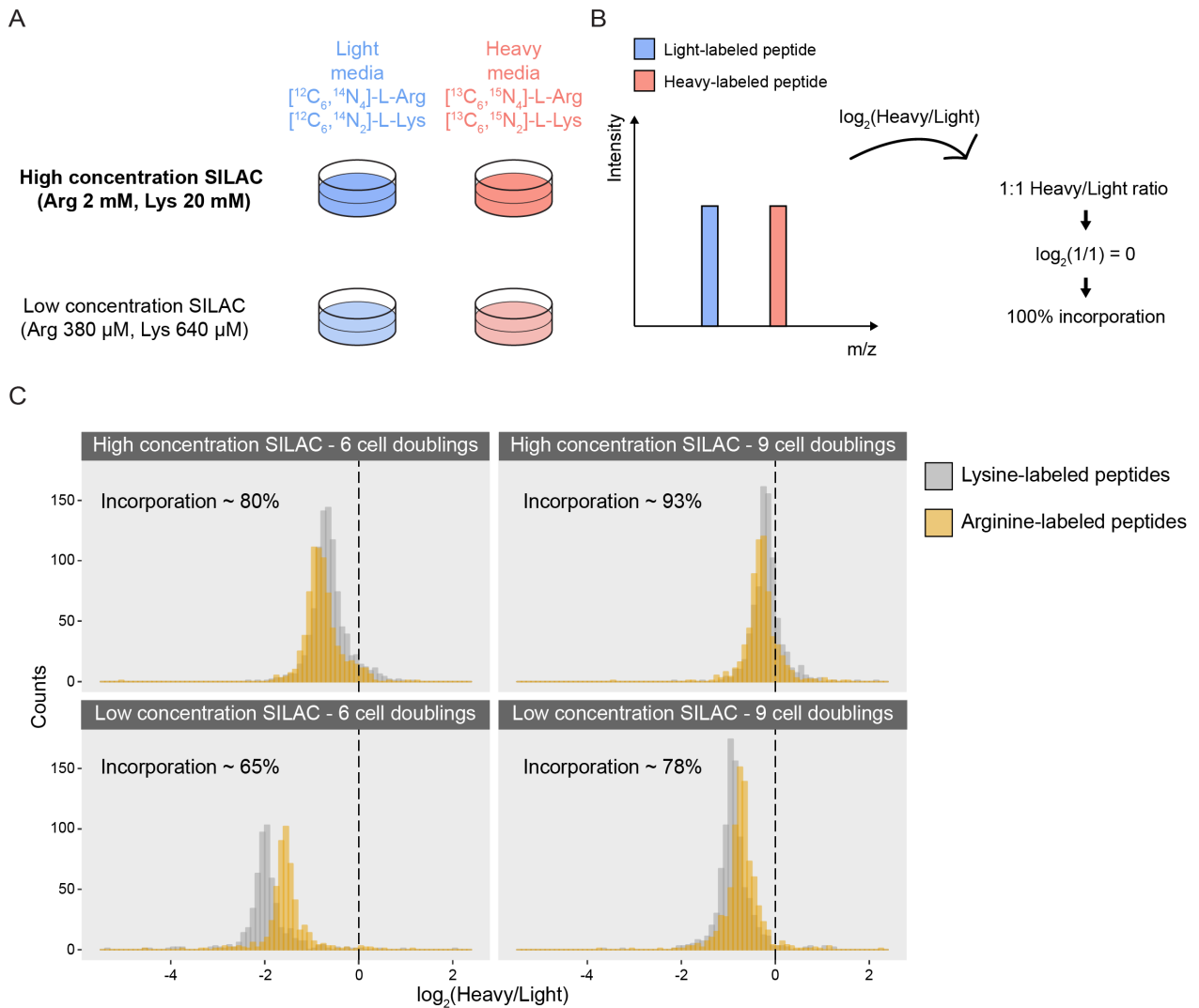
Figure 3.1. Incorporation analysis of fly cells.

(A) Schematic representation of the protocol for SILAC labeling of *Drosophila* cells in culture. *Drosophila* S2 cells were grown in serum-free synthetic media containing light or heavy isotopes of lysine and arginine. Two concentrations of supplemented isotopic amino acids were tested. After 6 or 9 days of culturing, light and heavy cells were mixed 1:1 and processed for mass spectrometry analysis. (B) Complete incorporation is reached when the signal intensities from light and heavy peptides are in a 1:1 ratio, corresponding to a $\log_2$(ratio) of zero. (C) Incorporation of heavy lysine and arginine into proteins was monitored by mass spectrometry. The counts of labeled peptides are graphed. The percentages of incorporation were calculated from the heavy-to-light ratios.

After 9 doublings in cell density, we downregulated PP2A-Tws in the heavy cells using Tws RNAi. Since prolonged RNAi treatment could result in indirect physiological changes, we also used okadaic acid (OA) for acute inhibition of all forms of PP2A. As controls for each experiment, light cells were exposed to non-target RNAi or DMSO, respectively. Within each experiment, treated and control cells were harvested and equally mixed in a 1:1 ratio with three technical replicates for each independent experiment (Figure 3.2A). Cells were lysed in sodium deoxycholate (SDC) buffer, and proteins were digested with trypsin. Phosphopeptides were then enriched on titanium dioxide (TiO$_2$) affinity resin prior to tandem MS (LC-MS/MS) analysis. Three biological replicates (Runs 1-3) were realized for RNAi experiments and two biological replicates (Runs 1 and 3) were done with the drug treatments.

A Cells grow in light media → Control; Cells grow in heavy media → Tws RNAi or Okadaic acid → Harvest and cells mixing 1:1 → Cell lysis in SDC buffer → Trypsin digestion → TiO_2 phosphopeptide enrichment → LC-MS/MS → Quantification of relative phosphopeptide abundance

B Number of identified phosphopeptides

C **Run 1** Significantly more phosphorylated phosphosites

Tws RNAi (308 phosphosites); OA (186 phosphosites); 237 / 71 / 115

Run 3 Significantly more phosphorylated phosphosites

Tws RNAi (16 phosphosites); OA (89 phosphosites); 7 / 9 / 80

Systematically identified site: Map205_S283

D **Significantly more phosphorylated phosphosites following Tws RNAi treatment**

Run1 (308 phosphosites); Run2 (56 phophosites); Run3 (16 phosphosites); 288 / 9 / 6 / 1 / 10 / 45

Common sites runs 1 + 2:
SRP72_S620, SRP72_T627, dDyn_S764, Larp_S284, Parvin_S13, Parvin_T20, Parvin_S9, Parvin_T16, Nup358_S2304, Larp_T982

Common sites runs 1 + 3:
Map205_S283, IP15837p_S27, IP15837p_T29, Ote_S50, CG6693_S258, dos-RA_S519, eEF1delta_S37, Stim-RA_S453, CG13117_T43

Common sites runs 1 + 2 + 3:
KLC_S433

E % of phosphopeptide — Number of phosphosites identified per phosphopeptide — Run1, Run2, Run3

F **Phosphorylated residues**

Run 1: 31,17% / 45,78% / 19,16% / 3,89%
Run 2: 33,93% / 50,00% / 12,50% / 3,57%
Run 3: 37,50% / 43,75% / 12,50% / 6,25%

Non-P Ser (S); P-directed Ser (SP); Non-P Thr (T); P-directed Thr (TP)

G KLC_S433 — -AAKVD**S**PTVTT-; Map205_S283 — -DLVAE**S**PRKEF-; Ote_S50 — -IGGQA**S**PAASP-

Fold change ($\log_2$) — Runs — Tws RNAi / OA / Ø not tested / NA not detected

152

Figure 3.2. SILAC-based quantitative phosphoproteomic screen to identify PP2A-Tws substrates.

(A) SILAC phosphoproteomics workflow. Light cells were treated with DMSO or non-target RNAi, heavy cells were treated with okadaic acid or Tws RNAi. Harvested heavy and light cells were mixed in a 1:1 ratio. Cells were lysed in sodium deoxycholate (SDC) buffer, digested with trypsin and phosphopeptides were enriched using titanium dioxide (TiO_2). Tandem MS (LC-MS/MS) analysis was performed followed by phosphopeptide identification and quantification using MaxQuant. Three technical replicates were realized per treatment. Three biological replicates were realized for RNAi experiments. Two biological replicates were done with the drug treatments. (B) Total number of phosphopeptides reproducibly identified between technical replicates, for each biological replicate (runs). (C) Venn diagrams showing the overlap between the Tws RNAi and OA experiments for Run 1 and Run 3. Significantly more phosphorylated individual sites were used for the analysis. (D) Venn diagram showing the overlap of significantly hyperphosphorylated individual sites following Tws depletion between each of the three independent runs. Shared phosphosites are highlighted. (E) Number of phosphorylation sites identified on each phosphopeptide following Tws depletion for each of the three independent runs. (F) Proportion of identified phosphopeptides phosphorylated on proline-directed or non-proline-directed threonine and serine residues following Tws depletion for each of the three independent runs. (G) Three proline-directed phosphosites are reproducibly more phosphorylated across experiments.

The number of identified phosphopeptides was stable between conditions within a same run, however it was highly variable between the different runs (Figure 3.2B). A maximum of 2751 phosphopeptides were identified in the first run for the Tws RNAi experiment. We looked at the intersection of the datasets obtained from the Tws RNAi and the OA experiments to identify hits that are rapidly affected by PP2A-Tws inhibition (Figure 3.2C). Seventy-one sites were significantly more phosphorylated in both experiments for Run 1. In comparison, only nine sites are shared hyperphosphorylated hits in Run 3. This is not surprising given the highly reduced number of identified phosphopeptides in Run 3. We identified only one significantly more phosphorylated site common to Tws RNAi and OA datasets in Run 1 and Run 3: Ser283 of the microtubule-associated protein Map205. Interestingly, this site was previously reported to be phosphorylated by Cdk1 to disrupt the interaction between Map205 and the Polo kinase (Archambault et al., 2008).

We next examined the overlap of significantly hyperphosphorylated sites following Tws depletion between each of the three independent runs (Figure 3.2D). Again, few hits are shared between experiments. Run 1 has minor overlaps with Runs 2 and 3,

which include proteins of the actin cytoskeleton (dDynamin and Parvin), of the microtubule cytoskeleton (Map205) and of the nuclear envelope (Nup358 and Otefin). The unique phosphosite systematically identified as more phosphorylated in all three Tws RNAi runs is Ser433 of the microtubule-associated kinesin light chain (KLC). PP2A-Tws could target these phosphosites at mitotic exit to promote processes such as mitotic spindle elongation, nuclear envelope reformation and cytokinesis.

Interestingly, despite the low number of common hyperphosphorylation sites detected, we found that the three Tws RNAi experiments share common features. First, the majority of identified phosphopeptides contain only one phosphosite, with less than 20% of peptides having more than two sites (Figure 3.2E). Second, our analyses reveal that hyperphosphorylated sites mainly correspond to serines (77 to 84%) rather than threonines (16 to 23%) in all experiments. No phosphorylated tyrosines were identified (Figure 3.2F). Although PP2A-B55 has been shown to dephosphorylate more efficiently phosphothreonines over phosphoserines in yeast and mammalian systems (Agostinis et al., 1992; Cundell et al., 2016; Godfrey et al., 2017; Kruse et al., 2020), we obtained distributions that are highly similar to those reported for the *Drosophila* global phosphoproteome (78% pSer, 19% pThr, 3% pTyr) (Bodenmiller et al., 2007; Colinet et al., 2017; Zhai et al., 2008) and for mammalian mitotic cells (85% pSer, 15% pThr, <1% pTyr) (Dulla et al., 2010; McCloy et al., 2015; Olsen et al., 2010). These natural abundances may explain why our datasets are not enriched with phosphorylated threonines. Moreover, in every run, phosphorylated residues (56 to 65%) are mostly proline-directed sites (S/T-P), which correspond to minimal Cdk1 consensus motifs. Interestingly, proline-directed sites have previously been shown to be significantly more dephosphorylated at the onset of mitotic exit (McCloy et al., 2015; Rogers et al., 2016b). Taken together, our analyses suggest that the global phosphoproteome signature is reproducible across our experiments, with differences in the identity of the phosphosites caused by the variable number of phosphopeptides identified between runs. Notably, Ser283 of Map205, Ser433 of KLC and S50 of Ote are proline-directed phosphosites that are reproducibly more phosphorylated across experiments (Tws RNAi and OA) and biological replicates (runs), making them strong PP2A-Tws target candidates (Figure 3.2G).

The above results depict the challenge of efficiently and reproducibly identifying phosphopeptides using SILAC labeling in *Drosophila* cells. Nonetheless, our SILAC-based phosphoproteomic screen allowed identification of many significantly more phosphorylated sites following Tws depletion and/or PP2A chemical inhibtion.

3.5.2 Quantitative phosphoproteomics without labeling uncovers potential PP2A-Tws substrates

Considering the relatively low number of identified phosphopeptides and the poor fitness of our cells in the SILAC media, we wished to use a label-free approach for our phosphoproteomic screen. Label-free proteomics analysis is intrinsically more variable than methods exploiting molecular labeling. Nonetheless, we hypothesized that this drawback would be more than compensated by the larger fraction of cells undergoing division in our cultures when using a standard rich medium, thus allowing the identification of more PP2A-Tws-dependent mitotic phosphopeptides. To counterbalance the loss of accuracy, we included one more technical replicate for each condition (four replicates in total) (Figure 3.3A). Apart from samples pooling after cell harvesting, the mass spectrometry workflow remained the same. In addition to Tws RNAi and OA treatments, we also included Gwl and Endos RNAi treatments (Figure S3.1A). Since Gwl and Endos function to specifically inhibit PP2A-Tws, we expected their knockdown to promote the hypophosphorylated state of PP2A-Tws-dependent phosphosites (Figure 3.3B).

A

4 replicates → Cell lysis in SDC buffer → Trypsin digestion → TiO₂ phosphopeptide enrichment → LC-MS/MS

Control

Intensity / m/z

4 replicates → Cell lysis in SDC buffer → Trypsin digestion → TiO₂ phosphopeptide enrichment → LC-MS/MS

RNAi or Okadaic acid

Intensity / m/z

→ Quantification of relative phosphopeptide abundance

B

Treatments

Gwl RNAi or Endos RNAi

Tws RNAi or Okadaic acid

Expected response

HIGH PP2A-Tws activity

Hypophosphorylated peptides

LOW PP2A-Tws activity

Hyperphosphorylated peptides

(P) Gwl → (P) Endos ⊣ PP2A-Tws

C

Endos RNAI — 115 / 28

Gwl RNAI — 42 / 30

OA — 189 / 350 (Map205_S283, KLC_S433, Ote_S50_S54)

Tws RNAi — 25 / 73 (Ote_S50_S54, KLC_S433, Map205_S283)

x-axis: Fold change (log₂); y-axis: −log₁₀(p.value)

- Significantly less phosphorylated peptides
- Not significant
- Significantly more phosphorylated peptides

D

Endos RNAi Significantly less phosphorylated phosphosites

OA Significantly more phosphorylated phosphosites

Tws RNAi Significantly more phosphorylated phosphosites

Gwl RNAi Significantly less phosphorylated phosphosites

Venn diagram values: 44, 84, 318, 1, 10, 1, 18, 0, 2, 33, 1, 20, 1, 1, 0

Common site Gwl + OA: Ankle2_S1089

Common site Endos + Tws: Larp_S284

Common sites Gwl + Endos + OA: Endos_S68, Patronin_S997

Common site Gwl + Endos + Tws: CG15160_S548

Common site Gwl + Tws + OA: Jra_S82

Common site Gwl + Endos + Tws + OA: Unkempt_S411

E
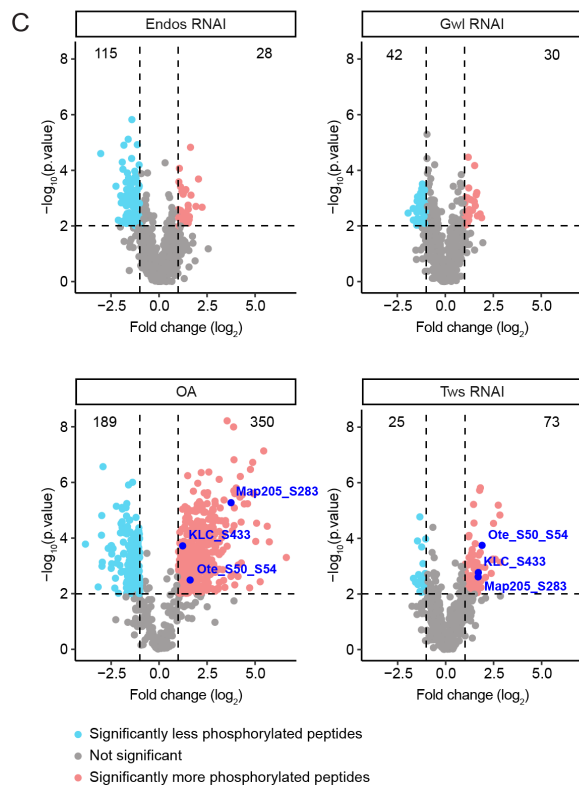
Significantly more phosphorylated phosphopeptides (Tws RNAi + OA)

Gene	Protein name	pSites	Fold change (log₂) Tws RNAi	OA
Capr	Caprin homolog	T738	2,85	3,94
ArfGAP3	ADP-ribosylation factor GTPase activating protein 3	S457	2,83	3,32
Akap200	A-kinase anchor protein 200	T111	2,59	4,88
Dlic	Dynein light intermediate chain	S434	2,46	2,40
CG6693	J domain-containing protein CG6693	S258	2,41	1,50
stwl	Stonewall	S442	2,38	4,28
dgt6	Augmin complex subunit dgt6	T394	2,08	3,13
Ote	Otefin	S50_S54	1,90	1,61
CG4747	Putative oxidoreductase GLYR1 homolog	T256	1,81	2,51
hts	Protein hu-li tai shao	T464	1,80	5,45
sle	Protein slender lobes	T140	1,77	1,73
Klc	Kinesin light chain	S433	1,70	1,20
Map205	205 kDa microtubule-associated protein	S283	1,69	3,75
lost	Lost	T479	1,65	2,95
H	Protein hairless	S791	1,63	1,52
MED1	Mediator of RNA polymerase II transcription subunit 1	S797	1,61	1,24
CG4747	Putative oxidoreductase GLYR1 homolog	S243_T256	1,59	2,01
gro	Protein groucho	T287	1,51	2,59
Gl	Dynactin subunit 1	S135_S138	1,46	2,22
MEP-1	MEP-1	S387	1,38	2,00

Figure 3.3. Label-free quantitative phosphoproteomics to uncover potential PP2A-Tws substrates.

(A) Label-free phosphoproteomics workflow. The mass spectrometry workflow remained the same than the one used for the SILAC-based screen, with the exception of one more technical replicate included per condition (four replicates in total) and the absence of sample pooling (control vs treated) after cell harvesting. (B) Gwl and Endos RNAi treatments were performed, in addition to Tws RNAi and OA treatments. Gwl and Endos function together to inhibit PP2A-Tws. Expected responses following treatments are indicated. (C) Volcano plots showing significantly altered phosphopeptides identified. Log-transformed p-values associated with individual phosphopeptides are plotted against log-transformed fold change in abundance between control and treated samples. Pink dots: hyperphosphorylated phosphopeptides (log$_2$ fold change > 1 (2-fold)). Light blue dots: hypophosphorylated phosphopeptides (log$_2$ fold change < 1 (0.5-fold)). p-value $\leq$ 0.01 are considered significant (the horizontal dashed line indicates p-value = 0.01). Blue labels depict the three highly reproducible proline-directed phosphosites identified in the SILAC-based screen. (D) Venn diagram showing the overlap between the significantly hypophosphorylated sites following Gwl/Endos RNAi and the hyperphosphorylated individual sites following Tws RNAi and OA treatment. Shared phosphosites are highlighted. (E) List of the top 20 (based on fold change) hyperphosphorylated phosphopeptides common to the Tws RNAi and OA datasets.

As expected, cells appeared much healthier and proliferated faster (doubling time of approximatively 24 h, which is approximately 1.5-2-fold faster than what we observed for cells grown in SILAC media) in standard rich medium (Express Five + 2 mM glutamine). In our experiments, we harvested twice as many cells per condition as in the SILAC experiments (40 x 10^6 vs 20 x 10^6) within a much shorter culture time. In average, over 10 000 phosphopeptides were identified per condition (Figure S3.1B), for a total of 749 significantly modified phosphopeptides. The total number of identified phosphophopeptides is more than 3-fold higher than the number obtained in the best SILAC run (Run 1). Like SILAC experiments, label-free experiments enriched monophosphorylated peptides (Figure S3.1C). We were able to identify significantly (p-value $\leq$ 0.01) hyper- (log$_2$ fold change > 1 (2-fold)) and hypophosphorylated (log$_2$ fold change < 1 (0.5-fold)) phosphopeptides for each condition (Figure 3.3C). Interestingly, depletion of Gwl or Endos resulted in datasets enriched for hypophosphorylated peptides. This is consistent with the hyperactivation of PP2A-Tws expected from these treatments. However, the difference between hyper- and hypophosphorylated peptides following Gwl depletion is less pronounced. As expected, Tws RNAi and OA treatments shift the datasets towards hyperphosphorylated peptides. Interestingly, the significantly

altered phosphosites we examined are mostly proline-directed sites for the three RNAi treatments while OA treatment impacts a majority of non-proline-directed sites (Figure S3.1D). Strikingly, Tws RNAi alters a higher proportion (37%) of proline-directed phosphothreonines compared to the other three conditions (21% for OA, 15% for Endos RNAi, 9% for Gwl RNAi). The distributions obtained for Gwl RNAi and Endos RNAi datasets are very similar, as expected for proteins cooperating in a common signaling pathway. They however differ from the distribution observed for the Tws RNAi dataset. This could suggest that Gwl affects the phosphoproteome through PP2A-B55 regulation but also through other pathways, as previously proposed (Bisteau et al., 2020). It could also suggest that the phosphoproteins altered by a gain of function of PP2A-Tws in mitosis are not the same as those altered by a loss of PP2A-Tws activity in interphase.

We decided to look at the intersection of the hypophosphorylated sites from Gwl and Endos RNAi with the hyperphosphorylated sites from Tws RNAi and OA inhibition to identify potential PP2A-Tws targets (Figure 3.3D). Among shared phosphosites, Ser1089 of the endoplasmic reticulum protein Ankle2 is less phosphorylated after Gwl depletion while being more phosphorylated after chemical inhibition of PP2A. Ser284 of the La-related protein (Larp) is less phosphorylated in the Endos-depleted cells and more phosphorylated in the Tws-depleted cells. This site was also identified in two of the Tws RNAi runs from SILAC experiments (Runs 1 and 2). Larp is an RNA-binding protein that is highly abundant in the cell. Two sites are less phosphorylated when Gwl and Endos are depleted while being more phosphorylated after OA treatment: Ser68 of Endos and Ser997 of Patronin. Endos[pS68], the Gwl phosphorylation site required for PP2A-Tws inhibition by Endos (see Chapters 1 and 2), is known to be dephosphorylated by PP2A-Tws (Mochida, 2014; Williams et al., 2014). This result indicates that Gwl and Endos depletions efficiently lead to more active PP2A-Tws in our experiments. Patronin is a protein binding the minus end of microtubules and contributing to mitotic spindle stabilization (Pavlova et al., 2019). Ser82 of Jra, the *Drosophila* Jun protein, a member of the activating protein 1 (AP-1) transcription factor family, is less phosphorylated after Gwl depletion and more phosphorylated in the Tws RNAi and OA datasets. Ser411 of Unkempt, a component of the mTOR pathway, is the sole phosphosite shared by all four intersected conditions. We also looked into the list of hyperphosphorylated peptides

shared by the Tws RNAi and OA datasets (Figure 3.3E). Strikingly, we found all three hits that were highly reproducible in our SILAC experiments: Map205^{pS283}, KLC^{pS433} and Ote^{pS50} (Figure 3.3C, E). An additional site, Ser54, is also hyperphosphorylated on Ote in the label-free experiment.

We compared hits from the most successful run of our SILAC-based proteomics analysis (494 significantly hyperphosphorylated sites upon Tws RNAi or OA treatments) with the ones obtained following the same treatments in the label-free screen. The intersection of the datasets sheds light on some interesting candidates (Figure 3.4A). In addition to Map205^{pS283}, KLC^{pS433} and Ote^{pS50}, other proteins regulating the nuclear envelope and the microtubule cytoskeleton are shared hits. Dgt6, a subunit of the augmin complex, is more phosphorylated at Thr394 in three experiments. The augmin complex functions at the minus ends of microtubules to generate a centrosome-independent spindle (Goshima et al., 2008). A recent study reports similar localizations for Dgt6 and Patronin, and suggests a possible Dgt6-dependent association of Patronin with metaphase microtubules bundles (Pavlova et al., 2019). We also identify three other proteins of the nuclear envelope as common hyperphosphorylated hits. Ser483 and Thr503 of NHK-1, the kinase phosphorylating BAF, are more phosphorylated following Tws depletion in our first SILAC experiment and after OA treatment in the label-free experiment. These two experiments also identified Ser1089 of Ankle2 as a hit. Finally, MSP-300, a KASH protein that anchors nuclei to the actin cytoskeleton, is more phosphorylated at Ser2289 in three experiments.

A

SILAC - Run 1 (S1)   Label-free (LF)

OA   Tws RNAi

Tws RNAi   OA

208   310
61   14   16
114   42
6   16
3
1   3
0   1
0

Common sites
S1-OA + S1-Tws + LF-OA + LF-Tws
Caprin_T738
Map205_S283
Rtnl-1_S263

Common sites
S1-Tws + LF-OA
4E-BP_T70
Ankle2_S1089
dFOG_S997
EF-1-delta_S37
Hbs1_S196
NHK-1_S483
NHK-1_T503
PR2_S1001
Shark_T553
Sle_T330
Vulcan_S273
Xpc_T231
β-Spec_T2160
CG15099_S1371

Common site
S1-OA + LF-OA
NAT1_S400

Common sites
S1-Tws + LF-Tws
Larp_S284
Sle_T22
Taf6_S532

Common sites
S1-OA + S1-Tws + LF-OA
SRP72_S620
CG46280_S158
MSP-300_S2289
Pzg_S194
Rbcn-3A_S1362
RpS3_S241

Common site
S1-OA + S1-Tws + LF-Tws
NAT1_S1022

Common sites
S1-Tws + LF-OA + LF-Tws
Akap200_T111
ArfGAP3_S457
CG42232_T114
CG5477_T53
CG6693_S258
KLC_S433
Dgt6_T394
Gorab_S185
HBS1_T204
Hts_T464
Jra_S82
NDF_S243
NDF_T256
Ote_S50
Rbcn-3A_T1366
Srrm234_S921

B

Otefin   LEM-D   TM
1   47   401 424

S50 S54

Figure 3.4. SILAC-based and label-free phosphoproteomics datasets uncover Otefin as a potential PP2A-Tws target.

(A) Venn diagram showing the overlap of significantly hyperphosphorylated individual sites following Tws depletion between the SILAC-based (Run 1) and the label-free datasets. Shared phosphosites are highlighted. The three highly reproducible proline-directed phosphosites identified across experiments (Map205^{pS283}, KLC^{pS433} and Ote^{pS50}) are indicated in bold. (B) Primary structure of the nuclear envelope protein Otefin. Yellow: LEM domain. Pink: transmembrane domain. The two hyperphosphorylated sites identified (in blue) are adjacent to the LEM domain of Otefin.

160

Among our most reproducible hits, Otefin is a LEM-D protein that is required for *Drosophila* germline stem cell maintenance and for BAF localization at the nuclear envelope (Figure 3.4B) (Barton et al., 2018; Barton et al., 2016; Duan et al., 2020b). As loss of PP2A-Tws delays nuclear envelope reformation (Mehsen et al., 2018), we decided to investigate further the PP2A-Tws – Otefin relationship.

3.5.3 Loss of Otefin impairs development of *Drosophila* embryos

otefin null flies are viable but sterile (Barton et al., 2014; Jiang et al., 2008). Otefin silencing alters nuclear lamina structure in *Drosophila* germline stem cells and disperses BAF from the nuclear lamina in fly tissues (Duan et al., 2020b). To assess the importance of Otefin in the context of meiosis and mitosis, we examined the consequences of RNAi-silencing of Otefin in *Drosophila* developing eggs and embryos. We used *mat-α-tub-GAL4* to drive two different *UAS-Otefin* RNAi constructions, targeting the coding sequence (CDS) or the 3'UTR of *otefin*, in mid-late oogenesis and the early embryo. Germline specific RNAi knockdown of Otefin allows its depletion in mature oocytes, thereby avoiding the severe early oogenesis defects arising from mutants (Zhang et al., 2018). While the 3'UTR-targeting RNAi does not lead to any hatching defects, less than half of the eggs laid by mothers expressing the *UAS-Ote^{CDS}* RNAi construct hatch, indicating that Otefin is required for embryonic development (Figure 3.5A).
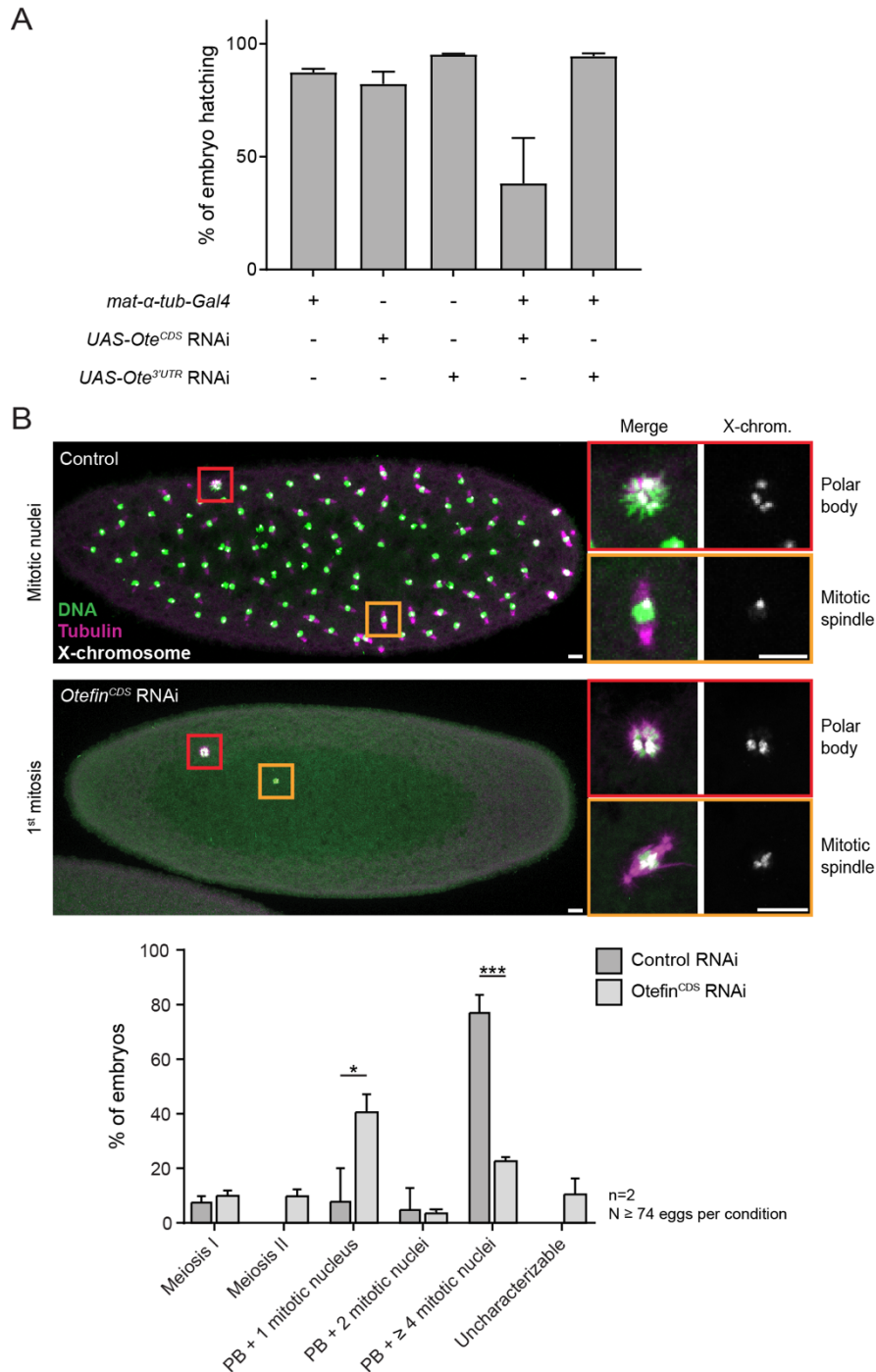
Figure 3.5. Loss of Otefin impairs development of *Drosophila* embryos.

(A) Germline specific RNAi knockdown of Otefin. Eggs from mothers of the indicated genotypes were scored for their hatching rate. Three technical replicates were performed per condition. *n* = 1 biological replicate. (B) Eggs from control and *mat-α-tub-GAL4/UAS-Ote^CDS^* RNAi mothers. Green: DNA. Magenta: tubulin. White: FISH for pericentric DNA of the X chromosome. Mitotic spindles are recognized by the presence

of astral microtubules, co-occurrence with a polar body (PB), and 1 or 2 foci of pericentromeric X-chromosome DNA. Insets from the red and orange boxes are enlarged on the right panel Scale bars: 10 μm. (C) Quantification of the embryonic phenotypes. n = 2. At least 74 eggs were scored for each condition. Error bars: mean ± SD. *p < 0.05, ***p < 0.001.

We next examined the intracellular phenotypes of these non-developing eggs. We stained the microtubules, the total DNA and the pericentric region of the X-chromosome (Figure 3.5B). Nuclear divisions occur normally in control embryos, with the majority of them (almost 80%) displaying more than four mitotic nuclei (stages 2-4 of embryogenesis) (Figure 3.5C). By contrast, most embryos knocked down for Otefin (around 40%) arrest early in embryonic development, during metaphase of the first zygotic division (stage 1 of embryogenesis). Only around 20% of the eggs have more than four mitotic nuclei. This indicates that silencing *otefin* in the female germline does not prevent meiosis completion, but rather interferes with the early stages of zygotic mitosis. Interestingly, it has previously been reported that RNAi knockdown of NHK-1, the kinase phosphorylating BAF, in *Drosophila* germline causes the embryos to arrest before completion of their first zygotic division (Zhang et al., 2018). Moreover, the protein Young arrest (YA), a component of the nuclear lamina expressed only during *Drosophila* early embryo development, is dispensable for egg activation but is required to transit from meiosis to mitosis (Sackton et al., 2009). As the nuclear envelope is presumably required for migration and apposition of the male and female pronuclei (Wolfner, 2002), loss of Otefin may also result in structural defects that prevent correct initiation of zygotic mitosis.

3.5.4 Phosphomimetic mutations at Ser50 and Ser54 of Otefin negatively impact its interaction with BAF

The two hyperphosphorylated sites identified in our screens, Ser50 and Ser54, are adjacent to the LEM domain of Otefin (Figure 3.4B). Both are proline-directed sites that have previously been reported to be phosphorylated by Cdk1 (Ashery-Padan et al., 1997; Habermann et al., 2012). From these observations, we hypothesized that phosphorylation at these sites at mitotic entry disrupts the interaction between Otefin

and BAF as part of the nuclear envelope breakdown process. Conversely, dephosphorylation of these sites by PP2A-Tws at the end of mitosis could later promote the BAF-Otefin interaction (Figure 3.6A) as part of an orderly nuclear envelope reformation process.
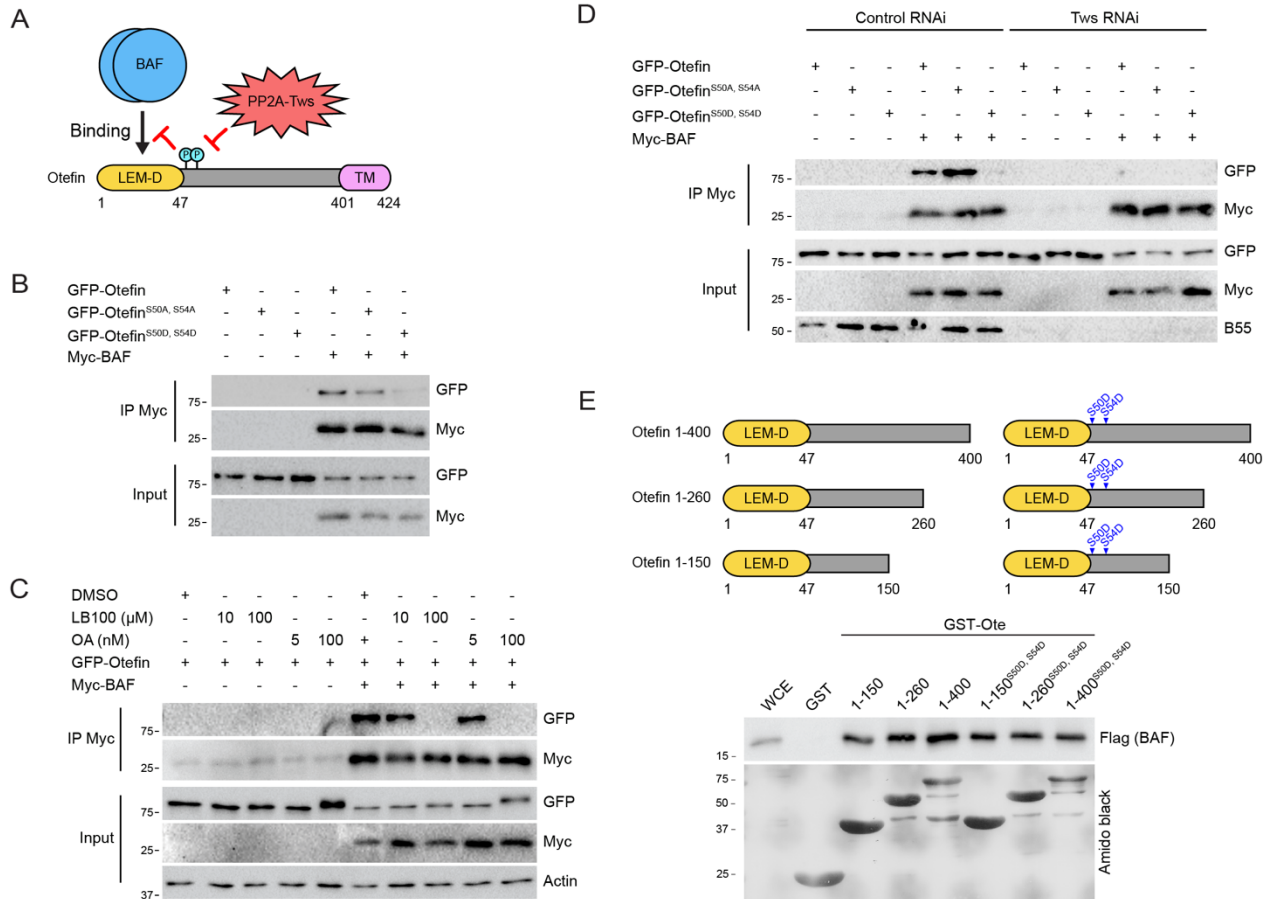
Figure 3.6. Phosphomimetic mutations at Ser50 and Ser54 of Otefin decrease its association with BAF in cells.

(A) Proposed model for the role of the identified phosphosites of Otefin during mitosis. (B) D-Mel cells transfected with the indicated proteins were submitted to Myc-BAF immunoprecipitation (IP), and products were analyzed by Western blot (WB) for GFP and Myc. (C) D-Mel cells transfected with the indicated proteins and treated with the indicated chemical inhibitors were submitted to Myc-BAF immunoprecipitation (IP), and products were analyzed by Western blot (WB) for GFP, Myc and actin. (D) D-Mel cells transfected with the indicated proteins and double-stranded RNAs were submitted to Myc-BAF immunoprecipitation (IP). Products were analyzed by Western blot (WB) for GFP, Myc and B55. (E) The indicated variants of GST-Otefin (or GST alone) were tested for their ability to pull down Flag-BAF from cell extracts (detected with anti-Flag).

To test this hypothesis, we generated double phosphodeficient (Ote$^{S50A, S54A}$) and phosphomimetic (Ote$^{S50D, S54D}$) GFP-tagged mutants and probed their interaction with Myc-BAF in a coprecipitation assay (Figure 3.6B). As expected, the phosphomimetic mutations strongly weakens, without completely preventing, GFP-Otefin association with BAF. This is consistent with the idea that phosphorylation of Ser50 and Ser54 negatively regulates the interaction. We next sought to test if the Otefin – BAF interaction is PP2A-dependent. We therefore treated cells co-expressing GFP-Otefin and Myc-BAF with OA or LB100 (Figure 3.6C). In both cases, PP2A inhibition prevents the association between GFP-Otefin and Myc-BAF. However, none of the two tested chemical inhibitors is specific to PP2A-Tws. To specifically inactivate PP2A-Tws, we used Tws RNAi, in cells expressing GFP-Otefin (WT, phosphodeficient and phosphomimetic) and Myc-BAF (Figure 3.6D). As expected, knockdown of Tws disrupts the interaction of Myc-BAF with GFP-Ote. Surprisingly, the interaction with BAF is not rescued by the S50A,S54A mutations in GFP-Ote. This might be due to increased BAF phosphorylation that may also contribute to disrupt the BAF-Ote interaction, as BAF is also a PP2A-B55/Tws target (Asencio et al., 2012; Mehsen et al., 2018). To test it, the use of a phosphodeficient variant of BAF would be informative. Additional phosphorylation sites in Otefin could also participate in regulating the interaction. Altogether, our results reinforce the idea that the phosphoregulation of Otefin's Ser50 and Ser54 involves PP2A-Tws and is important for its association with BAF.

To test if phosphorylation at these two sites directly impacts the ability of Otefin to interact with BAF, we decided to use a GST pulldown assay (Figure 3.6E). To increase Otefin's solubility and allow expression of our GST fusions in bacteria, we removed its transmembrane domain (residues 401-424). To further map the region of Otefin required for its association with BAF, we tested three truncations that all contain the LEM domain but have differential lengths for the disordered region. Finally, to test the phosphorylation requirements, we compared WT to phosphomimetic variants. We probed the interaction of the GST fusions with Flag-BAF expressed in cultured cells. We found that the phosphomimetic mutations in Otefin did not abrogate its interaction with BAF in this *in vitro* context, unlike in co-precipitations from cells. It is possible that the decrease in Otefin-BAF association due to the S50D,S54D mutations in cells depends on the

presence of another protein in the complex, such as lamin. Moreover, as the phosphomimetic mutations do not completely prevent the interaction between Otefin and BAF in co-precipitation experiments from D-Mel cells (Figure 3.6B), these mutations could induce merely a decrease in affinity between Otefin and BAF that may not be detectable in our pulldown assay where GST-Otefin is probably present in large excess relative to Flag-BAF. Expressing BAF in bacteria and optimizing molar ratios could solve these potential issues.

3.5.5 Mutation of the phosphosites impacts Otefin recruitment at the reforming nuclear envelope

To investigate if the phosphosites mutations affect Otefin's protein interaction dynamics during cell division, we used live fluorescence microscopy. We reasoned that removing the transmembrane domain (TM) in Otefin would uncover localization changes depending on interactions with proteins such as BAF at reassembling nuclei. We generated GFP-tagged variants with deletions of the N-terminal TM. As expected, while GFP-Otefin localizes to the NE, GFP-OtefinΔTM is diffuse in the nucleoplasm, as previously observed (Jiang et al., 2008) (Figure 3.7A). We expressed GFP-OtefinΔTM (WT, S50A,S54A and S50D,S54D) together with mCherry-tubulin in D-Mel cells and filmed their divisions. Quantification of GFP fluorescence intensity at the reforming nuclei using spindle elongation as time 0 shows a delay in the recruitment of GFP-OtefinΔTM[S50D,S54D] on chromosomes in telophase compared to WT and phosphodeficient forms (Figure 3.7B-C). This suggests that phosphorylation of Otefin retards, without preventing, its recruitment at the chromosomes during mitotic exit, possibly by regulating its interaction with BAF. Phosphodeficient mutations seem to slightly accelerate Otefin's recruitment, however quantified values are not significantly different in that case.
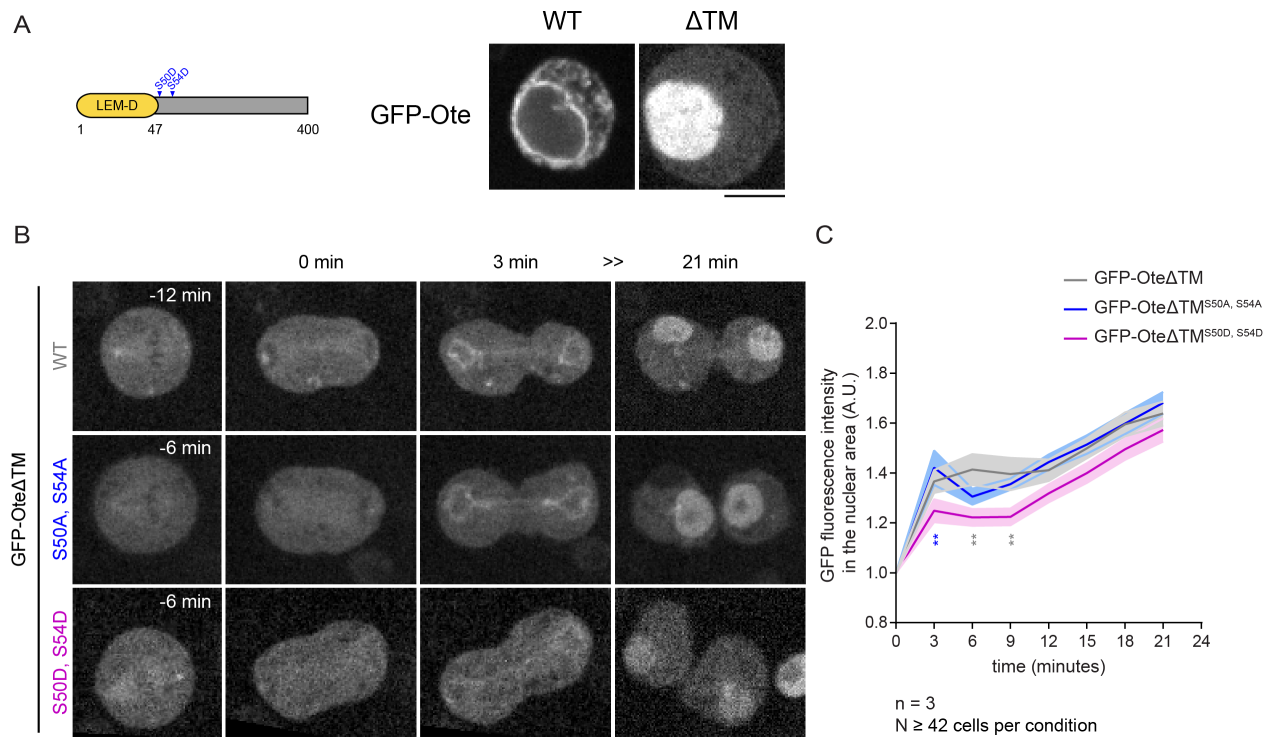
Figure 3.7. Mutation of the identified phosphosites impacts Otefin timely recruitment at the reassembling nuclei during mitotic exit.

(A) Removing Otefin's transmembrane domain (TM) to uncover localization changes depending on protein interactions. On the left, schematic representation of the primary structure of Otefin without the transmembrane domain. On the right, representative images of the indicated Otefin variants. GFP-Otefin localizes to the nuclear envelope. GFP-OtefinΔTM is diffuse in the nucleoplasm. Scale bar: 5 µm. (B) Live-imaging of cells expressing GFP-OtefinΔTM (WT, S50A,S54A and S50D,S54D) and mCH-tubulin (not shown). Time 0 corresponds to spindle elongation. Scale bar: 5 µm. (C) Quantification of GFP-OtefinΔTM (WT, S50A,S54A and S50D,S54D) recruitment on reassembling nuclei from the experiments in B. The fluorescence intensity was measured at a single z-plane for a region of interest (ROI) containing the nucleus for each time point. Values are averages of three independent experiments in which between 42 and 51 dividing cells were quantified for each condition. Shaded areas indicate standard error of the mean (SEM). Two-way ANOVA followed by Tukey's and Dunnetts's multiple comparisons was performed. Recruitment of GFP-OtefinΔTM[S50D,S54D] on chromosomes in telophase is significantly delayed compared to WT (grey asterisks) and phosphodeficient (blue asterisks) forms. **$p < 0.01$.

167

3.5.6 Phosphoregulation of Otefin impacts its association with other proteins

Phosphorylation of Otefin at Ser50 and Ser54 may alternatively alter its binding to another protein of the nuclear envelope that is in complex with BAF. To investigate this, we purified GFP-Otefin (WT and phosphomutants) from D-Mel cells using a GFP-affinity resin, eluted the purification products and analyzed interactors by mass spectrometry. Band patterns reveal purified GFP-Otefin variants and are informative about the amount of co-purified proteins (Figure 3.8A). We can detect many protein bands in our Flag-GFP negative control, but expression and purification levels of this construct are highly superior. To identify high-confidence interactors, mass spectrometry data from biological duplicates were analyzed using SAINTexpress in the CRAPome interface (Choi et al., 2012; Teo et al., 2014). Seventeen proteins scored as high-confidence binding partners (SAINT score $\geq$ 0.9) for at least one GFP-tagged Otefin variant (Figure 3.8B). Of these, Lamin and BAF are identified as interactors for all three GFP-Otefin forms, but are more abundant in the GFP-Ote$^{S50A,\ S54A}$ datasets. Another identified interactor is Girdin, a protein involved in actin organization. Interestingly, the relative abundance of Girdin retrieved with GFP-Ote$^{S50D,\ S54D}$ is higher than with the other variants, suggesting that phosphorylation of Otefin enhances the interaction. In accordance with our hypothesis, GFP-Ote$^{S50A,\ S54A}$ is the variant with the most high-confidence specific interactors, including 14-3-3ζ, AFG3L2, Droj2 and RpL3. Gene ontology (GO) analysis revealed an enrichment for proteins involved in ribosome biogenesis and modification, and microtubules organization (Figure 3.8C-D). Of note, two subunits of the H/ACA ribonucleoprotein complex, which catalyzes pseudouridylation of rRNA during ribosome biogenesis, score as high-confidence interactors for GFP-Otefin and GFP-Ote$^{S50A,\ S54A}$, respectively: Nop60B and GCR101. These two proteins localize to the nucleolus.
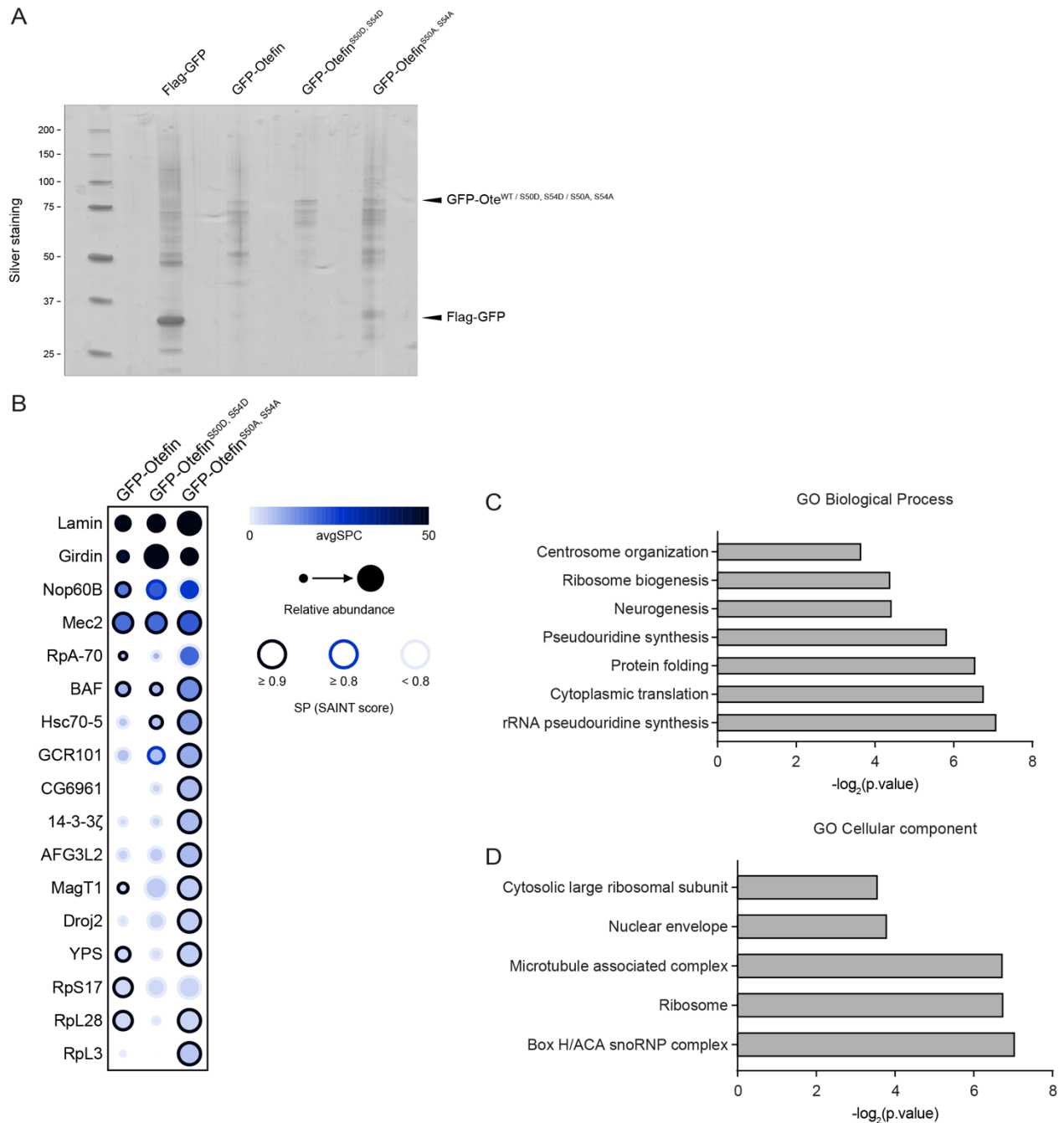
Figure 3.8. Mutation of the identified phosphosites of Otefin impacts its association with other proteins.

(A) D-Mel cells expressing GFP-Otefin (WT and phosphomutants) were submitted to GFP-affinity purification for mass spectrometry analysis. Purified complexes were visualized on a silver-stained gel. Arrows: GFP-tagged proteins. (B) Dotplot of AP-MS data with GFP-Otefin (WT and phosphomutants) in D-Mel cells from two biological replicates. Dot color represents the abundance (average spectral counts, avgSPC; see legend) detected for the indicated prey proteins listed for the indicated bait (GFP-Otefin

169

variants). Dot size indicates relative abundance detected for prey proteins across baits. Dot outline indicates SAINT score (SP) of interaction (determined by SAINTexpress). (C-D) Gene Ontology (GO) enrichment for Biological Process (C) and Cellular Component (D) analysis was performed on identified preys using DAVID. Log-transformed p-values calculated using Fisher's Exact test to measure the gene-enrichment are graphed.

Our results are consistent with our hypothesis that phosphorylation of Otefin near its LEM domain reduces its binding to BAF. Preventing phosphorylation at these sites allows other protein interactions, notably with ribosomal proteins. Moreover, we uncovered interactions between unphosphorylated Otefin and nucleolar proteins involved in rRNA processing. We cannot conclude that identified interactors are direct partners of Otefin; they could also be part of complexes involving other proteins, like BAF and Lamin.

3.6 Discussion

SILAC is a robust method broadly applied in large-scale screens to identify protein post-translational modifications, as it allows more accurate peptide quantification than unlabeled techniques (Olsen and Mann, 2013; Ong, 2012; Ong et al., 2002). Indeed, metabolic labeling of amino acids facilitates peptide pairs identification by mass spectrometry. SILAC is efficiently used in a wide variety of animal models (Ong, 2012). Despite numerous well-developed genetic and biochemical tools, only few SILAC-based proteomic studies have been conducted in *Drosophila*. One general caveat of SILAC is the arginine-to-proline conversion reported in several organisms, which can lead to the undesired labeling of prolines and a reduced global labeling (Bicho et al., 2010). Adding unlabeled proline to cell media can help reducing this phenomenon. In *Drosophila* however, labeled amino acid conversion is not limited to proline *in vivo*, as both heavy arginine and heavy lysine have been found to be converted in multiple other amino acids (Chang et al., 2013). This can introduce a shift in the isotopic pattern and affect the quantification accuracy. Such conversions have not been reported for SILAC S2 cell culture system (Bonaldi et al., 2008; Chang et al., 2013). However, high concentrations of labeled amino acids are typically used in *Drosophila*, possibly supplying enough amino acids to reduce metabolic conversion.

Our experiments are reminiscent of this, as only cells cultured in synthetic SILAC media with high concentrations of lysine and arginine reached satisfying labeling. The slower proliferation rates we observed for cells growing in SILAC media were also reported by another group, who suggested serum and yeast extract dialysis could remove important components of low molecular weight such as salts and protein-derived peptides (Bonaldi et al., 2008). Importantly, heavy and light SILAC media affected cell populations similarly and therefore did not affect subsequent proteomic quantifications. Unfortunately, supplementing SILAC media with unlabeled proline and glutamine did not accelerate cell proliferation (data not shown). Other tested cell lines (D-Mel and Kc) had a similar behavior than S2 cells in SILAC media. A healthy population of frequently dividing cells is crucial to the identification of PP2A-Tws mitotic substrates by phosphoproteomics, especially as fly cell synchronization is challenging. Moreover, SILAC proved to be expensive and time-consuming.

Altogether, these technical issues led us to look for an alternative phosphoproteomics approach. We decided to switch to label-free screening. Cell culture in label-free media allowed for faster cell proliferation, efficient RNAi silencing, and harvesting of bigger amounts of cells. This allowed a more than 3-fold increase in the number of identified phosphopeptides. We think these gains in quality and quantity of the biological material largely compensate for any loss of quantification accuracy due to the unlabeling. Moreover, label-free quantifications have made significant advances in the recent years, making them increasingly comparable to techniques like SILAC in terms of accuracy and reproducibility (Cox et al., 2014; Schober et al., 2021). Thus, from our experience, a label-free approach is more suitable to the study of the mitotic phosphoproteome in *Drosophila* cells in culture.

Yet, data obtained from our SILAC-based screens remain informative, especially when combined with data generated by label-free quantification. The intersection of our different datasets indeed points towards some reproducibly identified phosphosites that could correspond to PP2A-Tws targets. The most systematically identified hyperphosphorylated site after PP2A-Tws depletion and PP2A chemical inhibition is the Ser283 of the microtubule-associated protein Map205. Strikingly, Cdk1 phosphorylation

at this site was previously reported to disrupt the interaction between Map205 and the Polo kinase, thereby releasing Polo from the microtubules at mitotic entry (Archambault et al., 2008). Our phosphoproteomic results suggest dephosphorylation of this site during mitotic is PP2A-Tws-dependent. This event could promote Polo recruitment, via its interaction with Map205, at the spindle midzone during anaphase (Archambault et al., 2008; Kachaner et al., 2014).

We found other phosphosites in proteins of the microtubule cytoskeleton organization as high-confidence PP2A-Tws potential targets, including KLC^{pS433}, Dgt6^{pT394} and Patronin^{pS997}. Sites on proteins involved in nuclear envelope regulation were also repeatedly identified across experiments: NHK-1^{pS483}, NHK-1^{pT503}, Ankle2^{pS1089}, Nup358^{pS2304}, MSP-300^{pS2289} and Otefin$^{pS50, pS54}$. These results suggest that multiple dephosphorylation events driven by PP2A-Tws are necessary for proper NER. Targeting of Nup358 may promote NPC reassembly. Interestingly, previous results from *C. elegans* and human cells suggest that Ankle2 collaborates with PP2A to counteract NHK-1 and promote BAF dephosphorylation during mitotic exit (Asencio et al., 2012). Our group later reported PP2A-Tws-dependent dephosphoryltation of BAF in *Drosophila* (Mehsen et al., 2018). Our phosphoproteomic results reinforce the idea of a coordinated interplay between PP2A-Tws, Ankle2, NHK-1 and BAF to promote NER. MSP-300^{pS2289} was also identified in multiple experiments. MSP-300 is the *Drosophila* ortholog of the actin-binding nesprins, members of the linker of nucleoskeleton and cytoskeleton (LINC) complex.

Finally, our top-scoring nuclear envelope hit, Otefin, was identified through two proline-directed serines (Ser50 and Ser54) localized near its LEM domain. Otefin is a well-known BAF interactor that promotes its localization at the NE in interphase cells. BAF plays a central role in the nuclear architecture by bridging chromatin and NE proteins. We found Ser50 and Ser54 to be hyperphosphorylated upon PP2A-Tws depletion. Accordingly, these residues were previously identified as Cdk1 sites (Ashery-Padan et al., 1997; Habermann et al., 2012). Multiple NE proteins, including BAF and the LEM-D proteins, are phosphorylated at mitotic entry to trigger their mutual dissociation and NEB (Huguet et al., 2019). In *Xenopus*, dissociation of emerin from

BAF is phosphodependent during mitosis (Berk et al., 2013; Hirano et al., 2005). Our results suggest that PP2A-Tws-dependent dephosphorylation of Otefin at Ser50 and Ser54 promotes its interaction with BAF. We can imagine a simple model in which Cdk1 phosphorylation of Otefin at Ser50 and Ser54 at mitotic entry abrogates the association of its LEM domain to BAF dimers. This event probably contributes to dissociate the chromatin from the NE, which is required for NEB and mitotic progression. Otefin dephosphorylation by PP2A-Tws at mitotic exit would be part of a coordinated series of modifications leading to complete NER. The following paragraphs will present increasing evidence that however suggests a more complicated picture involving other layers of regulation.

Sites near emerin's LEM domain, that could correspond to the ones we identified in Otefin, can be modified with phosphate and *O*-linked *β–N*-acetylglucosamine (*O*-GlcNAcylation) (Berk et al., 2013). While phosphomimetic mutations reduce interaction with BAF, *O*-GlcNAc modifications seem to promote it (Berk et al., 2013; Hirano et al., 2005). As *O*-GlcNAcylation is globally reduced during mitosis (Liu and Li, 2018), phosphorylation and *O*-GlcNAcylation events could compete in a cell cycle-dependent manner to modulate Otefin/emerin – BAF association. Hence, *O*-GlcNAcylation could collaborate with PP2A-Tws for NER.

Other studies suggest that phosphorylation of emerin near its LEM domain may promote its oligomerization. Indeed, the LEM domain of emerin can interact with the central disorganized region of emerin (Berk et al., 2014; Samson et al., 2017). Altering the folding of the LEM domain promotes emerin oligomerization (Samson et al., 2017). Moreover, residues adjacent to the LEM domain (a.a. 48-53) participate in the LEM interaction with the central region (Berk et al., 2014). Phosphorylation of emerin near its LEM domain could modify its conformation, thereby promoting emerin-emerin interactions rather than emerin-BAF interactions (Fernandez et al., 2021; Samson et al., 2017; Samson et al., 2018).

Post-translational modifications on Otefin could also modulate interactions with other proteins. Our results indicate that the unphosphorylatable mutant engages with other partners, including nucleolar and actin-binding proteins. The nucleolus, the hub for

ribosomal DNA transcription and ribosome biogenesis, also contributes to cell cycle progression through the nucleolar stress response pathway (NSP), which mediates p53 stability (Nunez Villacis et al., 2018; Tiku and Antebi, 2018). Ribosomal proteins and nuclear actin are involved in the NSP (Boulon et al., 2010; Kelpsch and Tootle, 2018). Interestingly, it was recently suggested that Otefin, as an actin capping protein, could regulate nucleoplasmic and nucleolar actin structures (Duan et al., 2020a). Could Otefin be involved in the NSP, connecting cellular stresses to p53-mediated cell cycle arrest? A similar mechanotransducing role has been attributed to oligomeric emerin/Otefin, through interactions with lamins and the LINC complex proteins, for signaling mechanical stresses between the cytoskeleton and the nucleus (Fernandez et al., 2021; Haque et al., 2010; Mislow et al., 2002; Unnikannan et al., 2020).

In this study, we have used two phosphoproteomic approaches in *Drosophila* to identify novel PP2A-Tws substrates. We found interesting high-confidence candidates and began to dissect the phosphoregulation of the nuclear envelope protein Otefin. The mitotic roles of the LEM-D proteins are yet to be characterized. Our work is a step towards a better understanding of the LEM-D/BAF complexes regulation in mitosis.

3.7 Materials and methods

3.7.1 Plasmids and mutagenesis

Drosophila cells expression vectors were generated by Gateway recombination (Invitrogen). Coding sequences were first cloned into the pDONR221 entry vector and then recombined into the relevant destination vectors for expression from copper-inducible (pMT) or constitutive (pAC5) promoters. The following expression vectors were generated: pAc5-Flag-BAF, pMT-GFP-Ote, pMT-GFP-Ote$^{S50A, S54A}$, pMT-GFP-Ote$^{S50D, S54D}$, pMT-GFP-OteΔTM, pMT-GFP-OteΔTM$^{S50A, S54A}$, pMT-GFP-OteΔTM$^{S50D, S54D}$, pAc5-mCherry-tubulin. GST- OteΔTM (1-150, 1-150$^{S50D, S54D}$, 1-260, 1-260$^{S50D, S54D}$, 1-400, 1-400$^{S50D, S54D}$) plasmids were constructed into the pGEX4T vector. Amino-acid substitution mutants were generated using QuikChange Lightning Site-Directed

Mutagenesis Kit (Agilent) following the manufacturer's protocol. All sequences of oligonucleotides used for the generation of plasmids used in this study are provided in Tableau S3.1.

3.7.2 Cell culture, transfections and cell lines

Except for SILAC experiments that were performed using S2 cells, all cells were in the D-Mel (d.mel-2) background and were cultured in Express Five medium (Invitrogen) supplemented with glutamine, penicillin and streptomycin (Wisent). Transfections were performed using X-tremeGENE HP DNA Transfection Reagent (Roche) following the manufacturer's instructions. All stable cell lines were selected in medium containing 20 µg/ml blasticidin. While inducible pMT-based vectors contain the blasticidin resistance gene, pAc5-based vectors were co-transfected with pCoBlast to confer blasticidin resistance to the cells. Expression of the copper-inducible transgenes was induced with $CuSO_4$ (300 µM) for at least 8 h before experiments.

For phosphoproteomics, cells were treated with okadaic acid (5 nM or 100 nM) for 1 hour to inhibit PP2A. For immunoprecipitations, cells were treated with okadaic acid (5 nM or 100 nM) for 1 hour, with LB100 (10 µM or 100 µM) for 1 hour or with DMSO.

For RNA interference, dsRNAs were generated from PCR amplicons using a Ribomax kit (Promega). All sequences of oligonucleotides used in the PCRs are provided in Tableau S3.1.

For SILAC phosphoproteomics, cells were transfected in 25-cm^2 flasks with 80 µg of Tws (or control) dsRNA using Transfast reagent (Promega). 3 technical replicates were done for each experiment (each run). After a 4-day treatment, 20 x 10^6 heavy labeled cells and 20 x 10^6 light labeled cells were mixed. Cells were washed with cold PBS (3x). For label-free phosphoproteomics, cells were transfected in 25-cm^2 flasks with 150 µg of dsRNA (Endos, Gwl, Tws or control) using Transfast reagent (Promega). 4 technical replicates were done for each treatment. 40 x 10^6 were harvested 72 h later. For immunoprecipitations, cells were transfected in six-well plates with 20 µg of Tws (or

control) dsRNA using Transfast reagent (Promega). Cells were analyzed 24 h or 48 h later by immunoblotting. For all experiments, the control dsRNA was generated against the sequence of the bacterial kanamycin resistance gene.

3.7.3 SILAC of *Drosophila* cells

SILAC protocol was based on (Sap et al., 2015). Briefly, S2 cells were cultured in custom-made Schneider's *Drosophila* medium (Athena Enzyme Systems, Baltimore, MD), based on Invitrogen's formulation (Invitrogen, #21720-001), modified as follow: dialyzed yeastolate (3500 Da MWCO) and deficient for lysine and arginine. The medium was supplemented with 5% dialyzed FBS (F0392, Sigma-Aldrich), 1% penicillin-streptomycin and light $[^{12}C_6, {}^{14}N_4]$-L-Arginine and light $[^{12}C_6, {}^{14}N_2]$-L-Lysine, or heavy $[^{13}C_6, {}^{15}N_4]$-L-Arginine and $[^{13}C_6, {}^{15}N_2]$-L-Lysine (Silantes). Two concentrations were tested: Arg 380 µM and Lys 640 µM, or Arg 2 mM and Lys 20 mM. S2 cells were cultured at 25°C in concentrated (Arg 380 µM, Lys 640 µM) SILAC medium at 25°C for at least nine cell doublings to reach complete labeling. Light labeled cells were exposed to control conditions (dsKan or DMSO). Heavy labeled cells were either exposed to 4-day treatment with dsTws or to 1h treatment with okadaic acid 5 nM (Run1) or 100 nM (Run 3).

3.7.4 Protein purifications

For GFP affinity purifications, D-Mel cells expressing Flag-GFP, GFP-Otefin, GFP-Otefin[S50A, S54A] or GFP-Otefin[S50D, S54D] from 4 confluent 175-cm^2 flasks were harvested and resuspended in lysis buffer (75 mM K-HEPES pH 7.5, 150 mM NaCl, 2 mM EGTA, 2 mM MgCl$_2$, 1 mM DTT, 10 µg/ml aprotinin, 10 µg/ml leupeptin, 1 mM PMSF, 5% glycerol, 0.5% Triton X-100). Lysates were incubated with GFP-trap nanobeads (Cromotek) for 2 hours. Beads were washed 5 times with lysis buffer and 5 times with PBS containing protease inhibitors. The purification products were then eluted from the nanobeads using a buffer containing 0.5 M NH4OH and 0.5 mM EDTA.

Eluates were dessicated using a Speedvac centrifuge. 90% of each sample was sent for mass spectrometry. The remaining 10% was resuspended in 1X Laemmli buffer and used for SDS-PAGE analysis by silver nitrate staining. Protein purification products were analyzed by LC-MS by the Proteomics Facility in IRIC.

3.7.5 Mass spectrometry

For phosphoproteomics, harvested cells were lysed in ice cold 1% (w/v) SDC (Sodium deoxycholate, Sigma D6750) in 50 mM NH_4HCO_3. Protein concentration was measured by BCA assay (Thermo Fisher Scientific). Protein disulfide bonds were reduced by adding Tris(2-carboxyethyl)phosphine hydrochloride (TCEP, 5 mM final) to the lysates. Alkylation of cysteine residues was achieved by adding chloroacetamide (CAA, 20 mM final). Samples were incubated at 37 °C with 500 rpm shaking for 30 minutes for the reduction/alkylation procedure and then digested (overnight, 37°C) with trypsin (Sigma-Aldrich) using an enzyme to substrate ratio of 1:25 (w:w). Tryptic digests were acidified with 1% formic acid (FA), centrifuged (17,000x*g*, 10 min) and desalted on Oasis HLB cartridges (Waters) previously conditioned with acetonitrile (1% FA), solid-phase extraction (SPE) buffer (50% acetonitrile, 1% FA), and finally 1% aqueous FA. Peptide samples were applied, desalted with 3 ml of 1% FA and eluted in 1 ml of SPE buffer. Peptide eluates were snap-frozen in liquid nitrogen, lyophilized in a SpeedVac centrifuge and stored at -80°C. Phosphopeptide enrichment was performed on 5 µm titansphere particles (Canadian Life Science, Peterborough, ON, Canada) according to published protocols (Kanshin et al., 2012; Kanshin et al., 2013). Loading of protein extracts on the titansphere beads, washing, and elution steps were performed using custom spin columns (Ishihama et al., 2006) made from 200 µl pipette tip containing a SDB-XC membrane (Empore, 3M) frit and filled with TiO_2 beads. Peptides were desalted in 100 µl of 1% FA and subsequently eluted from spin columns using 100 µl of 50% acetonitrinile, 0.5% FA. LC-MS/MS analyses were per-formed on a Q-Exactive HF or an Orbitrap tribrid Fusion mass spectrometer using homemade capillary LC columns (18 cm length, 150 µm inner diameter, 360 µm outer diameter). Capillary LC columns were

packed with C18 Jupiter 3 μm particles (Phenomenex, Torrance, CA) at 1,000 psi. Samples were directly injected on LC-columns and separations were performed at a flow rate of 0.6 μl/min using a linear gradient of 5–35% aqueous acetonitrile (0.2% FA) in 150 min. Raw data analysis of SILAC experiments was performed using Maxquant software 1.5.3.8. The false discovery rate (FDR) for peptide, protein, and site identification was set to 1%, the minimum peptide length was set to 6. The Uniprot fly proteome database was used for all database searches. Further bioinformatics analyses were performed in R.

For affinity purification mass spectrometry (AP-MS), eluted protein purification products were analyzed by Liquid Chromatography—Mass Spectrometry (LC-MS) as described (Garrido et al., 2020). Samples were reconstituted in 50 mM ammonium bicarbonate with 10 mM TCEP [Tris (2-carboxyethyl) phosphine hydrochloride; Thermo Fisher Scientific], and vortexed for 1h at 37˚C. Chloroacetamide (Sigma-Aldrich) was added for alkylation to a final concentration of 55 mM. Samples were vortexed for another hour at 37˚C. One microgram of trypsin was added, and digestion was performed for 8 h at 37˚C. Supernatants were desalted on stage-tips (The Nest Group). Samples were dried down and solubilized in 5% acetonitrile (ACN)-0.2% formic acid (FA). The samples were loaded on a home-made reversed-phase column (150-μm i.d. by 150 mm) with a 220-min gradient from 10 to 30% ACN-0.2% FA and a 600-nl/min flow rate on an Easy nLC-1000 connected to an Orbitrap Fusion (Thermo Fisher Scientific, San Jose, CA). Each full MS spectrum acquired at a resolution of 240,000 was followed by tandem-MS (MS-MS) spectra acquisition on the most abundant multiply charged precursor ions for a maximum of 3s. Tandem-MS experiments were performed using collision-induced dissociation (CID) at a collision energy of 30%. The data were processed using PEAKS X (Bioinformatics Solutions, Waterloo, ON) and a Uniprot *Drosophila* unreviewed database. Scaffold version 5.0.0 (Proteome Sofware Inc., Portland, OR) was used to validate MS/MS-based peptide and protein identifications. Spectral counts were exported from Scaffold and were formatted according to SAINT algorithm guidelines. SAINTexpress statistical analyses were carried out including 3xFLAG-GFP controls using the CRAPome interface. Proteins with a SAINT score ≥0.9 were deemed genuine interactors. The dot plot was generated using ProHits-viz (Knight

et al., 2017). Gene Ontology (GO) enrichment analyses were performed using the Database for Annotation, Visualization and Integrated Discovery (DAVID) version 6.8 (Huang da et al., 2009a; Huang da et al., 2009b).

3.7.6 Western blotting and immunofluorescence

Primary antibodies used in western blotting were anti-Flag M2 from mouse (#F1804, Sigma, 1:2000 dilution), anti-GFP from rabbit (TP401, Torrey Pines, 1:2000 dilution), mouse monoclonal anti-actin (#MAB1501, Millipore, dilution 1:5000), anti-Myc A-14 from rabbit (#sc-789, Santa Cruz Biotechnology, Inc.), anti-Endos from rabbit (custom-made by Thermo Fisher Scientific, dilution 1:500), anti-Gwl (custom-made against full-length Gwl by Genscript), anti-PP2A B subunit from rabbit (#2290P, NEB, at 1:1000 dilution for WB). Secondary antibodies were coupled to Peroxidase (Jackson, at 1:5000 dilution).

For Fluorescence *In Situ* Hybridization (FISH), flies were allowed to lay eggs on grape-juice containing agar in a cage. Embryos were collected every 2 h and dechorionated in 50% bleach and then washed 3 times in 0.7% NaCl, 0.05% Triton X-100. Eggs were fixed in methanol:heptane (1:1) while shaking vigorously. Eggs were stored at -20˚C for later use, or immediately rehydrated successively in 9:1, 7:3 and 1:1 methanol:PBS solutions. FISH was performed using a probe against the 359-base pair peri-centromeric repeat on the X chromosome (Dernburg, 2011). Anti-α-tubulin YL1/2 from rat (#MCA77G, Sigma, dilution 1:2000) and anti-rat Alexa 647 (#A21247, Invitrogen, dilution 1:1000) were used to immunostain tubulin. DNA was stained with QUANT-IT Oli-green 1:5000 (#O7582, Invitrogen). Eggs were mounted using 1,2,3,4-Tetrahydronaphthalene (Sigma).

3.7.7 Immunoprecipitation

For immunoprecipitation of Myc-BAF, pelleted cells from confluent 9-cm^2 wells were lysed in 50 mM Tris-HCl pH 7.5, 150 mM NaCl, 1mM EDTA, 10% glycerol, 0.2%

Triton X-100, 1 mM PMSF, 10 µg/ml aprotinin and 10 µg/ml leupeptin, and lysates were centrifuged at 19 000xg during 10 min at 4 °C. Lysates were incubated with anti-Myc 9E10 from mouse (#sc-40, Santa Cruz Biotechnology, Inc.) for 90 min at 4 °C and then incubated with 20 µl of Protein G-conjugated Dynabeads (Invitrogen) for 30 min at 4 °C, before being washed in lysis buffer four times.

3.7.8 Production of GST-fusion proteins

Overnight cultures of BL21 *Escherichia coli* transformed with pGEX-OtefinΔTM (WT or mutants), were used to inoculate 110 ml of LB medium. At an OD$_{600}$ between 0.4 and 0.6, expression was induced with 1 mM IPTG for 3 h at 37°C. Cells were pelleted at 3000g for 10 min at 4°C and resuspended in 5 ml of PBS, 0.4% Sarcosyl and supplemented with 1 mM phenylmethylsulfonyl fluoride (PMSF), 10 µg/ml aprotinin and 10 µg/ml leupeptin. Bacterial cell suspensions were lysed by sonication and Triton X-100 was added (1% final). Extracts were incubated on wheel for 20 min at 4°C and centrifugated at 23,500xg for 20 min. For preparation of beads, 10 ml of clarified extract were incubated with 300 µl of washed Glutathion Sepharose 4B beads (GE Healthcare) for 1 h at 4°C. Beads were washed four times with PBS, 1 mM PMSF, 10 µg/ml aprotinin, 10 µg/ml leupeptin, 1% Triton X-100. Beads were flash freezed and stored in 90-µl aliquots at -80°C until use.

3.7.9 GST-pulldown assay

Pelleted D-Mel cells expressing Flag-BAF from confluent 75-cm^2 flasks were lysed in 75 mM K-HEPES pH 7.5, 150 mM KCl, 2 mM EGTA, 2 mM MgCl$_2$, 5% glycerol, 0.2% Triton X-100, 1 mM PMSF, 10 µg/ml aprotinin and 10 µg/ml leupeptin, and lysates were centrifuged at 4900xg during 15 min at 4 °C. Clarified lysates were incubated with sepharose beads bound to purified GST–OtefinΔTM (WT or mutants) or GST during 90 min at 4 °C. Beads were washed five times with lysis buffer before SDS–PAGE and immunoblotting.

3.7.10 Microscopy

Fixed embryos were imaged using a TCS SP8 DLS laser scanning microscope (Leica) using 63X (NA 1.4) oil objectives. Live imaging was performed using a Spinning-Disk confocal system (Yokogawa CSU-X1 5000) mounted on a fluorescence microscope (Zeiss Axio Observer.Z1) using an Axiocam 506 mono camera (Zeiss), 63X oil objective (NA 1.4), and Zen software. For time-lapse microscopy, D-Mel cells in culture were plated in a Lab-Tek II chambered coverglass (#155409, Thermo Fisher Scientific).

Fluorescence quantifications and images treatment were performed using Fiji software (NIH). For images in Figure 3.5, a final projection was made on the z-planes containing the nuclei. Figure 3.7 presents images of single z-planes containing the nuclei. Fluorescence intensity was measured at a single z-plane for a region of interest (ROI) containing the nucleus with the Fiji software. Background signal was substracted.

3.7.11 Fly genetics

Fly husbandry was conducted according to standard procedures. All crosses were performed at 25 °C. The WT strains used were W1118 and Oregon R. The Ote[HMS01926] (#39009, targets the 3'UTR) and Ote[HMC05269] RNAi (#62262, targets the coding sequence) strains used for depletion of Otefin were obtained from Bloomington *Drosophila* Stock Center (#20177). Expression of transgenes in the early embryo was driven by *mat-α-tub-GAL4* (#7062, Bloomington *Drosophila* Stock Center).

For fertility tests, between 5 and 10 well-fed females were mixed with 3 males in tubes containing grape juice agar with yeast paste and allowed to lay eggs for 1 day before being removed. The percentage of egg hatching was counted 24 h later. Three technical replicates were performed per condition.

3.7.12 Statistical Analyses

GraphPad software was used for graphing and statistical analyses. All results are expressed as mean ± SD unless otherwise indicated. Sample size (n) is given in each figure legend. Two-way ANOVA followed by Sidak's multiple comparisons was used in Figure 3.5B. Two-way ANOVA followed by Tukey's and Dunnetts's multiple comparisons was used in Figure 3.7C. In all figures, p-values are represented as follows: *$p < 0.05$, **$p < 0.01$, ***$p < 0.001$, ****$p \leq 0.0001$, and n.s. (not significant) is $p > 0.05$. Data distribution was assumed to be normal, but this was not formally tested.

3.8 Supplemental material

3.8.1 Supplementary figures
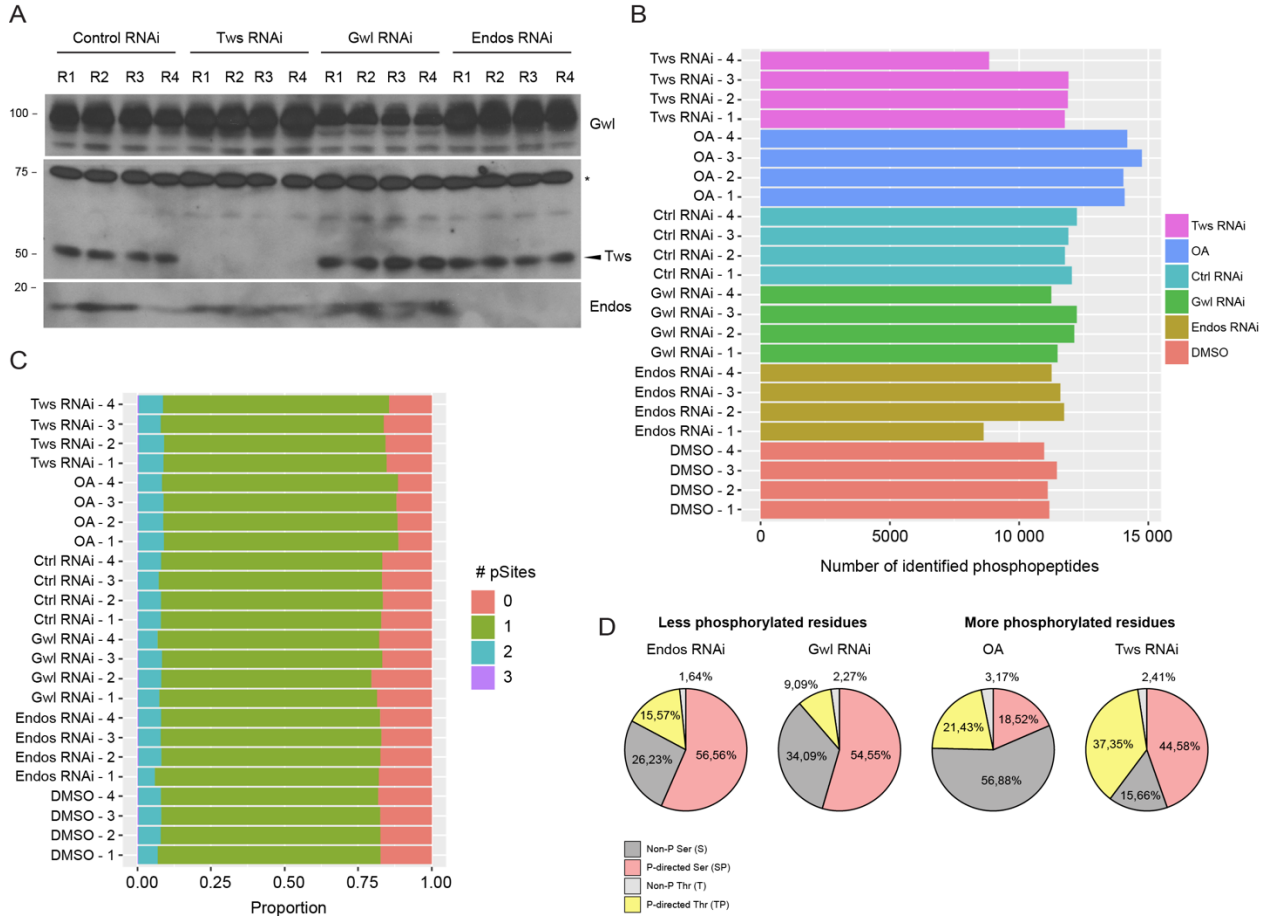
Figure S3.1. Label-free quantitative phosphoproteomics (complements to Figure 3.3). (A) WB validation of RNAi depletion for experiments in Figure 3.3. (B) Total number of phosphopeptides identified for each technical replicate across treatments. (C) Number of phosphorylation sites identified per phosphopeptide following for each technical replicate across treatments. (D) Proportion of identified hypophosphorylated (for Gwl and Endos RNAi treatments) and hyperphosphorylated (for Tws RNAi and OA treatments) proline-directed or non-proline-directed threonine and serine sites.

3.8.2 Supplementary tables

Tableau S3.1. Oligonucleotides used in this study.

Name	Sequence
Gateway cloning	
attB1-Ote-F	5'-GGGGACAAGTTTGTACAAAAAAGCAGGCTTAATGGCCGATGTGGACGATTTTGATTC-3'
attB2-Ote-R	5'-GGGGACCACTTTGTACAAGAAAGCTGGGTATCAGTAGAATATGTAATAAACGCCGAT TAACAAAAGGAC-3'
attB2-<u>Stop</u>-OteΔTM(1-400)-R	5'-GGGGACCACTTTGTACAAGAAAGCTGGGTA<u>TCA</u>CTTCTGCTCCAGGCTGTTCAACC -3'
pGEX-4T cloning	
*Nco*I-Otefin-F	5'-GGGGCCATGGGAATGGCCGATGTGGACGATTTTGATTCTC-3'
*Sma*I-Otefin400-R	5'-GGGGCCCGGGTCACTTCTGCTCCAGGCTGTTCAACC-3'
*Sma*I-Otefin260-R	5'-GGGGCCCGGGTCAAGATGGCGGCAGCACGGG-3'
*Sma*I-Otefin150-R	5'-GGGGCCCGGGTCAGCGCCGGGTCTGTACGGGTTG-3'
Mutagenesis	
Otefin-**S50D**-**S54D**-F	5'-GGTGGCCAGGCG**GAC**CCGGCCGCT**GAT**CCCAAGAAGACC-3'
Otefin-**S50D**-**S54D**-R	5'-GGTCTTCTTGGG**ATC**AGCGGCCGG**GTC**CGCCTGGCCACC-3'
dsRNA	
T7-Tws-F	5'-<u>TAATACGACTCACTATAGGGAGA</u>TCCTGCCTCAAAAGCC-3'
T7-Tws-R	5'-<u>TAATACGACTCACTATAGGGAGA</u>GAAGGTCTCCTGATCCGA-3'
T7-Kan-F	5'-<u>TAATACGACTCACTATAGGGAGA</u>CGACAATCTATCGCTTGTATGG-3'
T7-Kan-R	5'-<u>TAATACGACTCACTATAGGGAGA</u>CCGTCAGCCAGTTTAGTCTG-3'

3.9 Acknowledgements

Chapitre 4

4. Discussion et perspectives

La phosphatase mitotique PP2A-B55/Tws est l'élément central de ma thèse de doctorat. Je me suis intéressée dans un premier temps aux acteurs moléculaires agissant en amont de PP2A-Tws pour réguler son activité (Chapitre 2). Ce travail a permis d'approfondir notre compréhension du module composé de Gwl, Endos et PP2A-Tws, notamment de sa régulation spatiotemporelle. En autres, nos résultats apportent un nouvel éclairage sur la nécessité de la relocalisation de Gwl en prophase. De fait, nous avons trouvé qu'Endos et PP2A-Tws accomplissent leurs fonctions essentielles au cytoplasme. Dans un deuxième temps, je me suis penchée sur les protéines en aval de PP2A-Tws en tentant d'identifier ses substrats (Chapitre 3). Pour y arriver, j'ai adopté une stratégie de criblage phosphoprotéomique qui a permis d'identifier des candidats intéressants, dont la protéine de l'enveloppe nucléaire Otefin. La phosphorégulation d'Otefin par PP2A-Tws semble contrôler son interaction avec BAF et donc son recrutement à la chromatine lors de la reformation de l'enveloppe nucléaire. Dans les prochaines sections, je prendrai quelques pas de recul pour réfléchir à la façon dont mes résultats s'inscrivent dans des contextes mitotiques et cellulaires plus globaux.

4.1 Les phosphatases contre-attaquent

Longtemps négligées parmi les régulateurs de la mitose, les phosphatases ont depuis une vingtaine d'années commencé à susciter un intérêt plus marqué auprès des chercheurs. Une des raisons derrière ce désintérêt est leur nombre plus restreint que celui des kinases. Chez l'humain, on dénombre 539 gènes codant pour des kinases contre 189 gènes identifiés ou prédits pour les phosphatases (Chen et al., 2007). Bien que moins nombreuses, l'incorporation dynamique des sous-unités catalytiques des phosphatases au sein de complexes multimériques leur confère malgré tout un très large spectre de spécificité de substrats (Chen et al., 2017; Manning et al., 2002; Moorhead et al., 2007). Tel que présenté au Chapitre 1, les sites actifs de PP1 et PP2A contribuent à la reconnaissance spécifique des substrats, mais ce sont les sous-unités

régulatrices qui leur sont associées qui définissent majoritairement leur spécificité. Par leur interaction spécifique avec d'autres protéines, les sous-unités régulatrices contrôlent la localisation et l'activité des complexes.

4.1.1 Une compétition déloyale…et répandue?

Tout comme les kinases, PP1 et PP2A-B55 sont régulées au cours du cycle cellulaire. La liaison de petites phosphoprotéines non structurées est un mécanisme d'inhibition commun à PP1 et PP2A. Mon travail de thèse s'est intéressé de près au module inhibiteur de PP2A-B55, composé de Gwl et des endosulfines. Les endosulfines phosphorylées agissent comme inhibiteurs compétitifs de PP2A-B55 en entrée de mitose. Similairement, deux petites protéines (Inhibitor 1 et Inhibitor 2), phosphorylées par PKA et Cdk1 respectivement, lient PP1 et sont nécessaires à son inhibition en entrée de mitose (Ceulemans and Bollen, 2004; Leach et al., 2003; Wang et al., 2008a; Wang et al., 2008b; Wu et al., 2009). De façon intéressante, le complexe PP2A-B56, impliqué dans la transition métaphase-anaphase, est inhibé aux kinétochores par la liaison de la petite protéine Bod1 lorsqu'elle est phosphorylée par Cdk1 (Porter et al., 2013).

Ainsi, la liaison de petites phosphoprotéines inhibitrices semble être un mécanisme de régulation conservé parmi les phosphatases mitotiques. Inhibitor-1, Inhibitor-2, Bod1 et les endosulfines sont de petites protéines désordonnées et thermostables, qui lient et inhibent leur phosphatase cible suite à leur phosphorylation (Porter et al., 2013). Il n'est pas clair pour l'instant si PP1 et PP2A-B56 sont inhibées par compétition déloyale pendant la mitose. Par contre, l'inhibition par compétition déloyale a été proposée comme mode de régulation de la fonction non mitotique de PP1 dans la contraction musculaire (Filter et al., 2017). Ce mode d'inhibition découvert pour le module Gwl – endosulfines – PP2A pourrait donc constituer un mécanisme général, conservé évolutivement, de régulation de l'activité des phosphatases de la famille des PPPs.

4.1.2 Inhibiteurs spécifiques recherchés

L'intérêt relativement nouveau de l'étude des phosphatases combiné au fait que les sous-unités catalytiques sont communes à plusieurs complexes ayant des fonctions distinctes complique le développement d'inhibiteurs spécifiques. Parmi les inhibiteurs chimiques disponibles pour les PPPs, l'acide okadaïque est couramment utilisé. Initialement isolé de l'éponge de mer *Halichondira okadai*, l'acide okadaïque est une toxine qui inhibe les phosphatases des familles PP1 et PP2A (Bialojan et al., 1988; Bialojan and Takai, 1988; Tachibana et al., 1981; Takai et al., 1987; Takai and Mieskes, 1991; Takai et al., 1992). Bien qu'elle ait des affinités différentielles pour PP1 et PP2A (K_i ~ 150 nM et 30 pM, respectivement), cette molécule ne permet pas de cibler sélectivement les différents hétérocomplexes à l'intérieur des familles PP1 et PP2A (Takai and Mieskes, 1991; Takai et al., 1992). Cela s'explique par le fait qu'elle lie le site actif des sous-unités catalytiques et les ions métalliques qui s'y trouvent, sans égard aux sous-unités régulatrices associées (Xing et al., 2006; Zhang et al., 2013). Les autres toxines inhibitrices des phosphatases ont également un large spectre. Même un inhibiteur comme le LB-100, initialement présenté comme un inhibiteur spécifique de PP2A, n'est pas sélectif puisqu'il s'associe également avec le centre catalytique des phosphatases PPP5C (D'Arcy et al., 2019).

Comme ce sont les sous-unités régulatrices qui confèrent leur spécificité aux complexes PP1 et PP2A, une avenue possible pour le développement d'inhibiteurs spécifiques serait d'empêcher sélectivement leur recrutement (Moura and Conde, 2019; Nasa and Kettenbach, 2018; Nilsson, 2019). Pour développer des inhibiteurs spécifiques, une possibilité serait de bloquer sélectivement la formation des holoenzymes. On peut imaginer des composés synthétiques qui lieraient les surfaces d'interaction permettant le recrutement des sous-unités régulatrices : cela empêcherait la formation de certains complexes phosphatases et donc la déphosphorylation de leurs substrats (Zhang et al., 2013). Cette approche pourrait toutefois s'avérer difficile compte tenu de la taille des surfaces d'interactions impliquées. Une autre stratégie serait de cibler directement l'interaction avec le substrat. À cet effet, les progrès réalisés dans les dernières années pour identifier les motifs de reconnaissance des phosphatases sont

importants. Des molécules liant compétitivement les SLIMs identifiés pour empêcher la liaison des substrats aux phosphatases pourraient par exemple être développées. Comme les SLIMs diffèrent quelque peu d'un substrat à l'autre, il pourrait toutefois être plus efficace de cibler les motifs des phosphatases qui reconnaissent les SLIMs. La poursuite de la caractérisation structurelle des motifs de reconnaissance pourrait ainsi permettre d'identifier des façons de perturber l'interaction phosphatase – substrat. Le développement d'inhibiteurs spécifiques facilitera la dissection des mécanismes moléculaires régissant l'activité des phosphatases tout comme l'identification de leurs « phosphatasomes » respectifs. Plus généralement, l'identification des contributions spécifiques des phosphatases permettra de mieux comprendre les différents réseaux de phosphorylation et de mieux cerner les fonctions biologiques qui leur sont associées.

4.2 De l'importance d'être au bon endroit au bon moment

On représente souvent les voies de signalisation cellulaire comme un enchaînement linéaire d'étapes d'activation et d'inhibition de protéines. Bien qu'informatives, ces représentations omettent un aspect clé de toute voie de signalisation : la spatialité de ses composantes. La cellule est un environnement très dense et complexe dans lequel les localisations des macromolécules ne sont pas le fruit du hasard. Le contrôle spatiotemporel est clé dans de nombreux processus biologiques, comme l'établissement de la polarité cellulaire pendant le développement, la migration cellulaire et la division cellulaire. Gradients, compartiments, points d'ancrage, interactions protéiques; différents mécanismes contribuent à la régulation spatiotemporelle.

En entrée de mitose, l'import nucléaire de Cycline B – Cdk1 concentre son activité kinase au noyau, à l'abri des phosphatases cytoplasmiques. La localisation nucléaire de Gwl favorise probablement sa pleine activation en l'exposant à Cdk1 tout en l'éloignant de PP2A-B55. L'export de Gwl au cytoplasme mène ensuite à l'inhibition complète de PP2A-B55 avant que l'enveloppe nucléaire ne se brise et que le nucléoplasme ne se mélange au cytoplasme. En absence de mécanismes d'inhibition

190

robustes de PP1 et PP2A-B55, le mélange des contenus des deux compartiments dilue l'activité de Cdk1 et fait basculer la balance en faveur des phosphatases, empêchant l'établissement de l'état mitotique.

J'ai présenté précédemment le code biochimique intrinsèque régissant la déphosphorylation des substrats pendant la sortie de mitose. À ce code intrinsèque, il faut ajouter la localisation cellulaire des complexes phosphatases comme déterminant de leur spécificité. De fait, PP1 et PP2A peuvent être recrutées à diverses structures cellulaires via leur sous-unité régulatrice associée. Ainsi, on retrouve des populations de PP1 dans la région des kinétochores, au cortex cellulaire et à l'enveloppe nucléaire alors qu'une localisation au fuseau mitotique a été rapportée pour PP2A-B55 (Bollen et al., 2010; Peti et al., 2013; Reinhardt and Yaffe, 2013; Seshacharyulu et al., 2013). Le contrôle de la localisation des phosphatases dicte donc leur accès à différents substrats.

Mon travail de doctorat nous a permis de mieux comprendre certains aspects de la régulation spatiotemporelle du module Gwl – endosulfines – PP2A. Il a également soulevé de nouvelles questions, sur lesquelles il sera intéressant de se pencher.

4.2.1 Des fonctions nucléaires pour le module Gwl-endosulfines-PP2A?

Gwl est une protéine activée au noyau qui se relocalise au cytoplasme en entrée de mitose. Nous proposons un modèle dans lequel cette translocation permet à Gwl de phosphoryler son substrat au cytoplasme pour efficacement inhiber PP2A-B55. Nos travaux ont par ailleurs permis d'identifier un signal de localisation nucléaire (NLS) dans la séquence de B55/Tws (Larouche et al., 2021). Lorsque l'export nucléaire est bloqué, nous avons observé que Tws s'accumulait au noyau via son NLS (Larouche et al., 2021). Tws semble donc pouvoir transiter par le noyau, sans toutefois que cette localisation ne soit nécessaire à ses fonctions essentielles (Larouche et al., 2021). Quelle serait donc la raison physiologique d'une telle localisation nucléaire pour Tws?

Des résultats préliminaires obtenus par le précédent étudiant au doctorat Peng Wang suggèrent que Tws-GFP s'accumule au noyau suite au traitement de cellules de

drosophile avec l'agent alkylant méthanesulfonate de méthyle (MMS, methyl methanesulfonate). Or, une étude menée chez la drosophile suggère un rôle pour Tws dans le maintien de l'intégrité génomique (Merigliano et al., 2017). En présence de dommages à l'ADN, la kinase ATM phosphoryle le variant d'histone H2AX (appelé H2Av chez *Drosophila melanogaster*), qui s'appelle γ-H2AX/γ-H2Av dans sa forme phosphorylée, pour favoriser le recrutement des protéines de réparation (Fernandez-Capetillo et al., 2004; Rogakou et al., 1998; Stewart et al., 2003; Stucki et al., 2005). Chez la drosophile, la mutation de *tws* cause des aberrations chromosomiques et la persistance de foci nucléaires de γ-H2Av (Merigliano et al., 2017). Par leurs résultats de génétique, les auteurs suggèrent que PP2A-Tws est responsable de la déphosphorylation de γ-H2Av, déphosphorylation requise pour le désassemblage des complexes de réparation, la complétion de la réponse aux dommages et le retour de la chromatine à un état « pré-stress » (Merigliano et al., 2017). Chez les mammifères, PP2A a été la première famille de phosphatases impliquée dans la déphosphorylation de γ-H2AX (Chowdhury et al., 2005). La sous-unité catalytique de PP2A est en complexe et colocalise avec γ-H2AX, en plus de pouvoir le déphosphoryler *in vitro* (Chowdhury et al., 2005). La localisation nucléaire de Tws que nous avons observée pourrait donc être requise pour ce rôle proposé de PP2A dans la réponse aux dommages à l'ADN.

Pour tester les implications de Tws dans ce processus, il serait intéressant d'investiguer si l'accumulation nucléaire induite par des agents alkylants ou des irradiations dépend du NLS que nous avons identifié. Il serait important de tester biochimiquement si PP2A-Tws est directement responsable de la déphosphorylation de γ-H2Av. Il serait par ailleurs intéressant de vérifier si Tws colocalise avec γ-H2Av, et si cette potentielle colocalisation est dépendante du NLS de Tws.

Gwl joue également un rôle dans la protection de l'intégrité du génome en permettant la reprise du cycle cellulaire en aval de la réponse aux dommages à l'ADN (Pavey et al., 2020; Peng et al., 2010; Wong et al., 2016). Comme en mitose, la fonction de Gwl dans cette reprise est d'inhiber PP2A-B55. Est-ce que l'activité de Gwl permet d'inactiver PP2A-B55 suite à la déphosphorylation de γ-H2AX, pour permettre au cycle

cellulaire de se poursuivre? Une telle implication du module dans la réponse au dommage à l'ADN impliquerait la présence au noyau d'au moins une fraction d'Endos. Nous avons observé que la localisation d'Endos était majoritairement cytoplasmique et qu'elle semblait moins dynamique que celles de Gwl et de Tws (Larouche et al., 2021). Il n'est pas impossible qu'Endos ait la capacité de se retrouver au noyau. Une localisation nucléaire a d'ailleurs été proposée pour ses homologues humains dans des cellules HeLa (Charrasse et al., 2017; Hached et al., 2019). La participation du module dans la réponse aux dommages à l'ADN signifie aussi une activation de Gwl en amont de la mitose. Est-ce que l'activité basale de Gwl pourrait suffire pour cette fonction? Ou Gwl serait-elle partiellement activée en dehors de la mitose par une autre CDK que Cdk1?

4.2.2 Localisation des endosulfines : des questions demeurent sans réponse

Nous avons observé une localisation cytoplasmique pour Endos chez la mouche, localisation qui, entre nos mains, semble conservée pour ses homologues humains (Larouche et al., 2021). Nous avons également déterminé que PP2A-Tws accomplissait ses fonctions essentielles au cytoplasme (Larouche et al., 2021). Ces localisations expliquent la nécessité d'un export nucléaire de Gwl en prophase. Les mécanismes derrière la localisation cytoplasmique d'Endos demeurent toutefois à caractériser. De fait, de par sa petite taille de 13 kDa, il serait attendu qu'Endos (et ses homologues) puisse diffuser librement par les pores nucléaires. Comment expliquer l'enrichissement d'Endos au cytoplasme?

L'une des possibilités, mentionnée rapidement dans le Chapitre 2, est qu'Endos soit retenue au cytoplasme par une interaction avec une protéine ou une structure cytoplasmique. De façon intéressante, son homologue ENSA peut lier les membranes de phospholipides *in vitro* (Boettcher et al., 2008). Cette liaison aux phospholipides induit la formation d'hélices-α comprenant plusieurs résidus basiques (Boettcher et al., 2008). Ainsi, les régions chargées positivement d'ENSA pourraient être responsables des interactions avec les phospholipides chargés négativement des membranes. Nos

immunofluorescences révèlent un patron de localisation d'Endos qui ressemble à celui de certaines endomembranes, telles celles du réticulum endoplasmique, de l'appareil de Golgi ou encore des endosomes (Larouche et al., 2021). De plus, nous avons des résultats préliminaires de fractionnement cellulaire pour lesquels Endos est enrichie dans la fraction membranaire (Figure 4.1).
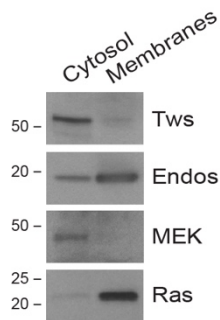
Figure 4.1. Enrichissement d'Endos dans la fraction membranaire.

Fractionnement cellulaire et Western blots montrant les quantités relatives d'Endos cytosolique et membranaire. La fraction membranaire contient les protéines membranaires intégrales ainsi que les protéines associées aux membranes. La fraction nucléaire a été isolée et exclue. MEK et Ras sont des contrôles cytosolique et membranaire, respectivement.

J'ai toutefois éprouvé des difficultés avec la reproductibilité de cette expérience; un travail d'optimisation sera requis pour en poursuivre l'investigation. Il serait néanmoins intéressant d'explorer davantage la liaison des endosulfines avec les endomembranes. Des marqueurs du Golgi, du réticulum endoplasmique et des différents endosomes pourraient être utilisés pour des expériences de colocalisation avec les endosulfines. Nous pourrions tenter de perturber le patron de localisation des endosulfines en introduisant des mutations dans leurs régions chargées positivement qui forment les hélices-α. Enfin, il a été proposé que le site de phosphorylation de PKA soit impliqué dans le contrôle du repliement d'ENSA et de son interaction avec les membranes (Boettcher et al., 2008). Il serait intéressant de tester si un rôle semblable pourrait être attribué au site de phosphorylation par Gwl. Dans leur état non phosphorylé, les endosulfines seraient recrutées aux endomembranes; en entrée de mitose, leur

phosphorylation par Gwl les délocaliserait en plus de promouvoir leur interaction avec PP2A-B55.

Une autre possibilité pour expliquer la localisation cytoplasmique observée pour Endos pourrait venir de sa séquence particulière. Les endosulfines sont décrites comme étant des protéines intrinsèquement désordonnées : elles fonctionnent sans adopter de structure tridimensionnelle fixe (Boettcher et al., 2007; Boettcher et al., 2008; Huang et al., 2001; Thapa et al., 2021; Uversky et al., 2000; Wright and Dyson, 1999). De plus, elles présentent une alternance de régions chargées positivement et négativement dans leurs séquences, ce qui pourrait leur permettre d'établir de faibles interactions électrostatiques entre elles. Ces deux caractéristiques en font des candidates plausibles pour l'homo-oligomérisation par séparation de phase liquide-liquide (Radivojac et al., 2004). Ce phénomène se produit lorsque des molécules à l'état liquide se séparent pour former deux phases distinctes; comme l'eau et l'huile. L'étude de ce type de phénomène est croissante en biologie et apporte de nouvelles perspectives dans la compréhension de l'organisation cellulaire. De fait, plusieurs organelles sans membranes, comme les nucléoles, les centrosomes, les complexes des pores nucléaires et la matrice du fuseau, forment des condensés biomoléculaires grâce à la séparation de phase (Decker et al., 2011; Johansen and Johansen, 2009; Johansen et al., 2011; Schmidt and Gorlich, 2015; Shav-Tal et al., 2005). Certaines de ces structures ont des propriétés plutôt liquides, d'autres se rapprochent des gels. Les rôles proposés pour la séparation de phase intracellulaire incluent la concentration locale de certaines molécules pour favoriser des réactions enzymatiques, la séquestration de molécules de signalisation pour empêcher des effets hors cibles (« *off target* ») et l'organisation de l'espace intracellulaire (Shin and Brangwynne, 2017).

Lorsque nous avons analysé la localisation d'Endos dans les embryons syncytiaux de la drosophile, nous avons observé qu'elle devient enrichie dans la région entourant le fuseau mitotique (Larouche et al., 2021). Cet enrichissement se produit en aval du bris de l'enveloppe nucléaire et semble colocaliser avec la matrice du fuseau (Johansen and Johansen, 2009; Johansen et al., 2011; Larouche et al., 2021). Est-ce que les propriétés d'Endos, qui sont caractéristiques des protéines qui peuvent faire de

la séparation de phase, pourraient lui permettre de s'accumuler dans la matrice du fuseau afin d'inhiber efficacement PP2A-Tws autour des structures mitotiques? Il serait intéressant de tester la colocalisation d'Endos avec les protéines connues de la matrice du fuseau chez la drosophile, soit Megator, Skeletor, Chromator et EAST (Qi et al., 2005; Qi et al., 2004; Rath et al., 2004; Walker et al., 2000). Par ailleurs, il serait important de valider l'hypothèse selon laquelle Endos peut former des condensés par séparation de phase liquide-liquide. Pour ce faire, il serait possible de purifier Endos et de tester sa capacité à former des micro-gouletettes dans un milieu aqueux. Pour les protéines qui font de la séparation de phase, cette capacité à former des micro-gouletettes est dépendante de leur concentration, de la température et de la concentration en sels (Brangwynne, 2013; Brangwynne et al., 2015; Zhu and Brangwynne, 2015). Il serait par la suite possible de tester si l'introduction de mutations dans les régions chargées d'Endos perturbe ses (potentielles) capacités à faire de la séparation de phase.

4.3 Cibler le module Gwl – endosulfines – PP2A en contexte pathologique?

La machinerie cellulaire est déréglée chez les cellules cancéreuses, ce qui leur permet de proliférer anormalement. Tel que mentionné au Chapitre 1, les niveaux de Gwl et des endosulfines sont surélevés dans plusieurs cancers (Alvarez-Fernandez et al., 2018; Cao et al., 2019; Dahlhaus et al., 2016; Rogers et al., 2018; Sun et al., 2017; Tian et al., 2017; Uppada et al., 2018; Vera et al., 2015; Zhuge et al., 2017). À l'inverse, PP2A-B55 tend à être inactivée; bien qu'elle semble avoir des propriétés oncogéniques dans certains contextes (Cheng et al., 2011; Curtis et al., 2012; Kamada et al., 2012; Mosca et al., 2013; Shouse et al., 2016).

Gwl agit comme oncogène en augmentant la prolifération, la migration et l'invasion des cellules cancéreuses (Rogers et al., 2018; Uppada et al., 2018; Vera et al., 2015; Wang et al., 2014a). En plus de son rôle en mitose, Gwl promeut l'oncogenèse en favorisant l'activation de la kinase AKT et de la voie Wnt/ β-catenin

(Uppada et al., 2018; Vera et al., 2015). Par ailleurs, Gwl favorise la reprise du cycle cellulaire après des dommages à l'ADN; son inhibition profite donc aux thérapies qui induisent des dommages à l'ADN (Wong et al., 2016).

L'inhibition de Gwl réduit la croissance tumorale *in vitro* et *in vivo* (Alvarez-Fernandez et al., 2018; Anania et al., 2015; Vera et al., 2015; Wang et al., 2014a). Dans les cellules de cancer du sein, la déplétion de Gwl augmente l'activation de PP2A, provoque l'échec de la mitose et augmente la sensibilité à la radiothérapie (Yoon et al., 2018). La sensibilisation à la radiothérapie a également été observée suite à la déplétion de Gwl dans des cellules de cancer du poumon (Nagel et al., 2015; Uppada et al., 2018). Son expression élevée dans les cellules cancéreuses, ses capacités oncogéniques ainsi que les effets bénéfiques de sa déplétion sur la croissance et la résistance tumorales font de Gwl une cible thérapeutique prometteuse.

Alternativement, il pourrait être intéressant de tenter d'augmenter l'activité de PP2A-B55 en contexte cancéreux en bloquant la liaison de ses inhibiteurs, les endosulfines (Zhang et al., 2013). Cette approche est en développement pour deux autres inhibiteurs endogènes de PP2A, le proto-oncogène nucléaire SET et CIP2A (pour *Cancerous Inhibitor of PP2A*). SET lie le centre catalytique de la sous-unité catalytique pour inhiber l'activité de PP2A (Arnaud et al., 2011; Li et al., 1995). CIP2A agit plutôt en liant la sous-unité B56 des complexes PP2A-B56 (Li et al., 1995). L'inhibition de ces inhibiteurs endogènes bloque la tumorigenèse et la prolifération cellulaire maligne *in vivo* (Junttila et al., 2007; Laine et al., 2013; Neviani et al., 2005). Différents types d'inhibiteurs (dérivés des céramides, peptides antagonistes, petites molécules) de l'interaction PP2A-SET présentement à l'étude permettent d'augmenter l'activité de PP2A dans les cellules cancéreuses (Janghorban et al., 2014; Liu et al., 2015; Neviani et al., 2007; Switzer et al., 2011; Wang et al., 2015). Les inhibiteurs de CIP2A présentement étudiés fonctionnent plutôt en réduisant les niveaux d'expression de CIP2A, en agissant au niveau transcriptionnel ou en induisant sa dégradation par le protéasome (Chen et al., 2010; Chen et al., 2012; Liu et al., 2014). Cibler les inhibiteurs endogènes semble donc être une approche prometteuse qui pourrait être explorée pour les endosulfines.

L'identification des contributions précises de PP2A-B55 en sortie de mitose pourrait également apporter de nouvelles pistes thérapeutiques. À titre d'exemple, des problèmes de ségrégation des chromosomes et des défauts de reformation de l'enveloppe, deux processus nécessitant PP2A-B55, peuvent mener à la formation de micronoyaux (Cimini et al., 2004; Cimini et al., 2003; Fenech et al., 2011; Thompson and Compton, 2011). Ceux-ci sont généralement plus perméables aux nucléases et deviennent donc des sites de dommages à l'ADN (Crasta et al., 2012; Hatch et al., 2013). Le système immunitaire peut détecter les micronoyaux et éliminer les cellules en contenant via la voie c-GAS – STING (Cai et al., 2014; Gaston et al., 2016; Legrier et al., 2016). Les taxanes, agents anticancers qui ciblent les microtubules, induisent la formation de micronoyaux (Chen and Horwitz, 2002; Jordan et al., 1996). La réaction inflammatoire induite par les micronoyaux pourrait donc contribuer à l'action anti-tumorale des taxanes (Mitchison et al., 2017). Fait intéressant, la déplétion de BAF, l'une des cibles de PP2A-B55, ou de la kinase VRK1/NHK-1, qui cible BAF et que nous avons identifiée dans nos cribles de phosphoprotéomique (Chapitre 3), induit de la micronucléation dans les cellules en division (Molitor and Traktman, 2014; Samwer et al., 2017). Perturber la reformation de l'enveloppe nucléaire pourrait donc s'avérer un moyen efficace d'augmenter l'immunogénicité des cellules cancéreuses.

Bref, l'exploration de questions fondamentales en lien avec le module Gwl-endosulfines-PP2A est certes essentielle à l'amélioration de notre compréhension de la division cellulaire, mais elle peut également déboucher sur des avenues thérapeutiques intéressantes.

4.4 Conclusion

L'une des raisons motivant la recherche scientifique est de mieux comprendre le monde qui nous entoure. Je pense que les résultats générés pendant mon doctorat contribueront à leur façon à approfondir notre compréhension de la division cellulaire et paveront la voie vers de nouvelles pistes à explorer. En cela, je me réjouis bien humblement de participer à l'effort scientifique.

Avant mon arrivée, le laboratoire Archambault a grandement participé à la dissection des mécanismes moléculaires régissant l'activation et la localisation de la kinase Greatwall. Mon travail aura contribué à améliorer notre compréhension du module Gwl – endosulfines – PP2A. Nous comprenons maintenant que Gwl doit sortir du noyau quelques minutes avant le bris de l'enveloppe nucléaire pour phosphoryler Endos au cytoplasme, ce qui résulte en l'inhibition de PP2A-Tws au moment requis. Par des cribles de phosphoprotéomique, j'ai également participé à l'effort d'identification de substrats mitotiques de PP2A-Tws. J'ai commencé la validation d'un candidat, la protéine de l'enveloppe nucléaire Otefin. La poursuite de mon travail permettra de mieux comprendre la régulation d'Otefin et de l'enveloppe nucléaire en mitose. D'autres candidats restent à tester; les données générées par les cribles pourront éventuellement aider à mieux cerner les contributions spécifiques de PP2A-Tws pour la sortie de mitose.

En somme, les deux études présentées se sont penchées sur deux aspects moins bien caractérisés de la mitose : la régulation spatiotemporelle de ses régulateurs et les contributions spécifiques des phosphatases. Bien qu'étudiée depuis plus d'un siècle, la mitose recèle encore nombre de questions; leur investigation nous permettra de mieux comprendre les mécanismes moléculaires sous-jacents de ce phénomène fondamental et hautement spectaculaire.

Annexes

Annexe 1. Genetic rescues of *endos* mutant flies.

(A) PCR validation of the transgenic flies. (B) Western blots to monitor protein expression levels. Polo-GFP was used as a control. We do not detect protein expression with the *nanos-Gal4* driver. (C) Genetic rescue of $endos^1/endos^{EY01105}$ mutant flies by the expression of the indicated Endos variants. None of the Endos-Flag variants can rescue the fertility of the sterile $endos^1/endos^{EY01105}$ hypomorphic mutant when driven by the female germline driver *nanos-Gal4*. (D) Genetic rescue of $endos^1/Df(3L)ED4536$ mutant flies by the expression of the indicated Endos variants. Values correspond to percentages of eclosed $endos^1/Df(3L)ED4536$ pupae (Tb^+) relative to the expected number calculated from the total number of eclosed pupae. All Endos-Flag variants can rescue the viability of the $endos^1/Df(3L)ED4536$ null mutant when driven by the driver *Ubi-Gal4*.
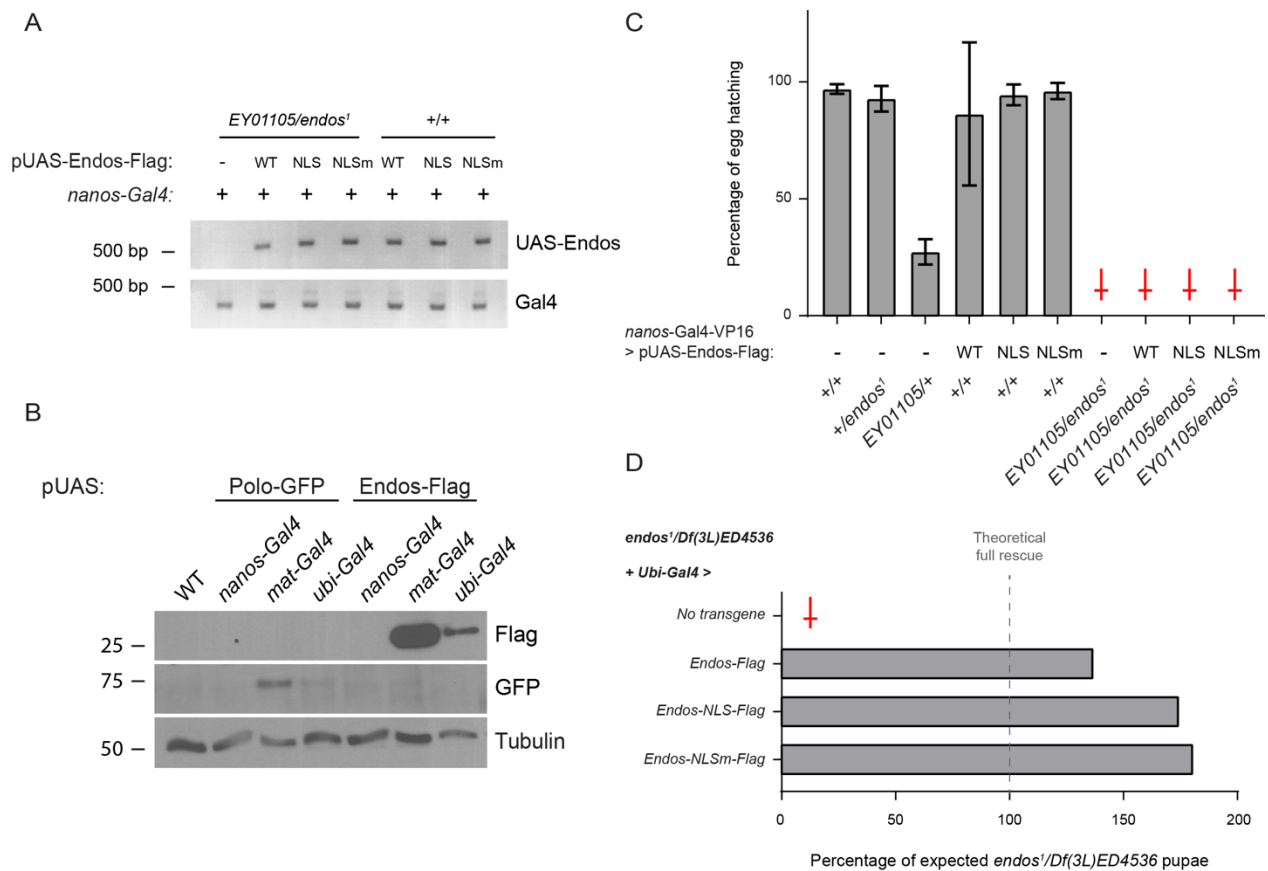
Annexe 2. Bande dessinée réalisée par la bédéiste Zviane dans le cadre du concours de vulgarisation scientifique L'Illustre recherche – Édition 2020, organisé par la Fédération des associations étudiantes des campus de l'Université de Montréal (FAÉCUM).

parce que les protéines forment parfois un **RÉSEAU DE SWITCHS** ON/OFF.

T'as une protéine, au doux nom de **CYCLINE B-CDK1**

son rôle, c'est de starter la mitose, en mettant plein de protéines à <u>ON</u>, dont une autre, nommée **GREATWALL**

dont le rôle (ENTRE AUTRES) est de mettre une autre protéine à <u>ON</u>, qui s'appelle **ENDOS**

dont le rôle est de mettre une autre protéine, **PP2A-TWINS**, à <u>OFF</u> !!!

clic!

clic!

cloc!

Pis c'est vraiment important que PP2A-TWINS soit à OFF au <u>début</u> de la mitose et qu'elle soit à ON juste <u>à la fin</u>, sinon il se passe des **problèmes**.

Si ces protéines-là font pas leur job au <u>bon moment</u> ou sont pas au <u>bon endroit</u>, il se passe plein d'affaires fuckées

GENRE:

Les chromosomes sont pas *tout à fait* alignés

ça donne:

Une mitose ratée

ça peut donner:

• destruction de la cellule
• cancer
• vous voyez le genre.

MYREILLE LAROUCHE doctorante en biochimie

Elle étudie la petite série de switchs Greatwall − Endos-PP2A-Twins.

Elle essaie de les faire s'activer à différents moments et à différents endroits pour mieux comprendre leur rôle.

Elle fait ça sur des mouches à fruits parce que c'est plus simple qu'une cellule humaine (y a juste 4 paires de chromosomes à la place de 23, tsé.)

Un jour, on va comprendre mieux le rôle des protéines et on pourra aussi l'enseigner en bio sec. 3 !!!

espoir

futur

EH BOY.

better world

Dans une cellule, des protéines, y en a genre <u>20 000</u>.

203

Références bibliographiques

Abbas, T., U. Sivaprasad, K. Terai, V. Amador, et al. 2008. PCNA-dependent regulation of p21 ubiquitylation and degradation via the CRL4Cdt2 ubiquitin ligase complex. *Genes Dev*. 22:2496-2506.

Adams, M.D., S.E. Celniker, R.A. Holt, C.A. Evans, et al. 2000. The genome sequence of Drosophila melanogaster. *Science*. 287:2185-2195.

Adhikari, D., M.K. Diril, K. Busayavalasa, S. Risal, et al. 2014. Mastl is required for timely activation of APC/C in meiosis I and Cdk1 reactivation in meiosis II. *J Cell Biol*. 206:843-853.

Afonso, O., I. Matos, A.J. Pereira, P. Aguiar, et al. 2014. Feedback control of chromosome separation by a midzone Aurora B gradient. *Science*. 345:332-336.

Agostinis, P., R. Derua, S. Sarno, J. Goris, et al. 1992. Specificity of the polycation-stimulated (type-2A) and ATP,Mg-dependent (type-1) protein phosphatases toward substrates phosphorylated by P34cdc2 kinase. *Eur J Biochem*. 205:241-248.

Agostinis, P., J. Goris, L.A. Pinna, F. Marchiori, et al. 1990. Synthetic peptides as model substrates for the study of the specificity of the polycation-stimulated protein phosphatases. *Eur J Biochem*. 189:235-241.

Agostinis, P., J. Goris, E. Waelkens, L.A. Pinna, et al. 1987. Dephosphorylation of phosphoproteins and synthetic phosphopeptides. Study of the specificity of the polycation-stimulated and MgATP-dependent phosphorylase phosphatases. *J Biol Chem*. 262:1060-1064.

Agrawal, A., and T.P. Lele. 2019. Mechanics of nuclear membranes. *J Cell Sci*. 132.

Ahonen, L.J., M.J. Kallio, J.R. Daum, M. Bolton, et al. 2005. Polo-like kinase 1 creates the tension-sensing 3F3/2 phosphoepitope and modulates the association of spindle-checkpoint proteins at kinetochores. *Curr Biol*. 15:1078-1089.

Aist, J.R., C.J. Bayles, W. Tao, and M.W. Berns. 1991. Direct experimental evidence for the existence, structural basis and function of astral forces during anaphase B in vivo. *J Cell Sci*. 100 (Pt 2):279-288.

Alber, F., S. Dokudovskaya, L.M. Veenhoff, W. Zhang, et al. 2007. The molecular architecture of the nuclear pore complex. *Nature*. 450:695-701.

Alexiades, M.R., and C. Cepko. 1996. Quantitative analysis of proliferation and cell cycle length during development of the rat retina. *Dev Dyn*. 205:293-307.

Alfieri, C., L. Chang, Z. Zhang, J. Yang, et al. 2016. Molecular basis of APC/C regulation by the spindle assembly checkpoint. *Nature*. 536:431-436.

Alvarez-Fernandez, M., and M. Malumbres. 2014. Preparing a cell for nuclear envelope breakdown: Spatio-temporal control of phosphorylation during mitotic entry. *Bioessays*. 36:757-765.

Alvarez-Fernandez, M., R. Sanchez-Martinez, B. Sanz-Castillo, P.P. Gan, et al. 2013. Greatwall is essential to prevent mitotic collapse after nuclear envelope breakdown in mammals. *Proc Natl Acad Sci U S A*. 110:17374-17379.

Alvarez-Fernandez, M., M. Sanz-Flores, B. Sanz-Castillo, M. Salazar-Roa, et al. 2018. Therapeutic relevance of the PP2A-B55 inhibitory kinase MASTL/Greatwall in breast cancer. *Cell Death Differ*. 25:828-840.

Anania, M., F. Gasparri, E. Cetti, I. Fraietta, et al. 2015. Identification of thyroid tumor cell vulnerabilities through a siRNA-based functional screening. *Oncotarget*. 6:34629-34648.

Andersen, S.S. 1999. Balanced regulation of microtubule dynamics during the cell cycle: a contemporary view. *Bioessays*. 21:53-60.

Andrade, E.C., V. Musante, A. Horiuchi, H. Matsuzaki, et al. 2017. ARPP-16 Is a Striatal-Enriched Inhibitor of Protein Phosphatase 2A Regulated by Microtubule-Associated Serine/Threonine Kinase 3 (Mast 3 Kinase). *J Neurosci*. 37:2709-2722.

Ang, X.L., and J. Wade Harper. 2005. SCF-mediated protein degradation and cell cycle control. *Oncogene*. 24:2860-2870.

Archambault, V., P.P. D'Avino, M.J. Deery, K.S. Lilley, et al. 2008. Sequestration of Polo kinase to microtubules by phosphopriming-independent binding to Map205 is relieved by phosphorylation at a CDK site in mitosis. *Genes Dev*. 22:2707-2720.

Archambault, V., and D.M. Glover. 2009. Polo-like kinases: conservation and divergence in their functions and regulation. *Nat Rev Mol Cell Biol*. 10:265-275.

Archambault, V., A.E. Ikui, B.J. Drapkin, and F.R. Cross. 2005. Disruption of mechanisms that prevent rereplication triggers a DNA damage response. *Mol Cell Biol*. 25:6707-6721.

Archambault, V., G. Lepine, and D. Kachaner. 2015. Understanding the Polo Kinase machine. *Oncogene*. 34:4799-4807.

Archambault, V., X. Zhao, H. White-Cooper, A.T. Carpenter, et al. 2007. Mutations in Drosophila Greatwall/Scant Reveal Its Roles in Mitosis and Meiosis and Interdependence with Polo Kinase. *PLoS Genet*. 3:e200.

Arellano, M., and S. Moreno. 1997. Regulation of CDK/cyclin complexes during the cell cycle. *Int J Biochem Cell Biol*. 29:559-573.

Arino, J., E. Perez-Callejon, N. Cunillera, M. Camps, et al. 1993. Protein phosphatases in higher plants: multiplicity of type 2A phosphatases in Arabidopsis thaliana. *Plant Mol Biol*. 21:475-485.

Arino, J., C.W. Woon, D.L. Brautigan, T.B. Miller, Jr., et al. 1988. Human liver phosphatase 2A: cDNA and amino acid sequence of two catalytic subunit isotypes. *Proc Natl Acad Sci U S A*. 85:4252-4256.

Arnaud, L., S. Chen, F. Liu, B. Li, et al. 2011. Mechanism of inhibition of PP2A activity and abnormal hyperphosphorylation of tau by I2(PP2A)/SET. *FEBS Lett*. 585:2653-2659.

Asencio, C., I.F. Davidson, R. Santarella-Mellwig, T.B. Ly-Hartig, et al. 2012. Coordination of kinase and phosphatase activities by Lem4 enables nuclear envelope reassembly during mitosis. *Cell*. 150:122-135.

Ashery-Padan, R., N. Ulitzur, A. Arbel, M. Goldberg, et al. 1997. Localization and posttranslational modifications of otefin, a protein required for vesicle attachment to chromatin, during Drosophila melanogaster development. *Mol Cell Biol*. 17:4114-4123.

Assoian, R.K., and X. Zhu. 1997. Cell anchorage and the cytoskeleton as partners in growth factor dependent cell cycle progression. *Curr Opin Cell Biol*. 9:93-98.

Asteriti, I.A., F. De Mattia, and G. Guarguaglini. 2015. Cross-Talk between AURKA and Plk1 in Mitotic Entry and Spindle Assembly. *Front Oncol*. 5:283.

Aureille, J., N. Belaadi, and C. Guilluy. 2017. Mechanotransduction via the nuclear envelope: a distant reflection of the cell surface. *Curr Opin Cell Biol*. 44:59-67.

Bahe, S., Y.D. Stierhof, C.J. Wilkinson, F. Leiss, et al. 2005. Rootletin forms centriole-associated filaments and functions in centrosome cohesion. *J Cell Biol*. 171:27-33.

Bai, C., R. Richman, and S.J. Elledge. 1994. Human cyclin F. *EMBO J*. 13:6087-6098.

Bai, C., P. Sen, K. Hofmann, L. Ma, et al. 1996. SKP1 connects cell cycle regulators to the ubiquitin proteolysis machinery through a novel motif, the F-box. *Cell*. 86:263-274.

Bajpai, R., K. Makhijani, P.R. Rao, and L.S. Shashidhara. 2004. Drosophila Twins regulates Armadillo levels in response to Wg/Wnt signal. *Development*. 131:1007-1016.

Barford, D. 1996. Molecular mechanisms of the protein serine/threonine phosphatases. *Trends Biochem Sci*. 21:407-412.

Barford, D., A.K. Das, and M.P. Egloff. 1998. The structure and mechanism of protein phosphatases: insights into catalysis and regulation. *Annu Rev Biophys Biomol Struct*. 27:133-164.

Barr, A.R., and F. Gergely. 2007. Aurora-A: the maker and breaker of spindle poles. *J Cell Sci*. 120:2987-2996.

Bartek, J., J. Bartkova, and J. Lukas. 1996. The retinoblastoma protein pathway and the restriction point. *Curr Opin Cell Biol*. 8:805-814.

Barton, L.J., T. Duan, W. Ke, A. Luttinger, et al. 2018. Nuclear lamina dysfunction triggers a germline stem cell checkpoint. *Nat Commun*. 9:3960.

Barton, L.J., K.E. Lovander, B.S. Pinto, and P.K. Geyer. 2016. Drosophila male and female germline stem cell niches require the nuclear lamina protein Otefin. *Dev Biol*. 415:75-86.

Barton, L.J., S.R. Wilmington, M.J. Martin, H.M. Skopec, et al. 2014. Unique and shared functions of nuclear lamina LEM domain proteins in Drosophila. *Genetics*. 197:653-665.

Baserga, R. 1965. The Relationship of the Cell Cycle to Tumor Growth and Control of Cell Division: A Review. *Cancer Res*. 25:581-595.

Beck, H., V. Nahse, M.S. Larsen, P. Groth, et al. 2010. Regulators of cyclin-dependent kinases are crucial for maintaining genome integrity in S phase. *J Cell Biol*. 188:629-638.

Bell, S.P., and A. Dutta. 2002. DNA replication in eukaryotic cells. *Annu Rev Biochem*. 71:333-374.

Belmont, L.D., A.A. Hyman, K.E. Sawin, and T.J. Mitchison. 1990. Real-time visualization of cell cycle-dependent changes in microtubule dynamics in cytoplasmic extracts. *Cell*. 62:579-589.

Bement, W.M., H.A. Benink, and G. von Dassow. 2005. A microtubule-dependent zone of active RhoA during cleavage plane specification. *J Cell Biol*. 170:91-101.

Bement, W.M., A.L. Miller, and G. von Dassow. 2006. Rho GTPase activity zones and transient contractile arrays. *Bioessays*. 28:983-993.

Berdnik, D., and J.A. Knoblich. 2002. Drosophila Aurora-A is required for centrosome maturation and actin-dependent asymmetric protein localization during mitosis. *Curr Biol*. 12:640-647.

Berdougo, E., M.V. Nachury, P.K. Jackson, and P.V. Jallepalli. 2008. The nucleolar phosphatase Cdc14B is dispensable for chromosome segregation and mitotic exit in human cells. *Cell Cycle*. 7:1184-1190.

Bergeron-Sandoval, L.P., N. Safaee, and S.W. Michnick. 2016. Mechanisms and Consequences of Macromolecular Phase Separation. *Cell*. 165:1067-1079.

Berk, J.M., D.N. Simon, C.R. Jenkins-Houk, J.W. Westerbeck, et al. 2014. The molecular basis of emerin-emerin and emerin-BAF interactions. *J Cell Sci*. 127:3956-3969.

Berk, J.M., K.E. Tifft, and K.L. Wilson. 2013. The nuclear envelope LEM-domain protein emerin. *Nucleus*. 4:298-314.

Bettencourt-Dias, M., R. Giet, R. Sinka, A. Mazumdar, et al. 2004. Genome-wide survey of protein kinases required for cell cycle progression. *Nature*. 432:980-987.

Bialojan, C., J.C. Ruegg, and A. Takai. 1988. Effects of okadaic acid on isometric tension and myosin phosphorylation of chemically skinned guinea-pig taenia coli. *J Physiol*. 398:81-95.

Bialojan, C., and A. Takai. 1988. Inhibitory effect of a marine-sponge toxin, okadaic acid, on protein phosphatases. Specificity and kinetics. *Biochem J*. 256:283-290.

Bianconi, E., A. Piovesan, F. Facchin, A. Beraudi, et al. 2013. An estimation of the number of cells in the human body. *Ann Hum Biol*. 40:463-471.

Bicho, C.C., F. de Lima Alves, Z.A. Chen, J. Rappsilber, et al. 2010. A genetic engineering solution to the "arginine conversion problem" in stable isotope labeling by amino acids in cell culture (SILAC). *Mol Cell Proteomics*. 9:1567-1577.

Bischoff, J.R., L. Anderson, Y. Zhu, K. Mossie, et al. 1998. A homologue of Drosophila aurora kinase is oncogenic and amplified in human colorectal cancers. *EMBO J*. 17:3052-3065.

Bisteau, X., J. Lee, V. Srinivas, J.H.S. Lee, et al. 2020. The Greatwall kinase safeguards the genome integrity by affecting the kinome activity in mitosis. *Oncogene*. 39:6816-6840.

Blagosklonny, M.V., and A.B. Pardee. 2002. The restriction point of the cell cycle. *Cell Cycle*. 1:103-110.

Blake-Hodek, K.A., B.C. Williams, Y. Zhao, P.V. Castilho, et al. 2012. Determinants for Activation of the Atypical AGC Kinase Greatwall during M Phase Entry. *Mol Cell Biol*. 32:1337-1353.

Bluemn, E.G., E.S. Spencer, B. Mecham, R.R. Gordon, et al. 2013. PPP2R2C loss promotes castration-resistance and is associated with increased prostate cancer-specific mortality. *Mol Cancer Res*. 11:568-578.

Bodenmiller, B., J. Malmstrom, B. Gerrits, D. Campbell, et al. 2007. PhosphoPep--a phosphoproteome resource for systems biology research in Drosophila Kc167 cells. *Mol Syst Biol*. 3:139.

Boettcher, J.M., K.L. Hartman, D.T. Ladror, Z. Qi, et al. 2007. (1)H, (13)C, and (15)N resonance assignment of the cAMP-regulated phosphoprotein endosulfine-alpha in free and micelle-bound states. *Biomol NMR Assign*. 1:167-169.

Boettcher, J.M., K.L. Hartman, D.T. Ladror, Z. Qi, et al. 2008. Membrane-induced folding of the cAMP-regulated phosphoprotein endosulfine-alpha. *Biochemistry*. 47:12357-12364.

Bollen, M., W. Peti, M.J. Ragusa, and M. Beullens. 2010. The extended PP1 toolkit: designed to create specificity. *Trends Biochem Sci*. 35:450-458.

Bonaldi, T., T. Straub, J. Cox, C. Kumar, et al. 2008. Combined use of RNAi and quantitative proteomics to study gene function in Drosophila. *Mol Cell*. 31:762-772.

Boni, A., A.Z. Politi, P. Strnad, W. Xiang, et al. 2015. Live imaging and modeling of inner nuclear membrane targeting reveals its molecular requirements in mammalian cells. *J Cell Biol*. 209:705-720.

Bontron, S., M. Jaquenoud, S. Vaga, N. Talarek, et al. 2013. Yeast endosulfines control entry into quiescence and chronological life span by inhibiting protein phosphatase 2A. *Cell Rep*. 3:16-22.

Booher, R., and D. Beach. 1989. Involvement of a type 1 protein phosphatase encoded by bws1+ in fission yeast mitotic control. *Cell*. 57:1009-1016.

Booher, R.N., C.E. Alfa, J.S. Hyams, and D.H. Beach. 1989. The fission yeast cdc2/cdc13/suc1 protein kinase: regulation of catalytic activity and nuclear localization. *Cell*. 58:485-497.

Bouchoux, C., and F. Uhlmann. 2011. A quantitative model for ordered Cdk substrate dephosphorylation during mitotic exit. *Cell*. 147:803-814.

Boulon, S., B.J. Westman, S. Hutten, F.M. Boisvert, et al. 2010. The nucleolus under stress. *Mol Cell*. 40:216-227.

Brangwynne, C.P. 2013. Phase transitions and size scaling of membrane-less organelles. *J Cell Biol*. 203:875-881.

Brangwynne, Clifford P., P. Tompa, and Rohit V. Pappu. 2015. Polymer physics of intracellular phase transitions. *Nature Physics*. 11:899-904.

Brene, S., N. Lindefors, M. Ehrlich, T. Taubes, et al. 1994. Expression of mRNAs encoding ARPP-16/19, ARPP-21, and DARPP-32 in human brain tissue. *J Neurosci*. 14:985-998.

Brown, E.J., and D. Baltimore. 2003. Essential and dispensable roles of ATR in cell cycle arrest and genome maintenance. *Genes Dev*. 17:615-628.

Brown, J.R., K.K. Koretke, M.L. Birkeland, P. Sanseau, et al. 2004. Evolutionary relationships of Aurora kinases: implications for model organism studies and the development of anti-cancer drugs. *BMC Evol Biol*. 4:39.

Bruinsma, W., J.A. Raaijmakers, and R.H. Medema. 2012. Switching Polo-like kinase-1 on and off in time and space. *Trends Biochem Sci*. 37:534-542.

Bryant, J.C., R.S. Westphal, and B.E. Wadzinski. 1999. Methylated C-terminal leucine residue of PP2A catalytic subunit is important for binding of regulatory Balpha subunit. *Biochem J*. 339 (Pt 2):241-246.

Bunz, F., A. Dutriaux, C. Lengauer, T. Waldman, et al. 1998. Requirement for p53 and p21 to sustain G2 arrest after DNA damage. *Science*. 282:1497-1501.

Burgess, A., S. Vigneron, E. Brioudes, J.C. Labbe, et al. 2010. Loss of human Greatwall results in G2 arrest and multiple mitotic defects due to deregulation of the cyclin B-Cdc2/PP2A balance. *Proc Natl Acad Sci U S A*. 107:12564-12569.

Burgos, M.H., and D.W. Fawcett. 1955. Studies on the fine structure of the mammalian testis. I. Differentiation of the spermatids in the cat (Felis domestica). *J Biophys Biochem Cytol*. 1:287-300.

Burke, D.J., and D. Church. 1991. Protein synthesis requirements for nuclear division, cytokinesis, and cell separation in Saccharomyces cerevisiae. *Mol Cell Biol*. 11:3691-3698.

Byers, B., and D.H. Abramson. 1968. Cytokinesis in HeLa: post-telophase delay and microtubule-associated motility. *Protoplasma*. 66:413-435.

Caballe, A., and J. Martin-Serrano. 2011. ESCRT machinery and cytokinesis: the road to daughter cell separation. *Traffic*. 12:1318-1326.

Cai, M., Y. Huang, R. Ghirlando, K.L. Wilson, et al. 2001. Solution structure of the constant region of nuclear envelope protein LAP2 reveals two LEM-domain structures: one binds BAF and the other binds DNA. *EMBO J*. 20:4399-4407.

Cai, M., Y. Huang, J.Y. Suh, J.M. Louis, et al. 2007. Solution NMR structure of the barrier-to-autointegration factor-Emerin complex. *J Biol Chem*. 282:14525-14535.

Cai, M., Y. Huang, R. Zheng, S.Q. Wei, et al. 1998. Solution structure of the cellular factor BAF responsible for protecting retroviral DNA from autointegration. *Nat Struct Biol*. 5:903-909.

Cai, X., Y.H. Chiu, and Z.J. Chen. 2014. The cGAS-cGAMP-STING pathway of cytosolic DNA sensing and signaling. *Mol Cell*. 54:289-296.

Campbell, K., J. Westholm, S. Kasvandik, F. Di Bartolomeo, et al. 2020. Building blocks are synthesized on demand during the yeast cell cycle. *Proc Natl Acad Sci U S A*. 117:7575-7583.

Cao, L., F. Chen, X. Yang, W. Xu, et al. 2014. Phylogenetic analysis of CDK and cyclin proteins in premetazoan lineages. *BMC Evol Biol*. 14:10.

Cao, L., W.J. Li, J.H. Yang, Y. Wang, et al. 2019. Inflammatory cytokine-induced expression of MASTL is involved in hepatocarcinogenesis by regulating cell cycle progression. *Oncol Lett*. 17:3163-3172.

Carmena, M., and W.C. Earnshaw. 2003. The cellular geography of aurora kinases. *Nat Rev Mol Cell Biol*. 4:842-854.

Carmena, M., X. Pinson, M. Platani, Z. Salloum, et al. 2012a. The chromosomal passenger complex activates Polo kinase at centromeres. *PLoS Biol*. 10:e1001250.

Carmena, M., S. Ruchaud, and W.C. Earnshaw. 2009. Making the Auroras glow: regulation of Aurora A and B kinase function by interacting proteins. *Curr Opin Cell Biol*. 21:796-805.

Carmena, M., M. Wheelock, H. Funabiki, and W.C. Earnshaw. 2012b. The chromosomal passenger complex (CPC): from easy rider to the godfather of mitosis. *Nat Rev Mol Cell Biol*. 13:789-803.

Carnero, A., and G.J. Hannon. 1998. The INK4 family of CDK inhibitors. *Curr Top Microbiol Immunol*. 227:43-55.

Casenghi, M., P. Meraldi, U. Weinhart, P.I. Duncan, et al. 2003. Polo-like kinase 1 regulates Nlp, a centrosome protein involved in microtubule nucleation. *Dev Cell*. 5:113-125.

Castilho, P.V., B.C. Williams, S. Mochida, Y. Zhao, et al. 2009. The M phase kinase Greatwall (Gwl) promotes inactivation of PP2A/B55delta, a phosphatase directed against CDK phosphosites. *Mol Biol Cell*. 20:4777-4789.

Castro, A., Y. Arlot-Bonnemains, S. Vigneron, J.C. Labbe, et al. 2002. APC/Fizzy-Related targets Aurora-A kinase for proteolysis. *EMBO Rep*. 3:457-462.

Castro, A., C. Bernis, S. Vigneron, J.C. Labbe, et al. 2005. The anaphase-promoting complex: a key factor in the regulation of cell cycle. *Oncogene*. 24:314-325.

Castro, A., and T. Lorca. 2018. Greatwall kinase at a glance. *J Cell Sci*. 131.

Cavalier-Smith, T. 1974. Basal body and flagellar development during the vegetative cell cycle and the sexual cycle of Chlamydomonas reinhardii. *J Cell Sci*. 16:529-556.

Cavalier-Smith, T. 2010. Origin of the cell nucleus, mitosis and sex: roles of intracellular coevolution. *Biol Direct*. 5:7.

Cayla, X., J. Goris, J. Hermann, P. Hendrix, et al. 1990. Isolation and characterization of a tyrosyl phosphatase activator from rabbit skeletal muscle and Xenopus laevis oocytes. *Biochemistry*. 29:658-667.

Celniker, S.E., and G.M. Rubin. 2003. The Drosophila melanogaster genome. *Annu Rev Genomics Hum Genet*. 4:89-117.

Ceulemans, H., and M. Bollen. 2004. Functional diversity of protein phosphatase-1, a cellular economizer and reset button. *Physiol Rev*. 84:1-39.

Chang, W., H.J. Worman, and G.G. Gundersen. 2015. Accessorizing and anchoring the LINC complex for multifunctionality. *J Cell Biol*. 208:11-22.

Chang, Y.C., H.W. Tang, S.Y. Liang, T.H. Pu, et al. 2013. Evaluation of Drosophila metabolic labeling strategies for in vivo quantitative proteomic analyses with applications to early pupa formation and amino acid starvation. *J Proteome Res*. 12:2138-2150.

Chao, W.C., K. Kulkarni, Z. Zhang, E.H. Kong, et al. 2012. Structure of the mitotic checkpoint complex. *Nature*. 484:208-213.

Charrasse, S., A. Gharbi-Ayachi, A. Burgess, J. Vera, et al. 2017. Ensa controls S-phase length by modulating Treslin levels. *Nat Commun*. 8:206.

Chen, F., V. Archambault, A. Kar, P. Lio, et al. 2007. Multiple protein phosphatases are required for mitosis in Drosophila. *Curr Biol*. 17:293-303.

Chen, J.G., and S.B. Horwitz. 2002. Differential mitotic responses to microtubule-stabilizing and -destabilizing drugs. *Cancer Res*. 62:1935-1938.

Chen, K.F., C.Y. Liu, Y.C. Lin, H.C. Yu, et al. 2010. CIP2A mediates effects of bortezomib on phospho-Akt and apoptosis in hepatocellular carcinoma cells. *Oncogene*. 29:6257-6266.

Chen, K.F., K.C. Pao, J.C. Su, Y.C. Chou, et al. 2012. Development of erlotinib derivatives as CIP2A-ablating agents independent of EGFR activity. *Bioorg Med Chem*. 20:6144-6153.

Chen, M.J., J.E. Dixon, and G. Manning. 2017. Genomics and evolution of protein phosphatases. *Sci Signal*. 10.

Cheng, Y., W. Liu, S.T. Kim, J. Sun, et al. 2011. Evaluation of PPP2R2A as a prostate cancer susceptibility gene: a comprehensive germline and somatic study. *Cancer Genet*. 204:375-381.

Chica, N., A.E. Rozalen, L. Perez-Hidalgo, A. Rubio, et al. 2016. Nutritional Control of Cell Size by the Greatwall-Endosulfine-PP2A.B55 Pathway. *Curr Biol*. 26:319-330.

Choi, H., G. Liu, D. Mellacheruvu, M. Tyers, et al. 2012. Analyzing protein-protein interactions from affinity purification-mass spectrometry data with SAINT. *Curr Protoc Bioinformatics*. Chapter 8:Unit8 15.

Choo, D.W., H.J. Baek, N. Motoyama, K.H. Cho, et al. 2009. ATM is required for rapid degradation of cyclin D1 in response to gamma-irradiation. *Biochem Biophys Res Commun*. 378:847-850.

Chow, J.P., W.Y. Siu, H.T. Ho, K.H. Ma, et al. 2003. Differential contribution of inhibitory phosphorylation of CDC2 and CDK2 for unperturbed cell cycle control and DNA integrity checkpoints. *J Biol Chem*. 278:40815-40828.

Chowdhury, D., M.C. Keogh, H. Ishii, C.L. Peterson, et al. 2005. gamma-H2AX dephosphorylation by protein phosphatase 2A facilitates DNA double-strand break repair. *Mol Cell*. 20:801-809.

Choy, M.S., M. Hieke, G.S. Kumar, G.R. Lewis, et al. 2014. Understanding the antagonism of retinoblastoma protein dephosphorylation by PNUTS provides insights into the PP1 regulatory code. *Proc Natl Acad Sci U S A*. 111:4097-4102.

Christie, M., C.W. Chang, G. Rona, K.M. Smith, et al. 2016. Structural Biology and Regulation of Protein Import into the Nucleus. *J Mol Biol*. 428:2060-2090.

Cimini, D., L.A. Cameron, and E.D. Salmon. 2004. Anaphase spindle mechanics prevent mis-segregation of merotelically oriented chromosomes. *Curr Biol*. 14:2149-2155.

Cimini, D., B. Moree, J.C. Canman, and E.D. Salmon. 2003. Merotelic kinetochore orientation occurs frequently during early mitosis in mammalian tissue cells and error correction is achieved by two different mechanisms. *J Cell Sci*. 116:4213-4225.

Ciosk, R., W. Zachariae, C. Michaelis, A. Shevchenko, et al. 1998. An ESP1/PDS1 complex regulates loss of sister chromatid cohesion at the metaphase to anaphase transition in yeast. *Cell*. 93:1067-1076.

Civelekoglu-Scholey, G., and J.M. Scholey. 2007. Mitotic motors: kinesin-5 takes a brake. *Curr Biol*. 17:R544-547.

Clever, M., T. Funakoshi, Y. Mimura, M. Takagi, et al. 2012. The nucleoporin ELYS/Mel28 regulates nuclear envelope subdomain formation in HeLa cells. *Nucleus*. 3:187-199.

Cohen, P.T., N.D. Brewis, V. Hughes, and D.J. Mann. 1990. Protein serine/threonine phosphatases; an expanding family. *FEBS Lett*. 268:355-359.

Cohen-Fix, O., J.M. Peters, M.W. Kirschner, and D. Koshland. 1996. Anaphase initiation in Saccharomyces cerevisiae is controlled by the APC-dependent degradation of the anaphase inhibitor Pds1p. *Genes Dev*. 10:3081-3093.

Colanzi, A., C. Hidalgo Carcedo, A. Persico, C. Cericola, et al. 2007. The Golgi mitotic checkpoint is controlled by BARS-dependent fission of the Golgi ribbon into separate stacks in G2. *EMBO J*. 26:2465-2476.

Colinet, H., C. Pineau, and E. Com. 2017. Large scale phosphoprotein profiling to explore Drosophila cold acclimation regulatory mechanisms. *Sci Rep*. 7:1713.

Connell-Crowley, L., J.W. Harper, and D.W. Goodrich. 1997. Cyclin D1/Cdk4 regulates retinoblastoma protein-mediated cell cycle arrest by site-specific phosphorylation. *Mol Biol Cell*. 8:287-301.

Cormier, P., H.B. Osborne, T. Bassez, R. Poulhe, et al. 1991. Protein phosphatase 2A from Xenopus oocytes. Characterization during meiotic cell division. *FEBS Lett*. 295:185-188.

Cox, J., M.Y. Hein, C.A. Luber, I. Paron, et al. 2014. Accurate proteome-wide label-free quantification by delayed normalization and maximal peptide ratio extraction, termed MaxLFQ. *Mol Cell Proteomics*. 13:2513-2526.

Crasta, K., N.J. Ganem, R. Dagher, A.B. Lantermann, et al. 2012. DNA breaks and chromosome pulverization from errors in mitosis. *Nature*. 482:53-58.

Cundell, M.J., R.N. Bastos, T. Zhang, J. Holder, et al. 2013. The BEG (PP2A-B55/ENSA/Greatwall) Pathway Ensures Cytokinesis follows Chromosome Separation. *Mol Cell*. 52:393-405.

Cundell, M.J., L.H. Hutter, R. Nunes Bastos, E. Poser, et al. 2016. A PP2A-B55 recognition signal controls substrate dephosphorylation kinetics during mitotic exit. *J Cell Biol*. 214:539-554.

Curtis, C., S.P. Shah, S.F. Chin, G. Turashvili, et al. 2012. The genomic and transcriptomic architecture of 2,000 breast tumours reveals novel subgroups. *Nature*. 486:346-352.

D'Arcy, B.M., M.R. Swingle, C.M. Papke, K.A. Abney, et al. 2019. The Antitumor Drug LB-100 Is a Catalytic Inhibitor of Protein Phosphatase 2A (PPP2CA) and 5 (PPP5C) Coordinating with the Active-Site Catalytic Metals in PPP5C. *Mol Cancer Ther*. 18:556-566.

Dahlhaus, M., A. Burkovski, F. Hertwig, C. Mussel, et al. 2016. Boolean modeling identifies Greatwall/MASTL as an important regulator in the AURKA network of neuroblastoma. *Cancer Lett*. 371:79-89.

de Carcer, G., G. Manning, and M. Malumbres. 2011. From Plk1 to Plk5: functional evolution of polo-like kinases. *Cell Cycle*. 10:2255-2262.

de Castro, I.J., R.S. Gil, L. Ligammari, M.L. Di Giacinto, et al. 2018. CDK1 and PLK1 coordinate the disassembly and reassembly of the nuclear envelope in vertebrate mitosis. *Oncotarget*. 9:7763-7773.

de Castro, I.J., E. Gokhan, and P. Vagnarelli. 2016. Resetting a functional G1 nucleus after mitosis. *Chromosoma*. 125:607-619.

De Souza, C.P., and S.A. Osmani. 2007. Mitosis, not just open or closed. *Eukaryot Cell*. 6:1521-1527.

Deana, A.D., F. Marchiori, F. Meggio, and L.A. Pinna. 1982. Dephosphorylation of synthetic phosphopeptides by protein phosphatase-T, a phosphothreonyl protein phosphatase. *J Biol Chem*. 257:8565-8568.

Deana, A.D., and L.A. Pinna. 1988. Identification of pseudo 'phosphothreonyl-specific' protein phosphatase T with a fraction of polycation-stimulated protein phosphatase 2A. *Biochim Biophys Acta*. 968:179-185.

Decker, M., S. Jaensch, A. Pozniakovsky, A. Zinke, et al. 2011. Limiting amounts of centrosome material set centrosome size in C. elegans embryos. *Curr Biol*. 21:1259-1267.

Della Monica, R., R. Visconti, N. Cervone, A.F. Serpico, et al. 2015. Fcp1 phosphatase controls Greatwall kinase to promote PP2A-B55 activation and mitotic progression. *Elife*. 4.

DePamphilis, M.L. 2016. Genome Duplication: The Heartbeat of Developing Organisms. *Curr Top Dev Biol*. 116:201-229.

Dernburg, A.F. 2011. In situ hybridization to somatic chromosomes in Drosophila. *Cold Spring Harb Protoc*. 2011.

Descombes, P., and E.A. Nigg. 1998. The polo-like kinase Plx1 is required for M phase exit and destruction of mitotic regulators in Xenopus egg extracts. *EMBO J*. 17:1328-1335.

Dilworth, S.M. 2002. Polyoma virus middle T antigen and its role in identifying cancer-related molecules. *Nat Rev Cancer*. 2:951-956.

Ding, R., R.R. West, D.M. Morphew, B.R. Oakley, et al. 1997. The spindle pole body of Schizosaccharomyces pombe enters and leaves the nuclear envelope as the cell cycle proceeds. *Mol Biol Cell*. 8:1461-1479.

Dippell, R.V. 1968. The development of basal bodies in paramecium. *Proc Natl Acad Sci U S A*. 61:461-468.

Diril, M.K., X. Bisteau, M. Kitagawa, M.J. Caldez, et al. 2016. Loss of the Greatwall Kinase Weakens the Spindle Assembly Checkpoint. *PLoS Genet*. 12:e1006310.

Dohadwala, M., E.F. da Cruz e Silva, F.L. Hall, R.T. Williams, et al. 1994. Phosphorylation and inactivation of protein phosphatase 1 by cyclin-dependent kinases. *Proc Natl Acad Sci U S A*. 91:6408-6412.

Donella-Deana, A., H.E. Meyer, and L.A. Pinna. 1991. The use of phosphopeptides to distinguish between protein phosphatase and acid/alkaline phosphatase activities: opposite specificity toward phosphoseryl/phosphothreonyl substrates. *Biochim Biophys Acta*. 1094:130-133.

Doonan, J.H., and N.R. Morris. 1989. The bimG gene of Aspergillus nidulans, required for completion of anaphase, encodes a homolog of mammalian phosphoprotein phosphatase 1. *Cell*. 57:987-996.

Draetta, G., and D. Beach. 1988. Activation of cdc2 protein kinase during mitosis in human cells: cell cycle-dependent phosphorylation and subunit rearrangement. *Cell*. 54:17-26.

Draetta, G., L. Brizuela, J. Potashkin, and D. Beach. 1987. Identification of p34 and p13, human homologs of the cell cycle regulators of fission yeast encoded by cdc2+ and suc1+. *Cell*. 50:319-325.

Draetta, G., F. Luca, J. Westendorf, L. Brizuela, et al. 1989. Cdc2 protein kinase is complexed with both cyclin A and B: evidence for proteolytic inactivation of MPF. *Cell*. 56:829-838.

Drummond-Barbosa, D., and A.C. Spradling. 2004. Alpha-endosulfine, a potential regulator of insulin secretion, is required for adult tissue growth control in Drosophila. *Dev Biol*. 266:310-321.

Duan, T., N. Green, T.L. Tootle, and P.K. Geyer. 2020a. Nuclear architecture as an intrinsic regulator of Drosophila female germline stem cell maintenance. *Curr Opin Insect Sci*. 37:30-38.

Duan, T., S.C. Kitzman, and P.K. Geyer. 2020b. Survival of Drosophila germline stem cells requires the chromatin-binding protein Barrier-to-autointegration factor. *Development*. 147.

Dulla, K., H. Daub, R. Hornberger, E.A. Nigg, et al. 2010. Quantitative site-specific phosphorylation dynamics of human protein kinases during mitotic progression. *Mol Cell Proteomics*. 9:1167-1181.

Dulubova, I., A. Horiuchi, G.L. Snyder, J.A. Girault, et al. 2001. ARPP-16/ARPP-19: a highly conserved family of cAMP-regulated phosphoproteins. *J Neurochem*. 77:229-238.

Dupre, A., E. Buffin, C. Roustan, A.C. Nairn, et al. 2013. The phosphorylation of ARPP19 by Greatwall renders the auto-amplification of MPF independently of PKA in Xenopus oocytes. *J Cell Sci*. 126:3916-3926.

Dupre, A., E.M. Daldello, A.C. Nairn, C. Jessus, et al. 2014. Phosphorylation of ARPP19 by protein kinase A prevents meiosis resumption in Xenopus oocytes. *Nat Commun*. 5:3318.

Duronio, R.J., A. Brook, N. Dyson, and P.H. O'Farrell. 1996. E2F-induced S phase requires cyclin E. *Genes Dev*. 10:2505-2513.

Echalier, G., and A. Ohanessian. 1969. [Isolation, in tissue culture, of Drosophila melangaster cell lines]. *C R Acad Hebd Seances Acad Sci D*. 268:1771-1773.

Egloff, M.P., P.T. Cohen, P. Reinemer, and D. Barford. 1995. Crystal structure of the catalytic subunit of human protein phosphatase 1 and its complex with tungstate. *J Mol Biol*. 254:942-959.

Egloff, M.P., D.F. Johnson, G. Moorhead, P.T. Cohen, et al. 1997. Structural basis for the recognition of regulatory subunits by the catalytic subunit of protein phosphatase 1. *EMBO J*. 16:1876-1887.

Ellis, J.A., M. Craxton, J.R. Yates, and J. Kendrick-Jones. 1998. Aberrant intracellular targeting and cell cycle-dependent phosphorylation of emerin contribute to the Emery-Dreifuss muscular dystrophy phenotype. *J Cell Sci*. 111 (Pt 6):781-792.

Emanuele, M.J., W. Lan, M. Jwa, S.A. Miller, et al. 2008. Aurora B kinase and protein phosphatase 1 have opposing roles in modulating kinetochore assembly. *J Cell Biol*. 181:241-254.

Endicott, J.A., M.E. Noble, and J.A. Tucker. 1999. Cyclin-dependent kinases: inhibition and substrate recognition. *Curr Opin Struct Biol*. 9:738-744.

Espert, A., P. Uluocak, R.N. Bastos, D. Mangat, et al. 2014. PP2A-B56 opposes Mps1 phosphorylation of Knl1 and thereby promotes spindle assembly checkpoint silencing. *J Cell Biol*. 206:833-842.

Evans, D.R., and B.A. Hemmings. 2000. Mutation of the C-terminal leucine residue of PP2Ac inhibits PR55/B subunit binding and confers supersensitivity to microtubule destabilization in Saccharomyces cerevisiae. *Mol Gen Genet*. 264:425-432.

Evans, T., E.T. Rosenthal, J. Youngblom, D. Distel, et al. 1983. Cyclin: a protein specified by maternal mRNA in sea urchin eggs that is destroyed at each cleavage division. *Cell*. 33:389-396.

Fang, G., H. Yu, and M.W. Kirschner. 1998. The checkpoint protein MAD2 and the mitotic regulator CDC20 form a ternary complex with the anaphase-promoting complex to control anaphase initiation. *Genes Dev*. 12:1871-1883.

Fantes, P., and P. Nurse. 1977. Control of cell size at division in fission yeast by a growth-modulated size control over nuclear division. *Exp Cell Res*. 107:377-386.

Fantes, P.A. 1977. Control of cell size and cycle time in Schizosaccharomyces pombe. *J Cell Sci*. 24:51-67.

Faragher, A.J., and A.M. Fry. 2003. Nek2A kinase stimulates centrosome disjunction and is required for formation of bipolar mitotic spindles. *Mol Biol Cell*. 14:2876-2889.

Favreau, C., H.J. Worman, R.W. Wozniak, T. Frappier, et al. 1996. Cell cycle-dependent phosphorylation of nucleoporins and nuclear pore membrane protein Gp210. *Biochemistry*. 35:8035-8044.

Fawcett, D.W. 1961. Intercellular bridges. *Exp Cell Res*. Suppl 8:174-187.

Feldman, R.M., C.C. Correll, K.B. Kaplan, and R.J. Deshaies. 1997. A complex of Cdc4p, Skp1p, and Cdc53p/cullin catalyzes ubiquitination of the phosphorylated CDK inhibitor Sic1p. *Cell*. 91:221-230.

Fenech, M., M. Kirsch-Volders, A.T. Natarajan, J. Surralles, et al. 2011. Molecular mechanisms of micronucleus, nucleoplasmic bridge and nuclear bud formation in mammalian and human cells. *Mutagenesis*. 26:125-132.

Fernandez, A., M. Bautista, and F. Pinaud. 2021. Emerin oligomerization and nucleoskeletal coupling at the nuclear envelope regulate nuclear mechanics against stress. bioRxiv.

Fernandez-Capetillo, O., A. Lee, M. Nussenzweig, and A. Nussenzweig. 2004. H2AX: the histone guardian of the genome. *DNA Repair (Amst)*. 3:959-967.

Ferrigno, P., T.A. Langan, and P. Cohen. 1993. Protein phosphatase 2A1 is the major enzyme in vertebrate cell extracts that dephosphorylates several physiological substrates for cyclin-dependent protein kinases. *Mol Biol Cell*. 4:669-677.

Filter, J.J., B.C. Williams, M. Eto, D. Shalloway, et al. 2017. Unfair competition governs the interaction of pCPI-17 with myosin phosphatase (PP1-MYPT1). *Elife*. 6.

Fink, G., I. Schuchardt, J. Colombelli, E. Stelzer, et al. 2006. Dynein-mediated pulling forces drive rapid mitotic spindle elongation in Ustilago maydis. *EMBO J*. 25:4897-4908.

Fisher, L.A., L. Wang, L. Wu, and A. Peng. 2014. Phosphatase 1 nuclear targeting subunit is an essential regulator of M-phase entry, maintenance, and exit. *J Biol Chem*. 289:23745-23752.

Flemming, W. 1882. Zellsubstanz, Kern und Zelltheilung. Leipzig, F. C. W. Vogel.

Floyd, S., J. Pines, and C. Lindon. 2008. APC/C Cdh1 targets aurora kinase to control reorganization of the mitotic spindle at anaphase. *Curr Biol*. 18:1649-1658.

Foley, E.A., M. Maldonado, and T.M. Kapoor. 2011. Formation of stable attachments between kinetochores and microtubules depends on the B56-PP2A phosphatase. *Nat Cell Biol*. 13:1265-1271.

Fry, A.M., P. Meraldi, and E.A. Nigg. 1998. A centrosomal function for the human Nek2 protein kinase, a member of the NIMA family of cell cycle regulators. *EMBO J*. 17:470-481.

Fu, G., X. Ding, K. Yuan, F. Aikhionbare, et al. 2007. Phosphorylation of human Sgo1 by NEK2A is essential for chromosome congression in mitosis. *Cell Res*. 17:608-618.

Fujiki, H., and M. Suganuma. 1993. Tumor promotion by inhibitors of protein phosphatases 1 and 2A: the okadaic acid class of compounds. *Adv Cancer Res*. 61:143-194.

Fujimitsu, K., M. Grimaldi, and H. Yamano. 2016. Cyclin-dependent kinase 1-dependent activation of APC/C ubiquitin ligase. *Science*. 352:1121-1124.

Fuller, B.G., M.A. Lampson, E.A. Foley, S. Rosasco-Nitcher, et al. 2008. Midzone activation of aurora B in anaphase produces an intracellular phosphorylation gradient. *Nature*. 453:1132-1136.

Funabiki, H., K. Kumada, and M. Yanagida. 1996. Fission yeast Cut1 and Cut2 are essential for sister chromatid separation, concentrate along the metaphase spindle and form large complexes. *EMBO J*. 15:6617-6628.

Funabiki, H., and D.J. Wynne. 2013. Making an effective switch at the kinetochore by phosphorylation and dephosphorylation. *Chromosoma*. 122:135-158.

Garcia-Blanco, N., A. Vazquez-Bolado, and S. Moreno. 2019. Greatwall-Endosulfine: A Molecular Switch that Regulates PP2A/B55 Protein Phosphatase Activity in Dividing and Quiescent Cells. *Int J Mol Sci*. 20.

Garland, P., S. Quraishe, P. French, and V. O'Connor. 2008. Expression of the MAST family of serine/threonine kinases. *Brain Res*. 1195:12-19.

Garrido, D., M. Bourouh, E. Bonneil, P. Thibault, et al. 2020. Cyclin B3 activates the Anaphase-Promoting Complex/Cyclosome in meiosis and mitosis. *PLoS Genet*. 16:e1009184.

Gaston, J., L. Cheradame, V. Yvonnet, O. Deas, et al. 2016. Intracellular STING inactivation sensitizes breast cancer cells to genotoxic agents. *Oncotarget*. 7:77205-77224.

Gavet, O., and J. Pines. 2010a. Activation of cyclin B1-Cdk1 synchronizes events in the nucleus and the cytoplasm at mitosis. *J Cell Biol*. 189:247-259.

Gavet, O., and J. Pines. 2010b. Progressive activation of CyclinB1-Cdk1 coordinates entry to mitosis. *Dev Cell*. 18:533-543.

Gentry, M.S., Y. Li, H. Wei, F.F. Syed, et al. 2005. A novel assay for protein phosphatase 2A (PP2A) complexes in vivo reveals differential effects of covalent modifications on different Saccharomyces cerevisiae PP2A heterotrimers. *Eukaryot Cell*. 4:1029-1040.

Gerace, L., and M.D. Huber. 2012. Nuclear lamina at the crossroads of the cytoplasm and nucleus. *J Struct Biol*. 177:24-31.

Gharbi-Ayachi, A., J.C. Labbe, A. Burgess, S. Vigneron, et al. 2010. The substrate of Greatwall kinase, Arpp19, controls mitosis by inhibiting protein phosphatase 2A. *Science*. 330:1673-1677.

Giacinti, C., and A. Giordano. 2006. RB and cell cycle progression. *Oncogene*. 25:5220-5227.

Girard, F., U. Strausfeld, A. Fernandez, and N.J. Lamb. 1991. Cyclin A is required for the onset of DNA replication in mammalian fibroblasts. *Cell*. 67:1169-1179.

Girault, J.A., A. Horiuchi, E.L. Gustafson, N.L. Rosen, et al. 1990. Differential expression of ARPP-16 and ARPP-19, two highly related cAMP-regulated phosphoproteins, one of which is specifically associated with dopamine-innervated brain regions. *J Neurosci*. 10:1124-1133.

Glavy, J.S., A.N. Krutchinsky, I.M. Cristea, I.C. Berke, et al. 2007. Cell-cycle-dependent phosphorylation of the nuclear pore Nup107-160 subcomplex. *Proc Natl Acad Sci U S A*. 104:3811-3816.

Glotzer, M., A.W. Murray, and M.W. Kirschner. 1991. Cyclin is degraded by the ubiquitin pathway. *Nature*. 349:132-138.

Glover, D.M. 2005. Polo kinase and progression through M phase in Drosophila: a perspective from the spindle poles. *Oncogene*. 24:230-237.

Glover, D.M., M.H. Leibowitz, D.A. McLean, and H. Parry. 1995. Mutations in aurora prevent centrosome separation leading to the formation of monopolar spindles. *Cell*. 81:95-105.

Godfrey, M., S.A. Touati, M. Kataria, A. Jones, et al. 2017. PP2A(Cdc55) Phosphatase Imposes Ordered Cell-Cycle Phosphorylation by Opposing Threonine Phosphorylation. *Mol Cell*. 65:393-402 e393.

Goguet-Rubio, P., P. Amin, S. Awal, S. Vigneron, et al. 2020. PP2A-B55 Holoenzyme Regulation and Cancer. *Biomolecules*. 10.

Goldberg, M.L. 2010. Greatwall kinase protects mitotic phosphosites from barbarian phosphatases. *Proc Natl Acad Sci U S A*. 107:12409-12410.

Golsteyn, R.M., S.J. Schultz, J. Bartek, A. Ziemiecki, et al. 1994. Cell cycle analysis and chromosomal localization of human Plk1, a putative homologue of the mitotic kinases Drosophila polo and Saccharomyces cerevisiae Cdc5. *J Cell Sci*. 107 (Pt 6):1509-1517.

Gomes, R., R.E. Karess, H. Ohkura, D.M. Glover, et al. 1993. Abnormal anaphase resolution (aar): a locus required for progression through mitosis in Drosophila. *J Cell Sci*. 104 (Pt 2):583-593.

Gong, Y., W. Wu, X. Zou, F. Liu, et al. 2018. MiR-26a inhibits thyroid cancer cell proliferation by targeting ARPP19. *Am J Cancer Res*. 8:1030-1039.

Gorjanacz, M., E.P. Klerkx, V. Galy, R. Santarella, et al. 2007. Caenorhabditis elegans BAF-1 and its kinase VRK-1 participate directly in post-mitotic nuclear envelope assembly. *EMBO J*. 26:132-143.

Goshima, G., M. Mayer, N. Zhang, N. Stuurman, et al. 2008. Augmin: a protein complex required for centrosome-independent microtubule generation within the spindle. *J Cell Biol*. 181:421-429.

Goshima, G., R. Wollman, S.S. Goodwin, N. Zhang, et al. 2007. Genes required for mitotic spindle assembly in Drosophila S2 cells. *Science*. 316:417-421.

Goss, V.L., B.A. Hocevar, L.J. Thompson, C.A. Stratton, et al. 1994. Identification of nuclear beta II protein kinase C as a mitotic lamin kinase. *J Biol Chem*. 269:19074-19080.

Gotz, J., A. Probst, E. Ehler, B. Hemmings, et al. 1998. Delayed embryonic lethality in mice lacking protein phosphatase 2A catalytic subunit Calpha. *Proc Natl Acad Sci U S A*. 95:12370-12375.

Gould, K.L., and P. Nurse. 1989. Tyrosine phosphorylation of the fission yeast cdc2+ protein kinase regulates entry into mitosis. *Nature*. 342:39-45.

Grallert, A., E. Boke, A. Hagting, B. Hodgson, et al. 2015. A PP1-PP2A phosphatase relay controls mitotic progression. *Nature*. 517:94-98.

Green, B.M., and J.J. Li. 2005. Loss of rereplication control in Saccharomyces cerevisiae results in extensive DNA damage. *Mol Biol Cell*. 16:421-432.

Green, D.D., S.I. Yang, and M.C. Mumby. 1987. Molecular cloning and sequence analysis of the catalytic subunit of bovine type 2A protein phosphatase. *Proc Natl Acad Sci U S A*. 84:4880-4884.

Groves, M.R., N. Hanlon, P. Turowski, B.A. Hemmings, et al. 1999. The structure of the protein phosphatase 2A PR65/A subunit reveals the conformation of its 15 tandemly repeated HEAT motifs. *Cell*. 96:99-110.

Gu, P., X. Qi, Y. Zhou, Y. Wang, et al. 2012. Generation of Ppp2Ca and Ppp2Cb conditional null alleles in mouse. *Genesis*. 50:429-436.

Guizetti, J., and D.W. Gerlich. 2012. ESCRT-III polymers in membrane neck constriction. *Trends Cell Biol*. 22:133-140.

Guttinger, S., E. Laurell, and U. Kutay. 2009. Orchestrating nuclear envelope disassembly and reassembly during mitosis. *Nat Rev Mol Cell Biol*. 10:178-191.

Habermann, K., E. Mirgorodskaya, J. Gobom, V. Lehmann, et al. 2012. Functional analysis of centrosomal kinase substrates in Drosophila melanogaster reveals a new function of the nuclear envelope component otefin in cell cycle progression. *Mol Cell Biol*. 32:3554-3569.

Hached, K., P. Goguet, S. Charrasse, S. Vigneron, et al. 2019. ENSA and ARPP19 differentially control cell cycle progression and development. *J Cell Biol*. 218:541-558.

Haglund, K., I.P. Nezis, D. Lemus, C. Grabbe, et al. 2010. Cindr interacts with anillin to control cytokinesis in Drosophila melanogaster. *Curr Biol*. 20:944-950.

Hannak, E., M. Kirkham, A.A. Hyman, and K. Oegema. 2001. Aurora-A kinase is required for centrosome maturation in Caenorhabditis elegans. *J Cell Biol*. 155:1109-1116.

Hannus, M., F. Feiguin, C.P. Heisenberg, and S. Eaton. 2002. Planar cell polarization requires Widerborst, a B' regulatory subunit of protein phosphatase 2A. *Development*. 129:3493-3503.

Haque, F., D. Mazzeo, J.T. Patel, D.T. Smallwood, et al. 2010. Mammalian SUN protein interaction networks at the inner nuclear membrane and their role in laminopathy disease processes. *J Biol Chem*. 285:3487-3498.

Hara, M., Y. Abe, T. Tanaka, T. Yamamoto, et al. 2012. Greatwall kinase and cyclin B-Cdk1 are both critical constituents of M-phase-promoting factor. *Nat Commun*. 3:1059.

Haraguchi, T., T. Koujin, M. Segura-Totten, K.K. Lee, et al. 2001. BAF is required for emerin assembly into the reforming nuclear envelope. *J Cell Sci*. 114:4575-4585.

Hardwick, K.G., R.C. Johnston, D.L. Smith, and A.W. Murray. 2000. MAD3 encodes a novel component of the spindle checkpoint which interacts with Bub3p, Cdc20p, and Mad2p. *J Cell Biol*. 148:871-882.

Harper, J.W., G.R. Adami, N. Wei, K. Keyomarsi, et al. 1993. The p21 Cdk-interacting protein Cip1 is a potent inhibitor of G1 cyclin-dependent kinases. *Cell*. 75:805-816.

Harper, J.W., S.J. Elledge, K. Keyomarsi, B. Dynlacht, et al. 1995. Inhibition of cyclin-dependent kinases by p21. *Mol Biol Cell*. 6:387-400.

Hartwell, L.H., J. Culotti, J.R. Pringle, and B.J. Reid. 1974. Genetic control of the cell division cycle in yeast. *Science*. 183:46-51.

Hartwell, L.H., and T.A. Weinert. 1989. Checkpoints: controls that ensure the order of cell cycle events. *Science*. 246:629-634.

Harvey, S.L., G. Enciso, N. Dephoure, S.P. Gygi, et al. 2011. A phosphatase threshold sets the level of Cdk1 activity in early mitosis in budding yeast. *Mol Biol Cell*. 22:3595-3608.

Hatch, E.M., A.H. Fischer, T.J. Deerinck, and M.W. Hetzer. 2013. Catastrophic nuclear envelope collapse in cancer cell micronuclei. *Cell*. 154:47-60.

Heald, R., and F. McKeon. 1990. Mutations of phosphorylation sites in lamin A that prevent nuclear lamina disassembly in mitosis. *Cell*. 61:579-589.

Healy, A.M., S. Zolnierowicz, A.E. Stapleton, M. Goebl, et al. 1991. CDC55, a Saccharomyces cerevisiae gene involved in cellular morphogenesis: identification, characterization, and homology to the B subunit of mammalian type 2A protein phosphatase. *Mol Cell Biol*. 11:5767-5780.

Hegarat, N., C. Vesely, P.K. Vinod, C. Ocasio, et al. 2014. PP2A/B55 and Fcp1 regulate Greatwall and Ensa dephosphorylation during mitotic exit. *PLoS Genet*. 10:e1004004.

Heim, A., A. Konietzny, and T.U. Mayer. 2015. Protein phosphatase 1 is essential for Greatwall inactivation at mitotic exit. *EMBO Rep*. 16:1501-1510.

Hein, A.L., P. Seshacharyulu, S. Rachagani, Y.M. Sheinin, et al. 2016. PR55alpha Subunit of Protein Phosphatase 2A Supports the Tumorigenic and Metastatic Potential of Pancreatic Cancer Cells by Sustaining Hyperactive Oncogenic Signaling. *Cancer Res*. 76:2243-2253.

Hein, J.B., E.P.T. Hertz, D.H. Garvanska, T. Kruse, et al. 2017. Distinct kinetics of serine and threonine dephosphorylation are essential for mitosis. *Nat Cell Biol*. 19:1433-1440.

Hemmings, B.A., C. Adams-Pearson, F. Maurer, P. Muller, et al. 1990. alpha- and beta-forms of the 65-kDa subunit of protein phosphatase 2A have a similar 39 amino acid repeating structure. *Biochemistry*. 29:3166-3173.

Hendrickx, A., M. Beullens, H. Ceulemans, T. Den Abt, et al. 2009. Docking motif-guided mapping of the interactome of protein phosphatase-1. *Chem Biol*. 16:365-371.

Hershko, A. 1983. Ubiquitin: roles in protein modification and breakdown. *Cell*. 34:11-12.

Hershko, A., and A. Ciechanover. 1998. The ubiquitin system. *Annu Rev Biochem*. 67:425-479.

Hershko, A., D. Ganoth, V. Sudakin, A. Dahan, et al. 1994. Components of a system that ligates cyclin to ubiquitin and their regulation by the protein kinase cdc2. *J Biol Chem*. 269:4940-4946.

Hertz, E.P.T., T. Kruse, N.E. Davey, B. Lopez-Mendez, et al. 2016. A Conserved Motif Provides Binding Specificity to the PP2A-B56 Phosphatase. *Mol Cell*. 63:686-695.

Herzog, F., I. Primorac, P. Dube, P. Lenart, et al. 2009. Structure of the anaphase-promoting complex/cyclosome interacting with a mitotic checkpoint complex. *Science*. 323:1477-1481.

Hidalgo Carcedo, C., M. Bonazzi, S. Spano, G. Turacchio, et al. 2004. Mitotic Golgi partitioning is driven by the membrane-fissioning protein CtBP3/BARS. *Science*. 305:93-96.

Hilioti, Z., Y.S. Chung, Y. Mochizuki, C.F. Hardy, et al. 2001. The anaphase inhibitor Pds1 binds to the APC/C-associated protein Cdc20 in a destruction box-dependent manner. *Curr Biol*. 11:1347-1352.

Hime, G.R., J.A. Brill, and M.T. Fuller. 1996. Assembly of ring canals in the male germ line from structural components of the contractile ring. *J Cell Sci*. 109 (Pt 12):2779-2788.

Hindley, J., and G.A. Phear. 1984. Sequence of the cell division gene CDC2 from Schizosaccharomyces pombe; patterns of splicing and homology to protein kinases. *Gene*. 31:129-134.

Hirano, Y., Y. Iwase, K. Ishii, M. Kumeta, et al. 2009. Cell cycle-dependent phosphorylation of MAN1. *Biochemistry*. 48:1636-1643.

Hirano, Y., M. Segawa, F.S. Ouchi, Y. Yamakawa, et al. 2005. Dissociation of emerin from barrier-to-autointegration factor is regulated through mitotic phosphorylation of emerin in a xenopus egg cell-free system. *J Biol Chem*. 280:39925-39933.

Hitomi, M., K. Yang, A.W. Stacey, and D.W. Stacey. 2008. Phosphorylation of cyclin D1 regulated by ATM or ATR controls cell cycle progression. *Mol Cell Biol*. 28:5478-5493.

Holder, J., S. Mohammed, and F.A. Barr. 2020. Ordered dephosphorylation initiated by the selective proteolysis of cyclin B drives mitotic exit. *Elife*. 9.

Holder, J., E. Poser, and F.A. Barr. 2019. Getting out of mitosis: spatial and temporal control of mitotic exit and cytokinesis by PP1 and PP2A. *FEBS Lett*. 593:2908-2924.

Holtrich, U., G. Wolf, A. Brauninger, T. Karn, et al. 1994. Induction and down-regulation of PLK, a human serine/threonine kinase expressed in proliferating cells and tumors. *Proc Natl Acad Sci U S A*. 91:1736-1740.

Horiuchi, A., K.R. Williams, T. Kurihara, A.C. Nairn, et al. 1990. Purification and cDNA cloning of ARPP-16, a cAMP-regulated phosphoprotein enriched in basal ganglia, and of a related phosphoprotein, ARPP-19. *J Biol Chem*. 265:9476-9484.

Howard, A., and S.R. Pelc. 1953. Synthesis of deoxyribonucleic acid in

normal and irradiated cells and its relation to chromosome breakage. *Heredity (Suppl.)*:261-273.

Huang da, W., B.T. Sherman, and R.A. Lempicki. 2009a. Bioinformatics enrichment tools: paths toward the comprehensive functional analysis of large gene lists. *Nucleic Acids Res*. 37:1-13.

Huang da, W., B.T. Sherman, and R.A. Lempicki. 2009b. Systematic and integrative analysis of large gene lists using DAVID bioinformatics resources. *Nat Protoc*. 4:44-57.

Huang, H.B., Y.C. Chen, A. Horiuchi, L.H. Tsai, et al. 2001. Backbone 1H, 15N, and 13C resonance assignments of ARPP-19. *J Biomol NMR*. 19:383-384.

Huang, Y., T. Li, S.C. Ems-McClung, C.E. Walczak, et al. 2018. Aurora A activation in mitosis promoted by BuGZ. *J Cell Biol*. 217:107-116.

Hughes, B.T., J. Sidorova, J. Swanger, R.J. Monnat, Jr., et al. 2013. Essential role for Cdk2 inhibitory phosphorylation during replication stress revealed by a human Cdk2 knockin mutation. *Proc Natl Acad Sci U S A*. 110:8954-8959.

Huguet, F., S. Flynn, and P. Vagnarelli. 2019. The Role of Phosphatases in Nuclear Envelope Disassembly and Reassembly and Their Relevance to Pathologies. *Cells*. 8.

Hwang, H.C., and B.E. Clurman. 2005. Cyclin E in normal and neoplastic cell cycles. *Oncogene*. 24:2776-2786.

Imaoka, T., M. Imazu, H. Usui, N. Kinohara, et al. 1983. Resolution and reassociation of three distinct components from pig heart phosphoprotein phosphatase. *J Biol Chem*. 258:1526-1535.

Imoto, Y., Y. Yoshida, F. Yagisawa, H. Kuroiwa, et al. 2011. The cell cycle, including the mitotic cycle and organelle division cycles, as revealed by cytological observations. *J Electron Microsc (Tokyo)*. 60 Suppl 1:S117-136.

Ishihama, Y., J. Rappsilber, and M. Mann. 2006. Modular stop and go extraction tips with stacked disks for parallel and multidimensional Peptide fractionation in proteomics. *J Proteome Res*. 5:988-994.

Izawa, D., and J. Pines. 2015. The mitotic checkpoint complex binds a second CDC20 to inhibit active APC/C. *Nature*. 517:631-634.

Janghorban, M., A.S. Farrell, B.L. Allen-Petersen, C. Pelz, et al. 2014. Targeting c-MYC by antagonizing PP2A inhibitors in breast cancer. *Proc Natl Acad Sci U S A*. 111:9157-9162.

Janssens, V., and J. Goris. 2001. Protein phosphatase 2A: a highly regulated family of serine/threonine phosphatases implicated in cell growth and signalling. *Biochem J*. 353:417-439.

Jeffrey, P.D., A.A. Russo, K. Polyak, E. Gibbs, et al. 1995. Mechanism of CDK activation revealed by the structure of a cyclinA-CDK2 complex. *Nature*. 376:313-320.

Jeong, Y., J. Lee, K. Kim, J.C. Yoo, et al. 2007. Characterization of NIP2/centrobin, a novel substrate of Nek2, and its potential role in microtubule stabilization. *J Cell Sci*. 120:2106-2116.

Jiang, W., G. Jimenez, N.J. Wells, T.J. Hope, et al. 1998. PRC1: a human mitotic spindle-associated CDK substrate protein required for cytokinesis. *Mol Cell*. 2:877-885.

Jiang, X., L. Xia, D. Chen, Y. Yang, et al. 2008. Otefin, a nuclear membrane protein, determines the fate of germline stem cells in Drosophila via interaction with Smad complexes. *Dev Cell*. 14:494-506.

Johansen, J., and K.M. Johansen. 2009. The spindle matrix through the cell cycle in Drosophila. *Fly (Austin)*. 3:213-220.

Johansen, K.M., A. Forer, C. Yao, J. Girton, et al. 2011. Do nuclear envelope and intranuclear proteins reorganize during mitosis to form an elastic, hydrogel-like spindle matrix? *Chromosome Res*. 19:345-365.

Johnston, G.C., J.R. Pringle, and L.H. Hartwell. 1977. Coordination of growth with cell division in the yeast Saccharomyces cerevisiae. *Exp Cell Res*. 105:79-98.

Jones, T.A., H.M. Barker, E.F. da Cruz e Silva, R.E. Mayer-Jaekel, et al. 1993. Localization of the genes encoding the catalytic subunits of protein phosphatase 2A to human chromosome bands 5q23-->q31 and 8p12-->p11.2, respectively. *Cytogenet Cell Genet*. 63:35-41.

Jordan, M.A., K. Wendell, S. Gardiner, W.B. Derry, et al. 1996. Mitotic block induced in HeLa cells by low concentrations of paclitaxel (Taxol) results in abnormal mitotic exit and apoptotic cell death. *Cancer Res*. 56:816-825.

Joukov, V., J.C. Walter, and A. De Nicolo. 2014. The Cep192-organized aurora A-Plk1 cascade is essential for centrosome cycle and bipolar spindle assembly. *Mol Cell*. 55:578-591.

Juanes, M.A., R. Khoueiry, T. Kupka, A. Castro, et al. 2013. Budding Yeast Greatwall and Endosulfines Control Activity and Spatial Regulation of PP2A(Cdc55) for Timely Mitotic Progression. *PLoS Genet*. 9:e1003575.

Junttila, M.R., P. Puustinen, M. Niemela, R. Ahola, et al. 2007. CIP2A inhibits PP2A in human malignancies. *Cell*. 130:51-62.

Kachaner, D., D. Garrido, H. Mehsen, K. Normandin, et al. 2017. Coupling of Polo kinase activation to nuclear localization by a bifunctional NLS is required during mitotic entry. *Nat Commun*. 8:1701.

Kachaner, D., X. Pinson, K.B. El Kadhi, K. Normandin, et al. 2014. Interdomain allosteric regulation of Polo kinase by Aurora B and Map205 is required for cytokinesis. *J Cell Biol*. 207:201-211.

Kalderon, D., B.L. Roberts, W.D. Richardson, and A.E. Smith. 1984. A short amino acid sequence able to specify nuclear location. *Cell*. 39:499-509.

Kalev, P., M. Simicek, I. Vazquez, S. Munck, et al. 2012. Loss of PPP2R2A inhibits homologous recombination DNA repair and predicts tumor sensitivity to PARP inhibition. *Cancer Res*. 72:6414-6424.

Kamada, Y., M. Sakata-Yanagimoto, M. Sanada, A. Sato-Otsubo, et al. 2012. Identification of unbalanced genome copy number abnormalities in patients with multiple myeloma by single-nucleotide polymorphism genotyping microarray analysis. *Int J Hematol*. 96:492-500.

Kang, Y.H., J.E. Park, L.R. Yu, N.K. Soung, et al. 2006. Self-regulated Plk1 recruitment to kinetochores by the Plk1-PBIP1 interaction is critical for proper chromosome segregation. *Mol Cell*. 24:409-422.

Kanshin, E., S. Michnick, and P. Thibault. 2012. Sample preparation and analytical strategies for large-scale phosphoproteomics experiments. *Semin Cell Dev Biol*. 23:843-853.

Kanshin, E., S.W. Michnick, and P. Thibault. 2013. Displacement of N/Q-rich peptides on TiO2 beads enhances the depth and coverage of yeast phosphoproteome analyses. *J Proteome Res*. 12:2905-2913.

Karsenti, E., and I. Vernos. 2001. The mitotic spindle: a self-made machine. *Science*. 294:543-547.

Kelpsch, D.J., and T.L. Tootle. 2018. Nuclear Actin: From Discovery to Function. *Anat Rec (Hoboken)*. 301:1999-2013.

Keminer, O., and R. Peters. 1999. Permeability of single nuclear pores. *Biophys J*. 77:217-228.

Kettenbach, A.N., D.K. Schweppe, B.K. Faherty, D. Pechenick, et al. 2011. Quantitative phosphoproteomics identifies substrates and functional modules of Aurora and Polo-like kinase activities in mitotic cells. *Sci Signal*. 4:rs5.

Khew-Goodall, Y., R.E. Mayer, F. Maurer, S.R. Stone, et al. 1991. Structure and transcriptional regulation of protein phosphatase 2A catalytic subunit genes. *Biochemistry*. 30:89-97.

Kim, D.I., K.C. Birendra, and K.J. Roux. 2015. Making the LINC: SUN and KASH protein interactions. *Biol Chem*. 396:295-310.

Kim, M.Y., E. Bucciarelli, D.G. Morton, B.C. Williams, et al. 2012. Bypassing the Greatwall-Endosulfine pathway: plasticity of a pivotal cell-cycle regulatory module in Drosophila melanogaster and Caenorhabditis elegans. *Genetics*. 191:1181-1197.

Kim, Y., N.G. Starostina, and E.T. Kipreos. 2008. The CRL4Cdt2 ubiquitin ligase targets the degradation of p21Cip1 to control replication licensing. *Genes Dev*. 22:2507-2519.

Kimura, K., M. Hirano, R. Kobayashi, and T. Hirano. 1998. Phosphorylation and activation of 13S condensin by Cdc2 in vitro. *Science*. 282:487-490.

King, R.W., P.K. Jackson, and M.W. Kirschner. 1994. Mitosis in transition. *Cell*. 79:563-571.

King, R.W., J.M. Peters, S. Tugendreich, M. Rolfe, et al. 1995. A 20S complex containing CDC27 and CDC16 catalyzes the mitosis-specific conjugation of ubiquitin to cyclin B. *Cell*. 81:279-288.

Kinoshita, N., H. Ohkura, and M. Yanagida. 1990. Distinct, essential roles of type 1 and 2A protein phosphatases in the control of the fission yeast cell division cycle. *Cell*. 63:405-415.

Kirschner, M., and T. Mitchison. 1986. Beyond self-assembly: from microtubules to morphogenesis. *Cell*. 45:329-342.

Kitagawa, M., H. Higashi, H.K. Jung, I. Suzuki-Takahashi, et al. 1996. The consensus motif for phosphorylation by cyclin D1-Cdk4 is different from that for phosphorylation by cyclin A/E-Cdk2. *EMBO J*. 15:7060-7069.

Knight, J.D.R., H. Choi, G.D. Gupta, L. Pelletier, et al. 2017. ProHits-viz: a suite of web tools for visualizing interaction proteomics data. *Nat Methods*. 14:645-646.

Knockenhauer, K.E., and T.U. Schwartz. 2016. The Nuclear Pore Complex as a Flexible and Dynamic Gate. *Cell*. 164:1162-1171.

Ko, L.J., and C. Prives. 1996. p53: puzzle and paradigm. *Genes Dev*. 10:1054-1072.

Kraft, C., F. Herzog, C. Gieffers, K. Mechtler, et al. 2003. Mitotic regulation of the human anaphase-promoting complex by phosphorylation. *EMBO J*. 22:6598-6609.

Kramer, A., I. Liashkovich, Y. Ludwig, and V. Shahin. 2008. Atomic force microscopy visualises a hydrophobic meshwork in the central channel of the nuclear pore. *Pflugers Arch*. 456:155-162.

Kramer, E.R., N. Scheuringer, A.V. Podtelejnikov, M. Mann, et al. 2000. Mitotic regulation of the APC activator proteins CDC20 and CDH1. *Mol Biol Cell*. 11:1555-1569.

Krek, W., and E.A. Nigg. 1991. Differential phosphorylation of vertebrate p34cdc2 kinase at the G1/S and G2/M transitions of the cell cycle: identification of major phosphorylation sites. *EMBO J*. 10:305-316.

Kremmer, E., K. Ohst, J. Kiefer, N. Brewis, et al. 1997. Separation of PP2A core enzyme and holoenzyme with monoclonal antibodies against the regulatory A subunit: abundant expression of both forms in cells. *Mol Cell Biol*. 17:1692-1701.

Kruse, T., S.P. Gnosa, I. Nasa, D.H. Garvanska, et al. 2020. Mechanisms of site-specific dephosphorylation and kinase opposition imposed by PP2A regulatory subunits. *EMBO J*. 39:e103695.

Kuilman, T., A. Maiolica, M. Godfrey, N. Scheidel, et al. 2015. Identification of Cdk targets that control cytokinesis. *EMBO J*. 34:81-96.

Kumar, G.S., E. Gokhan, S. De Munter, M. Bollen, et al. 2016. The Ki-67 and RepoMan mitotic phosphatases assemble via an identical, yet novel mechanism. *Elife*. 5.

Kunda, P., N.T. Rodrigues, E. Moeendarbary, T. Liu, et al. 2012. PP1-mediated moesin dephosphorylation couples polar relaxation to mitotic exit. *Curr Biol*. 22:231-236.

Kuriyama, R., and G.G. Borisy. 1983. Cytasters induced within unfertilized sea-urchin eggs. *J Cell Sci*. 61:175-189.

Kwon, Y.G., S.Y. Lee, Y. Choi, P. Greengard, et al. 1997. Cell cycle-dependent phosphorylation of mammalian protein phosphatase 1 by cdc2 kinase. *Proc Natl Acad Sci U S A*. 94:2168-2173.

L'Allemain, G., J.N. Lavoie, N. Rivard, V. Baldin, et al. 1997. Cyclin D1 expression is a major target of the cAMP-induced inhibition of cell cycle entry in fibroblasts. *Oncogene*. 14:1981-1990.

Labandera, A.M., A.R. Vahab, S. Chaudhuri, D. Kerk, et al. 2015. The mitotic PP2A regulator ENSA/ARPP-19 is remarkably conserved across plants and most eukaryotes. *Biochem Biophys Res Commun*. 458:739-744.

Labit, H., K. Fujimitsu, N.S. Bayin, T. Takaki, et al. 2012. Dephosphorylation of Cdc20 is required for its C-box-dependent activation of the APC/C. *EMBO J*. 31:3351-3362.

Lad, C., N.H. Williams, and R. Wolfenden. 2003. The rate of hydrolysis of phosphomonoester dianions and the exceptional catalytic proficiencies of protein and inositol phosphatases. *Proc Natl Acad Sci U S A*. 100:5607-5610.

Laguri, C., B. Gilquin, N. Wolff, R. Romi-Lebrun, et al. 2001. Structural characterization of the LEM motif common to three human inner nuclear membrane proteins. *Structure*. 9:503-511.

Laine, A., H. Sihto, C. Come, M.T. Rosenfeldt, et al. 2013. Senescence sensitivity of breast cancer cells is defined by positive feedback loop between CIP2A and E2F1. *Cancer Discov*. 3:182-197.

LaJoie, D., and K.S. Ullman. 2017. Coordinated events of nuclear assembly. *Curr Opin Cell Biol*. 46:39-45.

Lambrecht, C., D. Haesen, W. Sents, E. Ivanova, et al. 2013. Structure, Regulation, and Pharmacological Modulation of PP2A Phosphatases. *Methods Mol Biol*. 1053:283-305.

Lampson, M.A., K. Renduchitala, A. Khodjakov, and T.M. Kapoor. 2004. Correcting improper chromosome-spindle attachments during cell division. *Nat Cell Biol*. 6:232-237.

Lane, H.A., and E.A. Nigg. 1996. Antibody microinjection reveals an essential role for human polo-like kinase 1 (Plk1) in the functional maturation of mitotic centrosomes. *J Cell Biol*. 135:1701-1713.

Larouche, M., D. Kachaner, P. Wang, K. Normandin, et al. 2021. Spatiotemporal coordination of Greatwall-Endos-PP2A promotes mitotic progression. *J Cell Biol*. 220.

Laurell, E., K. Beck, K. Krupina, G. Theerthagiri, et al. 2011. Phosphorylation of Nup98 by multiple kinases is crucial for NPC disassembly during mitotic entry. *Cell*. 144:539-550.

Leach, C., S. Shenolikar, and D.L. Brautigan. 2003. Phosphorylation of phosphatase inhibitor-2 at centrosomes during mitosis. *J Biol Chem*. 278:26015-26020.

Lee, J., and J. Stock. 1993. Protein phosphatase 2A catalytic subunit is methyl-esterified at its carboxyl terminus by a novel methyltransferase. *J Biol Chem*. 268:19192-19195.

Lee, K.K., T. Haraguchi, R.S. Lee, T. Koujin, et al. 2001. Distinct functional domains in emerin bind lamin A and DNA-bridging protein BAF. *J Cell Sci*. 114:4567-4573.

Lee, M.G., and P. Nurse. 1987. Complementation used to clone a human homologue of the fission yeast cell cycle control gene cdc2. *Nature*. 327:31-35.

Lee, M.H., I. Reynisdottir, and J. Massague. 1995. Cloning of p57KIP2, a cyclin-dependent kinase inhibitor with unique domain structure and tissue distribution. *Genes Dev*. 9:639-649.

Legrier, M.E., I. Bieche, J. Gaston, A. Beurdeley, et al. 2016. Activation of IFN/STAT1 signalling predicts response to chemotherapy in oestrogen receptor-negative breast cancer. *Br J Cancer*. 114:177-187.

Lew, D.J., and S. Kornbluth. 1996. Regulatory roles of cyclin dependent kinase phosphorylation in cell cycle control. *Curr Opin Cell Biol*. 8:795-804.

Li, J., M. Dallmayer, T. Kirchner, J. Musa, et al. 2018. PRC1: Linking Cytokinesis, Chromosomal Instability, and Cancer Evolution. *Trends Cancer*. 4:59-73.

Li, M., H. Guo, and Z. Damuni. 1995. Purification and characterization of two potent heat-stable protein inhibitors of protein phosphatase 2A from bovine kidney. *Biochemistry*. 34:1988-1996.

Li, Y.H., H. Kang, Y.N. Xu, Y.T. Heo, et al. 2013. Greatwall kinase is required for meiotic maturation in porcine oocytes. *Biol Reprod*. 89:53.

Lillo, C., A.R. Kataya, B. Heidari, M.T. Creighton, et al. 2014. Protein phosphatases PP2A, PP4 and PP6: mediators and regulators in development and responses to environmental cues. *Plant Cell Environ*. 37:2631-2648.

Lin, F., D.L. Blake, I. Callebaut, I.S. Skerjanc, et al. 2000. MAN1, an inner nuclear membrane protein that shares the LEM domain with lamina-associated polypeptide 2 and emerin. *J Biol Chem*. 275:4840-4847.

Lin, F.C., and K.T. Arndt. 1995. The role of Saccharomyces cerevisiae type 2A phosphatase in the actin cytoskeleton and in entry into mitosis. *EMBO J*. 14:2745-2759.

Lince-Faria, M., S. Maffini, B. Orr, Y. Ding, et al. 2009. Spatiotemporal control of mitosis by the conserved spindle matrix protein Megator. *J Cell Biol*. 184:647-657.

Linder, M.I., M. Kohler, P. Boersema, M. Weberruss, et al. 2017. Mitotic Disassembly of Nuclear Pore Complexes Involves CDK1- and PLK1-Mediated Phosphorylation of Key Interconnecting Nucleoporins. *Dev Cell*. 43:141-156 e147.

Lindon, C., and J. Pines. 2004. Ordered proteolysis in anaphase inactivates Plk1 to contribute to proper mitotic exit in human cells. *J Cell Biol*. 164:233-241.

Lindqvist, A., V. Rodriguez-Bravo, and R.H. Medema. 2009. The decision to enter mitosis: feedback and redundancy in the mitotic entry network. *J Cell Biol*. 185:193-202.

Lipinszki, Z., P. Wang, R. Grant, C. Lindon, et al. 2014. Affinity purification of protein complexes from Drosophila embryos in cell cycle studies. *Methods Mol Biol*. 1170:571-588.

Liu, C., and J. Li. 2018. O-GlcNAc: A Sweetheart of the Cell Cycle and DNA Damage Response. *Front Endocrinol (Lausanne)*. 9:415.

Liu, D., M. Vleugel, C.B. Backer, T. Hori, et al. 2010. Regulated targeting of protein phosphatase 1 to the outer kinetochore by KNL1 opposes Aurora B kinase. *J Cell Biol*. 188:809-820.

Liu, H., Y. Gu, H. Wang, J. Yin, et al. 2015. Overexpression of PP2A inhibitor SET oncoprotein is associated with tumor progression and poor prognosis in human non-small cell lung cancer. *Oncotarget*. 6:14913-14925.

Liu, Q., S. Guntuku, X.S. Cui, S. Matsuoka, et al. 2000. Chk1 is an essential kinase that is regulated by Atr and required for the G(2)/M DNA damage checkpoint. *Genes Dev*. 14:1448-1459.

Liu, Z., L. Ma, Z.S. Wen, Z. Hu, et al. 2014. Cancerous inhibitor of PP2A is targeted by natural compound celastrol for degradation in non-small-cell lung cancer. *Carcinogenesis*. 35:905-914.

Llamazares, S., A. Moreira, A. Tavares, C. Girdham, et al. 1991. polo encodes a protein kinase homolog required for mitosis in Drosophila. *Genes Dev*. 5:2153-2165.

Lohka, M.J., M.K. Hayes, and J.L. Maller. 1988. Purification of maturation-promoting factor, an intracellular regulator of early mitotic events. *Proc Natl Acad Sci U S A*. 85:3009-3013.

Longin, S., K. Zwaenepoel, J.V. Louis, S. Dilworth, et al. 2007. Selection of protein phosphatase 2A regulatory subunits is mediated by the C terminus of the catalytic Subunit. *J Biol Chem*. 282:26971-26980.

Lorca, T., C. Bernis, S. Vigneron, A. Burgess, et al. 2010. Constant regulation of both the MPF amplification loop and the Greatwall-PP2A pathway is required for metaphase II arrest and correct entry into the first embryonic cell cycle. *J Cell Sci*. 123:2281-2291.

Lorca, T., A. Devault, P. Colas, A. Van Loon, et al. 1992. Cyclin A-Cys41 does not undergo cell cycle-dependent degradation in Xenopus extracts. *FEBS Lett*. 306:90-93.

Lorincz, A.T., and S.I. Reed. 1984. Primary structure homology between the product of yeast cell division control gene CDC28 and vertebrate oncogenes. *Nature*. 307:183-185.

Lou, Y., J. Yao, A. Zereshki, Z. Dou, et al. 2004. NEK2A interacts with MAD1 and possibly functions as a novel integrator of the spindle checkpoint signaling. *J Biol Chem*. 279:20049-20057.

Lowe, M., N.K. Gonatas, and G. Warren. 2000. The mitotic phosphorylation cycle of the cis-Golgi matrix protein GM130. *J Cell Biol*. 149:341-356.

Lowe, M., C. Rabouille, N. Nakamura, R. Watson, et al. 1998. Cdc2 kinase directly phosphorylates the cis-Golgi matrix protein GM130 and is required for Golgi fragmentation in mitosis. *Cell*. 94:783-793.

Lu, M., K. Ding, G. Zhang, M. Yin, et al. 2015. MicroRNA-320a sensitizes tamoxifen-resistant breast cancer cells to tamoxifen by targeting ARPP-19 and ERRgamma. *Sci Rep*. 5:8735.

Ma, S., S. Vigneron, P. Robert, J.M. Strub, et al. 2016. Greatwall dephosphorylation and inactivation upon mitotic exit is triggered by PP1. *J Cell Sci*. 129:1329-1339.

Ma, Y., Y. Liu, Y.S. Pu, M.L. Cui, et al. 2020. LncRNA IGFL2-AS1 functions as a ceRNA in regulating ARPP19 through competitive binding to miR-802 in gastric cancer. *Mol Carcinog*. 59:311-322.

MacKintosh, R.W., G. Haycox, D.G. Hardie, and P.T. Cohen. 1990. Identification by molecular cloning of two cDNA sequences from the plant Brassica napus which are very similar to mammalian protein phosphatases-1 and -2A. *FEBS Lett*. 276:156-160.

Macurek, L., A. Lindqvist, D. Lim, M.A. Lampson, et al. 2008. Polo-like kinase-1 is activated by aurora A to promote checkpoint recovery. *Nature*. 455:119-123.

Maddox, P.S., K.S. Bloom, and E.D. Salmon. 2000. The polarity and dynamics of microtubule assembly in the budding yeast Saccharomyces cerevisiae. *Nat Cell Biol*. 2:36-41.

Magidson, V., R. Paul, N. Yang, J.G. Ault, et al. 2015. Adaptive changes in the kinetochore architecture facilitate proper spindle assembly. *Nat Cell Biol*. 17:1134-1144.

Mailand, N., S. Bekker-Jensen, J. Bartek, and J. Lukas. 2006. Destruction of Claspin by SCFbetaTrCP restrains Chk1 activation and facilitates recovery from genotoxic stress. *Mol Cell*. 23:307-318.

Mailand, N., J. Falck, C. Lukas, R.G. Syljuasen, et al. 2000. Rapid destruction of human Cdc25A in response to DNA damage. *Science*. 288:1425-1429.

Makela, E., E. Loyttyniemi, U. Salmenniemi, O. Kauko, et al. 2019. Arpp19 Promotes Myc and Cip2a Expression and Associates with Patient Relapse in Acute Myeloid Leukemia. *Cancers (Basel)*. 11.

Makkerh, J.P., C. Dingwall, and R.A. Laskey. 1996. Comparative mutagenesis of nuclear localization signals reveals the importance of neutral and acidic amino acids. *Curr Biol*. 6:1025-1027.

Malik, R., R. Lenobel, A. Santamaria, A. Ries, et al. 2009. Quantitative analysis of the human spindle phosphoproteome at distinct mitotic stages. *J Proteome Res*. 8:4553-4563.

Mall, M., T. Walter, M. Gorjanacz, I.F. Davidson, et al. 2012. Mitotic lamin disassembly is triggered by lipid-mediated signaling. *J Cell Biol*. 198:981-990.

Maller, J.L. 1986. Mitogenic signalling and protein phosphorylation in Xenopus oocytes. *J Cyclic Nucleotide Protein Phosphor Res*. 11:543-555.

Malone, C.J., W.D. Fixsen, H.R. Horvitz, and M. Han. 1999. UNC-84 localizes to the nuclear envelope and is required for nuclear migration and anchoring during C. elegans development. *Development*. 126:3171-3181.

Malumbres, M. 2014. Cyclin-dependent kinases. *Genome Biol*. 15:122.

Malumbres, M., and M. Barbacid. 2001. To cycle or not to cycle: a critical decision in cancer. *Nat Rev Cancer*. 1:222-231.

Malumbres, M., and M. Barbacid. 2005. Mammalian cyclin-dependent kinases. *Trends Biochem Sci*. 30:630-641.

Manchado, E., M. Guillamot, G. de Carcer, M. Eguren, et al. 2010. Targeting mitotic exit leads to tumor regression in vivo: Modulation by Cdk1, Mastl, and the PP2A/B55alpha,delta phosphatase. *Cancer Cell*. 18:641-654.

Manchado, E., M. Guillamot, and M. Malumbres. 2012. Killing cells by targeting mitosis. *Cell Death Differ*. 19:369-377.

Maniotis, A.J., C.S. Chen, and D.E. Ingber. 1997. Demonstration of mechanical connections between integrins, cytoskeletal filaments, and nucleoplasm that stabilize nuclear structure. *Proc Natl Acad Sci U S A*. 94:849-854.

Manning, G., D.B. Whyte, R. Martinez, T. Hunter, et al. 2002. The protein kinase complement of the human genome. *Science*. 298:1912-1934.

Mansharamani, M., and K.L. Wilson. 2005. Direct binding of nuclear membrane protein MAN1 to emerin in vitro and two modes of binding to barrier-to-autointegration factor. *J Biol Chem*. 280:13863-13870.

Mant, C.T., J.M. Kovacs, H.M. Kim, D.D. Pollock, et al. 2009. Intrinsic amino acid side-chain hydrophilicity/hydrophobicity coefficients determined by reversed-phase high-performance liquid chromatography of model peptides: comparison with other hydrophilicity/hydrophobicity scales. *Biopolymers*. 92:573-595.

Margalit, A., A. Brachner, J. Gotzmann, R. Foisner, et al. 2007. Barrier-to-autointegration factor--a BAFfling little protein. *Trends Cell Biol*. 17:202-208.

Margalit, A., M. Segura-Totten, Y. Gruenbaum, and K.L. Wilson. 2005. Barrier-to-autointegration factor is required to segregate and enclose chromosomes within the nuclear envelope and assemble the nuclear lamina. *Proc Natl Acad Sci U S A*. 102:3290-3295.

Marguerat, S., A. Schmidt, S. Codlin, W. Chen, et al. 2012. Quantitative analysis of fission yeast transcriptomes and proteomes in proliferating and quiescent cells. *Cell*. 151:671-683.

Martinez-Balbas, M.A., A. Dey, S.K. Rabindran, K. Ozato, et al. 1995. Displacement of sequence-specific transcription factors from mitotic chromatin. *Cell*. 83:29-38.

Martino, L., S. Morchoisne-Bolhy, D.K. Cheerambathur, L. Van Hove, et al. 2017. Channel Nucleoporins Recruit PLK-1 to Nuclear Pore Complexes to Direct Nuclear Envelope Breakdown in C. elegans. *Dev Cell*. 43:157-171 e157.

Marzec, K., and A. Burgess. 2018. The Oncogenic Functions of MASTL Kinase. *Front Cell Dev Biol*. 6:162.

Masai, H., S. Matsumoto, Z. You, N. Yoshizawa-Sugata, et al. 2010. Eukaryotic chromosome DNA replication: where, when, and how? *Annu Rev Biochem*. 79:89-130.

Matsuoka, S., M. Huang, and S.J. Elledge. 1998. Linkage of ATM to cell cycle regulation by the Chk2 protein kinase. *Science*. 282:1893-1897.

Matthews, L.M., and J.P. Evans. 2014. alpha-endosulfine (ENSA) regulates exit from prophase I arrest in mouse oocytes. *Cell Cycle*. 13:1639-1649.

Mayer, R.E., P. Hendrix, P. Cron, R. Matthies, et al. 1991. Structure of the 55-kDa regulatory subunit of protein phosphatase 2A: evidence for a neuronal-specific isoform. *Biochemistry*. 30:3589-3597.

Mayer-Jaekel, R.E., S. Baumgartner, G. Bilbe, H. Ohkura, et al. 1992. Molecular cloning and developmental expression of the catalytic and 65-kDa regulatory subunits of protein phosphatase 2A in Drosophila. *Mol Biol Cell*. 3:287-298.

Mayer-Jaekel, R.E., H. Ohkura, P. Ferrigno, N. Andjelkovic, et al. 1994. Drosophila mutants in the 55 kDa regulatory subunit of protein phosphatase 2A show strongly reduced ability to dephosphorylate substrates of p34cdc2. *J Cell Sci*. 107 (Pt 9):2609-2616.

Mayer-Jaekel, R.E., H. Ohkura, R. Gomes, C.E. Sunkel, et al. 1993. The 55 kd regulatory subunit of Drosophila protein phosphatase 2A is required for anaphase. *Cell*. 72:621-633.

Mayor, T., Y.D. Stierhof, K. Tanaka, A.M. Fry, et al. 2000. The centrosomal protein C-Nap1 is required for cell cycle-regulated centrosome cohesion. *J Cell Biol*. 151:837-846.

McCloy, R.A., B.L. Parker, S. Rogers, R. Chaudhuri, et al. 2015. Global Phosphoproteomic Mapping of Early Mitotic Exit in Human Cells Identifies Novel Substrate Dephosphorylation Motifs. *Mol Cell Proteomics*. 14:2194-2212.

McCloy, R.A., S. Rogers, C.E. Caldon, T. Lorca, et al. 2014. Partial inhibition of Cdk1 in G 2 phase overrides the SAC and decouples mitotic events. *Cell Cycle*. 13:1400-1412.

McGowan, C.H., and P. Russell. 1993. Human Wee1 kinase inhibits cell division by phosphorylating p34cdc2 exclusively on Tyr15. *EMBO J*. 12:75-85.

McIntosh, J.R. 2016. Mitosis. *Cold Spring Harb Perspect Biol*. 8.

McIntosh, J.R., K.L. McDonald, M.K. Edwards, and B.M. Ross. 1979. Three-dimensional structure of the central mitotic spindle of Diatoma vulgare. *J Cell Biol*. 83:428-442.

Meghini, F., T. Martins, X. Tait, K. Fujimitsu, et al. 2016. Targeting of Fzr/Cdh1 for timely activation of the APC/C at the centrosome during mitotic exit. *Nat Commun*. 7:12607.

Mehsen, H., V. Boudreau, D. Garrido, M. Bourouh, et al. 2018. PP2A-B55 promotes nuclear envelope reformation after mitosis in Drosophila. *J Cell Biol*. 217:4106-4123.

Melixetian, M., A. Ballabeni, L. Masiero, P. Gasparini, et al. 2004. Loss of Geminin induces rereplication in the presence of functional p53. *J Cell Biol*. 165:473-482.

Merigliano, C., A. Marzio, F. Renda, M.P. Somma, et al. 2017. A Role for the Twins Protein Phosphatase (PP2A-B55) in the Maintenance of Drosophila Genome Integrity. *Genetics*. 205:1151-1167.

Min, M., U. Mayor, G. Dittmar, and C. Lindon. 2014. Using in vivo biotinylated ubiquitin to describe a mitotic exit ubiquitome from human cells. *Mol Cell Proteomics*. 13:2411-2425.

Minshull, J., R. Golsteyn, C.S. Hill, and T. Hunt. 1990. The A- and B-type cyclin associated cdc2 kinases in Xenopus turn on and off at different times in the cell cycle. *EMBO J*. 9:2865-2875.

Minshull, J., A. Straight, A.D. Rudner, A.F. Dernburg, et al. 1996. Protein phosphatase 2A regulates MPF activity and sister chromatid cohesion in budding yeast. *Curr Biol*. 6:1609-1620.

Mishima, M., S. Kaitna, and M. Glotzer. 2002. Central spindle assembly and cytokinesis require a kinesin-like protein/RhoGAP complex with microtubule bundling activity. *Dev Cell*. 2:41-54.

Mishra, P., and D.C. Chan. 2014. Mitochondrial dynamics and inheritance during cell division, development and disease. *Nat Rev Mol Cell Biol*. 15:634-646.

Mislow, J.M., J.M. Holaska, M.S. Kim, K.K. Lee, et al. 2002. Nesprin-1alpha self-associates and binds directly to emerin and lamin A in vitro. *FEBS Lett*. 525:135-140.

Mitchison, T., L. Evans, E. Schulze, and M. Kirschner. 1986. Sites of microtubule assembly and disassembly in the mitotic spindle. *Cell*. 45:515-527.

Mitchison, T.J., J. Pineda, J. Shi, and S. Florian. 2017. Is inflammatory micronucleation the key to a successful anti-mitotic cancer drug? *Open Biol*. 7.

Miyazaki, W.Y., and T.L. Orr-Weaver. 1994. Sister-chromatid cohesion in mitosis and meiosis. *Annu Rev Genet*. 28:167-187.

Mocciaro, A., E. Berdougo, K. Zeng, E. Black, et al. 2010. Vertebrate cells genetically deficient for Cdc14A or Cdc14B retain DNA damage checkpoint proficiency but are impaired in DNA repair. *J Cell Biol*. 189:631-639.

Mochida, S. 2014. Regulation of alpha-endosulfine, an inhibitor of protein phosphatase 2A, by multisite phosphorylation. *FEBS J*. 281:1159-1169.

Mochida, S., and T. Hunt. 2007. Calcineurin is required to release Xenopus egg extracts from meiotic M phase. *Nature*. 449:336-340.

Mochida, S., S. Ikeo, J. Gannon, and T. Hunt. 2009. Regulated activity of PP2A-B55 delta is crucial for controlling entry into and exit from mitosis in Xenopus egg extracts. *Embo J*. 28:2777-2785.

Mochida, S., S.L. Maslen, M. Skehel, and T. Hunt. 2010. Greatwall phosphorylates an inhibitor of protein phosphatase 2A that is essential for mitosis. *Science*. 330:1670-1673.

Mohr, D., S. Frey, T. Fischer, T. Guttler, et al. 2009. Characterisation of the passive permeability barrier of nuclear pore complexes. *EMBO J*. 28:2541-2553.

Molitor, T.P., and P. Traktman. 2014. Depletion of the protein kinase VRK1 disrupts nuclear envelope morphology and leads to BAF retention on mitotic chromosomes. *Mol Biol Cell*. 25:891-903.

Mollinari, C., J.P. Kleman, W. Jiang, G. Schoehn, et al. 2002. PRC1 is a microtubule binding and bundling protein essential to maintain the mitotic spindle midzone. *J Cell Biol*. 157:1175-1186.

Montes de Oca, R., P.R. Andreassen, and K.L. Wilson. 2011. Barrier-to-Autointegration Factor influences specific histone modifications. *Nucleus*. 2:580-590.

Moorhead, G.B., L. Trinkle-Mulcahy, and A. Ulke-Lemee. 2007. Emerging roles of nuclear protein phosphatases. *Nat Rev Mol Cell Biol*. 8:234-244.

Moreno-Torres, M., M. Jaquenoud, and C. De Virgilio. 2015. TORC1 controls G1-S cell cycle transition in yeast via Mpk1 and the greatwall kinase pathway. *Nat Commun*. 6:8256.

Morgan, D.O. 1995. Principles of CDK regulation. *Nature*. 374:131-134.

Morgan, D.O. 1997. Cyclin-dependent kinases: engines, clocks, and microprocessors. *Annu Rev Cell Dev Biol*. 13:261-291.

Morgan, D.O. 2007. The Cell Cycle: Principles of Control. New Science Press, London. 297 pp.

Mosca, L., P. Musto, K. Todoerti, M. Barbieri, et al. 2013. Genome-wide analysis of primary plasma cell leukemia identifies recurrent imbalances associated with changes in transcriptional profiles. *Am J Hematol*. 88:16-23.

Moura, M., and C. Conde. 2019. Phosphatases in Mitosis: Roles and Regulation. *Biomolecules*. 9.

Moutinho-Santos, T., P. Sampaio, I. Amorim, M. Costa, et al. 1999. In vivo localisation of the mitotic POLO kinase shows a highly dynamic association with the mitotic apparatus during early embryogenesis in Drosophila. *Biol Cell*. 91:585-596.

Mueller, P.R., T.R. Coleman, A. Kumagai, and W.G. Dunphy. 1995. Myt1: a membrane-associated inhibitory kinase that phosphorylates Cdc2 on both threonine-14 and tyrosine-15. *Science*. 270:86-90.

Mullins, J.M., and J.J. Biesele. 1977. Terminal phase of cytokinesis in D-98s cells. *J Cell Biol*. 73:672-684.

Musacchio, A., and E.D. Salmon. 2007. The spindle-assembly checkpoint in space and time. *Nat Rev Mol Cell Biol*. 8:379-393.

Myers, J.S., R. Zhao, X. Xu, A.J. Ham, et al. 2007. Cyclin-dependent kinase 2 dependent phosphorylation of ATRIP regulates the G2-M checkpoint response to DNA damage. *Cancer Res*. 67:6685-6690.

Nagel, R., M. Stigter-van Walsum, M. Buijze, J. van den Berg, et al. 2015. Genome-wide siRNA Screen Identifies the Radiosensitizing Effect of Downregulation of MASTL and FOXM1 in NSCLC. *Mol Cancer Ther*. 14:1434-1444.

Nakayama, K.I., and K. Nakayama. 2006. Ubiquitin ligases: cell-cycle control and cancer. *Nat Rev Cancer*. 6:369-381.

Nasa, I., and A.N. Kettenbach. 2018. Coordination of Protein Kinase and Phosphoprotein Phosphatase Activities in Mitosis. *Front Cell Dev Biol*. 6:30.

Neer, E.J., C.J. Schmidt, R. Nambudripad, and T.F. Smith. 1994. The ancient regulatory-protein family of WD-repeat proteins. *Nature*. 371:297-300.

Neurohr, G., A. Naegeli, I. Titos, D. Theler, et al. 2011. A midzone-based ruler adjusts chromosome compaction to anaphase spindle length. *Science*. 332:465-468.

Neviani, P., R. Santhanam, J.J. Oaks, A.M. Eiring, et al. 2007. FTY720, a new alternative for treating blast crisis chronic myelogenous leukemia and Philadelphia chromosome-positive acute lymphocytic leukemia. *J Clin Invest*. 117:2408-2421.

Neviani, P., R. Santhanam, R. Trotta, M. Notari, et al. 2005. The tumor suppressor PP2A is functionally inactivated in blast crisis CML through the inhibitory activity of the BCR/ABL-regulated SET protein. *Cancer Cell*. 8:355-368.

Nguyen, K.M., and L. Busino. 2020. The Biology of F-box Proteins: The SCF Family of E3 Ubiquitin Ligases. *Adv Exp Med Biol*. 1217:111-122.

Nichols, R.J., M.S. Wiebe, and P. Traktman. 2006. The vaccinia-related kinases phosphorylate the N' terminus of BAF, regulating its interaction with DNA and its retention in the nucleus. *Mol Biol Cell*. 17:2451-2464.

Nigg, E.A. 1995. Cyclin-dependent protein kinases: key regulators of the eukaryotic cell cycle. *Bioessays*. 17:471-480.

Nigg, E.A. 1996. Cyclin-dependent kinase 7: at the cross-roads of transcription, DNA repair and cell cycle control? *Curr Opin Cell Biol*. 8:312-317.

Nigg, E.A. 2001. Mitotic kinases as regulators of cell division and its checkpoints. *Nat Rev Mol Cell Biol*. 2:21-32.

Nilsson, J. 2019. Protein phosphatases in the regulation of mitosis. *J Cell Biol*. 218:395-409.

Norbury, C., J. Blow, and P. Nurse. 1991. Regulatory phosphorylation of the p34cdc2 protein kinase in vertebrates. *EMBO J*. 10:3321-3329.

Norbury, C., and P. Nurse. 1992. Animal cell cycles and their control. *Annu Rev Biochem*. 61:441-470.

Nunez Villacis, L., M.S. Wong, L.L. Ferguson, N. Hein, et al. 2018. New Roles for the Nucleolus in Health and Disease. *Bioessays*. 40:e1700233.

Nurse, P. 1990. Universal control mechanism regulating onset of M-phase. *Nature*. 344:503-508.

Nurse, P., P. Thuriaux, and K. Nasmyth. 1976. Genetic control of the cell division cycle in the fission yeast Schizosaccharomyces pombe. *Mol Gen Genet*. 146:167-178.

O'Connell, M.J., M.J. Krien, and T. Hunter. 2003. Never say never. The NIMA-related protein kinases in mitotic control. *Trends Cell Biol*. 13:221-228.

O'Connell, M.J., J.M. Raleigh, H.M. Verkade, and P. Nurse. 1997. Chk1 is a wee1 kinase in the G2 DNA damage checkpoint inhibiting cdc2 by Y15 phosphorylation. *EMBO J*. 16:545-554.

Ogris, E., D.M. Gibson, and D.C. Pallas. 1997. Protein phosphatase 2A subunit assembly: the catalytic subunit carboxy terminus is important for binding cellular B subunit but not polyomavirus middle tumor antigen. *Oncogene*. 15:911-917.

Ohkura, H., I.M. Hagan, and D.M. Glover. 1995. The conserved Schizosaccharomyces pombe kinase plo1, required to form a bipolar spindle, the actin ring, and septum, can drive septum formation in G1 and G2 cells. *Genes Dev*. 9:1059-1073.

Ohtsubo, M., A.M. Theodoras, J. Schumacher, J.M. Roberts, et al. 1995. Human cyclin E, a nuclear protein essential for the G1-to-S phase transition. *Mol Cell Biol*. 15:2612-2624.

Okumura, E., A. Morita, M. Wakai, S. Mochida, et al. 2014. Cyclin B-Cdk1 inhibits protein phosphatase PP2A-B55 via a Greatwall kinase-independent mechanism. *J Cell Biol*. 204:881-889.

Olsen, J.V., and M. Mann. 2013. Status of large-scale analysis of post-translational modifications by mass spectrometry. *Mol Cell Proteomics*. 12:3444-3452.

Olsen, J.V., M. Vermeulen, A. Santamaria, C. Kumar, et al. 2010. Quantitative phosphoproteomics reveals widespread full phosphorylation site occupancy during mitosis. *Sci Signal*. 3:ra3.

Ong, S.E. 2012. The expanding field of SILAC. *Anal Bioanal Chem*. 404:967-976.

Ong, S.E., B. Blagoev, I. Kratchmarova, D.B. Kristensen, et al. 2002. Stable isotope labeling by amino acids in cell culture, SILAC, as a simple and accurate approach to expression proteomics. *Mol Cell Proteomics*. 1:376-386.

Orgad, S., N.D. Brewis, L. Alphey, J.M. Axton, et al. 1990. The structure of protein phosphatase 2A is as highly conserved as that of protein phosphatase 1. *FEBS Lett*. 275:44-48.

Orthwein, A., A. Fradet-Turcotte, S.M. Noordermeer, M.D. Canny, et al. 2014. Mitosis inhibits DNA double-strand break repair to guard against telomere fusions. *Science*. 344:189-193.

Ory, S., M. Zhou, T.P. Conrads, T.D. Veenstra, et al. 2003. Protein phosphatase 2A positively regulates Ras signaling by dephosphorylating KSR1 and Raf-1 on critical 14-3-3 binding sites. *Curr Biol*. 13:1356-1364.

Osmanagic-Myers, S., T. Dechat, and R. Foisner. 2015. Lamins at the crossroads of mechanosignaling. *Genes Dev*. 29:225-237.

Osmani, A.H., S.L. McGuire, and S.A. Osmani. 1991. Parallel activation of the NIMA and p34cdc2 cell cycle-regulated protein kinases is required to initiate mitosis in A. nidulans. *Cell*. 67:283-291.

Osmani, S.A., R.T. Pu, and N.R. Morris. 1988. Mitotic induction and maintenance by overexpression of a G2-specific gene that encodes a potential protein kinase. *Cell*. 53:237-244.

Paine, P.L., and C.M. Feldherr. 1972. Nucleocytoplasmic exchange of macromolecules. *Exp Cell Res*. 74:81-98.

Paine, P.L., L.C. Moore, and S.B. Horowitz. 1975. Nuclear envelope permeability. *Nature*. 254:109-114.

Pal, G., M.T. Paraz, and D.R. Kellogg. 2008. Regulation of Mih1/Cdc25 by protein phosphatase 2A and casein kinase 1. *J Cell Biol*. 180:931-945.

Palazzo, R.E., J.M. Vogel, B.J. Schnackenberg, D.R. Hull, et al. 2000. Centrosome maturation. *Curr Top Dev Biol*. 49:449-470.

Pardee, A.B. 1974. A restriction point for control of normal animal cell proliferation. *Proc Natl Acad Sci U S A*. 71:1286-1290.

Patel, J.T., A. Bottrill, S.L. Prosser, S. Jayaraman, et al. 2014. Mitotic phosphorylation of SUN1 loosens its connection with the nuclear lamina while the LINC complex remains intact. *Nucleus*. 5:462-473.

Patterson, D.J. 1999. The Diversity of Eukaryotes. *Am Nat*. 154:S96-S124.

Pavey, S., A. Pinder, W. Fernando, N. D'Arcy, et al. 2020. Multiple interaction nodes define the postreplication repair response to UV-induced DNA damage that is defective in melanomas and correlated with UV signature mutation load. *Mol Oncol*. 14:22-41.

Pavlova, G.A., A.V. Razuvaeva, J.V. Popova, E.N. Andreyeva, et al. 2019. The role of Patronin in Drosophila mitosis. *BMC Mol Cell Biol*. 20:7.

Paweletz, N. 2001. Walther Flemming: pioneer of mitosis research. *Nat Rev Mol Cell Biol*. 2:72-75.

Peng, A., T.M. Yamamoto, M.L. Goldberg, and J.L. Maller. 2010. A novel role for greatwall kinase in recovery from DNA damage. *Cell Cycle*. 9:4364-4369.

Pepling, M.E., M. de Cuevas, and A.C. Spradling. 1999. Germline cysts: a conserved phase of germ cell development? *Trends Cell Biol*. 9:257-262.

Peter, M., J. Nakagawa, M. Doree, J.C. Labbe, et al. 1990. In vitro disassembly of the nuclear lamina and M phase-specific phosphorylation of lamins by cdc2 kinase. *Cell*. 61:591-602.

Peters, J.M. 2006. The anaphase promoting complex/cyclosome: a machine designed to destroy. *Nat Rev Mol Cell Biol*. 7:644-656.

Peti, W., A.C. Nairn, and R. Page. 2013. Structural basis for protein phosphatase 1 regulation and specificity. *FEBS J*. 280:596-611.

Pettersen, E.F., T.D. Goddard, C.C. Huang, G.S. Couch, et al. 2004. UCSF Chimera--a visualization system for exploratory research and analysis. *J Comput Chem*. 25:1605-1612.

Pettersen, E.F., T.D. Goddard, C.C. Huang, E.C. Meng, et al. 2021. UCSF ChimeraX: Structure visualization for researchers, educators, and developers. *Protein Sci*. 30:70-82.

Pfleger, C.M., and M.W. Kirschner. 2000. The KEN box: an APC recognition signal distinct from the D box targeted by Cdh1. *Genes Dev*. 14:655-665.

Piekny, A., M. Werner, and M. Glotzer. 2005. Cytokinesis: welcome to the Rho zone. *Trends Cell Biol*. 15:651-658.

Pines, J., and T. Hunter. 1991. Human cyclins A and B1 are differentially located in the cell and undergo cell cycle-dependent nuclear transport. *J Cell Biol*. 115:1-17.

Pinsky, B.A., C. Kung, K.M. Shokat, and S. Biggins. 2006. The Ipl1-Aurora protein kinase activates the spindle checkpoint by creating unattached kinetochores. *Nat Cell Biol*. 8:78-83.

Pintard, L., and V. Archambault. 2018. A unified view of spatio-temporal control of mitotic entry: Polo kinase as the key. *Open Biol*. 8.

Polyak, K., M.H. Lee, H. Erdjument-Bromage, A. Koff, et al. 1994. Cloning of p27Kip1, a cyclin-dependent kinase inhibitor and a potential mediator of extracellular antimitogenic signals. *Cell*. 78:59-66.

Porter, I.M., K. Schleicher, M. Porter, and J.R. Swedlow. 2013. Bod1 regulates protein phosphatase 2A at mitotic kinetochores. *Nat Commun*. 4:2677.

Posch, M., G.A. Khoudoli, S. Swift, E.M. King, et al. 2010. Sds22 regulates aurora B activity and microtubule-kinetochore interactions at mitosis. *J Cell Biol*. 191:61-74.

Prescott, D.M., and M.A. Bender. 1962. Synthesis of RNA and protein during mitosis in mammalian tissue culture cells. *Exp Cell Res*. 26:260-268.

Primorac, I., and A. Musacchio. 2013. Panta rhei: the APC/C at steady state. *J Cell Biol*. 201:177-189.

Qi, H., U. Rath, Y. Ding, Y. Ji, et al. 2005. EAST interacts with Megator and localizes to the putative spindle matrix during mitosis in Drosophila. *J Cell Biochem*. 95:1284-1291.

Qi, H., U. Rath, D. Wang, Y.Z. Xu, et al. 2004. Megator, an essential coiled-coil protein that localizes to the putative spindle matrix during mitosis in Drosophila. *Mol Biol Cell*. 15:4854-4865.

Qian, J., M. Beullens, J. Huang, S. De Munter, et al. 2015. Cdk1 orders mitotic events through coordination of a chromosome-associated phosphatase switch. *Nat Commun*. 6:10215.

Qiao, R., F. Weissmann, M. Yamaguchi, N.G. Brown, et al. 2016. Mechanism of APC/CCDC20 activation by mitotic phosphorylation. *Proc Natl Acad Sci U S A*. 113:E2570-2578.

Rabinowitz, W. 1941. Studies of the cytology and early embryology of the egg of Drosophila melanogaster. *Journal of Morphology*. 69.

Radivojac, P., Z. Obradovic, D.K. Smith, G. Zhu, et al. 2004. Protein flexibility and intrinsic disorder. *Protein Sci*. 13:71-80.

Rainey, M.D., M.E. Charlton, R.V. Stanton, and M.B. Kastan. 2008. Transient inhibition of ATM kinase is sufficient to enhance cellular sensitivity to ionizing radiation. *Cancer Res*. 68:7466-7474.

Rangarajan, A., and R.A. Weinberg. 2003. Opinion: Comparative biology of mouse versus human cells: modelling human cancer in mice. *Nat Rev Cancer*. 3:952-959.

Rangone, H., E. Wegel, M.K. Gatt, E. Yeung, et al. 2011. Suppression of scant identifies Endos as a substrate of greatwall kinase and a negative regulator of protein phosphatase 2A in mitosis. *PLoS Genet*. 7:e1002225.

Rath, U., D. Wang, Y. Ding, Y.Z. Xu, et al. 2004. Chromator, a novel and essential chromodomain protein interacts directly with the putative spindle matrix protein skeletor. *J Cell Biochem*. 93:1033-1047.

Rattner, J.B., and S.G. Phillips. 1973. Independence of centriole formation and DNA synthesis. *J Cell Biol*. 57:359-372.

Reed, S.I., J.A. Hadwiger, and A.T. Lorincz. 1985. Protein kinase activity associated with the product of the yeast cell division cycle gene CDC28. *Proc Natl Acad Sci U S A*. 82:4055-4059.

Reinhardt, H.C., A.S. Aslanian, J.A. Lees, and M.B. Yaffe. 2007. p53-deficient cells rely on ATM- and ATR-mediated checkpoint signaling through the p38MAPK/MK2 pathway for survival after DNA damage. *Cancer Cell*. 11:175-189.

Reinhardt, H.C., and M.B. Yaffe. 2013. Phospho-Ser/Thr-binding domains: navigating the cell cycle and DNA damage response. *Nat Rev Mol Cell Biol*. 14:563-580.

Reiter, L.T., and E. Bier. 2002. Using Drosophila melanogaster to uncover human disease gene function and potential drug target proteins. *Expert Opin Ther Targets*. 6:387-399.

Ren, D., L.A. Fisher, J. Zhao, L. Wang, et al. 2017. Cell cycle-dependent regulation of Greatwall kinase by protein phosphatase 1 and regulatory subunit 3B. *J Biol Chem*. 292:10026-10034.

Resnitzky, D., and S.I. Reed. 1995. Different roles for cyclins D1 and E in regulation of the G1-to-S transition. *Mol Cell Biol*. 15:3463-3469.

Ribbeck, K., and D. Gorlich. 2001. Kinetic analysis of translocation through nuclear pore complexes. *EMBO J*. 20:1320-1330.

Ribeiro, P.S., F. Josue, A. Wepf, M.C. Wehr, et al. 2010. Combined functional genomic and proteomic approaches identify a PP2A complex as a negative regulator of Hippo signaling. *Mol Cell*. 39:521-534.

Rieder, C.L., and A. Khodjakov. 2003. Mitosis through the microscope: advances in seeing inside live dividing cells. *Science*. 300:91-96.

Robbins, E., G. Jentzsch, and A. Micali. 1968. The centriole cycle in synchronized HeLa cells. *J Cell Biol*. 36:329-339.

Robinson, D.N., and L. Cooley. 1996. Stable intercellular bridges in development: the cytoskeleton lining the tunnel. *Trends Cell Biol*. 6:474-479.

Robinson, D.N., and L. Cooley. 1997. Genetic analysis of the actin cytoskeleton in the Drosophila ovary. *Annu Rev Cell Dev Biol*. 13:147-170.

Rogakou, E.P., D.R. Pilch, A.H. Orr, V.S. Ivanova, et al. 1998. DNA double-stranded breaks induce histone H2AX phosphorylation on serine 139. *J Biol Chem*. 273:5858-5868.

Rogers, S., D. Fey, R.A. McCloy, B.L. Parker, et al. 2016a. PP1 initiates the dephosphorylation of MASTL, triggering mitotic exit and bistability in human cells. *J Cell Sci*. 129:1340-1354.

Rogers, S., R. McCloy, D.N. Watkins, and A. Burgess. 2016b. Mechanisms regulating phosphatase specificity and the removal of individual phosphorylation sites during mitotic exit. *Bioessays*. 38 Suppl 1:S24-32.

Rogers, S., R.A. McCloy, B.L. Parker, D. Gallego-Ortega, et al. 2018. MASTL overexpression promotes chromosome instability and metastasis in breast cancer. *Oncogene*. 37:4518-4533.

Roshak, A.K., E.A. Capper, C. Imburgia, J. Fornwald, et al. 2000. The human polo-like kinase, PLK, regulates cdc2/cyclin B through phosphorylation and activation of the cdc25C phosphatase. *Cell Signal*. 12:405-411.

Russell, P., and P. Nurse. 1987. Negative regulation of mitosis by wee1+, a gene encoding a protein kinase homolog. *Cell*. 49:559-567.

Ruvolo, P.P. 2016. The broken "Off" switch in cancer signaling: PP2A as a regulator of tumorigenesis, drug resistance, and immune surveillance. *BBA Clin*. 6:87-99.

Ruvolo, P.P., Y.H. Qui, K.R. Coombes, N. Zhang, et al. 2011. Low expression of PP2A regulatory subunit B55alpha is associated with T308 phosphorylation of AKT and shorter complete remission duration in acute myeloid leukemia patients. *Leukemia*. 25:1711-1717.

Sackton, K.L., J.M. Lopez, C.L. Berman, and M.F. Wolfner. 2009. YA is needed for proper nuclear organization to transition between meiosis and mitosis in Drosophila. *BMC Dev Biol*. 9:43.

Salimian, K.J., E.R. Ballister, E.M. Smoak, S. Wood, et al. 2011. Feedback control in sensing chromosome biorientation by the Aurora B kinase. *Curr Biol*. 21:1158-1165.

Samson, C., F. Celli, K. Hendriks, M. Zinke, et al. 2017. Emerin self-assembly mechanism: role of the LEM domain. *FEBS J*. 284:338-352.

Samson, C., A. Petitalot, F. Celli, I. Herrada, et al. 2018. Structural analysis of the ternary complex between lamin A/C, BAF and emerin identifies an interface disrupted in autosomal recessive progeroid diseases. *Nucleic Acids Res*. 46:10460-10473.

Samwer, M., M.W.G. Schneider, R. Hoefler, P.S. Schmalhorst, et al. 2017. DNA Cross-Bridging Shapes a Single Nucleus from a Set of Mitotic Chromosomes. *Cell*. 170:956-972 e923.

Sanchez, I., and B.D. Dynlacht. 1996. Transcriptional control of the cell cycle. *Curr Opin Cell Biol*. 8:318-324.

Santamaria, D., C. Barriere, A. Cerqueira, S. Hunt, et al. 2007. Cdk1 is sufficient to drive the mammalian cell cycle. *Nature*. 448:811-815.

Santos, S.D., R. Wollman, T. Meyer, and J.E. Ferrell, Jr. 2012. Spatial positive feedback at the onset of mitosis. *Cell*. 149:1500-1513.

Sap, K.A., K. Bezstarosti, D.H. Dekkers, M. van den Hout, et al. 2015. Global quantitative proteomics reveals novel factors in the ecdysone signaling pathway in Drosophila melanogaster. *Proteomics*. 15:725-738.

Saxton, W.M., D.L. Stemple, R.J. Leslie, E.D. Salmon, et al. 1984. Tubulin dynamics in cultured mammalian cells. *J Cell Biol*. 99:2175-2186.

Schellhaus, A.K., P. De Magistris, and W. Antonin. 2016. Nuclear Reformation at the End of Mitosis. *J Mol Biol*. 428:1962-1985.

Schirmer, E.C., and L. Gerace. 2005. The nuclear membrane proteome: extending the envelope. *Trends Biochem Sci*. 30:551-558.

Schmidt, H.B., and D. Gorlich. 2015. Nup98 FG domains from diverse species spontaneously phase-separate into particles with nuclear pore-like permselectivity. *Elife*. 4.

Schmit, T.L., and N. Ahmad. 2007. Regulation of mitosis via mitotic kinases: new opportunities for cancer management. *Mol Cancer Ther*. 6:1920-1931.

Schmitz, M.H., M. Held, V. Janssens, J.R. Hutchins, et al. 2010. Live-cell imaging RNAi screen identifies PP2A-B55alpha and importin-beta1 as key mitotic exit regulators in human cells. *Nat Cell Biol*. 12:886-893.

Schneider, A. 1873. Untersuchungen über Plathelminthen. *Jahrb. Oberhess. Ges. Naturwiss. Heilk.*:69–81.

Schneider, I. 1972. Cell lines derived from late embryonic stages of Drosophila melanogaster. *J Embryol Exp Morphol*. 27:353-365.

Schober, F.A., I. Atanassov, D. Moore, J. Calvo-Garrido, et al. 2021. Stable Isotope Labeling of Amino Acids in Flies (SILAF) Reveals Differential Phosphorylation of Mitochondrial Proteins Upon Loss of OXPHOS Subunits. *Mol Cell Proteomics*. 20:100065.

Schumacher, J.M., A. Golden, and P.J. Donovan. 1998. AIR-2: An Aurora/Ipl1-related protein kinase associated with chromosomes and midbody microtubules is required for polar body extrusion and cytokinesis in Caenorhabditis elegans embryos. *J Cell Biol*. 143:1635-1646.

Schwager, S.C., P.V. Taufalele, and C.A. Reinhart-King. 2019. Cell-Cell Mechanical Communication in Cancer. *Cell Mol Bioeng*. 12:1-14.

Schweizer, N., M. Weiss, and H. Maiato. 2014. The dynamic spindle matrix. *Curr Opin Cell Biol*. 28:1-7.

Seki, A., J.A. Coppinger, C.Y. Jang, J.R. Yates, et al. 2008. Bora and the kinase Aurora a cooperatively activate the kinase Plk1 and control mitotic entry. *Science*. 320:1655-1658.

Sen, S., H. Zhou, and R.A. White. 1997. A putative serine/threonine kinase encoding gene BTAK on chromosome 20q13 is amplified and overexpressed in human breast cancer cell lines. *Oncogene*. 14:2195-2200.

Seshacharyulu, P., P. Pandey, K. Datta, and S.K. Batra. 2013. Phosphatase: PP2A structural importance, regulation and its aberrant expression in cancer. *Cancer Lett*. 335:9-18.

Shaltiel, I.A., L. Krenning, W. Bruinsma, and R.H. Medema. 2015. The same, only different - DNA damage checkpoints and their reversal throughout the cell cycle. *J Cell Sci*. 128:607-620.

Shao, H., Y. Huang, L. Zhang, K. Yuan, et al. 2015. Spatiotemporal dynamics of Aurora B-PLK1-MCAK signaling axis orchestrates kinetochore bi-orientation and faithful chromosome segregation. *Sci Rep*. 5:12204.

Sharma, K., R.C. D'Souza, S. Tyanova, C. Schaab, et al. 2014. Ultradeep human phosphoproteome reveals a distinct regulatory nature of Tyr and Ser/Thr-based signaling. *Cell Rep*. 8:1583-1594.

Sharp, D.J., G.C. Rogers, and J.M. Scholey. 2000. Cytoplasmic dynein is required for poleward chromosome movement during mitosis in Drosophila embryos. *Nat Cell Biol*. 2:922-930.

Shav-Tal, Y., J. Blechman, X. Darzacq, C. Montagna, et al. 2005. Dynamic sorting of nuclear components into distinct nucleolar caps during transcriptional inhibition. *Mol Biol Cell*. 16:2395-2413.

Sherr, C.J. 1994. G1 phase progression: cycling on cue. *Cell*. 79:551-555.

Sherr, C.J. 1996. Cancer cell cycles. *Science*. 274:1672-1677.

Sherr, C.J., and J.M. Roberts. 1995. Inhibitors of mammalian G1 cyclin-dependent kinases. *Genes Dev*. 9:1149-1163.

Shibata, A., O. Barton, A.T. Noon, K. Dahm, et al. 2010. Role of ATM and the damage response mediator proteins 53BP1 and MDC1 in the maintenance of G(2)/M checkpoint arrest. *Mol Cell Biol*. 30:3371-3383.

Shin, J.Y., I. Mendez-Lopez, Y. Wang, A.P. Hays, et al. 2013. Lamina-associated polypeptide-1 interacts with the muscular dystrophy protein emerin and is essential for skeletal muscle maintenance. *Dev Cell*. 26:591-603.

Shin, Y., and C.P. Brangwynne. 2017. Liquid phase condensation in cell physiology and disease. *Science*. 357.

Shouse, G., R. de Necochea-Campion, S. Mirshahidi, X. Liu, et al. 2016. Novel B55alpha-PP2A mutations in AML promote AKT T308 phosphorylation and sensitivity to AKT inhibitor-induced growth arrest. *Oncotarget*. 7:61081-61092.

Shumaker, D.K., K.K. Lee, Y.C. Tanhehco, R. Craigie, et al. 2001. LAP2 binds to BAF.DNA complexes: requirement for the LEM domain and modulation by variable regions. *EMBO J*. 20:1754-1764.

Siliciano, J.D., C.E. Canman, Y. Taya, K. Sakaguchi, et al. 1997. DNA damage induces phosphorylation of the amino terminus of p53. *Genes Dev*. 11:3471-3481.

Simanis, V., and P. Nurse. 1986. The cell cycle control gene cdc2+ of fission yeast encodes a protein kinase potentially regulated by phosphorylation. *Cell*. 45:261-268.

Sivan, G., N. Kedersha, and O. Elroy-Stein. 2007. Ribosomal slowdown mediates translational arrest during cellular division. *Mol Cell Biol*. 27:6639-6646.

Skoczylas, C., K.M. Fahrbach, and K. Rundell. 2004. Cellular targets of the SV40 small-t antigen in human cell transformation. *Cell Cycle*. 3:606-610.

Skoufias, D.A., R.L. Indorato, F. Lacroix, A. Panopoulos, et al. 2007. Mitosis persists in the absence of Cdk1 activity when proteolysis or protein phosphatase activity is suppressed. *J Cell Biol*. 179:671-685.

Snaith, H.A., C.G. Armstrong, Y. Guo, K. Kaiser, et al. 1996. Deficiency of protein phosphatase 2A uncouples the nuclear and centrosome cycles and prevents attachment of microtubules to the kinetochore in Drosophila microtubule star (mts) embryos. *J Cell Sci*. 109 (Pt 13):3001-3012.

Solomon, M.J., M. Glotzer, T.H. Lee, M. Philippe, et al. 1990. Cyclin activation of p34cdc2. *Cell*. 63:1013-1024.

Song, H., J. Pan, Y. Liu, H. Wen, et al. 2014. Increased ARPP-19 expression is associated with hepatocellular carcinoma. *Int J Mol Sci*. 16:178-192.

Songyang, Z., S. Blechner, N. Hoagland, M.F. Hoekstra, et al. 1994. Use of an oriented peptide library to determine the optimal substrates of protein kinases. *Curr Biol*. 4:973-982.

Sonn, S., Y. Jeong, and K. Rhee. 2009. Nip2/centrobin may be a substrate of Nek2 that is required for proper spindle assembly during mitosis in early mouse embryos. *Mol Reprod Dev*. 76:587-592.

Sorensen, C.S., C. Lukas, E.R. Kramer, J.M. Peters, et al. 2001. A conserved cyclin-binding domain determines functional interplay between anaphase-promoting complex-Cdh1 and cyclin A-Cdk2 during cell cycle progression. *Mol Cell Biol*. 21:3692-3703.

Sosa, B.A., U. Kutay, and T.U. Schwartz. 2013. Structural insights into LINC complexes. *Curr Opin Struct Biol*. 23:285-291.

Starr, D.A., and M. Han. 2002. Role of ANC-1 in tethering nuclei to the actin cytoskeleton. *Science*. 298:406-409.

Steen, R.L., M. Beullens, H.B. Landsverk, M. Bollen, et al. 2003. AKAP149 is a novel PP1 specifier required to maintain nuclear envelope integrity in G1 phase. *J Cell Sci*. 116:2237-2246.

Stegmeier, F., and A. Amon. 2004. Closing mitosis: the functions of the Cdc14 phosphatase and its regulation. *Annu Rev Genet*. 38:203-232.

Stewart, G.S., B. Wang, C.R. Bignell, A.M. Taylor, et al. 2003. MDC1 is a mediator of the mammalian DNA damage checkpoint. *Nature*. 421:961-966.

Stone, S.R., J. Hofsteenge, and B.A. Hemmings. 1987. Molecular cloning of cDNAs encoding two isoforms of the catalytic subunit of protein phosphatase 2A. *Biochemistry*. 26:7215-7220.

Strack, S., D. Chang, J.A. Zaucha, R.J. Colbran, et al. 1999. Cloning and characterization of B delta, a novel regulatory subunit of protein phosphatase 2A. *FEBS Lett*. 460:462-466.

Strack, S., J.A. Zaucha, F.F. Ebner, R.J. Colbran, et al. 1998. Brain protein phosphatase 2A: developmental regulation and distinct cellular and subcellular localization by B subunits. *J Comp Neurol*. 392:515-527.

Strausfeld, U., J.C. Labbe, D. Fesquet, J.C. Cavadore, et al. 1991. Dephosphorylation and activation of a p34cdc2/cyclin B complex in vitro by human CDC25 protein. *Nature*. 351:242-245.

Stucki, M., J.A. Clapperton, D. Mohammad, M.B. Yaffe, et al. 2005. MDC1 directly binds phosphorylated histone H2AX to regulate cellular responses to DNA double-strand breaks. *Cell*. 123:1213-1226.

Sudakin, V., G.K. Chan, and T.J. Yen. 2001. Checkpoint inhibition of the APC/C in HeLa cells is mediated by a complex of BUBR1, BUB3, CDC20, and MAD2. *J Cell Biol*. 154:925-936.

Sudakin, V., D. Ganoth, A. Dahan, H. Heller, et al. 1995. The cyclosome, a large complex containing cyclin-selective ubiquitin ligase activity, targets cyclins for destruction at the end of mitosis. *Mol Biol Cell*. 6:185-197.

Suijkerbuijk, S.J., M. Vleugel, A. Teixeira, and G.J. Kops. 2012. Integration of kinase and phosphatase activities by BUBR1 ensures formation of stable kinetochore-microtubule attachments. *Dev Cell*. 23:745-755.

Sullivan, M., and D.O. Morgan. 2007. Finishing mitosis, one step at a time. *Nat Rev Mol Cell Biol*. 8:894-903.

Sun, X.J., Y.L. Li, L.G. Wang, L.Q. Liu, et al. 2017. Mastl overexpression is associated with epithelial to mesenchymal transition and predicts a poor clinical outcome in gastric cancer. *Oncol Lett*. 14:7283-7287.

Sunkel, C.E., and D.M. Glover. 1988. polo, a mitotic mutant of Drosophila displaying abnormal spindle poles. *J Cell Sci*. 89 (Pt 1):25-38.

Switzer, C.H., R.Y. Cheng, T.M. Vitek, D.J. Christensen, et al. 2011. Targeting SET/I(2)PP2A oncoprotein functions as a multi-pathway strategy for cancer therapy. *Oncogene*. 30:2504-2513.

Tachibana, K., P. Scheuer, Y. Tsukitani, H. Kikuchi, et al. 1981. Okadaic acid, a cytotoxic polyether from two marine sponges of the genus

Halichondria. *J Am Chem Soc*. 103:2469–2471.

Takai, A., C. Bialojan, M. Troschka, and J.C. Ruegg. 1987. Smooth muscle myosin phosphatase inhibition and force enhancement by black sponge toxin. *FEBS Lett*. 217:81-84.

Takai, A., and G. Mieskes. 1991. Inhibitory effect of okadaic acid on the p-nitrophenyl phosphate phosphatase activity of protein phosphatases. *Biochem J*. 275 (Pt 1):233-239.

Takai, A., M. Murata, K. Torigoe, M. Isobe, et al. 1992. Inhibitory effect of okadaic acid derivatives on protein phosphatases. A study on structure-affinity relationship. *Biochem J*. 284 (Pt 2):539-544.

Takai, H., K. Tominaga, N. Motoyama, Y.A. Minamishima, et al. 2000. Aberrant cell cycle checkpoint function and early embryonic death in Chk1(-/-) mice. *Genes Dev*. 14:1439-1447.

Talarek, N., E. Cameroni, M. Jaquenoud, X. Luo, et al. 2010. Initiation of the TORC1-regulated G0 program requires Igo1/2, which license specific mRNAs to evade degradation via the 5'-3' mRNA decay pathway. *Mol Cell*. 38:345-355.

Tanaka, K., E. Kitamura, Y. Kitamura, and T.U. Tanaka. 2007. Molecular mechanisms of microtubule-dependent kinetochore transport toward spindle poles. *J Cell Biol*. 178:269-281.

Tanenbaum, M.E., N. Stern-Ginossar, J.S. Weissman, and R.D. Vale. 2015. Regulation of mRNA translation during mitosis. *Elife*. 4.

Taylor, J.H. 1960. Nucleic acid synthesis in relation to the cell division cycle. *Ann N Y Acad Sci*. 90:409-421.

Teo, G., G. Liu, J. Zhang, A.I. Nesvizhskii, et al. 2014. SAINTexpress: improvements and additional features in Significance Analysis of INTeractome software. *J Proteomics*. 100:37-43.

Terasawa, M., A. Shinohara, and M. Shinohara. 2014. Canonical non-homologous end joining in mitosis induces genome instability and is suppressed by M-phase-specific phosphorylation of XRCC4. *PLoS Genet*. 10:e1004563.

Terrak, M., F. Kerff, K. Langsetmo, T. Tao, et al. 2004. Structural basis of protein phosphatase 1 regulation. *Nature*. 429:780-784.

Thapa, C., P. Roivas, T. Haataja, P. Permi, et al. 2021. The Interaction Mechanism of Intrinsically Disordered PP2A Inhibitor Proteins ARPP-16 and ARPP-19 With PP2A. *Front Mol Biosci*. 8:650881.

Theillet, F.X., A. Binolfi, T. Frembgen-Kesner, K. Hingorani, et al. 2014. Physicochemical properties of cells and their effects on intrinsically disordered proteins (IDPs). *Chem Rev*. 114:6661-6714.

Thompson, S.L., and D.A. Compton. 2011. Chromosome missegregation in human cells arises through specific types of kinetochore-microtubule attachment errors. *Proc Natl Acad Sci U S A*. 108:17974-17978.

Tian, J., Y. Lin, and J. Yu. 2017. E2F8 confers cisplatin resistance to ER+ breast cancer cells via transcriptionally activating MASTL. *Biomed Pharmacother*. 92:919-926.

Tiku, V., and A. Antebi. 2018. Nucleolar Function in Lifespan Regulation. *Trends Cell Biol*. 28:662-672.

Tolstykh, T., J. Lee, S. Vafai, and J.B. Stock. 2000. Carboxyl methylation regulates phosphoprotein phosphatase 2A by controlling the association of regulatory B subunits. *EMBO J*. 19:5682-5691.

Torres, J.Z., K.H. Ban, and P.K. Jackson. 2010. A specific form of phospho protein phosphatase 2 regulates anaphase-promoting complex/cyclosome association with spindle poles. *Mol Biol Cell*. 21:897-904.

Torvaldson, E., V. Kochin, and J.E. Eriksson. 2015. Phosphorylation of lamins determine their structural properties and signaling functions. *Nucleus*. 6:166-171.

Touati, S.A., M. Kataria, A.W. Jones, A.P. Snijders, et al. 2018. Phosphoproteome dynamics during mitotic exit in budding yeast. *EMBO J*. 37.

Toyoshima-Morimoto, F., E. Taniguchi, N. Shinya, A. Iwamatsu, et al. 2001. Polo-like kinase 1 phosphorylates cyclin B1 and targets it to the nucleus during prophase. *Nature*. 410:215-220.

Trinkle-Mulcahy, L., and A.I. Lamond. 2006. Mitotic phosphatases: no longer silent partners. *Curr Opin Cell Biol*. 18:623-631.

Tseng, L.C., and R.H. Chen. 2011. Temporal control of nuclear envelope assembly by phosphorylation of lamin B receptor. *Mol Biol Cell*. 22:3306-3317.

Uemura, T., K. Shiomi, S. Togashi, and M. Takeichi. 1993. Mutation of twins encoding a regulator of protein phosphatase 2A leads to pattern duplication in Drosophila imaginal discs. *Genes Dev*. 7:429-440.

Uhlmann, F. 2001. Chromosome cohesion and segregation in mitosis and meiosis. *Curr Opin Cell Biol*. 13:754-761.

Uhlmann, F., F. Lottspeich, and K. Nasmyth. 1999. Sister-chromatid separation at anaphase onset is promoted by cleavage of the cohesin subunit Scc1. *Nature*. 400:37-42.

Ungricht, R., M. Klann, P. Horvath, and U. Kutay. 2015. Diffusion and retention are major determinants of protein targeting to the inner nuclear membrane. *J Cell Biol*. 209:687-703.

Unnikannan, C.P., A. Reuveny, D. Grunberg, and T. Volk. 2020. Recruitment of BAF to the nuclear envelope couples the LINC complex to endoreplication. *Development*. 147.

Uppada, S.B., S. Gowrikumar, R. Ahmad, B. Kumar, et al. 2018. MASTL induces Colon Cancer progression and Chemoresistance by promoting Wnt/beta-catenin signaling. *Mol Cancer*. 17:111.

Uversky, V.N., J.R. Gillespie, and A.L. Fink. 2000. Why are "natively unfolded" proteins unstructured under physiologic conditions? *Proteins*. 41:415-427.

Vagnarelli, P. 2021. Back to the new beginning: Mitotic exit in space and time. *Semin Cell Dev Biol*.

van der Horst, A., and S.M. Lens. 2014. Cell division: control of the chromosomal passenger complex in time and space. *Chromosoma*. 123:25-42.

Van Hoof, C., F. Ingels, X. Cayla, I. Stevens, et al. 1995. Molecular cloning and developmental regulation of expression of two isoforms of the catalytic subunit of protein phosphatase 2A from Xenopus laevis. *Biochem Biophys Res Commun*. 215:666-673.

van Vugt, M.A., A.K. Gardino, R. Linding, G.J. Ostheimer, et al. 2010. A mitotic phosphorylation feedback network connects Cdk1, Plk1, 53BP1, and Chk2 to inactivate the G(2)/M DNA damage checkpoint. *PLoS Biol*. 8:e1000287.

Vandre, D.D., F.M. Davis, P.N. Rao, and G.G. Borisy. 1986. Distribution of cytoskeletal proteins sharing a conserved phosphorylated epitope. *Eur J Cell Biol*. 41:72-81.

Vera, J., L. Lartigue, S. Vigneron, G. Gadea, et al. 2015. Greatwall promotes cell transformation by hyperactivating AKT in human malignancies. *Elife*. 4.

Vigneron, S., E. Brioudes, A. Burgess, J.C. Labbe, et al. 2009. Greatwall maintains mitosis through regulation of PP2A. *Embo J*. 28:2786-2793.

Vigneron, S., A. Gharbi-Ayachi, A.A. Raymond, A. Burgess, et al. 2011. Characterization of the mechanisms controlling Greatwall activity. *Mol Cell Biol*. 31:2262-2275.

Viquez, N.M., C.R. Li, Y.P. Wairkar, and A. DiAntonio. 2006. The B' protein phosphatase 2A regulatory subunit well-rounded regulates synaptic growth and cytoskeletal stability at the Drosophila neuromuscular junction. *J Neurosci*. 26:9293-9303.

Virshup, D.M., and S. Shenolikar. 2009. From promiscuity to precision: protein phosphatases get a makeover. *Mol Cell*. 33:537-545.

Visconti, R., L. Palazzo, R. Della Monica, and D. Grieco. 2012. Fcp1-dependent dephosphorylation is required for M-phase-promoting factor inactivation at mitosis exit. *Nat Commun*. 3:894.

Visintin, R., K. Craig, E.S. Hwang, S. Prinz, et al. 1998. The phosphatase Cdc14 triggers mitotic exit by reversal of Cdk-dependent phosphorylation. *Mol Cell*. 2:709-718.

Visintin, R., S. Prinz, and A. Amon. 1997. CDC20 and CDH1: a family of substrate-specific activators of APC-dependent proteolysis. *Science*. 278:460-463.

Voets, E., and R.M. Wolthuis. 2010. MASTL is the human orthologue of Greatwall kinase that facilitates mitotic entry, anaphase and cytokinesis. *Cell Cycle*. 9:3591-3601.

Von Stetina, J.R., S. Tranguch, S.K. Dey, L.A. Lee, et al. 2008. alpha-Endosulfine is a conserved protein required for oocyte meiotic maturation in Drosophila. *Development*. 135:3697-3706.

Vorobjev, I.A., and S. Chentsov Yu. 1982. Centrioles in the cell cycle. I. Epithelial cells. *J Cell Biol*. 93:938-949.

Walczak, C.E., and S.L. Shaw. 2010. A MAP for bundling microtubules. *Cell*. 142:364-367.

Walker, D.H., and J.L. Maller. 1991. Role for cyclin A in the dependence of mitosis on completion of DNA replication. *Nature*. 354:314-317.

Walker, D.L., D. Wang, Y. Jin, U. Rath, et al. 2000. Skeletor, a novel chromosomal protein that redistributes during mitosis provides evidence for the formation of a spindle matrix. *J Cell Biol*. 151:1401-1412.

Wall, M.A., D.E. Coleman, E. Lee, J.A. Iniguez-Lluhi, et al. 1995. The structure of the G protein heterotrimer Gi alpha 1 beta 1 gamma 2. *Cell*. 83:1047-1058.

Walter, G., F. Ferre, O. Espiritu, and A. Carbone-Wiley. 1989. Molecular cloning and sequence of cDNA encoding polyoma medium tumor antigen-associated 61-kDa protein. *Proc Natl Acad Sci U S A*. 86:8669-8672.

Wang, L., V.Q. Luong, P.J. Giannini, and A. Peng. 2014a. Mastl kinase, a promising therapeutic target, promotes cancer recurrence. *Oncotarget*. 5:11479-11489.

Wang, P., J.A. Galan, K. Normandin, E. Bonneil, et al. 2013. Cell cycle regulation of Greatwall kinase nuclear localization facilitates mitotic progression. *J Cell Biol*. 202:277-293.

Wang, P., M. Larouche, K. Normandin, D. Kachaner, et al. 2016. Spatial regulation of greatwall by Cdk1 and PP2A-Tws in the cell cycle. *Cell Cycle*. 15:528-539.

Wang, P., M. Malumbres, and V. Archambault. 2014b. The Greatwall-PP2A axis in cell cycle control. *Methods Mol Biol*. 1170:99-111.

Wang, P., X. Pinson, and V. Archambault. 2011. PP2A-twins is antagonized by greatwall and collaborates with polo for cell cycle progression and centrosome attachment to nuclei in drosophila embryos. *PLoS Genet*. 7:e1002227.

Wang, S., W. Xie, D. Wang, Z. Peng, et al. 2015. Discovery of a small molecule targeting SET-PP2A interaction to overcome BCR-ABLT315I mutation of chronic myeloid leukemia. *Oncotarget*. 6:12128-12140.

Wang, W., C. Cronmiller, and D.L. Brautigan. 2008a. Maternal phosphatase inhibitor-2 is required for proper chromosome segregation and mitotic synchrony during Drosophila embryogenesis. *Genetics*. 179:1823-1833.

Wang, W., P.T. Stukenberg, and D.L. Brautigan. 2008b. Phosphatase inhibitor-2 balances protein phosphatase 1 and aurora B kinase for chromosome segregation and cytokinesis in human retinal epithelial cells. *Mol Biol Cell*. 19:4852-4862.

Wanke, V., I. Pedruzzi, E. Cameroni, F. Dubouloz, et al. 2005. Regulation of G0 entry by the Pho80-Pho85 cyclin-CDK complex. *EMBO J*. 24:4271-4278.

Watanabe, N., M. Broome, and T. Hunter. 1995. Regulation of the human WEE1Hu CDK tyrosine 15-kinase during the cell cycle. *EMBO J*. 14:1878-1891.

Wei, H., D.G. Ashby, C.S. Moreno, E. Ogris, et al. 2001. Carboxymethylation of the PP2A catalytic subunit in Saccharomyces cerevisiae is required for efficient interaction with the B-type subunits Cdc55p and Rts1p. *J Biol Chem*. 276:1570-1577.

Wei, R., B. Ngo, G. Wu, and W.H. Lee. 2011. Phosphorylation of the Ndc80 complex protein, HEC1, by Nek2 kinase modulates chromosome alignment and signaling of the spindle assembly checkpoint. *Mol Biol Cell*. 22:3584-3594.

Wente, S.R., and M.P. Rout. 2010. The nuclear pore complex and nuclear transport. *Cold Spring Harb Perspect Biol*. 2:a000562.

West, M., N. Zurek, A. Hoenger, and G.K. Voeltz. 2011. A 3D analysis of yeast ER structure reveals how ER domains are organized by membrane curvature. *J Cell Biol*. 193:333-346.

Wheatley, S.P., and Y. Wang. 1996. Midzone microtubule bundles are continuously required for cytokinesis in cultured epithelial cells. *J Cell Biol*. 135:981-989.

White-Cooper, H., M. Carmena, C. Gonzalez, and D.M. Glover. 1996. Mutations in new cell cycle genes that fail to complement a multiply mutant third chromosome of Drosophila. *Genetics*. 144:1097-1111.

Williams, B.C., J.J. Filter, K.A. Blake-Hodek, B.E. Wadzinski, et al. 2014. Greatwall-phosphorylated Endosulfine is both an inhibitor and a substrate of PP2A-B55 heterotrimers. *Elife*. 3:e01695.

Wilson, E.B. 1925. The cell in development and heredity. The MacMillan Co., New York.

Wlodarchak, N., and Y. Xing. 2016. PP2A as a master regulator of the cell cycle. *Crit Rev Biochem Mol Biol*. 51:162-184.

Wolf, F., R. Sigl, and S. Geley. 2007. '... The end of the beginning': cdk1 thresholds and exit from mitosis. *Cell Cycle*. 6:1408-1411.

Wolf, F., C. Wandke, N. Isenberg, and S. Geley. 2006. Dose-dependent effects of stable cyclin B1 on progression through mitosis in human cells. *EMBO J*. 25:2802-2813.

Wolff, N., B. Gilquin, K. Courchay, I. Callebaut, et al. 2001. Structural analysis of emerin, an inner nuclear membrane protein mutated in X-linked Emery-Dreifuss muscular dystrophy. *FEBS Lett*. 501:171-176.

Wolfner, M. 2002. Nuclear Envelope Dynamics in Drosophila Pronuclear Formation and in Embryos. Kluwer Academic/Plenum Publishers.

Wong, P.Y., H.T. Ma, H.J. Lee, and R.Y. Poon. 2016. MASTL(Greatwall) regulates DNA damage responses by coordinating mitotic entry after checkpoint recovery and APC/C activation. *Sci Rep*. 6:22230.

Woodruff, J.B. 2018. Assembly of Mitotic Structures through Phase Separation. *J Mol Biol*. 430:4762-4772.

Wright, P.E., and H.J. Dyson. 1999. Intrinsically unstructured proteins: re-assessing the protein structure-function paradigm. *J Mol Biol*. 293:321-331.

Wu, J., T. Tolstykh, J. Lee, K. Boyd, et al. 2000. Carboxyl methylation of the phosphoprotein phosphatase 2A catalytic subunit promotes its functional association with regulatory subunits in vivo. *EMBO J*. 19:5672-5681.

Wu, J.Q., J.Y. Guo, W. Tang, C.S. Yang, et al. 2009. PP1-mediated dephosphorylation of phosphoproteins at mitotic exit is controlled by inhibitor-1 and PP1 phosphorylation. *Nat Cell Biol*. 11:644-651.

Wurzenberger, C., and D.W. Gerlich. 2011. Phosphatases: providing safe passage through mitotic exit. *Nat Rev Mol Cell Biol*. 12:469-482.

Xie, F., G. Xie, and Q. Sun. 2020. Long Noncoding RNA DLX6-AS1 Promotes the Progression in Cervical Cancer by Targeting miR-16-5p/ARPP19 Axis. *Cancer Biother Radiopharm*. 35:129-136.

Xie, H., and S. Clarke. 1993. Methyl esterification of C-terminal leucine residues in cytosolic 36-kDa polypeptides of bovine brain. A novel eucaryotic protein carboxyl methylation reaction. *J Biol Chem*. 268:13364-13371.

Xie, H., and S. Clarke. 1994. Protein phosphatase 2A is reversibly modified by methyl esterification at its C-terminal leucine residue in bovine brain. *J Biol Chem*. 269:1981-1984.

Xing, Y., Y. Xu, Y. Chen, P.D. Jeffrey, et al. 2006. Structure of protein phosphatase 2A core enzyme bound to tumor-inducing toxins. *Cell*. 127:341-353.

Xu, N., S. Libertini, E.J. Black, Y. Lao, et al. 2012. Cdk-mediated phosphorylation of Chk1 is required for efficient activation and full checkpoint proficiency in response to DNA damage. *Oncogene*. 31:1086-1094.

Xu, Y., Y. Chen, P. Zhang, P.D. Jeffrey, et al. 2008. Structure of a protein phosphatase 2A holoenzyme: insights into B55-mediated Tau dephosphorylation. *Mol Cell*. 31:873-885.

Yamaguchi, M., R. VanderLinden, F. Weissmann, R. Qiao, et al. 2016. Cryo-EM of Mitotic Checkpoint Complex-Bound APC/C Reveals Reciprocal and Conformational Regulation of Ubiquitin Ligation. *Mol Cell*. 63:593-607.

Yamamoto, T.M., L. Wang, L.A. Fisher, F.D. Eckerdt, et al. 2014. Regulation of Greatwall kinase by protein stabilization and nuclear localization. *Cell Cycle*. 13:3565-3575.

Yamano, H. 2019. APC/C: current understanding and future perspectives. *F1000Res*. 8.

Yamashiro, S., Y. Yamakita, G. Totsukawa, H. Goto, et al. 2008. Myosin phosphatase-targeting subunit 1 regulates mitosis by antagonizing polo-like kinase 1. *Dev Cell*. 14:787-797.

Yanagawa, S., J.S. Lee, and A. Ishimoto. 1998. Identification and characterization of a novel line of Drosophila Schneider S2 cells that respond to wingless signaling. *J Biol Chem*. 273:32353-32359.

Yang, H., W. Jiang, M. Gentry, and R.L. Hallberg. 2000. Loss of a protein phosphatase 2A regulatory subunit (Cdc55p) elicits improper regulation of Swe1p degradation. *Mol Cell Biol*. 20:8143-8156.

Yang, L., T. Guan, and L. Gerace. 1997. Integral membrane proteins of the nuclear envelope are dispersed throughout the endoplasmic reticulum during mitosis. *J Cell Biol*. 137:1199-1210.

Yao, C., U. Rath, H. Maiato, D. Sharp, et al. 2012. A nuclear-derived proteinaceous matrix embeds the microtubule spindle apparatus during mitosis. *Mol Biol Cell*. 23:3532-3541.

Yao, C., C. Wang, Y. Li, M. Zavortink, et al. 2018. Evidence for a role of spindle matrix formation in cell cycle progression by antibody perturbation. *PLoS One*. 13:e0208022.

Yip, S.C., S. Cotteret, and J. Chernoff. 2012. Sumoylated protein tyrosine phosphatase 1B localizes to the inner nuclear membrane and regulates the tyrosine phosphorylation of emerin. *J Cell Sci*. 125:310-316.

Yoon, Y.N., M.H. Choe, K.Y. Jung, S.G. Hwang, et al. 2018. MASTL inhibition promotes mitotic catastrophe through PP2A activation to inhibit cancer growth and radioresistance in breast cancer cells. *BMC Cancer*. 18:716.

Yu, J., S.L. Fleming, B. Williams, E.V. Williams, et al. 2004. Greatwall kinase: a nuclear protein required for proper chromosome condensation and mitotic progression in Drosophila. *J Cell Biol*. 164:487-492.

Yu, J., Y. Zhao, Z. Li, S. Galas, et al. 2006. Greatwall kinase participates in the Cdc2 autoregulatory loop in Xenopus egg extracts. *Mol Cell*. 22:83-91.

Yu, X.X., X. Du, C.S. Moreno, R.E. Green, et al. 2001. Methylation of the protein phosphatase 2A catalytic subunit is essential for association of Balpha regulatory subunit but not SG2NA, striatin, or polyomavirus middle tumor antigen. *Mol Biol Cell*. 12:185-199.

Yudkovsky, Y., M. Shteinberg, T. Listovsky, M. Brandeis, et al. 2000. Phosphorylation of Cdc20/fizzy negatively regulates the mammalian cyclosome/APC in the mitotic checkpoint. *Biochem Biophys Res Commun*. 271:299-304.

Zachariae, W., M. Schwab, K. Nasmyth, and W. Seufert. 1998. Control of cyclin ubiquitination by CDK-regulated binding of Hct1 to the anaphase promoting complex. *Science*. 282:1721-1724.

Zachariae, W., T.H. Shin, M. Galova, B. Obermaier, et al. 1996. Identification of subunits of the anaphase-promoting complex of Saccharomyces cerevisiae. *Science*. 274:1201-1204.

Zani, B.G., and E.R. Edelman. 2010. Cellular bridges: Routes for intercellular communication and cell migration. *Commun Integr Biol*. 3:215-220.

Zhai, B., J. Villen, S.A. Beausoleil, J. Mintseris, et al. 2008. Phosphoproteome analysis of Drosophila melanogaster embryos. *J Proteome Res*. 7:1675-1682.

Zhang, D., and S. Oliferenko. 2013. Remodeling the nuclear membrane during closed mitosis. *Curr Opin Cell Biol*. 25:142-148.

Zhang, M., S.D. Yogesha, J.E. Mayfield, G.N. Gill, et al. 2013. Viewing serine/threonine protein phosphatases through the eyes of drug designers. *FEBS J*. 280:4739-4760.

Zhang, S., L. Chang, C. Alfieri, Z. Zhang, et al. 2016. Molecular mechanism of APC/C activation by mitotic phosphorylation. *Nature*. 533:260-264.

Zhang, Z., A.R. Krauchunas, S. Huang, and M.F. Wolfner. 2018. Maternal Proteins That Are Phosphoregulated upon Egg Activation Include Crucial Factors for Oogenesis, Egg Activation and Embryogenesis in Drosophila melanogaster. *G3 (Bethesda)*. 8:3005-3018.

Zhu, C., and W. Jiang. 2005. Cell cycle-dependent translocation of PRC1 on the spindle by Kif4 is essential for midzone formation and cytokinesis. *Proc Natl Acad Sci U S A*. 102:343-348.

Zhu, C., E. Lau, R. Schwarzenbacher, E. Bossy-Wetzel, et al. 2006. Spatiotemporal control of spindle midzone formation by PRC1 in human cells. *Proc Natl Acad Sci U S A*. 103:6196-6201.

Zhu, L., and C.P. Brangwynne. 2015. Nuclear bodies: the emerging biophysics of nucleoplasmic phases. *Curr Opin Cell Biol*. 34:23-30.

Zhu, W., Y. Chen, and A. Dutta. 2004. Rereplication by depletion of geminin is seen regardless of p53 status and activates a G2/M checkpoint. *Mol Cell Biol*. 24:7140-7150.

Zhuge, B.Z., B.R. Du, X.L. Meng, and Y.Q. Zhang. 2017. MASTL is a potential poor prognostic indicator in ER+ breast cancer. *Eur Rev Med Pharmacol Sci*. 21:2413-2420.

Zolnierowicz, S., C. Csortos, J. Bondor, A. Verin, et al. 1994. Diversity in the regulatory B-subunits of protein phosphatase 2A: identification of a novel isoform highly expressed in brain. *Biochemistry*. 33:11858-11867.

Zou, L., and S.J. Elledge. 2003. Sensing DNA damage through ATRIP recognition of RPA-ssDNA complexes. *Science*. 300:1542-1548.